Influence and reliance of Chlamydia trachomatis on host glucose metabolism

Maimouna Djamila Sadio N'Gadjaga

Sorbonne Université

Ecole doctorale Complexité du Vivant

Unité de Biologie Cellulaire de l'Infection Microbienne

Influence and reliance of *Chlamydia trachomatis* on host glucose metabolism

Par Maïmouna Djamila Sadio N'GADJAGA

Thèse de doctorat de Microbiologie Cellulaire

Dirigée par Agathe SUBTIL

Présentée et soutenue publiquement le 24 Septembre 2021

Devant un jury composé de :

Dr. Bertrand FRIGUET (Professeur à l'Sorbonne Université, Paris)	Président
Dr. Isabelle DERRE (Professeur l'Université de Virginie, USA)	Rapportrice
Dr. Benoit VIOLLET (Directeur de recherche, Institut Cochin, Paris)	Rapporteur
Dr. Alain CHARBIT (Directeur de recherche, INEM, Paris)	Examinateur
Dr. Agathe SUBTIL (Directrice de recherche CNRS, Institut Pasteur Paris)	Directrice de thèse

Acknowledgements

Here we are after 4 years. We are in the last few weeks and the best description for my feelings is “I can’t believe I am finally here”. Before I go any further, I would like to thank Dr. Bertrand FRIGUET, Dr. Isabelle DERRE, Dr. Benoit VIOLLET and Dr. Alain CHARBIT for agreeing to be part of my thesis committee. Thank you for your precious time and I am looking forward to our discussions about my work.

Yes, I indeed can’t believe I am already and finally here. I still remember the day Agathe called me to tell me I got the scholarship for the thesis as if it was yesterday. It went by very fast and it was full of emotions, of tears of joy (or not), and of amazing experiences. This journey was one rocky one, and I would have not been able to get here without Agathe. You were way more than a PI to us. You were my rock through this entire process. You were of amazing help and support whether it was for the science our for my personal life. I kept joking that you were the PhDs’ mom, but you really were. Thank you for guiding me, for the discussions, for the motivations whenever experiments didn’t work (and they did that a lot). Thank you for always believing in me and supporting me for my professional ambitions. You were there at every step of the way for way more than I could have asked for. Thank you for being so understanding for every time I couldn’t leave my bed, or when I had to go back to bed and for continuously checking on me. There is not enough “thank you” I can say to tell you how lucky and grateful and thankful I am for everything you did for me during this journey. You are simply awe-amazing (awesome/amazing).

I would also like to thank every member of my team, current and former. Every one of you made this experience way more fun and less challenging. A special thanks to Stephanie and Michael who helped me a lot though this project. Thank you so so so much for all the efforts. Thank you for your time and your contribution. It means the world to me. And to Stephanie thanks for all the advice since I got in the lab 5 years ago. You were always present and made yourself available when needed. I will miss you ☺.

I also want to thank Yongzheng for introducing me to the exciting and challenging world of primary cells, from extracting them to taking care of them. I can but only mention all of our struggles through data analysis which we always ended up figuring out. Thank you also for all the beautiful jazzy rides whenever I needed it. Thanks also to Chongfa and Laure for every time you had to help me out in the lab. It was amazing working with both of you. To

Chongfa with whom I shared an office, but also share a passion for photography, thank you for all the amazing pictures and advice on cameras. Thanks for all the chit chats we had and the restaurants recommendations. Those 3 years with you were really fun ☺. To my dear Chloe, thank you for all those foodie moments. We started this adventure together and I am so happy to call you Dr. now ☺. I already miss our tea and coffee and chocolate breaks. And of course, I can't forget our plant talks ☺. It was a pleasure working with you. Thank you to Sebastien who my teacher for the entire time he was in the lab. Thanks for answering my million questions. To Daniel, thank you for everything, your energy, your suggestions, your Deutch and Chinese learning phases (haha). Thanks for energizing our days. To Benoit, we were also office mate and it was awesome working with you. I am still hoping you will introduce me for real to Volleyball. Thanks for everything. Thanks also to Marine, who became a friend, and Chang for all of our shopping days ☺.

Béatrice, my one and only bibi. You are way way wayyy more than a colleague. You are a true friend and I'm going to miss you a bunch: from our chit chat/coffee breaks, to our get togethers and our hair journey. Thank you for always being there (for the science or in my personal life) and for brightening my days when everything was going wrong. I am sorry you will no longer have someone to bug when you have a break ;). In any case thank you for everything. I will miss you and my samoussas ☹.

To everyone I had the opportunity to collaborate with, whether it was on campus, or in elsewhere, I would like to thank you: Dr. Pouysségur for generously giving us the LS174T cells; Masa Zdralevic for helping me with the LS174T cells; Anna Spier for all the discussions concerning our projects and the advice for the seahorse; Dr. Aimanianda Bopaiah for helping set up a part of my project; Gael for the long hours of work on the statistics; every single one who helped me out with some chemicals or seahorse material… I am also thinking about everyone on our floor, from 3 teams but one big family. A very big and special thanks to Nicolas for the bike ☺ and for helping me with it constantly and for all the discussions. You are amazing ☺. Thanks to Maxime for initiating me to rock climbing and all of our discussions. Thanks to Matt and Michael for all the advice concerning my experiments. If I forgot anyone, please forgive me. Thank you everyone ☺.

I had the opportunity to work with two students which I believe only helped me grow as a scientist and a manager. It was challenging, mostly for personal reasons, but I definitely had a great time with both David and Emile. It was awesome working with you. I wish you the only best ☺.

Finally, I need to thank my family without whom none of this would have been possible. No matter the amount of doubt I had at any point of this journey, they were all there and supportive. This past year and a half have been more than challenging and they, with very important people in my life (Leatitia, Brice, Hamed, Marie-Claude, Nadine, Fadima), were there for me. Leatitia I love you to the moon and back. Thank you for being there every second I needed someone ☺. Thanks to my mom, my dad, my sister Nouria (who happened to help me for my report haha), and my brothers Ismaël and Kalifa. Thank you and Allah ka aou balo. Ka amina ko-ou bè nogoya. Allah ka aou sara, ka toro ni guèrè guèrè bo-a sra kan. A very special thanks to my uncle and aunty Daribi who I love like my own parents. Thank you for being there for me. You guys have a big special place in my heart, and I can't wait to see you guys again (and all the mountains and birds around your place haha). Thank you to Hamed. You came into my life not long ago but you have been there for me more than I can't count and describe. Thank you for always being there and supporting me through sunshine and rain, and even thunder lately. You are incredible and thank you for bringing my spirit up in all those hard times, and God knows we've had few of those. I am lucky and thankful for having such amazing people in my life and may Allah bless you all.

Table of Contents

Table of Figures

Abbreviations

2-DG	**2-Deoxy-D-Glucose**
ADP	Adenosine Diphosphate
Aldo A	Aldolase A
ATP	Adenosine Triphosphate
CDC	Center For Disease Control
CEP170	Centrosomal Protein 170 Kda
COMC	Chlamydial Outer Membrane Complex
CPAF	Chlamydial Protease-Like Activity Factor
CydAB	Cytochrome Bd Oxidase
cyt c	Cytochrome C
Drp1	Dynamin Protein Related 1
DTT	Dithiothreitol
EB	Elementary Body
ECAR	Extracellular Acidification Rates
F2,6BP	Fructose-2,6-Bisphosphate
F6P	Fructose-6-Phosphate
F6P	Fructose-6-Phosphate
FADH+	Flavin Adenine Dinucleotide
FADH2	Reduced Flavin Adenine Dinucleotide
FASII	Type II Fatty Acid Synthesis
FCCP	Carbonyl Cyanide-4 (Trifluoromethoxy) Phenylhydrazone
G1P	Glucose-1-Phosphate
G3P	Glyceraldehyde-3-Phosphate
G6P	Glucose-6-Phosphate
G6PD	Glucose-6-Phosphate Dehydrogenase
GFPT	Glucosamine-Fructose-6-Phosphate Amidotransferase
GLUT1	Glucose Transporter 1
GLUT3	Glucose Transporter 3
GSH	Glutathione
GTP	Guanosine Triphosphate
HBP	Hexosamine Biosynthesis Pathway
HIF-1	Hypoxia Inducible Factor 1
HK	Hexokinase
IPAM	Inclusion Protein Acting On Microtubules
LDHA	Lactate Dehydrogenase A
LGV	Lymphogranuloma Venereum
mDAP	Meso-Diaminopimelate
MLC2	Myosin Light Chain II
MLCK	Myosin Light Chain Kinase

MTOC	Microtubule Organizing Center
MYPT1	Myosin Phosphatase Targeting Subunit 1
Na^+-NQR	Sodim-Dependent NADH Dehydrogenase
NAD+	Nicotinamide Adenine Dinucleotide
NADH,H+	Reduced Nicotinamide Adenine Dinucleotide
NADPH	Nicotinamide Adenine Dinucleotide Phosphate
O_2	Oxygen
OCR	Oxygen Consumption Rates
OxPhos	Oxidative Phosphorylation
PDH	Pyruvate Dehydrogenase
PDK1	Pyruvate Dehydrogenase Kinase 1
PDPK1	3-Phosphoinositide-Dependent Protein Kinase-1
PEP	Phosphoenolpyruvate
PFK1	Phosphofructokinase-1
PFKFB	Phosphofructo-2-Kinase/Fructose-2,6-Bisphosphatases
PGM	Phosphoglucomutase
PI3K	Phosphoinositide-3-Kinase
PK	Pyruvate Kinase
PPAT	Phosphoribosyl Pyrophosphate Amidotransferase
PPP	Pentose Phosphate Pathway
PRA	5'-Phosphoribosylamine
PRPP	Phosphoribosyl Pyrophosphate
PRRs	Pathogen Recognition Receptors
R5P	Ribose-5-Phosphate
RB	Reticulate Body
ROS	Reactive Oxygen Species
SdhA-C	Succinate Dehydrogenase
SFKs	Src Family Kinases
SMVT	Sodium Multivitamin Transporter
STD	Sexually Transmitted Diseases
STI	Sexually Transmitted Infections
T2S	Type 2 Secretion
T3S	Type 3 Secretion
TCA	Tricarboxylic Acid
TG2	Transglutaminase 2
TKT	Transketolase
UDP-GlcNAc	UDP-N-Acetylglucosamine
VDAC	Voltage Dependent Anion Channel
WASP	Wiskott-Aldrich Syndrome Protein
WHO	World Health Organisation

Abstract

Microorganisms with an intracellular development lifestyle exert a strong pressure on the metabolism of their host, since they obtain all their nutriments from its cytoplasm. The obligate intracellular bacteria *Chlamydia trachomatis* provides an extreme illustration of this: they rely on the host not only for the supply of glucose, their main carbon source, but probably also, at least partially, for the supply of the energy currency generated through glucose catabolism, adenosine triphosphate (ATP). These bacteria undergo a particular biphasic developmental cycle: the infectious bacteria, or elementary bodies (EBs), adhere to the membrane of a host cell, typically of the epithelium of the genital tract, and trigger their internalization. Once inside a membrane-bound compartment, called an inclusion, the bacteria express a new set of genes and convert to reticulate bodies (RBs). This only replicative form of the bacteria has a higher metabolism than EBs. Bacteria multiply in the inclusion several times until RBs convert back to EBs, which, once released, can initiate a new infectious cycle. The metabolic pressure exerted by the bacteria on their host thus evolves with time. However, whether infection modulates the metabolism of its host, and the degree of the reliance of individual steps of the bacterial development cycle on host metabolism, remain largely unknown. In this work, using primary epithelial cells and a cell line of non-tumoral origin, we showed that the two main ATP producing pathways of the host, glycolysis and oxidative phosphorylation, remained fairly stable during infection. These results suggest that, against our expectations, there is no significant shift of the host metabolism towards glycolysis during infection. Inhibition of either pathway strongly reduced the capacity of the bacteria to undergo a developmental cycle. While EBs showed some degree of energetic autonomy in the synthesis of the first proteins expressed at the onset of infection, a functional glycolysis was necessary for the establishment of early inclusions, while oxidative phosphorylation is less needed at this early stage of development. The relative importance of the two pathways to sustain the initial steps of infection correlates with their relative contribution in maintaining ATP levels in epithelial cells, glycolysis being the main contributor. Altogether, this work confirms the dependence of the bacteria on the ATP production capacity of the host. However, ATP consumption by the bacteria appears to be fairly balanced with the normal production capacity of the host, and the autonomous production capacity of the bacteria, so that no major shift in host metabolism is required to meet bacterial needs.

Résumé

Les microorganismes à développement intracellulaire exercent une pression importante sur le métabolisme de leur hôte, car ils obtiennent tous leurs nutriments de son cytoplasme. Les bactéries intracellulaires obligatoires *Chlamydia trachomatis* en sont une illustration extrême : elles dépendent de leur hôte non seulement pour l'apport en glucose, leur source principale de carbone, mais probablement aussi, au moins partiellement, pour l'obtention de la monnaie énergétique issue du catabolisme du glucose, l'adénosine triphosphate (ATP). Ces bactéries effectuent un cycle de développement biphasique: les bactéries infectieuses, ou corps élémentaires (EBs), adhèrent à la membrane d'une cellule hôte, typiquement une cellules épithéliale du tractus génital, et provoquent leur internalisation. Une fois à l'intérieur d'un compartiment délimité par une membrane, appelé inclusion, les bactéries expriment un nouveau jeu de gènes et se transforment en corps réticulés (RBs). Le métabolisme des RBs, qui constitue la seule forme réplicative des bactéries, est plus élevé que celui des EBs. Les bactéries se multiplient plusieurs fois dans l'inclusion jusqu'à ce que les RBs se convertissent en EBs, qui, une fois relargués de la cellule-hôte, peuvent initier un nouveau cycle infectieux. La pression métabolique exercée par les bactéries sur leur hôte évolue donc tout au cours du temps. Savoir si l'infection module le métabolisme de son hôte, et dans quelle mesure les différentes étapes du cycle de développement dépendent de ce métabolisme, demeurent des questions ouvertes. Dans ce travail, en utilisant des cellules épithéliales primaires et une lignée cellulaire d'origine non tumorale, nous avons montré que les deux voies métaboliques principales pour la production d'ATP chez l'hôte, la glycolyse et la phosphorylation oxydative, restaient largement stables durant l'infection. Ces résultats indiquent que contrairement à nos attentes, il n'y a pas de basculement significatif du métabolisme de l'hôte vers la glycolyse durant l'infection. L'inhibition de l'une ou l'autre de ces deux voies diminue fortement la capacité des bactéries à effectuer leur cycle de développement. Bien que les EBs démontrent un certain degré d'autonomie énergétique pour la synthèse des protéines exprimées dans la phase initiale de l'infection, une glycolyse fonctionnelle est requise pour accompagner la formation des inclusions, tandis que la phosphorylation oxydative est moins nécessaire à ce stade précoce du développement. L'importance relative des deux voies pour soutenir les étapes initiales de l'infection corrèle avec leur contribution respective à maintenir le niveau d'ATP dans les cellules épithéliales, la glycolyse étant le contributeur principal. En conclusion, ce travail confirme la dépendance des bactéries vis à vis de la capacité de production d'ATP de l'hôte. Cependant, la consommation d'ATP par les bactéries semble en équilibre avec la production normale des cellules épithéliales et la production autonome par les bactéries, en sorte que le métabolisme de l'hôte ne nécessite pas de remodelage profond pour répondre aux besoins des bactéries.

Résumé Détaillé

Chlamydia trachomatis est une bactérie au développement intracellulaire obligatoire, qui se développe exclusivement chez l'Homme. Cette espèce est la première cause bactérienne d'infection sexuellement transmissible, avec plus de 100 millions de nouveaux cas par an. Souvent asymptomatique, ces infections des voies uro-génitales peuvent avoir des conséquences lourdes sur le long terme chez la femme (grossesse extra-utérine, inflammation pelvienne chronique, infertilité). Certains serovars distincts infectent eux la conjonctive de l'œil, pouvant conduire au trachome lorsque non traité à temps : c'est la première cause de cécité acquise au monde.

Chlamydia trachomatis appartient à la famille des *Chlamydiaceae*, qui regroupe, au sein du phylum des *Chlamydiae*, des espèces pathogènes d'animaux (mammifères, insectes, poissons, marsupiaux…) qui ont un impact en santé vétérinaire et humaine. Les autres familles sont moins bien connues, et sont trouvées dans toutes sortes de niches écologiques, avec une grande variété d'hôtes. Toutes les *Chlamydiae* sont des bactéries à Gram négatif partageant plusieurs caractéristiques originales : un mode de développement intracellulaire obligatoire, et un cycle de développement sous deux morphologies : le corps élémentaire (EB), métaboliquement peu actif et non réplicatif, et le corps réticulé (RB), métaboliquement plus actif car réplicatif. Seule la forme EB est infectieuse : après attachement à la surface d'une cellule-hôte, typiquement une cellule épithéliale du tractus génital ou de la conjonctive de l'œil selon les sérovars, la bactérie est internalisée au sein d'un compartiment d'endocytose, que l'on désigne sous le nom d'inclusion. Au cours des premières heures de l'infection, l'inclusion se déplace le long de microtubules, en utilisant des protéines motrices de l'hôte, pour rejoindre le centre organisateur des microtubules (MTOC). L'internalisation des bactéries déclenche aussi une modification de leur état, et rapidement un nouveau programme transcriptionnel est mis en place. Parmi les premiers gènes exprimés, plusieurs codent pour des protéines que les bactéries sécrètent grâce à un appareil de sécrétion de type 3. Ce mécanisme de sécrétion, retrouvé dans de nombreuses bactéries à Gram négatif pathogènes, permet aux chlamydiae de diriger certaines protéines soit dans le cytoplasme de l'hôte, soit dans la lumière ou dans la membrane de l'inclusion. Les protéines ainsi sécrétées sont appelées protéines effectrices, car elles jouent un rôle clé dans la prise de contrôle de l'hôte par le pathogène. La protéine Cap1 est l'une de ces protéines sécrétées précocement dans la membrane de l'inclusion. Le changement de

programme transcriptionnel s'accompagne d'un changement de morphologie des bactéries, avec une transformation graduelle vers la forme RB. Une première division des RBs a lieu environ 6 h après le début de l'infection (6 hpi), et les bactéries entament alors leur phase de division soutenue, avec un doublement du génome bactérien en environ 2-3 h. Dès 24 hpi certains RBs cessent de se diviser et se différencient en EBs. Cet évènement a lieu de manière asynchrone, de sorte que les inclusions contiennent un mélange entre RBs et EBs. Comme les besoins énergétiques des RBs sont supérieurs à ceux des EBs, on estime que le pic de la consommation énergétique de l'inclusion est atteinte vers 30-32 hpi, lorsque le nombre de RBs commence à décroitre car les conversions en EBs l'emportent sur les divisions. Quarante- huit hpi, l'inclusion contient très majoritairement des EBs, qui sont ensuite libérés soit par lyse de la cellule-hôte, soit par un processus d'extrusion où l'inclusion est relarguée dans le milieu extracellulaire entourée d'une membrane. Les EB libérés peuvent commencer un nouveau cycle infectieux sur les cellules adjacentes.

Le caractère intracellulaire obligatoire des chlamydiae va de pair avec une perte importante de gènes codant pour des fonctions métaboliques essentielles, ces fonctions étant assurées par l'hôte. Ainsi, le génome de *C. trachomatis* ne contient qu'environ 900 gènes, et les bactéries dépendent de leur hôte, entre-autre, pour la synthèse de plusieurs acides aminés, de tous les nucléotides, et de nombreux co-facteurs de réactions enzymatiques. Longtemps *C. trachomatis* a également été considéré comme un parasite énergétique, se développant au dépend de l'adénosine tri-phosphate (ATP) fourni par l'hôte. Le séquençage de son génome a révélé ses capacités glycolytiques, et la présence d'un cycle de Krebs (TCA) incomplet. Les études en protéomique et les mesures de synthèse protéique en milieu axénique suggèrent que les EBs utilisent la glycolyse, qui pourrait être alimentée par leurs stocks de glycogène. La question de savoir si cette réserve énergétique est suffisante pour initier l'infection avant la conversion en RBs sera posée dans ce travail. Plusieurs arguments soutiennent que la phase de réplication des RBs est quant à elle au moins partiellement dépendante de l'import d'ATP fourni par l'hôte. En effet, les bactéries expriment deux transporteurs permettant l'import d'ATP, les enzymes de la glycolyse sont peu exprimées et le glucose semble surtout soutenir la synthèse de lipopolysaccharide, et enfin, en milieu axénique, la synthèse protéiques des RBs nécessite la présence d'ATP.

Des données disparates de la littérature suggéraient que l'infection par *C. trachomatis* puisse s'accompagner d'une augmentation de la glycolyse. Il était assez tentant de faire un

parallèle entre les cellules infectées, dont les besoins énergétiques sont accrus pour soutenir le métabolisme des bactéries, et des cellules tumorales. Dans de nombreuses tumeurs, la prolifération cellulaire s'accompagne d'un rééquilibrage des voies métaboliques, qualifié d'effet Warburg, en faveur de la glycolyse. Cependant, il est à noter que dans le cas de *Chlamydia*, les données avaient été obtenues pour l'essentiel dans des cellules HeLa, qui d'origine cancéreuse et ont été maintenues en culture sur de nombreuses générations, de sorte que leur métabolisme est anormal. De plus, certaines des données indiquant que les cellules infectées puissent privilégier la glycolyse avaient été obtenues avec d'autres espèces de *Chlamydiaceae* que *C. trachomatis*, or ces espèces ont pu mettre en place des adaptations très spécifiques aux tissus qu'elles infectent. La question des conséquences de l'infection par *C. trachomatis* sur le métabolisme de l'hôte demeurait donc ouverte, et nous avons donc cherché à comprendre si les deux voies majeures de synthèse d'ATP dans l'hôte, la glycolyse et la respiration oxydative, se trouvaient modifiées au cours du temps par l'infection. Nous avons également cherché à comprendre si le développement des bactéries dépendait ou non du fonctionnement optimal de ces deux voies, et, si oui, à quelle étape du cycle bactérien.

Pour répondre à ces questions, nous nous sommes attachés à travailler dans des cellules épithéliales dites « primaires », c'est-à-dire maintenues en culture pendant moins de 5-6 passages depuis leur isolement sur des biopsies de patientes. La crise sanitaire liée à la pandémie de SARS-Cov2 a restreint notre accès aux cellules de patientes, nous avons parfois utilisé la lignée A2EN, qui sont des cellules épithéliales non tumorales de l'endocol, immortalisées (via les protéines E6 et E7 du virus de l'herpès). Pour tous les paramètres que nous avons pu analyser, les cellules A2EN présentent un métabolisme similaire aux cellules primaires, ce qui valide leur utilisation pour les questions posées ici.

Pour mener à bien cette étude nous avons choisi de créer une souche de *C. trachomatis* de serovar D (l'un des serovar prépondérant des infections génitales) exprimant de façon stable une protéine fluorescente, la mCherry. Nous avons montré que quoique cette souche diffèrait légèrement de la souche parentale, avec un gain d'infectivité *in vitro*, elle constituait un outil acceptable pour notre sujet de recherche. Pour aborder l'étude des modifications éventuelles du métabolisme de l'hôte nous avons commencé par mesurer la concentration d'ATP total dans les cellules infectées, et nous l'avons trouvée stable tout au long de l'infection, indiquant qu'un équilibre s'établit entre les deux partenaires. Nous avons ensuite comparé l'abondance de deux marqueurs de la glycolyse dans des cellules infectées et non-infectées : la production de lactate,

et l'acidification du milieu de culture. Le premier paramètre indique une stabilité de la glycolyse lors de l'infection, le second une augmentation de 30% lorsque le métabolisme des bactéries est à son maximum. Nous concluons que la glycolyse est stable, ou augmentée de façons modeste par l'infection par *C. trachomatis*. La phosphorylation oxydative (OxPhos) de l'hôte, mesurée par la consommation d'oxygène par les mitochondries, est quant à elle inchangée par l'infection. Ces résultats indiquent que l'infection par *C. trachomatis* n'entraine pas une augmentation significative des capacités de production d'ATP de l'hôte, indiquant que la production énergétique normale suffit aux besoins des bactéries. Nous avons ensuite utilisé des molécules inhibitrices de voies métaboliques spécifiques pour déterminer les conséquences de leur inhibition, même partielle, sur le cycle de développement des bactéries. Le GNE-140 est un inhibiteur spécifique des isoformes A et B de la lactate deshydrogenase. Nous avons mesuré une diminution dose dépendante de la concentration d'ATP dans les cellules épithéliales traitées par cette molécule, dès 2 h après le début du traitement. Appliqué lors d'une infection, le GNE-140 affecte à la fois les phases précoce et prolifération du développement des bactéries, avec globalement une importante réduction des bactéries infectieuses formées. Les drogues ciblant OxPhos (oligomycine et phenformine) ont quant à elles un effet modeste sur la phase précoce, qui corrèle avec leur moindre impact sur la production d'ATP que le GNE-140 dans ce type cellulaire. En revanche, comme le GNE-140 elles inhibent la production de particules infectieuses. Enfin, nos résultats illustrent combien il est important d'utiliser les cellules primaires pour ce type d'étude. En effet, la dépendance des bactéries au bon fonctionnement de la glycolyse n'est pas retrouvée dans deux lignées tumorales testées.

En résumé, contrairement à nos attentes, nous avons montré que les cellules épithéliales infectées par *C. trachomatis* ne subissent pas d' « effet Warburg ». En dépit de la prépondérance de la glycolyse pour la production d'ATP dans ces cellules, les bactéries ne peuvent pas se passer d'une OxPhos optimale dans leur phase réplicative. La dépendance des bactéries à la fois vis-à-vis de la glycolyse et de la respiration oxydative, pour leur phase de réplication, renforce l'hypothèse que les bactéries ne sont pas autonomes en besoin énergétique dans cette phase de leur développement, et qu'elles détournent l'ATP de l'hôte, faisant feu de tout bois. On ne peut exclure que d'autres métabolites affectés par l'usage de ces inhibiteurs soient impliqués dans les effets observés, en particulier la perte de renouvellement de NAD lorsque OxPhos est inhibée, car les bactéries sont entièrement dépendantes de l'hôte pour ce métabolite essentiel.

Mon travail doctoral a aussi porté un éclairage sur les capacités énergétiques de EBs. En effet, j'ai montré qu'en absence de glucose dans le milieu de culture de cellules HeLa, et par conséquent avec une concentration de glucose réduite dans ces cellules, les bactéries étaient capables de synthétiser la protéine Cap1, démontrant ainsi une certaine autonomie énergétique. Cependant, elles étaient moins regroupées au MTOC et les tubules émanant de l'inclusion moins long. Ces phénomènes s'expliquent probablement par le fait que la migration des inclusions vers le MTOC et l'élongation de tubules sont des phénomènes qui nécessitent un apport énergétique sous forme d'ATP dans le cytoplasme, c'est-à-dire par l'hôte. Or la privation de glucose réduit de moitié la concentration en ATP dans ces cellules. Cette hypothèse que la baisse du niveau d'ATP explique les phénotypes précoces est soutenue par la corrélation que nous avons observée entre l'effet des différentes drogues testées sur le niveau d'ATP dans les cellules primaires, et la migration des bactéries vers le MTOC. Nous en avons conclu que les EBs possèdent une autonomie toute relative car certaines étapes clés du développement de *C. trachomatis* mettent en jeu des processus eukaryotes dépendants de l'ATP.

La comparaison de notre travail sur *C. trachomatis* avec des données de la littérature sur d'autres espèces de *Chlamydiaceae* sont difficiles car les autres travaux ne portent pas sur des cellules primaires. Il est à noter que contrairement à celles de *C. trachomatis*, les inclusions de certaines espèces sont décrites comme en étroite association avec les mitochondries, suggérant des stratégies distinctes. Cette possibilité est en accord avec les conclusions du travail post-doctoral de Sébastien Triboulet, à la révision duquel j'ai participé. Dans cette étude, ST a montré que l'accumulation de glycogène dans l'inclusion de seulement certaines espèces de *Chlamydiaceae* (*C. trachomatis*, *C. suis* et *C. muridarum*) corrèle avec l'acquisition d'un signal de sécrétion de type 3 dans la phosphoglucomutase des dites espèces. Sa sécrétion dans la lumière de l'inclusion explique comment les bactéries peuvent tirer profit de leur capacité à y accumuler du glycogène, puisque l'enzyme assure la conversion de glucose-1-phosphate en glucose-6-phosphate, seule source de glucose captée par les bactéries. L'absence de sécrétion de la phosphoglucomutase dans d'autres *Chlamydiacae* testées (*C. caviae* et *C. pneumoniae*) renforce l'hypothèse que des stratégies métaboliques différentes ont été mises en place par ces différentes espèces, adaptées aux tissus qu'elles infectent. Les conclusions auxquelles nous sommes arrivées à l'issue de ce travail sont donc à considérer avec précaution si on s'intéresse à d'autres *Chlamydia* pathogènes pour l'Homme telle que *C. pneumoniae*. Enfin, la revue de la littérature concernant d'autres types de bactéries souligne le peu d'information disponible sur

les conséquences métaboliques des infections par des bactéries intracellulaires dans les cellules épithéliales primaires, et appelle à d'autres études de ce type.

Introduction

I. *Chlamydia trachomatis*, a human-adapted obligate intracellular pathogen

1. Once upon a time, the discovery of *Chlamydiae*…

The beginning of the 20th century marks the discovery of chlamydial inclusions in ocular infections. The responsible infectious agent was mistakenly taken for a protozoan, named "Chlamydozoa", then for a virus due to its small size, filterable characteristics and non-reproductive ability on media. Similar inclusions were later observed in diverse infections namely zoonotic pulmonary, ocular and sexual infections (Horn, 2008; Nunes and Gomes, 2014). In 1966, with the advent of electron microscopy, Moulder work allowed to finally classify the *Chlamydiae* phylum members as bacteria (Moulder, 1966). By the 2nd half of the 20th century, methods were developed to culture *Chlamydiae* first in embryonated egg, then in egg yolk (Black, 2013; Chen et al., 2019; Horn, 2008; Nunes and Gomes, 2014).

2. *Chlamydia trachomatis* and its numerous relatives

The *Chlamydiae* phylum exclusively contains obligate intracellular bacteria. That lifestyle has made it difficult to obtain a clear picture of the phylum members diversity due to the requirement of host co-culture for their studies. Moreover, since many universal bacterial primers have mismatches to chlamydial 16S rRNA genes, identification of unknown lineages requires the use of specific primers (Lagkouvardos et al., 2014).

Growing numbers of studies are now using novel approaches such as culture-independent metagenomics (Taylor-Brown et al., 2016, 2017) or single cell genomics (Collingro et al., 2017) enabling the establishment of a phylogenetic tree revealing unknown relationships (Pillonel et al., 2018; Taylor-Brown et al., 2015). The discovery of additional chlamydial species from diverse environment and or hosts such as amoeba, reptiles, birds, fishes and arthropods has also helped in building an up-to-date *Chlamydiae* phylogenetic tree (Fehr et al., 2013; Pillonel et al., 2018; Taylor-Brown et al., 2015) (Figure 1). A recent study discovered that chlamydial lineages are not only found but might dominate the bacterial community in deep marine anoxic environments. Using genome-resolved metagenomics, the authors were able to reconstruct 24 chlamydial genomes expanding the diversity of the phylum which is now composed of seven clades (Dharamshi et al., 2020) (Figure 1).

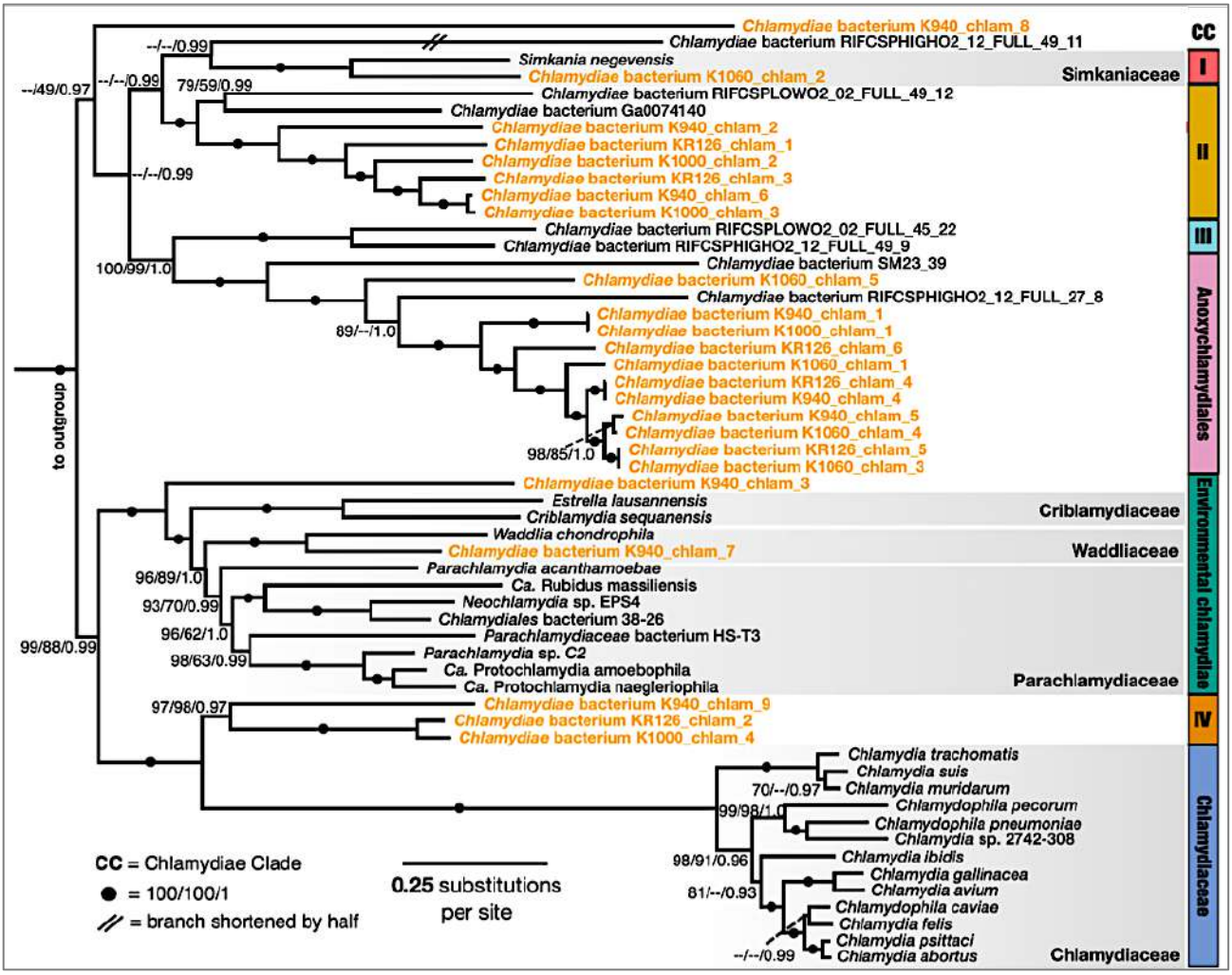

Figure 1. Updated *Chlamydiae* phylogenetic tree
Bayesian phylogenetic tree of 38 concatenated single-copy conserved marker proteins representing known chlamydial species (in black) and identified marine sediment *Chlamydiae* (in orange). *Chlamydiae* are organized into seven clades: chlamydial clade (CC) I (containing the *Simkaniaceae*) to IV; Environmental chlamydiae containing *Criblamydiaceae*, *Waddliaceae*, and *Parachlamydiaceae*; *Chlamydiaceae* and *Anoxychlamydiales*. Adapted from (Dharamshi et al., 2020)

Chlamydia trachomatis (C. trachomatis) is one of the 13 species members of *Chlamydiaceae*, a family of pathogens with a diverse range of eukaryotic hosts (Figure 2). *Chlamydiaceae* represents an entire clade on its own, and its members display the smallest genomes of the phylum (1-1,2 Mbp) (Dharamshi et al., 2020; Horn, 2008; Omsland et al., 2014). *C. trachomatis* along with *C. pneumoniae*, represent the two most important human pathogens. The former is strictly restricted to its human host while the latter can also infect horses, frogs and marsupials. Other species, such as *C. psittaci*, *C. abortus*, and to a lesser extent *C. felis*, can also infect humans through zoonotic transmission. Diseases caused by *Chlamydiaceae* are diverse and range from pneumonia or obstructive pulmonary disease caused

for instance by *C. pneumoniae, C. felis, C. pecorum, C. muridarum* or *C. suis,* to ovine enzootic abortion caused by *C. abortus* (Nunes and Gomes, 2014).

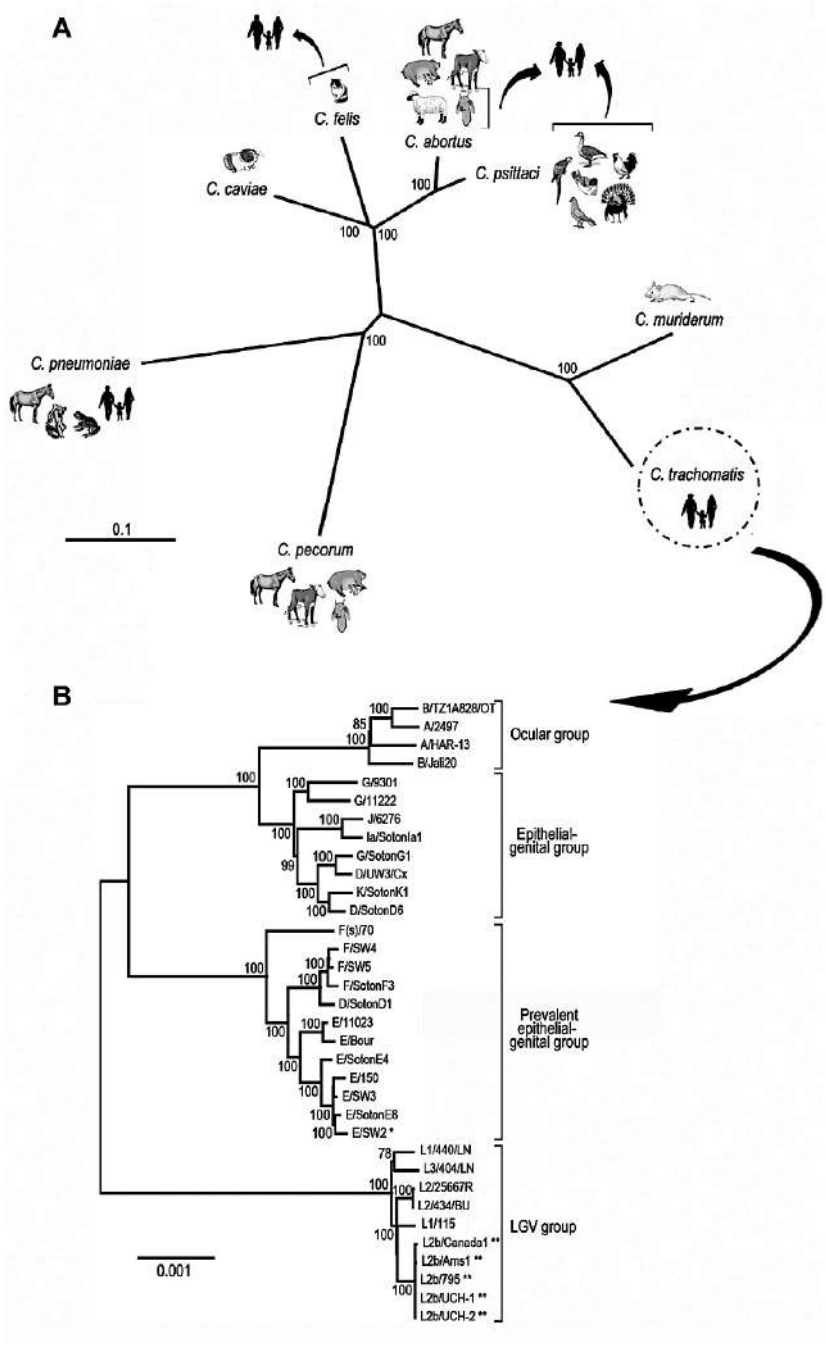

Figure 2. Phylogenetic reconstruction of *Chlamydia* genus
(A) *Chlamydia* species are represented with their respective hosts. *C. suis* is not represented in the tree due to missing genomic data. The tree was constructed using the Neighbour-Joining Tree method that is based here on 600 Orthologous genes. (B) Phylogenic reconstruction of *C. trachomatis*. The tree was made by comparing 819 genes conserved from the sequenced genomes of different serovars of *C. trachomatis*, showing a genetic correlation between tissue tropism and infection symptoms, and serovar (Nunes and Gomes, 2014)

3. *Chlamydia trachomatis* epidemiology

C. trachomatis, which is the pathogen of interest in this project, has been classified into about 15 serovars based on the major outer membrane protein (MOMP) antigenic variation. (Figure 2). Those serovars are grouped into three biovars that either infect ocular or genital tissues (Nunes and Gomes, 2014; O'Connell and Ferone, 2016). Post-genomic studies revealed the limits of using MOMP variation to categorize *C. trachomatis* strains, as gene recombination can occur (Harris et al., 2012). This is still however the commonly used classification system, because the correlation between tissue tropism, infection symptoms and serovars remains very strong.

a. Ocular infections

Ocular infections are caused by serovars A-C, which, when left untreated, can lead to trachoma, a chronic inflammatory disease. Transmission occurs through direct contact of infected people eye and nose discharges, or indirectly by the spread of those discharges by certain type of flies. Repeated infections often occur and lead first to eyelids' severe scarring (trachomatous conjunctival scarring) which eventually induces it to turn inward (trachomatous trichiasis), causing constant pain due to the eyelashes rubbing against the eye. With no treatment, irreversible opacities form on the cornea causing visual impairment or blindness.

Trachoma is the leading cause of preventable infectious blindness and visual impairment worldwide with 1.9 million cases and representing 1.4% of all blindness cases worldwide. About 2,5 million people have trachomatous trichiasis worldwide (discussed later in this section), and about 142 million people are still at risk of trachoma blindness. Trachoma is endemic in 44 countries in Africa, Asia, Central and South America, Australia and the Middle East, with Africa being the most severely affected continent (Figure 3). In those endemic areas, active trachoma affects both adults, with women being more at risk, and children, having a prevalence as high as 90% in the latter group. The economic consequences of trachoma are significant. When considering eye impairment, trichiasis and blindness, the economic loss is estimated at 8 billion US$. (Burton and Mabey, 2009; WHO | Trachoma, 2020).

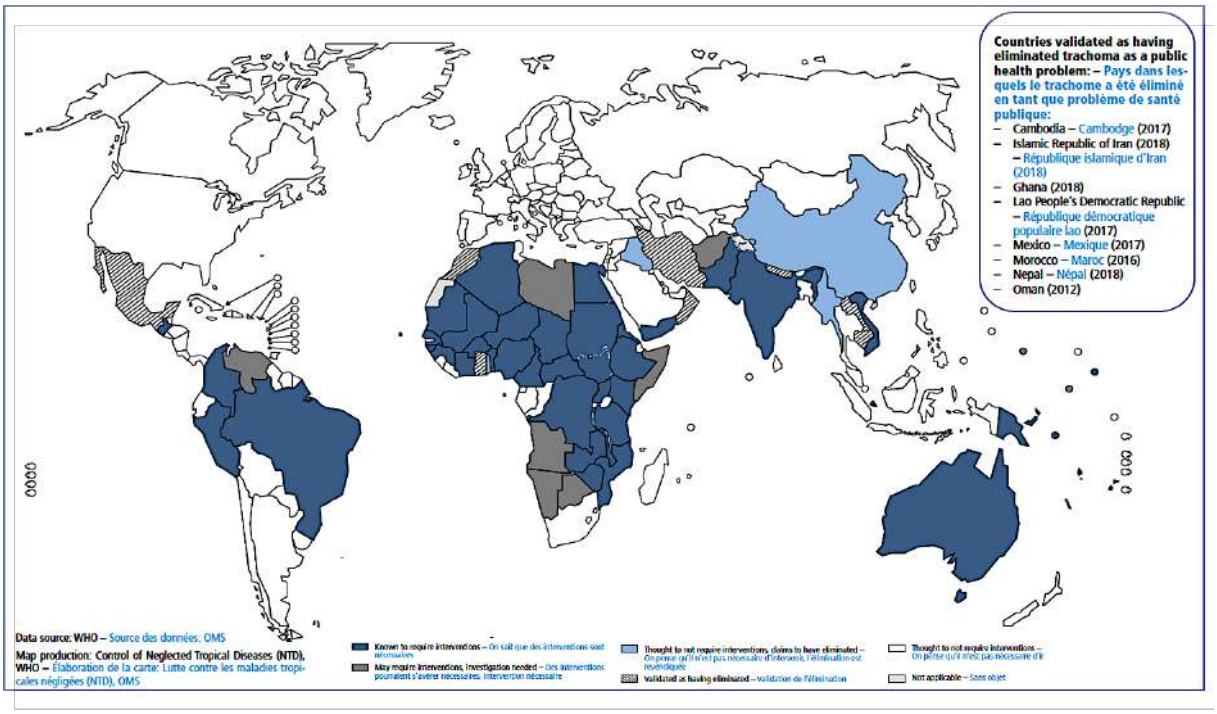

Figure 3. Elimination status of trachoma as a public health problem as of 2019
The SAFE program adopted to help eliminate trachoma as a public health problem by 2020 allowed its eradication in 8 countries (purple box). However, 44 countries are still endemic for trachoma as of 2021. Thus, a new target date has been set for 2030. Adapted from WHO epidemiological record 2019 (Rowley et al., 2019)

b. Genital infections

The two other *C. trachomatis* biovars infect the genital tract and represent the leading cause of sexually transmitted infections (STI) worldwide. According to the WHO, there were 127 million new cases of chlamydial genital infections in 2016, with women being more affected (WHO fact sheets on Chlamydia) (Figure 4, Figure 5). The global incidence (new cases per 100,000 persons at a particular time) of infection, for adults aged 15-49, increased by 4.1% between 2005 and 2008 (WHO 2019 Bulletin #97). In the USA alone, more than 1,8 million chlamydial infection were recorded in 2019, with adolescent and young adults being more affected. Indeed in 2019, almost two-third of all reported cases was among persons aged 15-24 years, with women more affected (CDC National overview of STDs 2019) (Figure 5).

Serovars D-K are responsible for non-invasive genital infections and mostly affect adolescents and young adults. They result in various symptoms such as cervicitis (inflammation of the cervix) in women and urethritis (inflammation of the urethra) in men. The disease being asymptomatic in most cases, it is left untreated and can worsen and lead to pelvic inflammatory diseases in women. This can cause drastic irreversible consequences such as infertility, spontaneous abortion, or ectopic pregnancies. The infection can also be transmitted to babies

during labor. Complications can also occur for men, leading to epididymitis and reactive arthritis (O'Connell and Ferone, 2016).

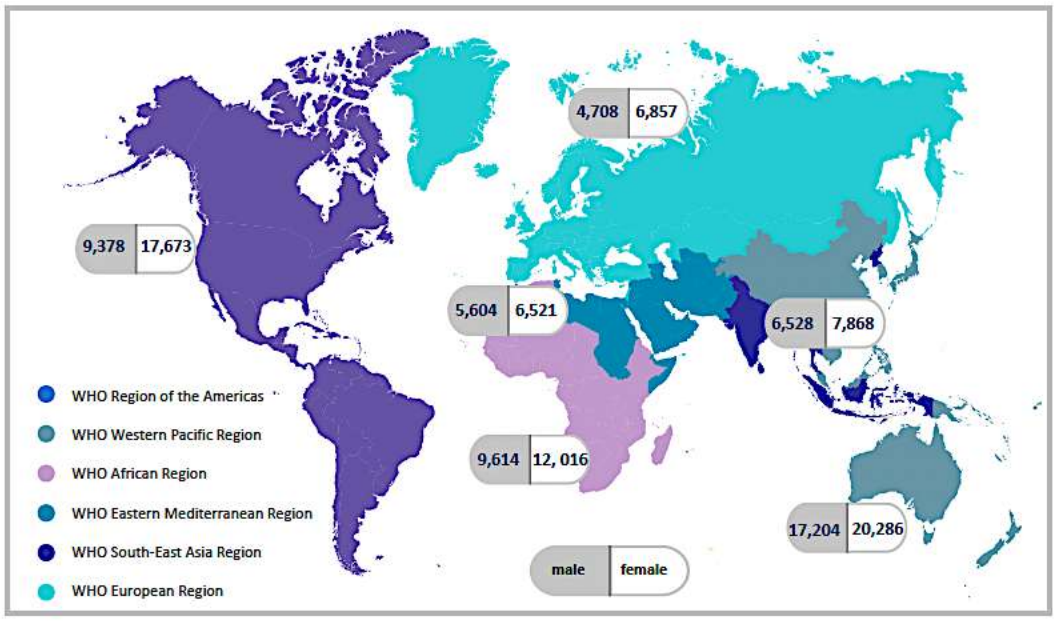

Figure 4. Estimation of prevalent cases of Chlamydial infections by WHO region in 2016
Prevalence (number of cases per 100000 persons) of chlamydial infection worldwide for the age group 15-49 years. Women are more affected than men. WHO Global Adult Estimates for 4 STIs.

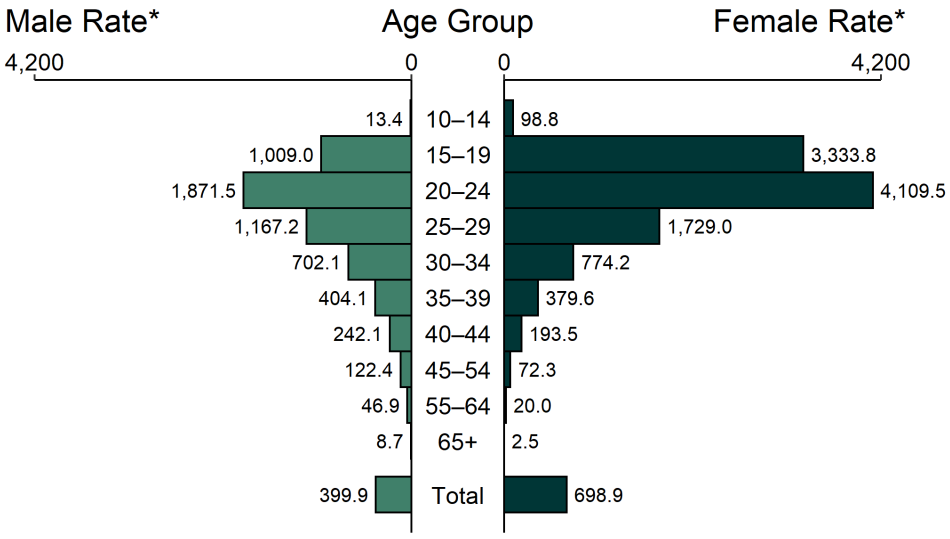

Figure 5. Chlamydia Rates of Reported Cases by Age Group and Sex, United States, 2019
In 2019, most reported chlamydial infection case was among the age group 15-24. CDC National overview of STDs 2019. * Per 100,000; Total includes all ages

The last group, serovars L1, L2 and L3, is responsible for more invasive sexually transmitted diseases. They can spread through the dissemination of infected macrophages and reach local, draining nymph nodes causing lymphogranuloma venereum or LGV. These infections are often symptomatic contrary to other chlamydial infections. They can lead to rectal stenosis and fibrosis, that are sometimes associated with HIV primarily in men engaging in receptive anal intercourse with men (Nunes and Gomes, 2014; O'Connell and Ferone, 2016).

4. Treatment

In 1998, the WHO established the WHO Alliance for the Global Elimination of Trachoma which aimed to eliminate trachoma as a public health disease by 2020 (GET2020). As of today, the new target date is 2030. Trachoma elimination strategy is based on the **SAFE** guidelines involving the following: **S**urgery for patients with trichiasis; **A**ntibiotic treatment with azithromycin to treat the infection; **F**acial cleanness; **E**nvironmental improvement. This program has resulted in a significant reduction of trachoma prevalence. Indeed, the number of people at risk of trachoma decreased by 91% between 2002 and 2019. Moreover, since 2011, 8 countries have been validated by the WHO to have eliminated trachoma as a public health issue (Figure 3). Results are thus encouraging, but with 44 countries still being endemic for trachoma, efforts to fight trachoma have to be pursued and even amplified (Burton and Mabey, 2009) (WHO | Trachoma, 2021).

Genital infections are also treated with azithromycin as a single dose, or with doxycycline for a weeklong treatment. Even though drug resistance has not been reported, antibiotic treatment might not be always effective at eliminating the bacteria, especially for chronic infections (Nunes and Gomes, 2014; O'Connell and Ferone, 2016). As of today, there is still no vaccine against *C. trachomatis* infections, however they are under development and the first phase I trial was recently successfully achieved (Abraham et al., 2019; de la Maza et al., 2021).

II. Prominent features of *C. trachomatis* developmental cycle

1. A closer look at the developmental cycle of *Chlamydia trachomatis*

A characteristic of *Chlamydiae* is their unique cycle divided in two parts, each relying on a morphologically and functionally different form of the bacteria. This developmental cycle concept was first introduced by Bedson and Bland after observing different forms of the pathogen at successive stages of infection (Bedson and Bland, 1932). The infectious particle, called elementary body (EB), is small (~300 nm), non-replicative, with compact DNA and was thought to be metabolically inactive, being described as a dormant spore-like structure for years (Stephens, 1998; Iliffe-Lee and McClarty, 1999; Omsland et al., 2014). Recent studies have shown that EBs are somewhat metabolically active (Haider et al., 2010; Omsland et al., 2012; Vandahl et al., 2004). Their highly disulfide cross-linked outer membrane allows them to resist potential harsh extracellular conditions including osmotic and physical stress. The replicative bacterial form, called reticulate body (RB), is larger (>1 μm) and in contrast to EBs, the proteins of their outer membrane are reduced, making it more fluid (Bavoil et al., 1984; Hackstadt et al., 1985; Hatch et al., 1986). Their replicative activity makes RBs more metabolically active than EBs, and we will give more details later on the metabolic requirements of each form.

EBs initiate *C. trachomatis* infection through binding epithelial cells. Internalization in endocytic vesicles quickly follows, which is in part triggered by the secretion of bacterial proteins as described later (Figure 6). Once internalized, bacteria remain in a membrane-bound compartment, known as "inclusion", throughout their entire cycle. Soon after entry, EBs differentiate into RBs, which replicate several times causing inclusions to grow significantly in size. Starting about 24 h post infection (hpi), RBs asynchronously differentiate back into EBs. Around 48 hpi, newly formed EBs are released by either cell lysis or inclusion extrusion, from which point a new infection can begin (AbdelRahman and Belland, 2005; Elwell et al., 2016; Gitsels et al., 2019; Nunes and Gomes, 2014).

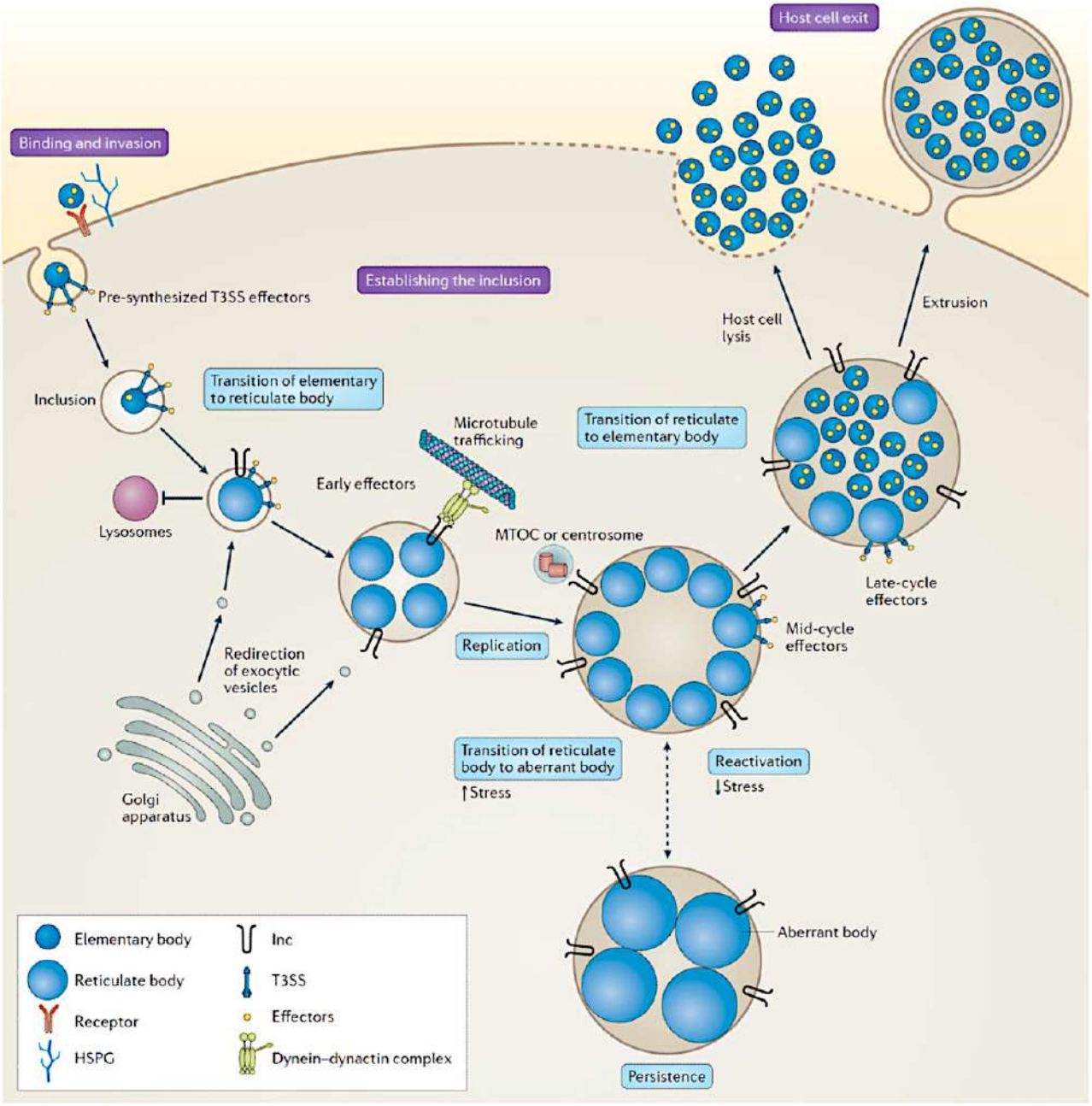

Figure 6. Development cycle of *C. trachomatis*
Elementary Bodies (EBs) attach to host cells then are quickly internalized in a parasitophorous vacuole called inclusion. EBs either convert into Reticulate Bodies (RB), which replicate inside inclusions, or into persistent form in stressful conditions. RBs differentiate back into EBs, which are released from host cells in order to initiate another round of infection (Elwell et al, 2016)

2. EBs and RBs successive roles during infection

a. EBs initiate infection

i. The adhesion

Even though *C. trachomatis'* target is typically a human epithelial cell, it can undergo a normal developmental cycle in a various range of cell types, from different mammalian species *in vitro*. This means that the tropism of *C. trachomatis* towards human is not due to specific binding to a human receptor, and in fact the bacteria likely use multiple attachment and entry routes, as detailed below. Still, part of the difference in tropism between serovars might be due to the use of different host receptors as was illustrated by Fadel and Eley for serovars E versus LGV (AbdelRahman and Belland, 2005; Fadel and Eley, 2008; Elwell et al., 2016; Gitsels et al., 2019).

C. trachomatis adhesion to host cells is a two-step process. The first one involves a low-affinity, reversible bacterial attachment through electrostatic interactions to herapan sulfate (HS) containing glycosaminoglycans (GAGs). In fact, treatment of cells with HS lysate inhibits adhesion (Su et al., 1996; Zhang and Stephens, 1992).

The second attachment step is irreversible with high affinity binding to host cell receptors. Multiple host receptors and their binding bacterial partners have been identified so far, but some grey areas remain to be elucidated (Gitsels et al., 2019). Some of the identified host receptors-chamydial adhesins (*C. trachomatis*) couples are: Cystic fibrosis transmembrane conductance regulator (CFTR) with LPS (Ajonuma et al., 2010); Beta-1 integrin (ITGB1) with CT017 or Ctad (Stallmann and Hegemann, 2016); and 3'sulfogalactolipid (3'SGL) with Hsp70 (Mamelak et al., 2001). Additional identified host receptors involved in chlamydial adhesion are the platelet-derived growth factor the receptor beta (PDGFRβ) (Elwell et al., 2008), the EphrinA2 receptor (Subbarayal et al., 2015), the fibroblast growth factor receptor (FGFR) via Fibroblast growth factor 2 (FGF2) as an intermediate (Kim et al., 2011), and the protein disulfide isomerase (PDI) (Abromaitis and Stephens, 2009; Conant and Stephens, 2007). PDI, a component of the estrogen receptor complex, has been shown to have two independent roles in infection. On one hand, it promotes bacterial attachment, and on the other hand, its active enzymatic activity is necessary for bacterial entry, possibly to reduce disulfide bridges in the type 3 secretion machinery (see below) (Abromaitis and Stephens, 2009; Betts-Hampikian and Fields, 2011). On the bacterial side, putative adhesins also include proteins of the outer membrane complex, namely OmcB (Fadel and Eley, 2007), the major outer protein, MOMP

(Stephens et al., 2001; Su et al., 1996) and also the polymorphic outer membrane proteins (Pmps) (Becker and Hegemann, 2014).

ii. The entry

One important feature of chlamydiae is that they all express a multi-component secretion machinery called the type 3 secretion (T3S) system, that we will describe in further detail later. Upon host cell binding, the T3S system is activated allowing injection of pre-packaged bacterial effectors into the host. That promotes rapid bacterial internalization favored by cytoskeletal rearrangements, which actually is a constant theme throughout infection (**Figure 7**) (Elwell et al., 2016; Gitsels et al., 2019). To this date, there are controversial findings regarding the involvement of clathrin-coated pits and caveola in *C. trachomatis* entry process (Gitsels et al., 2019). In any case, the internalization step is fast, with about 50% of the bacteria being internalized within 10 min in the case of bacteria of the LGV biovar (Vromman et al., 2014). *C. trachomatis* serovars A to K are internalized less efficiently, and a centrifugation step is commonly used in experimental conditions to enhance bacterial entry. In all cases, EBs play an active role in this internalization step, through the secretion of "effector" proteins, that contribute to rearrangement of the cytoskeleton and the plasma membrane.

Effectors mediating invasion identified so far are the actin recruiting phosphoprotein TarP (CT456) and TmeA (CT694). TarP mediates actin nucleation and enhance filament polymerization (Jewett et al., 2006). Phosphorylation of TarP post injection allows the Rac1 (RAS-related C3 botulin toxin) dependent recruitment and activation of the Arp2/3 complex, leading to a local actin remodeling (Carabeo et al., 2004, 2007; Elwell et al., 2008) (Figure 7). Rac1 is an actin polymerization regulator which is part of the Rho GTPases family. TmeA functions synergetically with TarP, by directly activating host N-WASP to promote Arp2/3-dependent actin polymerization (Keb et al., 2021).

Finally, our laboratory showed that genetic disruption of the effector CT622 (TaiP) resulted in a decrease in bacterial entry (Cossé et al., 2018). However, it is not clear at this stage whether this reflects a role for CT622 in the entry step per se, or whether it reflects a general defect in the formation of EBs at the preceding infectious cycle from which they were collected.

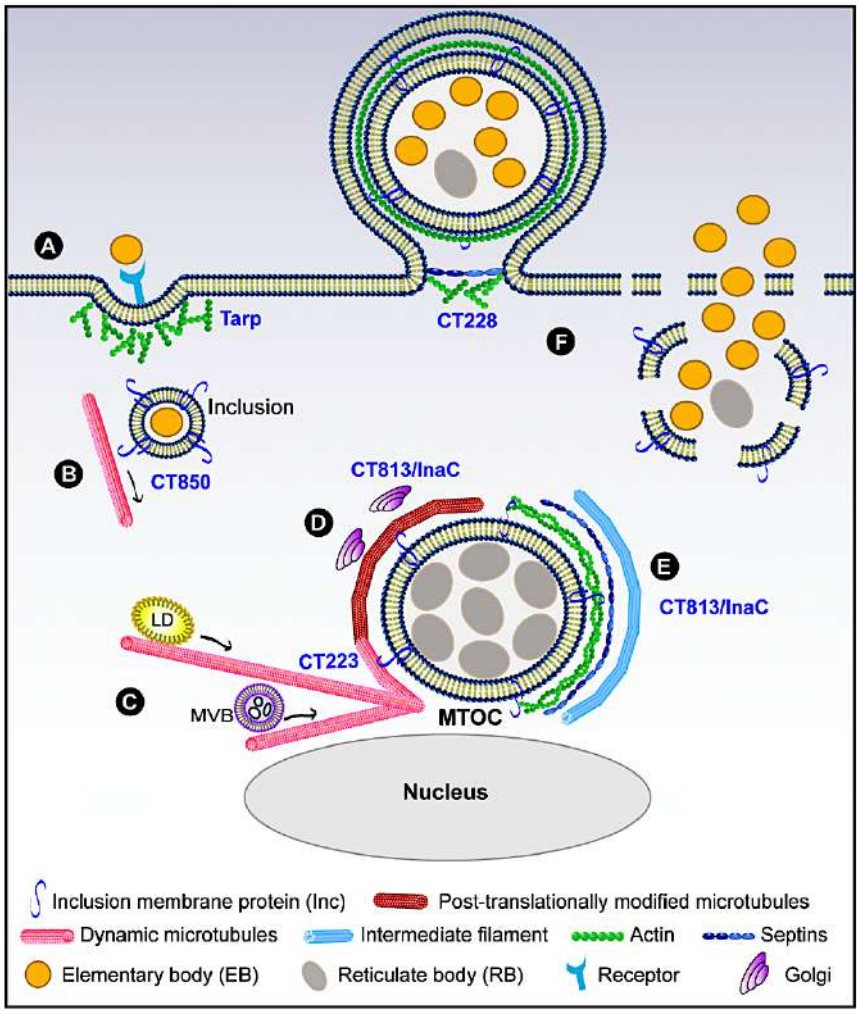

Figure 7. Cytoskeletal modulations during *C. trachomatis* infection
The cytoskeleton is reorganized throughout the course of chlamydial infection. (A) Upon entry the bacterial translocated actin-recruiting phosphoprotein (TarP) induces polymerization of actin. (B) The newly formed inclusion is transported to the microtubule organizing center (MTOC) with the help of CT850. (C) Microtubules cages form around the inclusion which involves probably CT223, with lipid droplets (LD) and multivesicular bodies (MVB) movements towards the inclusion. (D) Post-translational modifications of microtubule cages and mini-Golgi positioning around the inclusion is mediated by CT813/InaC. (E) CT813 is also involved in the stabilization of the inclusion with actin, septins and intermediate filaments fibers. (F) *Chlamydia* exit cell either through lysing cells (right), or through an extrusion process (left) (Wesolowski and Paumet, 2017)

b. RBs take over!

i. Conversion into RBs

During the first hours of infection, various events leading to EB to RB conversion are activated. The exact signal inducing EB to RB differentiation is not known (Belland et al., 2003; Shaw et al., 2000). Nevertheless, that conversion requires some significant changes. To begin with, the proteins of the chlamydial outer membrane complex (COMC) which are highly cross-linked in EBs get reduced, allowing EBs "relaxation" (Hackstadt et al., 1985; Hatch et al.,

1986). Furthermore, the EBs highly compact DNA decondenses through the dissociation of the histone-like proteins Hc1 and Hc2, allowing active gene transcription (Barry et al., 1993; Brickman et al., 1993; Christiansen, 1993). Changes in the gene expression profile and in bacterial morphology are detected as early as 2 hpi. Twenty-nine immediate early genes have thus been identified, which are mainly involved in nutrient acquisition and inclusion membrane modification. One of the early protein synthesized is Cap1 (CT529), a protein that associates with the inclusion membrane (Belland et al., 2003; Shaw et al., 2000). The first doubling of bacterial genome is completed at 6 hpi (Shaw et al., 2000).

ii. Translocation to the microtubule organizing center (MTOC)

The inclusion is progressively modified by secreted proteins that are incorporated into the inclusion membrane via a type 3 secretion process, called Inc proteins (Bannantine et al., 2000). This process, which will be described in more details in Chapter 3.2, allows interactions with the host in order to establish the replicative niche. The inclusion is transported along microtubules through interactions of the inclusion with dynein toward the microtubule organizing center (MTOC) at the peri-Golgi region. That transport is p50 dynamitin independent suggesting that *C. trachomatis* has effectors playing its role, linking cargo to microtubule (Grieshaber, 2003) (Figure 7).

During *C. trachomatis* infection, Src family kinases (SFKs) activation increases and active SFKs are recruited at the inclusion membrane. Those SFKs were proven to be essential for inclusions migration to the MTOC (Mital and Hackstadt, 2011; Mital et al., 2010). Moreover, several Inc proteins, namely IncB or CT232, CT101, and CT222, are located in cholesterol rich microdomain at the contact point of centrosomes and inclusion. They also colocalize with active SFKs indicating that they may be involved in inclusions transport (Mital et al., 2010). One identified contributor to this transport is CT850, which also colocalizes with active SFKs, binds directly to dynein light chain 1 (DYNLT1) to facilitate traffic to the MTOC (Mital et al., 2015) (**Figure** 7).

iii. RBs proliferation

RBs proliferate within the inclusion, with a doubling time of about 2-3 hours (Shaw et al., 2000). Bacterial division was long thought to occur through binary fission, a model that seems to be supported by three-dimensional reconstitution of inclusions viewed by electron

microscopy (Lee et al., 2018). However, some immunofluorescence data support a polarized cell division mechanism resembling budding (Abdelrahman et al., 2016), so the question remains opened, especially in light of the very peculiar features of *Chlamydiae* division machinery, and in particular the absence of a FtsZ orthologue, a protein involved in bacterial division mechanism (AbdelRahman and Belland, 2005; Stephens, 1998). In addition, *Chlamydia* cell wall has been a mystery for years, and was even coined the "chlamydial anomaly", based on the fact that numerous studies had failed to detect peptidoglycan in *Chlamydia* (Barbour et al., 1982; Fox et al., 1990) even though genomic studies showed the presence of a complete set of genes required for its synthesis (Stephens, 1998). To top that, chlamydial growth is sensitive peptidoglycans targeting antibiotics such as penicillin (Barbour et al., 1982). The peptidoglycan paradox has finally been resolved by their detection using different techniques *in vitro* (Liechti et al., 2014) or using cell lysates (Packiam et al., 2015). They were later shown to localize at the division septum of bacteria (Liechti et al., 2016). Their low abundance could be a strategy to prevent host immune activation through stimulation of pathogen recognition receptors (PRRs) such as NOD2 that is known to be activated by chlamydial peptidoglycan (Liechti et al., 2016; Packiam et al., 2015).

iv. The growing inclusion needs to be stabilized

As mentioned previously, RBs proliferation is accompanied by a considerable expansion of the inclusion; thus, inclusions need to be stabilized to preserve their integrity. This stabilization is achieved by multiple actors of the host cell. Already at 12 hpi, a network of post-translationally modified microtubule surrounds the inclusion, which remains until the end of the cycle (**Figure 7,** Figure 8) (Al-Zeer et al., 2014). The formation of this network depends on the interaction between the centrosomal protein 170 kDa (CEP170) and the Inc protein IPAM (inclusion protein acting on microtubules) (Dumoux et al., 2015). The effector CT813/ InaC has been proven to mediate the microtubules post-translational modifications in addition to the repositioning of Golgi mini stacks around the inclusion (Kokes et al., 2015; Wesolowski and Paumet, 2017).

Other stabilizing actors are F-actin and intermediate filaments, which form a dynamic scaffold around the inclusion to stabilize it (Bastidas et al., 2013; Kumar and Valdivia, 2008a). F-actin recruitment and assembly involve RhoA GTPase (Kumar and Valdivia, 2008b, 2008a), septins (Volceanov et al., 2014), epidermal growth factor receptor (EGFR) signaling (Patel et al., 2014) and the effector CT813.

Scaffold stability also involves intermediate filaments. Indeed glycosylation of vimentin, a cytoplasmic intermediate filament, which is important for intermediate filaments morphology, was shown to be required for *C. trachomatis* stability and development (Tarbet et al., 2018). Disruption of this cytoskeletal scaffold around the inclusion leads to leakage of its contents into the cytosol, followed with a strong host immune response. Therefore, re-organizing host cytoskeleton around the inclusion can be seen as an immune modulation mechanism (Kumar and Valdivia, 2008b, 2008a).

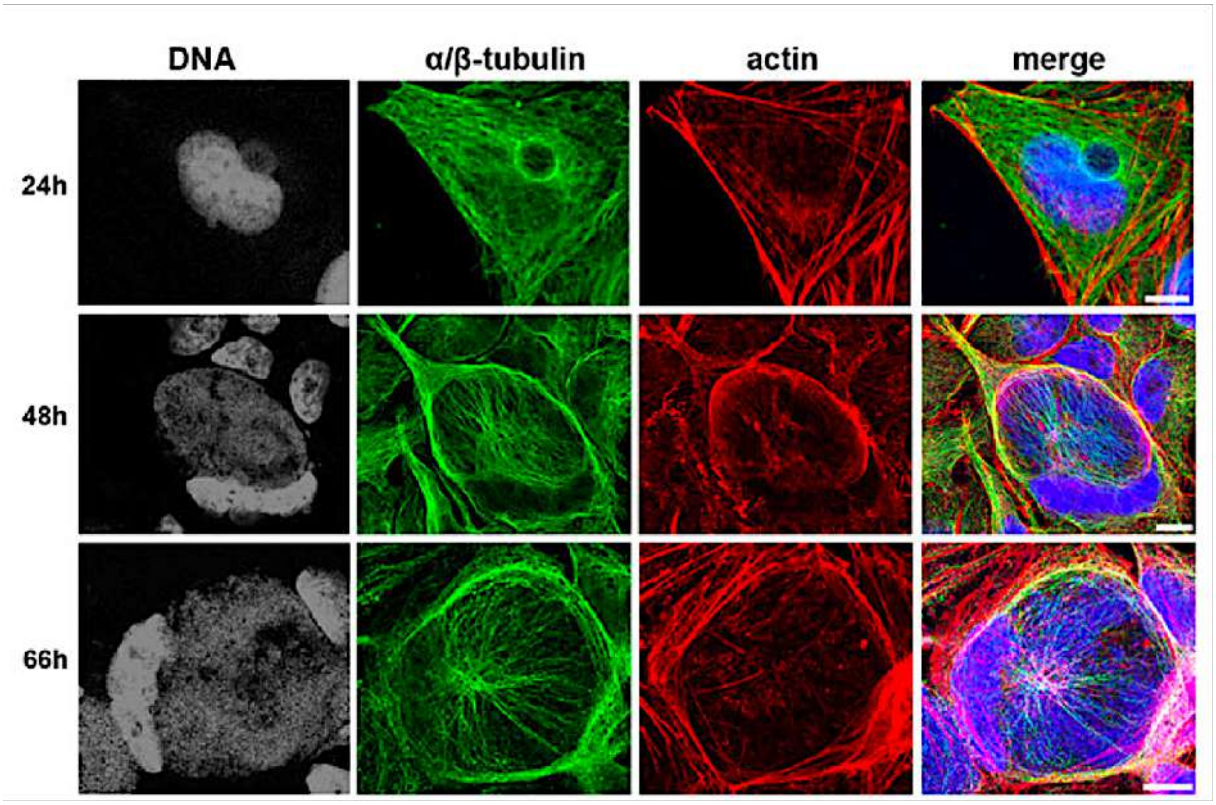

Figure 8. Organization of actin and tubulin around *C. trachomatis* inclusions
HeLa cells were infected with *C. trachomatis* and fixed at three time point (24, 48 and 66 h). Cells were stained for confocal microscopy which revealed tubulin (green) and actin (red) filaments surrounding the inclusion. DNA is represented in grey and inclusions are marked by stars. Maximum projections obtained from z-stacks are represented. Scale bars: 10 µm. (Dumoux et al., 2015)

c. Back to where we started

i. The RB to EB conversion

RBs differentiate back into EBs in an asynchronous manner, with the first EB appearing 24 hpi (Belland et al., 2003; Shaw et al., 2000). The trigger for RB to EB conversion remains to be elucidated, with several hypotheses being considered. The contact-dependent hypothesis speculates that the RBs conversion into EBs could be initiated through detachment of RBs from the inclusion membrane resulting in the disruption of the RBs T3S system activity (Wilson et

al., 2006). Wilson et al. (2009) tested that hypothesis by recording live-cell imaging of *C. trachomatis* infected cells and tracking individual chlamydial particles. They observed that RBs that were almost immobile were tethered to the membrane and coincidently detach from it preceding conversion into EBs (Wilson et al., 2009). A recent hypothesis proposes that the bacterial size itself, below a certain threshold, triggers the conversion. This hypothesis is based on the observation that the average diameter of RBs tends to diminish with time, and is supported by mathematical models (Lee et al., 2018). Finally, confrontation of mathematical models with video recording of bacteria expressing fluorescent tracers recently suggested that RB-to-EB development followed a cell-autonomous program that does not respond to environmental cues (Chiarelli et al., 2020).

Prior to RB to EB conversion, late cycle genes are expressed. Those include the *hctA* and *hctB* genes coding for the histone-like protein Hc1 and Hc2 whose role is to condense DNA (Barry et al., 1993; Brickman et al., 1993; Belland et al., 2003). Another step involved in this conversion is the expression of genes encoding proteins such as OmcA and OmcB necessary for re-assembly of the COMC. In addition, the COMC goes back to its highly disulfide cross-linked state, probably through isomerases that are expressed in the late cycle (AbdelRahman and Belland, 2005; Belland et al., 2003). The disulfide bonds in the T3S apparatus go through the same fate as in the COMC (Betts-Hampikian and Fields, 2011).

Various stress factors including antibiotics treatments or nutritional deficiency can trigger chlamydial persistence by mechanisms not fully understood yet. This state is characterized by the presence of enlarge, but still viable, aberrant bodies, with a quiescent metabolism (Reviewed in Mpiga and Ravaoarinoro, 2006).

ii. Cellular exit

Chlamydial egress from host cells happens through two mutually exclusive pathways, lysis and extrusion (Figure 6).

Lysis is a fast step-wise process, starting with inclusion membrane, followed by plasma membrane, permeabilization. Within 15 min, for *C. trachomatis* serovar L2, the cell lyses with the plasma membrane rupturing, a process relying on cysteine proteases.

During extrusion, inclusions exit cells which remain intact as well as inclusions themselves. Extrusion is a slower process than lysis, that can take up to 3 h. It starts with pinching of the inclusion, followed by a protrusion out of the cell then finally detachment from the cell (Hybiske and Stephens, 2007). Extrusion is a calcium dependent process. Indeed,

Nguyen et al. (2018), discovered an interaction between the Inc protein MrcA and a Ca^{2+} channel and proved, through knockdown and mutagenesis experiments, that Ca^{2+} signaling pathways are required for *C. trachomatis* release (Nguyen et al., 2018). This process requires actin polymerization, neuronal Wiskott-Aldrich syndrome protein (WASP), myosin II and the RhoA GTPase (Hybiske and Stephens, 2007). Extrusion also involves the myosin phosphatase pathway with the active myosin phosphatase targeting subunit 1 (MYPT1) interacting with an Inc protein which has been shown to be involved in cell exit, CT228. Moreover, silencing myosin light chain II (MLC2), myosin light chain kinase (MLCK), and myosin IIA and IIB reduced extrusion formation of *C. trachomatis* suggesting their importance in this exit mechanism (Lutter et al., 2013). Released inclusions being intact, extrusion enhances survival of EBs extracellularly and would prevent immune response from host cells. Moreover, extruded bacteria can be engulfed by macrophages and dendritic cells, and might lead to the release of still infectious particles if they survive in these cells (Sherrid and Hybiske, 2017; Zuck et al., 2017).

III. *Chlamydia trachomatis* interactions with its host cell

1. The central role of type 3 secretion

Over the course of infection, chlamydiae translocate a number of "effector" proteins across the inclusion membrane, to facilitate invasion and establish a suitable replication niche, as detailed below. Three different secretion systems are encoded in *Chlamydiaceae* genomes: type 2, 3 and 5 secretion system (T2S system, T3S system, and T5S system, respectively) (Fields, 2012; Henderson and Lam, 2001; Stephens, 1998) (Figure 9). The main mechanism for effectors' transport into the host cytoplasm is the T3S system. The T3S apparatus resembles a molecular syringe referred to as injectisome. It is composed of over 20 proteins coded by at least 4 gene clusters, spread across chlamydial genome (Galán et al., 2014). Phylogenetic studies reveal that the T3S system has evolved from a flagellum that lost its motion ability and gained a protein transport one (Abby and Rocha, 2012; Galán et al., 2014).

The T3S apparatus is activated upon contact of the tip of injectisome' needle and the host cell membrane (Nans et al., 2014). Effectors are then directly delivered in their target's cytoplasm with the help of chaperone proteins. Indeed, secretion through the injectisome requires effectors to be unfolded which is facilitated by chaperon proteins (Dai and Li, 2014; Pais et al., 2013; Parsot, 2003; Spaeth et al., 2009). T3S dependent effectors possess a secretion

signal in their first 20-25 amino acids, which is not fully characterized and is highly variable, (Galán et al., 2014). Machine learning techniques have been developed in order to predict which effector protein uses the T3S system (An et al., 2016). They are only partly successful at identifying T3S effectors in *Chlamydiaceae*.

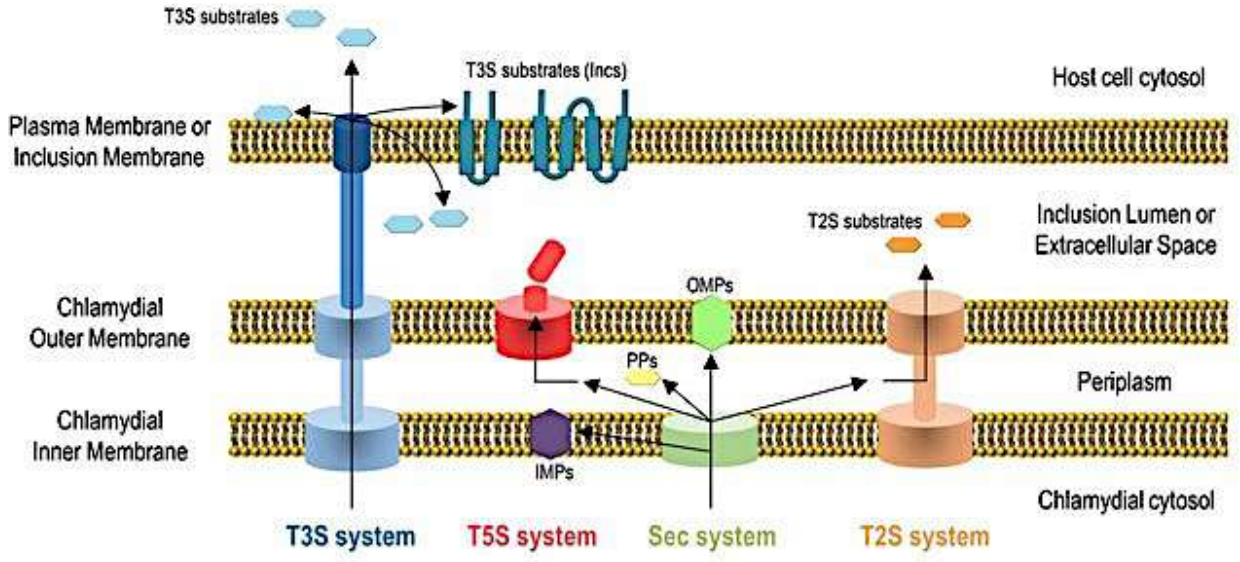

Figure 9. Diversity of *C. trachomatis* secretion systems
C. trachomatis as other members of the *Chlamydiaceae* family uses multiple systems in order to secrete effectors into the host. Secretion can be done in a one step process (through the T3S system), or in a two steps process (through the T2S system, T5S system, and the sec system). Abbreviations: OMPs: Outer membrane proteins; PPs: periplasmic proteins; IMPs: Inner membrane protein (Bugalhão and Mota, 2019)

Some effectors, such as CPAF (chlamydial protease-like activity factor), are secreted through other pathways. Indeed, CPAF is translocated into the chlamydial periplasm through a general secretory pathway, the Sec-dependent pathway. Its secretion into the host cytoplasm from the periplasm is unclear. It has been hypothesized that it process could happen through either the T2S pathway or through budding vesicles from the outer membrane that would fuse with the inclusion membrane prior to release in the cytoplasm (Chen et al., 2010).

2. T3S effectors target numerous cellular activities

C. trachomatis genome codes for probably close to 80-100 effectors that are either released into the host cytoplasm, in the inclusion lumen, or inserted in the inclusion membrane. The latter are called Inc proteins and represent probably the largest class of effectors. Indeed, over 50 effectors have been predicted to be Incs, based on the bilobed hydrophobic domain

which anchors Incs in the inclusion membrane, as they are exposed toward the cytosol (Bannantine et al., 2000; Dehoux et al., 2011; Li et al., 2008; Lutter et al., 2012).

Due to the fact that *Chlamydia* was intractable to genetic manipulations, identification of chlamydial T3S dependent effectors has been based for years on heterologous secretion assays using genetically tractable bacteria possessing a functional T3S system such as *Yersinia pseudotuberculosis* or *Shigella flexneri* (da Cunha et al., 2014; Subtil et al., 2005). The development of a transformation method for *C. trachomatis*, has since opened the door to more direct characterization of these effector proteins (Wang et al., 2011).

So far, multiple roles have been identified for chlamydial effectors, from protecting bacteria from the host to promoting a successful infection. As mentioned in the previous section, cytoskeleton reorganization is induced by infection upon bacterial entry (Balana, 2005; Carabeo et al., 2002; Clifton et al., 2005; Thalmann et al., 2010) and during the pathogen development (Dumoux et al., 2015). Effectors are also involved in apoptosis inhibition (Rajalingam et al., 2008a; Sarkar, 2015; Sixt et al., 2017; Weber et al., 2017), modulation of the immune response (Carpenter et al., 2017; Chen et al., 2014; Patton et al., 2016; Rajeeve, 2018), and also in interfering with various cellular trafficking routes, discussed more in detailed below (Paul et al., 2017; Stanhope et al., 2017; Wesolowski et al., 2017).

3. *Chlamydia* hijack resource from their hosts

a. The inclusion membrane is an interaction platform

The inclusion membrane represents a barrier protecting on one hand the pathogen during its development from the host, but on the other hand, it limits access to host nutrients. In fact, while the inclusion membrane is likely permeable to some ions (Grieshaber et al., 2002) and molecules larger than 520 Da cannot pass through (Heinzen and Hackstadt, 1997). Thus, obtaining various nutrients from the host requires transport channels, or fusion with various host compartments containing the nutrients needed (Figure 10) (Triboulet and Subtil, 2019). Several host proteins known to regulate intracellular traffic such as Rab GTPases and SNAREs proteins are present at the inclusion membrane, in such a way that this vacuole, which has co-evolved with the eukaryotic cell, can be considered just like another intracellular compartment, following the "rules" of intracellular traffic (Aeberhard et al., 2015; Herweg et al., 2015; Saka et al., 2011). Most interactions between the inclusion membrane and intracellular compartments are mediated by Incs, although it is likely not their exclusive role, as they also contribute to the maintenance of the integrity of the inclusion membrane (Moore and Ouellette, 2014).

b. *Chlamydia* hijack the vesicular traffic

i. *Chlamydia* control their interactions with host organelles

Chlamydia obtain nutrients required for their proper development by hijacking multiple organelles. Rab GTPases are key regulators in membrane trafficking. Multiple endosomal and Golgi associated Rabs have been associated with inclusions. Some are species specific, with Rab 6, for instance, which is only recruited by *C. trachomatis* or Rab 10 only by *C. pneumoniae* and *C. muridarum*, while Rab1, 4, and 11 are recruited by all three (Damiani et al., 2014; Rzomp et al., 2003) (Figure 10). Recruitment of Golgi associated Rabs such as Rab6, 11 an 14 allow the rerouting of exocytic vesicles rich in lipids (Rzomp et al., 2003). Another pathway hijacked by *Chlamydia* is the slow transferring recycling pathway, mediated by Rabs 4 and 11. Disrupting this pathway, which could be a source of iron for the pathogen impaired bacterial growth (Ouellette and Carabeo, 2010) and is mediated by the Inc protein CT229 (Faris et al., 2019). CT229 also regulates trafficking of mannose-6-phosphate receptor, a marker of late endosomes which have also been associated with the inclusion (Faris et al., 2019).

Rabs also allow vesicles fusion by recruiting lipid kinases. The latter enriches the inclusion membrane with Golgi-specific lipid phosphatidylinositol-4-phosphate (PI4P) probably disguising it as a Golgi compartment (Damiani et al., 2014; Moorhead et al., 2010) (Figure 10).

Vesicles fusion with the inclusion membrane is mediated by specific SNAREs which allow rerouting of the Golgi exocytic pathway for instance (Gitsels et al., 2019). Some effectors such as IncA, InaC and IPAM possess SNARE-like motifs. While SNARE-like molecules at the inclusion surface may facilitate fusion with some compartments, it might in some instances have an inhibitory role, for instance by limiting the fusion with lysosomes, (Delevoye et al., 2008; Kokes and Valdivia, 2012; Ronzone and Paumet, 2013). Nonetheless, even though *Chlamydia* inhibit lysosomal fusion, lysosomes remain in close proximity to inclusions. This allows the pathogen to hijack lysosomal derived amino acids and or oligopeptides (Ouellette et al., 2011). The same was also observed for autophagic vesicles, that remain close to the inclusion, without proceeding into a xenophagic stage. *Chlamydia* might intercept these vesicles to get more nutrients (Al-Younes et al., 2004).

Another target of *Chlamydia* is the Golgi apparatus. Infection induced Golgi fragmentation into mini stacks surrounding the inclusion (Heuer et al., 2009). This phenomenon involves multiple host proteins and at least the effector CT813/InaC which bind Arf GTPases and the 14-3-3 proteins to remodel F-actin and microtubule, and to recruit Golgi mini stacks to

the inclusion (Al-Zeer et al., 2014; Kokes et al., 2015). Those mini stacks could be a source of lipids, such as sphingomyelin and cholesterol, for bacteria. However, Golgi fragmentation (Gurumurthy et al., 2014) along with the presence of InaC (Kokes et al., 2015) were shown to be dispensable for lipids delivery in inclusions. Thus, this indicates that *Chlamydia* acquire lipids through multiple routes and that Golgi fragmentation may play another role during infection.

Mitochondria have also been reported to be associated with inclusions of *C. caviae* and *C. psittaci* (Vanrompay et al., 1996). Chlamydial dependence or exact interaction with mitochondria remain to be elucidated, especially since mitochondrial interactions seems to be species specific. Nonetheless, C*hlamydia* could use mitochondria for energy metabolites, or associate with them in order to prevent them to release cytochrome C, which is an apoptotic signal (Gitsels et al., 2019; Kokes and Valdivia, 2012).

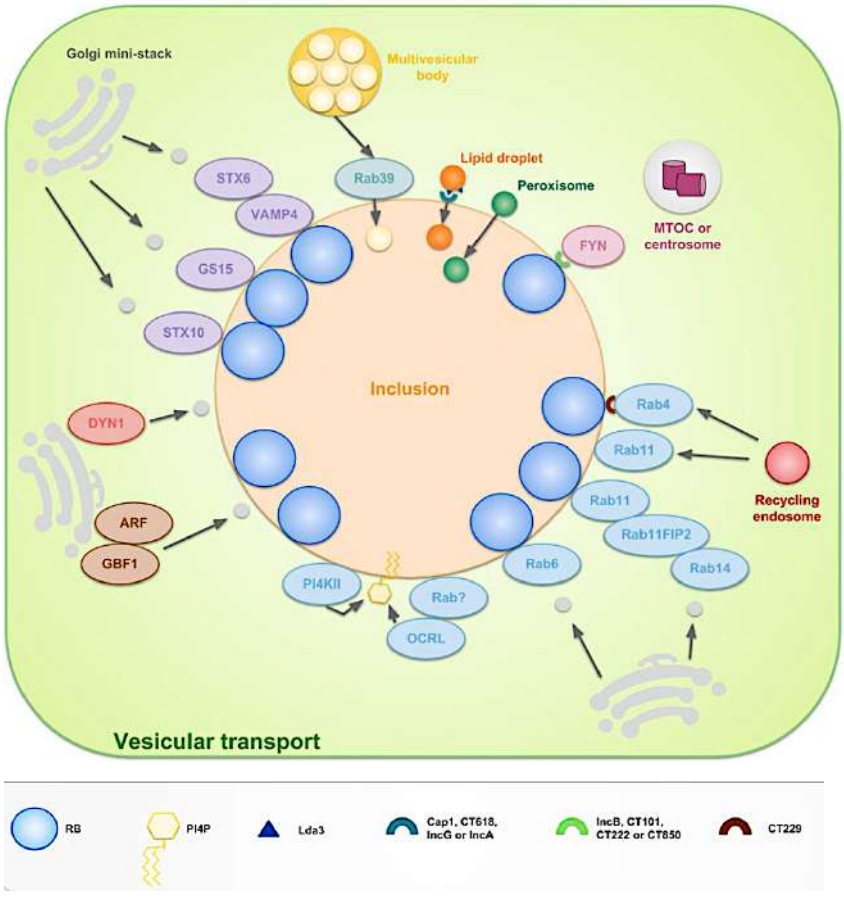

Figure 10. Schematic representation of *C. trachomatis* vesicular transport pathway
Throughout infection, *C. trachomatis* interacts selectively with host organelles. Those interactions are mediated by inclusions membrane proteins, recruitment of cellular trafficking regulators or direct uptake of host organelles. Endosomal (1, 4, 6, 11) and Golgi-associated Rab proteins (6, 11 and 14) allow interaction with those compartments. *C. trachomatis* also hijacks phosphatidylinositol-4-phosphate (PI4P) from fragmented Golgi surrounding the inclusion. It also interacts with Trans-Golgi SNARE proteins syntaxin 6 and 10 (STX10, STX6), vesicle associated membrane protein 4 (VAMP4), and GS15 which regulate the Golgi exocytic pathway. The inclusion membrane protein IncA, InaC and IPAM prevent lysosomal fusion

through their SNARE-like motifs. Some organelles are translocated directly into the inclusions, namely multivesicular bodies (MVBs), lipid droplets and peroxisomes which provide lipids to the bacteria. Acquisition of sphingomyelin from the host is regulated by the host FYN kinase and depends on the Arf1 GTPase/ Golgi-specific Brefeldin A resistance factor 1 (GBF1) pathway. Dynamin (DYN1) which allows formation of vesicles from the trans-Golgi network is required for *C. trachomatis* growth. Adapted from (Gitsels et al., 2019)

ii. Some organelles are translocated into the inclusion

Some of *Chlamydia* targets are lipid droplets (LDs) which are storage organelles from the ER for neutral lipids or long fatty chain acids. They are indeed observed in the lumen of inclusions where they could be used to generate energy or as a fatty acid source for the inclusion membrane (Figure 10) (Cocchiaro et al., 2008; Kokes and Valdivia, 2012; Martin and Parton, 2006). During infection, LDs proteome becomes enriched in proteins involved in lipid metabolism and biosynthesis (Saka et al., 2015). Some of those LD associated proteins are found inside inclusions and can even influence *Chlamydia* by modulating their effector activity. This is the case for CT775 whose acyltransferase activity is regulated by the ACBD6 protein (acyl-coA-binding domain containing protein 6) thus affecting phosphatidylcholine formation in *C. trachomatis* (Soupene et al., 2012, 2015). LDs are associated with the chlamydial proteins Lda1, 2, and 3. A mechanistic model has only been proposed for the role of Lda3 in lipid droplets translocation into the inclusion. Secreted Lda3 would bind LDs close to the inclusion, after what it will be tethered to the membrane by an hypothetical Inc protein, before being engulfed in the inclusion (Cocchiaro et al., 2008). Other chlamydial proteins are associated with LDs namely IncA, IncG, Cap1 and CTL0882 which may each have a specific role in LDs translocations (Cocchiaro et al., 2008; Saka et al., 2015).

Other chlamydial targets are peroxisomes and multivesicular bodies (MVBs) (Figure 10). Indeed both have been observed in the inclusions (Beatty, 2006; Boncompain et al., 2014). The mechanism of peroxisomes' import into the inclusion lumen is still unclear. In addition, they were shown to be dispensable to bacterial development as bacteria can develop and produce infectious progenies in cells deprived of peroxisomes biogenesis (Boncompain et al., 2014). As for MVBs, they are a source of lipids such as sphingomyelin, cholesterol and phospholipids for *Chlamydia* (Beatty, 2006). Effectors allowing MVBs translocation have not been identified, however, the host GTPase Rab39 contributes to its delivery in inclusions (Gambarte Tudela et al., 2015).

Chlamydia also hijack multiple vesicular pathways in order to acquire lipids (Figure 10). Some of them involve dynamin (Gurumurthy et al., 2014), the FYN kinase (Elwell and

Engel, 2012; Mital and Hackstadt, 2011), or the Arf GTPase and the Arf exchange factor GBF1 (Elwell et al., 2011; Moorhead et al., 2010; Reiling et al., 2013), just to name a few.

c. *Chlamydia* also acquires lipids through non-vesicular pathways

The fusion of host compartments with the inclusion membrane contributes to inclusion expansion. Another strategy used by *Chlamydia* to acquire lipids is by taking over non-vesicular pathways (Figure 11). The lipid transporter "CERamide transport protein" (CERT) is enriched at ER-inclusion membrane contact sites (MCSs), where it directly binds the effector IncD in order to redirect non-vesicular transport of ceramide to the inclusion. (Agaisse and Derré, 2014; Derré et al., 2011; Elwell et al., 2011). Once at the inclusion, ceramide is converted into sphingomyelin probably by the sphingomyelin synthase 2 (SMS2), also recruited at the MCSs (Derré et al. 2011; Elwell et al., 2011). The MCSs are also enriched with the ER-resident "vesicle-associated membrane protein-associated protein" (VAP) B, whose recruitment is mediated by the CERT/IncD interaction, others VAPs which interacts with IncV (Stanhope et al., 2017), and the ER calcium sensor Stromal interaction molecule 1 (STIM1) whose role is still unclear as its depletion does not affect *C. trachomatis* growth (Agaisse and Derre, 2015), in contrast to CERT and VAPB (Derré et al., 2011; Elwell et al., 2011).

In addition, even though the mechanism is still unclear, *Chlamydia* was shown to depend on members of the HDL (high density lipoprotein) biogenesis machinery, which controls cholesterol and phospholipids efflux (Cox et al., 2012; Samanta et al., 2017). *C. trachomatis* hijacks a host lipid transport system normally involved in the biogenesis of high-density lipoprotein (HDL) by mediating efflux of cholesterol and phospholipid. The lipid binding proteins ATP-binding cassette transporters A1 (ABCA1), CD36 and LIMPII Analogous-1 (CLA1) and Apolipoprotein A1 (ApoA) localize at the inclusion membrane. Moreover, inhibition of ABCA1 and CLA1 activity prevented phospholipid recruitment to the inclusion and prevented *C. trachomtis* growth (Cox et al., 2012). Host glycerophospholipids are also stolen by *Chlamydia* through the activation of the cytosolic phospholipase A2 (ERK-cPLA2) signaling pathway (Elwell and Engel, 2012; Su et al., 2004).

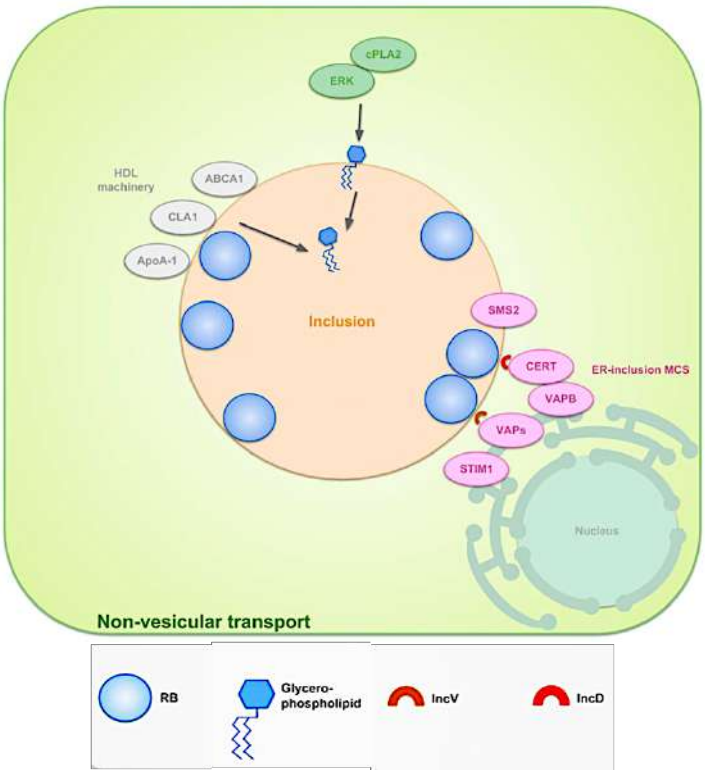

Figure 11. Schematic representation of *C. trachomatis* non-vesicular transport pathway
C. trachomatis also uses a non-vesicular pathway to acquire lipids. Glycerophospholipids are hijacked through activation of the cytosolic phospholipase A2 (ERK-cPLA2) signaling pathway. ER derived sphingomyelin is obtained at ER-inclusion membrane contact sites (MCS). The latter are enriched in "ceramide endoplasmic reticulum transport" (CERT) protein, ER-resident vesicle-associated membrane protein-associated protein (VAP) B, sphingomyelin synthase 2 (SMS2) and Stromal interaction molecule 1 (STIM1) which ER calcium sensor. CERT and other VAPs interacts at the inclusion membrane with IncD and IncV, respectively. HDL machinery is also recruited at the inclusion membrane to facilitate obtention of phospholipids. This includes ATP-binding cassette transporters A1 (ABCA1), CD36 and LIMPII Analogous-1 (CLA1) and Apolipoprotein A1 (ApoA)). Adapted from (Gitsels et al., 2019)

4. Nutriments transport across the inclusion membrane

Promoting fusion of selected organelles with the inclusion membrane allows the bacteria to feed the inclusion with nutriments contained within these fusing vesicles. It also provides a mean to supply the inclusion membrane with host-derived membrane transporters, that can now function to feed the bacteria. This seems to be the mechanism by which *Chlamydia* acquire biotin, a vitamin and a cofactor for carboxylase enzymes. Its uptake involves the host protein sodium multivitamin transporter (SMVT) which is recruited at the inclusion membrane allowing entry into the inclusion. Then, RBs import it into the bacterial cytoplasm through their biotin transporter, BioY (Fisher et al., 2012). Another illustration is glucose import into the inclusion which is mediated by the UDP-glucose transporter, SLC35D2, (Gehre et al., 2016) which is also an N-acetylglucosamine transporter.

Intriguingly, proteomic studies identified only one transporter at the inclusion membrane, SLC7A5 (a transporter for neutral amino acids) (Aeberhard et al., 2015). This is probably due to the fact that these membrane-imbedded proteins often escape identification by mass spectrometry. It is likely that many host-derived transporters remained to be identified at the inclusion membrane. Inc proteins might also contribute to nutrient transport across this lipidic barrier.

IV. Metabolism seen from two angles

1. Glucose metabolism in mammalian cells

    a. Glucose as a source of energy

Glucose is one of the main carbon sources used by mammalian cells to generate energy. (Figure 12). Upon entry into glycolysis, this six-carbon molecule is broken down into three-carbon molecules. Under normal oxygen levels the end product, pyruvate, is then tunneled into the Kreb's cycle, also designated as the tricarboxylic acid (TCA) cycle (Figure 13). Throughout those pathways, but mostly in the TCA cycle, the redox cofactors nicotinamide adenine dinucleotide (NAD+) and flavin adenine dinucleotide (FADH+) are reduced into NADH,H+ and FADH2, respectively (Figure 12, Figure 13).

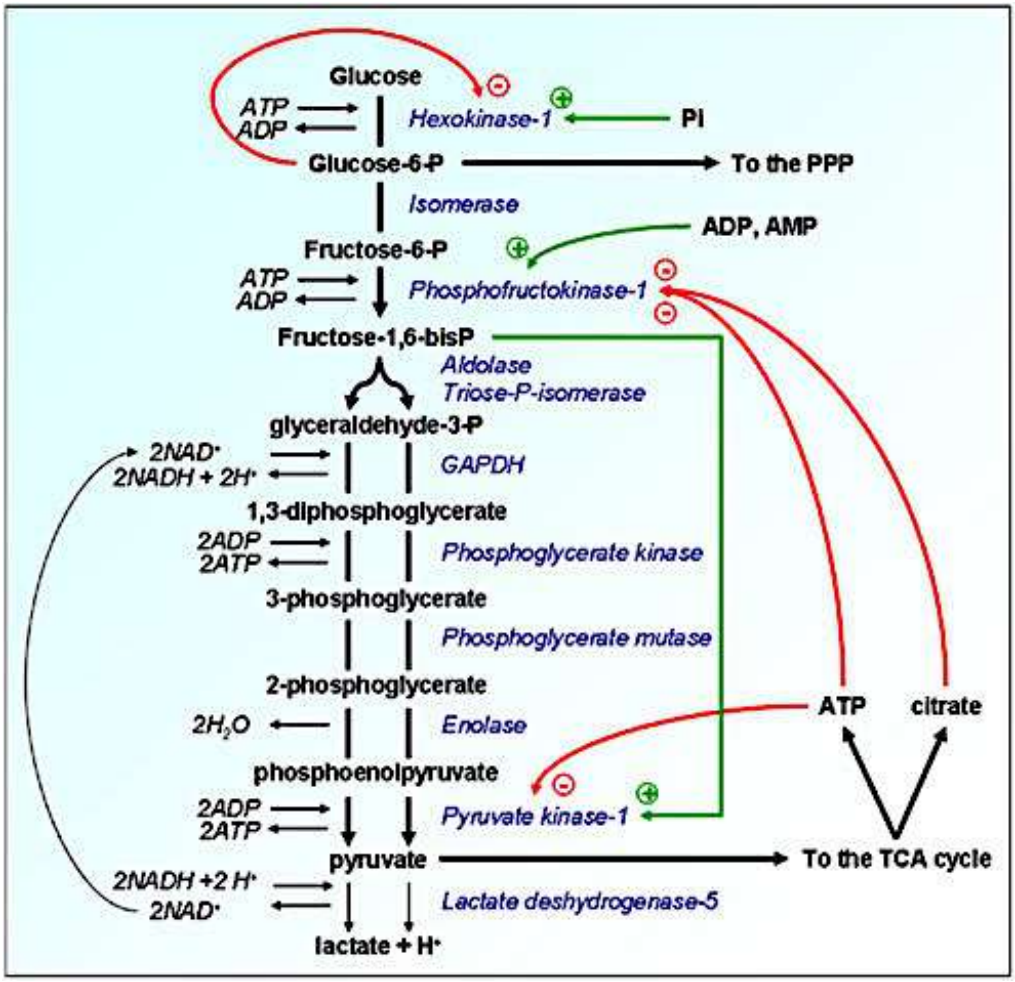

Figure 12. Glycolysis pathway and its regulation
In glycolysis, glucose is broken down after multiple steps into pyruvate. Under normal oxygen levels, the latter mostly enters the TCA cycle, otherwise, it is converted into lactate. Glycolysis flux is influenced by three key enzymes namely hexokinase, phosphofructokinase-1 and pyruvate kinase (Porporato et al., 2011)

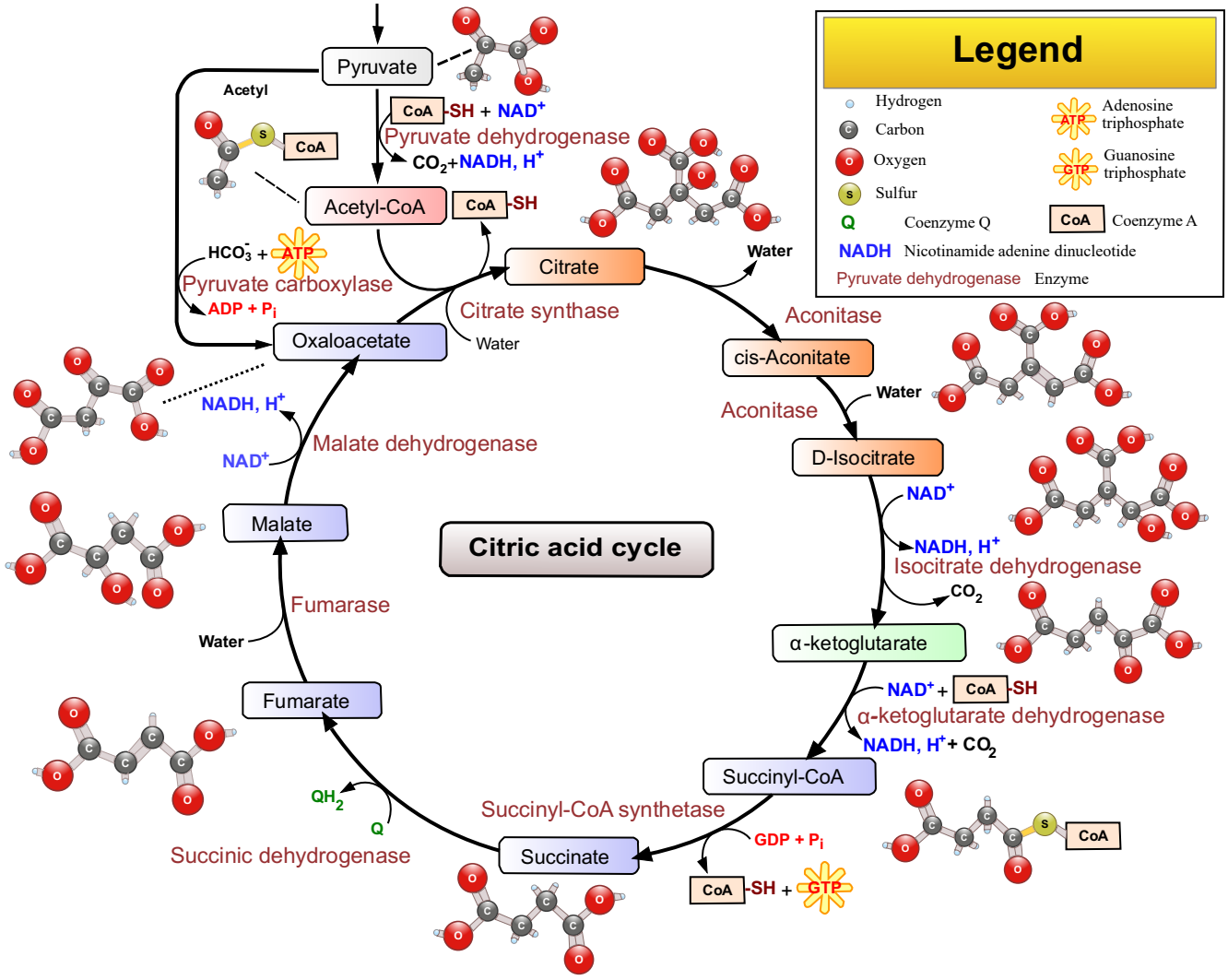

Figure 13. The citric acid or TCA cycle
The TCA cycle is initiated by the conversion of pyruvate into acetyl-CoA which is first converted itself into citrate followed by a succession of conversions leading back to citrate. In this pathway mostly, the redox cofactors NAD+ and FADH+ are converted into NADH,H+ or FADH2, providing them reducing power. Wikipedia.

The reduction power of the cofactors is used during oxidative phosphorylation (OxPhos) which occurs in the inner membrane of the mitochondria (Figure 14). Indeed, during this last step, an electron is transferred from either a molecule of NADH,H+ or FADH2 to a series of electron acceptor molecules, the last of which being a dioxygen molecule. This generates a water molecule on one hand and creates a proton gradient in the inner mitochondrial membrane, on the other hand. Proton then move down their concentration gradient into the mitochondrial matrix through ATP synthase, referred to as complex V. This results in the activation of the latter, which couples phosphate to adenosine diphosphate (ADP) producing cell's energy currency adenosine triphosphate (ATP) (Figure 14). The complete oxidation of one glucose molecule produces around 36 molecules of ATP (2 ATP from glycolysis, 2 ATP

equivalent, GTP, from the TCA cycle; 32 ATP from OxPhos), with OxPhos being the major contributor to ATP production.

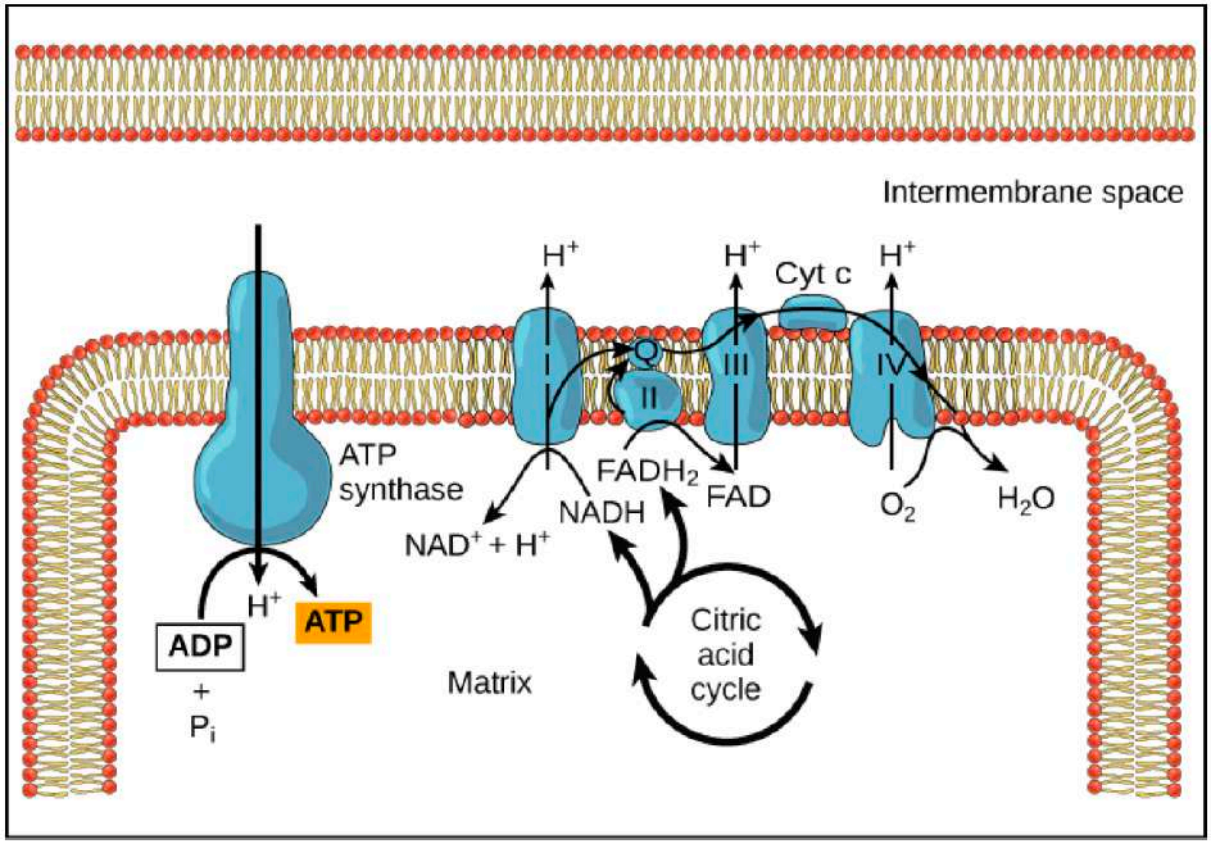

Figure 14. Oxidative phosphorylation (OxPhos) overview
OxPhos occurs in the inner mitochondrial membrane. NADH,H+ or FADH2 are re-oxidized by the complex I (I) and complex II (II), respectively. The resulting electrons produced through the oxidation reactions are transferred to other complexes (III and IV) and intermediate molecules (ubiquinone (Q), ant cytochrome c (cyt c)), then to the final electron acceptor oxygen (O_2). An efflux of protons from mitochondrial matrix into the intermembrane space is generated during this process which is stabilized by ATP synthase (complex V). The latter pumps protons back into the matrix coupling it with ATP molecules generation.
(https://courses.lumenlearning.com/wm-biology1/chapter/reading-electron-transport-chain/)

b. Glucose metabolism intertwines with other metabolic pathways

Glucose hydrolysis generates diverse intermediates than can feed other metabolic pathways. One of those pathways involves G6P which results from glucose phosphorylation. G6P is converted into glucose-1-phosphate (G1P) by a phosphoglucomutase (PGM), then into UDP-glucose. The latter is in turn used to produce a glucose storage molecule, glycogen, through the glycogen synthesis pathway. G6P can also be redirected into the PPP (pentose phosphate pathway) which is divided into the oxidative and the non-oxidative phase (Figure 15). The oxidative phase generates the reducing cofactor Nicotinamide Adenine Dinucleotide Phosphate (NADPH). NADPH is involved in both promoting and reducing oxidative stress,

through the formation of free radicals and the antioxidant glutathione (GSH), respectively (Fisher and Zhang, 2006). The non-oxidative phase leads to the synthesis of pentose sugars including ribose-5-phosphate (R5P) which is a starting point for nucleotides synthesis. This phase is characterized by series of non-oxidative reactions resulting in the interconversion of carbon sugars containing either 3, 5, 6 or 7 carbons (Figure 15). PPP is also interconnected to glycolysis through the reversible conversion of R5P into glyceraldehyde-3-phosphate (G3P) and fructose-6-phosphate (F6P), two intermediates of glycolysis (Figure 15, Figure 16).

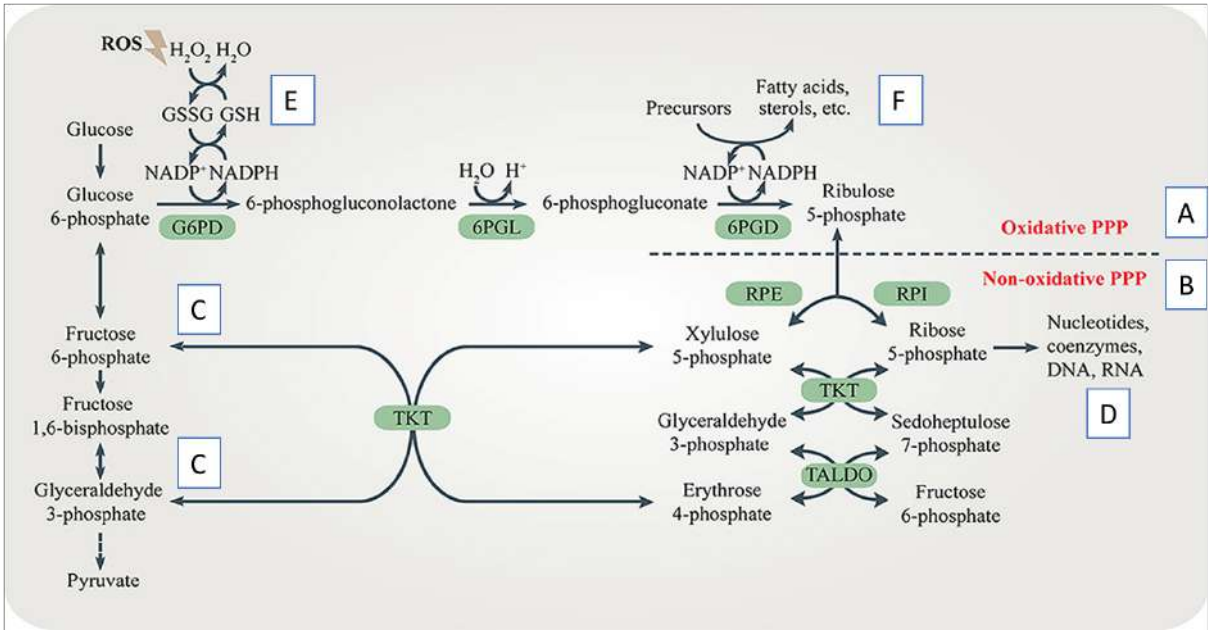

Figure 15. The Pentose Phosphate Pathway
PPP is divided in two phases: the oxidative phase where G6P is converted through multiple oxidation reactions into ribulose-5-phosphate (A), and the non-oxidative phase characterized by a series of reactions leading to various number-carbon molecules (B). Depending on cell needs, intermediates of the second phase can be re-shuffled into glycolysis (C). The two most important products of the PPP are ribose-5-phophate sugar that is used for nucleotides synthesis and NADPH which is involved in multiple cellular processes (E and F) (adapted from (Ge et al., 2020))

Some non-essential amino acids biosynthesis pathways also rely on various intermediates from glucose metabolism. Those include alanine, serine, glutamate, and aspartate, that are respectively derived from pyruvate, 3-phosphoglycerate, α-ketoglutarate (also known as oxoglutarate) and oxaloacetate (Figure 16).

Another pathway relying on glucose degradation is the lipid biosynthesis pathway which uses acetyl-coA for fatty acid elongation and/or cholesterol biogenesis, and glycerol-3-phosphate and ceramide for fatty acid and sphingolipids biogenesis (Figure 16).

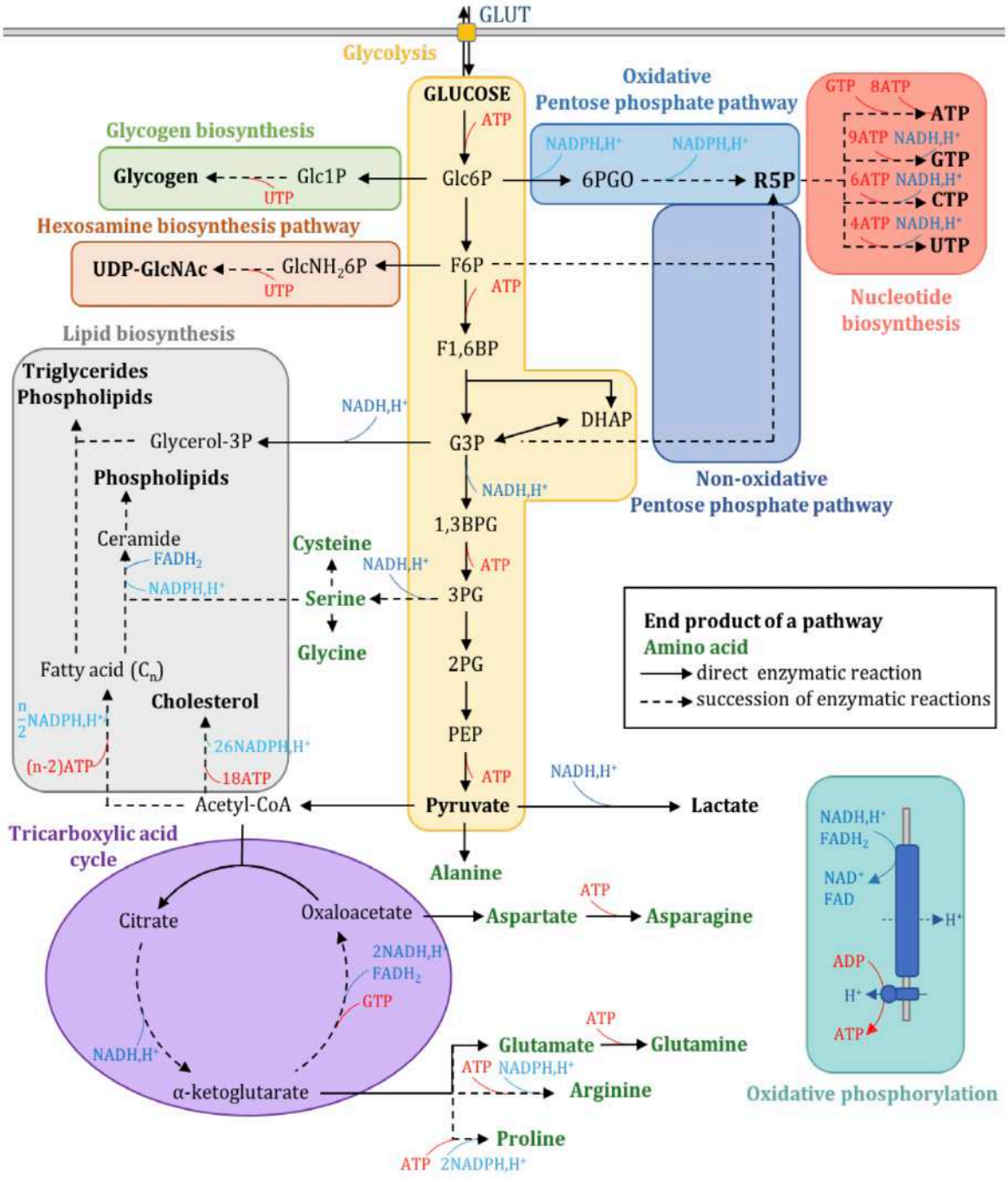

Figure 16. Metabolic network associated with Glucose metabolism
Abbreviations: Glucose-6-phosphate (Glc6P), fructose-6-phosphate (F6P), fructose-1,6-bisphosphate (F1,6BP), glyceraldehyde-3-phosphate (G3P), dihydroxyacetone-phosphate (DHAP), 1,3-bisphosphoglycerate (1,3BPG), 3-phosphoglycerate (3PG), 2-phosphoglycerate (2PG), phosphoenolpyruvate (PEP), Glucose-1-phosphate (Glc1P), 6-phosphogluconolactone (6PGO), ribose-5-phosphate (R5P), glucosamine-6-phosphate (GlcNH26P), uridine diphosphate-N-acetylglucosamine (UDP-GlcNAc). (Maffei, 2018)

One more pathway linked to glucose metabolism is the hexosamine biosynthesis pathway (HBP) which uses fructose-6-phosphate as its starting point (Figure 16). This pathway leads to the formation of UDP-N-acetylglucosamine (UDP-GlcNAc) which can further be

converted into other sugars that are in turn used in N- and O- linked glycosylation of Golgi and ER proteins. UDP-GlcNAc is also a substrate for *O*-N-acetylglycosylation, a post-translational modification that has been shown in vivo to modulate aging, cell proliferation, and histone remodeling or transcription (Denzel et al., 2014; Love and Hanover, 2005).

c. Glucose metabolism regulation

Three enzymes, namely hexokinase (HK), phosphofructokinase-1(PFK1) and pyruvate kinase (PK) tightly regulate glycolysis and its opposite pathway, gluconeogenesis that synthesizes glucose from lactate. Both pathways are regulated so that one is always more active than its counterpart. Stimulation of one pathway over the other is determined by the amount and activity of specific enzymes of the pathway. For instance, an increase of AMP or ADP, demonstrating the need for additional energy or upstream metabolites, triggers PFK1. In contrast, indicators that of the pathway saturation such as high levels of ATP or citrate accumulation would instead inhibit PFK1 as well as PK, turning off glycolysis (Figure 12) (Jm et al., 2002).

Furthermore, under hypoxic conditions either due to environmental constraints or in an oncogenic context, the transcription factor HIF-1 (hypoxia inducible factor 1) stimulates glycolysis at different levels (Figure **17**). On one hand, it increases the expression of both isoforms of glucose transporters, glucose transporter 1 and 3 (GLUT1 and GLUT3) resulting in an increase of glucose import, fueling glycolysis (Ebert et al., 1995, 1996). The HK isoform HK2 is also a target of HIF-1 which cooperates with the oncogene transcription factor c-Myc to activate it under hypoxia (Kim et al., 2007). HIF-1 and c-Myc duo also act together under hypoxia to transactivate pyruvate dehydrogenase kinase 1 (PDK1) (Figure **17**), an inhibitor of pyruvate dehydrogenase (PDH) (Kim et al., 2007). PDH is the enzyme determining entry into the TCA cycle. Its inhibition redirects pyruvate into lactate production, leading to replenishing NAD+ pools. With low levels of dioxygen in hypoxia, electrons produced from the respiratory chain are coupled to water molecules producing reactive oxygen species (ROS). Thus, an additional advantage to PDH inhibition is the reduction of ROS production through a decrease activity of the electron transport chain (Kim et al., 2006). HIF-1 also induces expression of lactate dehydrogenase A (*LDHA*) which, in contrast to its isoform *LDHB* which has a lower affinity for pyruvate, favors fermentation by converting pyruvate into lactate, instead of going through OxPhos (Figure **17**) (Doherty and Cleveland, 2013; Porporato et al., 2011)

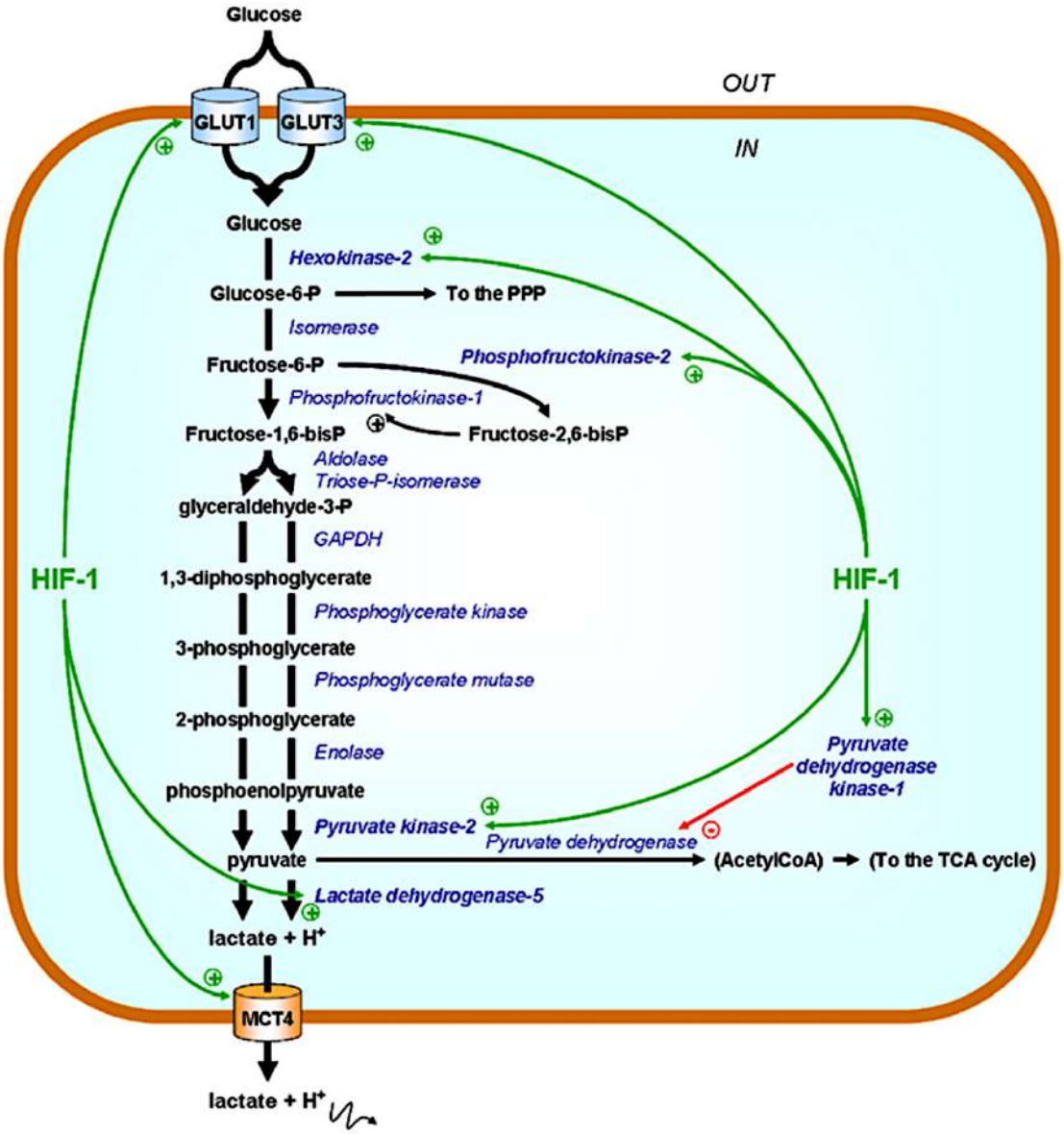

Figure 17. Glucose regulation by the transcription factor HIF-1
HIF-1 accelerates glycolytic flux by promoting the expression of glucose transporters, GLUT1 and GLUT3, and multiple glycolytic enzymes (green arrows) (Porporato et al., 2011)

Another key regulator of glycolysis is Fructose-2,6-bisphosphate (F2,6BP) which strongly stimulates PFK1 (Figure **17**). Its level decreases during starvation resulting is higher predominance of gluconeogenesis over glycolysis (Jm et al., 2002). F2,6BP is made from Fructose-6-Phosphate (F6P) by phosphofructo-2-kinase/fructose-2,6-bisphosphatases (PFKFB). PFKFB are bifunctional enzymes that either stimulate the formation (through PFK2 activity) or degradation (through FBPase activity) of F2,6BP. HIF-1 targets one isoform, the *PFKFB3* gene (Minchenko et al., 2002), which mostly has a PFK2 activity. Under hypoxic conditions, that activity is increased by an AMP-activated protein kinase (AMPK)-dependent phosphorylation (Marsin et al., 2002) (Figure **17**).

One of the four PK isoforms, PKM2 can transactivate glycolysis related genes by directly interacting with HIF-1 and enhancing its binding to its target genes (Luo et al., 2011). PKM2 is associated with increased nucleic acid synthesis in normal proliferating cells, embryonic cells and cancer cells (Porporato et al., 2011). It is more expressed in tumorigenic cells and it exists as an active tetrameric or a nearly inactive dimeric form. Its active form is stimulated by accumulation of upstream intermediates such as F1,6P and Serine, promoting glycolysis. The dimeric form is induced by accumulation of biosynthetic products downstream such as lipids, alanine and other amino acids (Mazurek, 2011). In addition, oxidative stress inhibits PKM2 activity along with another enzyme Glyceraldehyde phosphate dehydrogenase (GAPDH). GAPDH inhibition induces the accumulation of G6P which drives the metabolic flux into the PPP. This allows the generation of the antioxidant NADPH used to dampen the ROS effect (Anastasiou et al., 2011).

Other factors triggering entry into pathways linked to glycolysis is the amount of enzyme available. An example is the increase of glucose-6-phosphate dehydrogenase (G6PD) and transketolase (TKT) expression during replication. This probably results from the organism's needs of nucleotides for DNA synthesis, which is met through boosting the PPP (Vizán et al., 2009). In addition, glucosamine-fructose-6-phosphate amidotransferase (GFPT), the enzyme determining entry into HBP, is inhibited by the final product of that metabolic pathway, UDP-GlcNAc (Assrir et al., 2014).

d. The Warburg effect

Rapidly dividing cells such as cancer cells display high glycolytic rate similar to what occurs in fermentation, even in the presence of oxygen. This switch in metabolism is referred to as the Warburg effect (Figure 18). Under this state, key enzymes and transporters involved in glycolysis are upregulated, leading to an increase of lactate production and regeneration of redox cofactors. This metabolic state is not associated with dysfunctional mitochondria or OxPhos (Zu and Guppy, 2004).

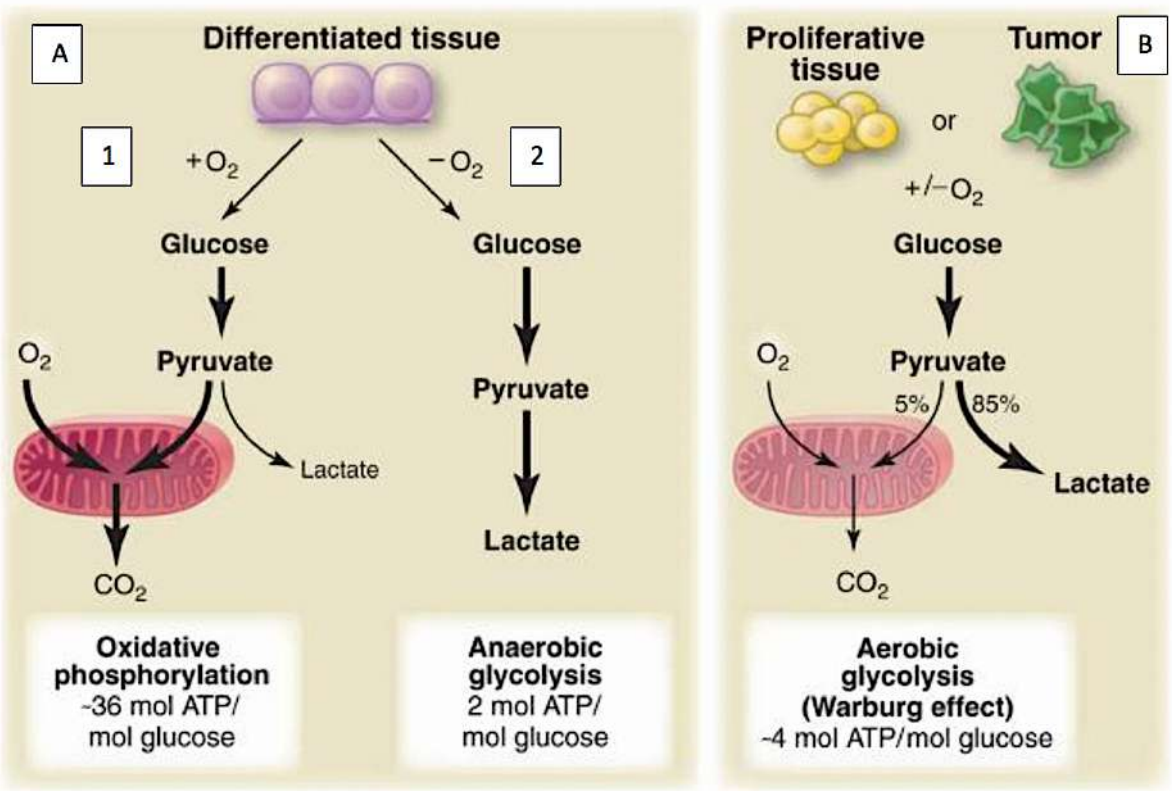

Figure 18 Glucose metabolism under different O_2 levels
Un normal levels of O_2, non-proliferating tissues metabolize glucose into pyruvate after what the latter mostly OxPhos (A.1). When O_2 becomes limiting, pyruvate can be redirected to lactate synthesis (anaerobic glycolysis, A.2) which however generates less ATP compared to OxPhos. In the Warburg effect (aerobic glycolysis), regardless of O2 levels, pyruvate is mostly used for lactate production (B) (Vander Heiden et al., 2009).

Knowing that glycolysis produces less ATP than OxPhos, the question raises as to why this would be a preferred pathway for proliferating cells. One explanation is that producing less ATP would only become detrimental to cells in situations where resources become scarce. As long as glucose and other nutrients are available, the ATP produced would be sufficient to sustain cell growth. One advantage of increasing the glycolytic flow is that dividing cells require amino acids, lipids and nucleotides in addition to energy to replicate their cellular content. This can be met by reshuffling intermediated of glycolysis in the PPP for instance for the required nucleotides, or even NADH both for its antioxidant properties but also for its role in lipids synthesis. Thus, under circumstances where cells need to commit most of their carbon source available to producing intermediates such as: acetyl-coA and NADPH for lipids synthesis; glycolysis intermediates for non-essential amino acids synthesis, and ribose for nucleotides, switching to aerobic glycolysis might be advantageous (Vander Heiden et al., 2009).

As for cancer cells, the Warburg effect can also be advantageous due to the acidic environment created by increased lactate production which favors tumor growth (Swietach et al., 2007). Moreover, levels of O_2, which is required for ATP production through OxPhos, can fluctuate in tumor due to the distance from blood vessels. It is then not beneficial to entirely depend on the latter for ATP production (Pouysségur et al., 2006).

2. An overview of *C. trachomatis'* metabolism

a. Investigating *Chlamydiae* metabolic features in the pre-genomic era

One technique for studying *Chlamydiae* involved infecting embryonated chicken eggs to cultivate the pathogen (Burnet and Rountree, 1935). Under these experimental conditions, amino acids such as glutamate (Perrin, 1952), and intermediates of glucose metabolism including glucose, glutamate, fumarate, succinate, α-ketoglutarate, and pyruvate (Allen and Bovarnick, 1957) were not oxidized by purified bacteria. This apparent lack of enzymatic capacities led to the theory that *Chlamydiae* entirely depended on their host's for energy supply, an idea presented by Moulder as the "energy parasite" hypothesis in the 1960s.

Further experiments began to clarify the metabolic capacities of *Chlamydiae* and to question that hypothesis. Weiss and colleagues demonstrated that *C. trachomatis* and *C. psittaci* are capable of utilizing glucose (Ormsbee and Weiss, 1963; Weiss et al., 1964). Indeed, they detected that high levels of radioactive CO_2 were released when using radio-labelled glucose (Ormsbee and Weiss, 1963). They also showed that the purified bacteria produced pyruvate from labelled D-glucose, confirming that glycolysis is active (Weiss et al., 1964). However, even though glycolysis should generate some ATP, several *Chlamydia* species surprisingly depended on exogenous addition of ATP in order to metabolize D-glucose (Weiss, 1965). Another study solved this paradox by demonstrating that addition of a co-purified host HK allowed the conversion of glucose into G6P, suggesting *Chlamydia* did not possess a functional HK (Vender and Moulder, 1967).

Conversely, Ormsbee and Weiss (1963) did not detect an increase in oxygen consumption in their experimental settings. Hence, they concluded that *Chlamydiae* did not have the capacity to perform OxPhos and speculated on their use of the PPP combined with additional decarboxylation (Ormsbee and Weiss, 1963). This hypothesis was later supported by enzymatic activity experiments proving the functionality of the PPP in *C. psittaci* (Moulder et al., 1965).

Following experiments also investigated the enzymatic activity of the TCA cycle related enzymes. The presence of TCA cycle was demonstrated in *C. psittaci* (Moulder, 1962). Indeed, when using labelled pyruvate at carbon 1, labelled CO_2, derived from acetyl-CoA conversion, was produced. Though, no other carbon molecules were produced suggesting that it was unlikely that acetyl-CoA progresses through the TCA cycle (Weiss, 1967).

Another observation supporting the "energy parasite" hypothesis was the fact that RNA synthesis in *C. psittaci*, was reliant on exogenous addition of nucleotides (Hatch, 1975a). Additionally, it was demonstrated that they import host ATP through an ATP-ADP exchange mechanism (Hatch et al., 1982). Hatch postulated that ATP hydrolysis is required to create a membrane potential for transport of molecules such as amino acids on which *Chlamydia* also rely on (Hatch et al., 1982).

b. The "energy parasite" unmasked

i. Some of *Chlamydiaceae*'s metabolic pathways are complete

It is not before the late 90s that *C. trachomatis* serovar D genome was sequenced, which brought the first global picture of the metabolic capacities of the bacterium (Stephens, 1998) (Figure 19). As of 2014, genome sequence of all *Chlamydiaceae* members was available. Genomic sequence confirmed previous observations such as the absence of HK enzyme, and the presence of a complete PPP. In addition, the presence of a complete glycolysis pathway, which relies on phosphorylated glucose supply from the host, was revealed (Stephens, 1998).

Regarding phospholipid synthesis, *C. trachomatis* encodes for all genes necessary for phospholipids biosynthesis via a type II fatty acid synthesis (FASII) pathway (Stephens, 1998). In fact, using a heterologous expression system in *E. coli*, was also shown to produce *de novo* phospholipids (Yao et al., 2014, 2015a, 2015b). They can synthesize branched-chain fatty acids using acetate, glycerol-3-phosphate, isoleucine, and serine (Yao et al., 2015a). Nevertheless, they hijack host phospholipids (Su et al., 2004; Wylie et al., 1997) that they modify through their acyl-acyl carrier protein synthetase, before they can incorporate them it in their own phospholipids (Yao et al., 2015b). However, FASII was shown to be required for bacterial replication indicating that the bacteria are not entirely dependent on host phospholipids (Yao et al., 2014).

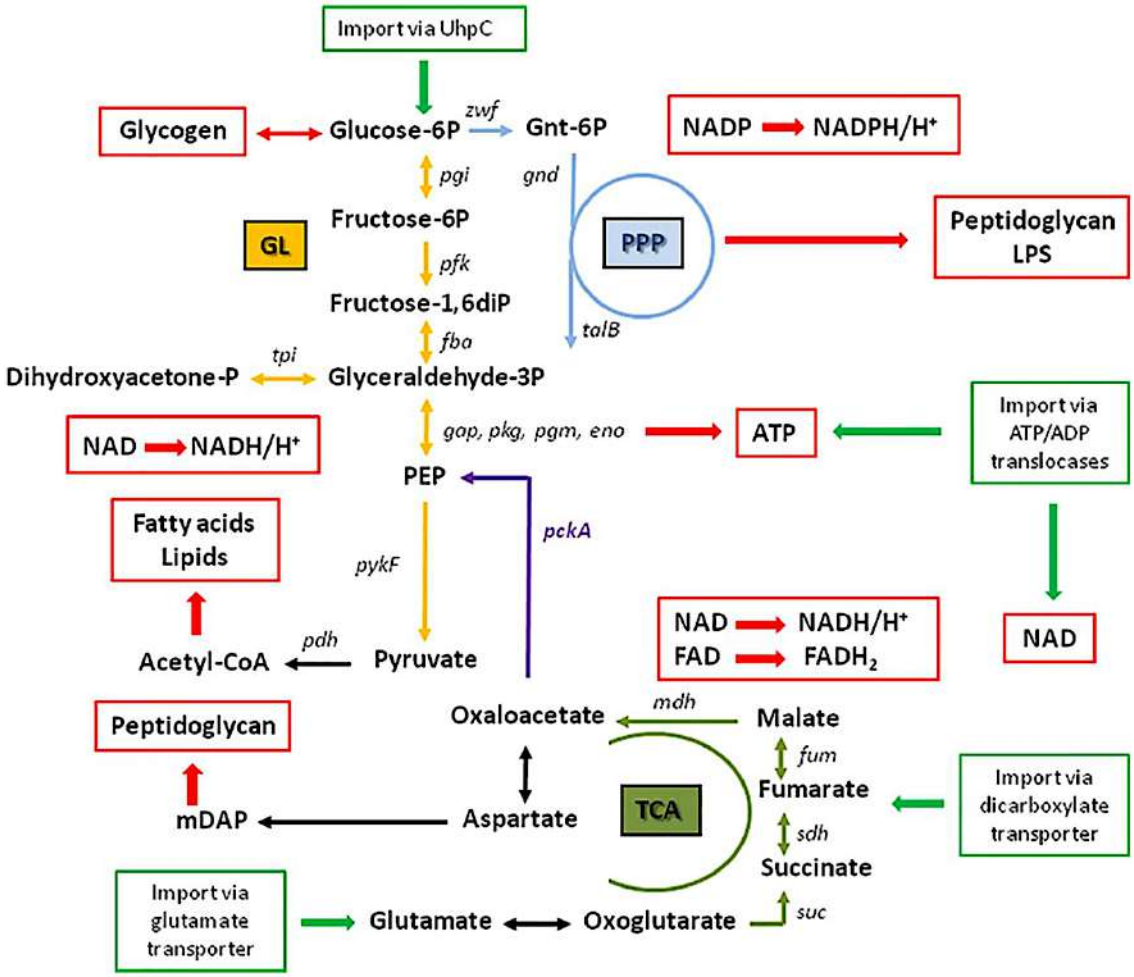

Figure 19. Schematic representation of the central *C. trachomatis* carbon metabolism based on published genomic data
C. trachomatis lacks HK but possesses a complete glycolysis pathway (yellow arrows) and PPP (blue arrows). Its TCA cycle (olive-green arrows), however, is incomplete and is connected to glycolysis by the PEP carboxylase PckA (purple arrows). Import of various metabolites is represented in green boxes and red arrows indicate major products of bacterial metabolism (Mehlitz et al., 2017)

ii. The TCA cycle is incomplete

All *Chlamydiaceae* have an incomplete TCA cycle. Genome sequence revealed that they lack the first three enzymes of that pathway, namely citrate synthase, aconitase and isocitrate dehydrogenase (Stephens, 1998). Citrate synthase is the enzyme responsible for converting acetyl-coA into citrate. Thus, even though *Chlamydiaceae* can synthesize acetyl Co-A, the latter can't be redirected into the TCA cycle (Figure 19). These revelations are consistent with earlier observations (Weiss 1967). The pathway thus relies on importing of various substrates from the host to fuel this pathway. To do so, McClarty (1999) hypothesized that the bacteria may import α-ketoglutarate (also called oxoglutarate) while exporting of malate, and

this potentially through a dicarboxylate transporter, SodTi. Another possibility may be the import of glutamate, that would be converted into α-ketoglutarate, or directly of α-ketoglutarate from the host (McClarty, 1999 Omsland) (Figure 19).

The TCA cycle is linked to glycolysis through the phosphoenolpyruvate carboxykinase (PckA) enzyme, which allows the bacteria to synthesize phosphoenolpyruvate (PEP) from oxaloacetate (Figure 19). This allows the pathogen to utilize various dicarboxylic acids from host TCA cycle as other carbon source than glucose. Indeed, using ^{13}C-malate, Mehlitz et al. showed that this metabolite is taken up by *C. trachomatis* and further converted into fumarate and succinate (Mehlitz et al., 2017).

Some enzymes of the TCA cycle, even though present, carry mutations preventing them to play their role in the pathway. Indeed, all strains of *C. trachomatis* sequenced present a frameshift mutation in succinate dehydrogenase resulting in a truncated non-functional protein. Another enzyme, fumarate hydratase has two frameshift mutations, in two *C. trachomatis* strains L2/434/Bu and L2/UCH-1/proctitis (Thomson et al., 2007).

iii. *Chlamydiaceae* are capable of producing energy

One way to make energy is through the electron transport chain. Genome data revealed that *Chlamydiaceae* are capable of producing ATP through OxPhos. They possess genes encoding for: a sodim-dependent NADH dehydrogenase (Na^+-NQR, complex I), succinate dehydrogenase (SdhA-C, complex II), cytochrome bd oxidase (CydAB, complex IV), and an A1–A0-ATPase (complex V) (Dibrov et al., 2004; Omsland et al., 2014; Stephens, 1998) (Figure 20). In contrast to mitochondrial complex I, Na+-NQR relies on Na+ transport, energizing their plasma membrane through a sodium gradient across it.

The observation that succinate dehydrogenase, as mentioned above, is a truncated protein raised questions as to the ability of the pathogen to produce energy. The capacity to do so has been demonstrated recently. Liang et al. were able to measure respiratory activity in *C. trachomatis* infected cells. They used inhibitors against various complexes of mitochondrial oxidative phosphorylation system which did not completely reduced respiratory activity. They were able to further inhibit that activity using an Na^+-NQR inhibitor proving its functionality (Liang et al., 2018). They also investigated the reliance on host ATP by inhibiting its production at two stages of infection: at early stages (1hpi) and in mid-cycle (12hpi). Their observations suggest that bacterial development depends only partially on host energy supply, with a stronger susceptibility in early steps of infection (Liang et al., 2018). The authors did not investigate the

steps of the developmental cycle that were impaired when the host respiratory chain was blocked, nor did they measure the consequences on the production of infectious particles.

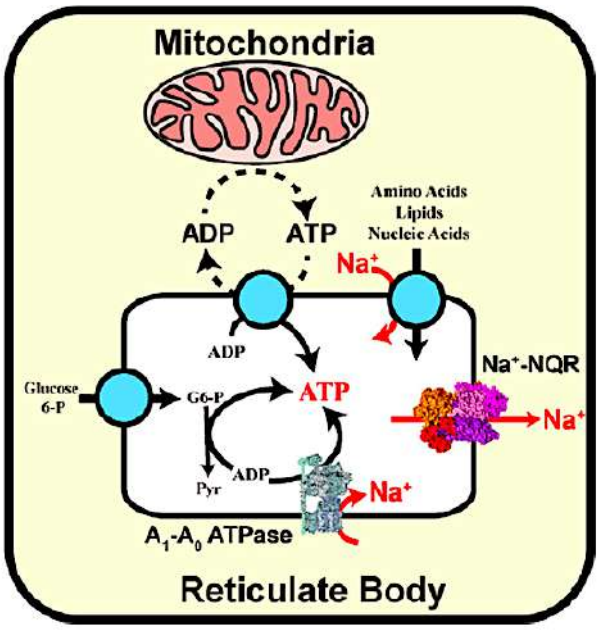

Figure 20. The chlamydial oxidative phosphorylation system
Chlamydiae are capable of producing ATP. Their oxidative phosphorylation system is composed of multiple components including a NADH dehydrogenase (Na^+-NQR), and an A1–A0-ATPase. Na^+-NQR generates a sodium gradient by pumping it out of reticulate bodies. External sodium is then pumped back in through the A1–A0-ATPase to produced ATP. Adapted from (Liang et al., 2018)

c. The limited biosynthetic capacities of *Chlamydiaceae*

Even though *Chlamydiaceae* were shown to be somewhat independent metabolically from the host, they remain dependent on diverse host precursors to fuel several of their pathways. Bader et al. (1958) showed that *C. trachomatis* required exogenous source of amino acids for replication (Bader and Morgan, 1958). Early work had shown that *C. trachomatis* require glutamine, histidine, phenylalanine, leucine, valine for their growth (Allan and Pearce, 1983; Hatch, 1975b). Genome sequencing confirmed that the bacteria were auxotroph for several amino acids, which they hijack from their host potentially using amino acid pumps they encode (Braun et al., 2008; Read, 2000; Stephens, 1998). Tracing the incorporation of heavy isotopes from donor metabolites showed that the bacteria conserved the ability to make some amino acids *de novo* such as alanine, asparagine or glutamine, using metabolites imported from the host (Mehlitz et al., 2017). Interestingly, although the bacteria have retained the capacity to make glutamine, this amino acid is also directly scavenged from the host to meet the high needs for peptidoglycan synthesis (Rajeeve et al., 2020). Peptidoglycan synthesis also uses meso-

diaminopimelate (mDAP) as crosslinkers. The precursor for the latter is aspartate whose pool could also be replenished through hijacking host TCA cycle intermediates such as malate, previously mentioned, before being redirected into *de novo* mDAP biosynthesis (Mehlitz et al., 2017).

Another important gap in the biogenesis capacities of *Chlamydiaceae* concerns nucleotides (Hatch, 1975a; Hatch et al., 1982). Bacterial transporters for ATP, GTP, CTP, UTP and NAD have been described (Fisher et al., 2013; Tjaden et al., 1999). This dependence from the host could be exploited for therapeutic intervention against *Chlamydiae*. In fact, it was shown indeed that inhibiting the *de novo* GMP (Guanine monophosphate) synthesis pathway of the host strongly impaired infection both in cell cultures and *in vivo* (Rother et al., 2018).

d. A second dogma revisited: the metabolic inertia of EBs

For years EBs have been considered as metabolically inert since early experiments failed to detect protein, RNA and DNA synthesis in this form of the bacteria as opposed to RBs (Crenshaw et al., 1990; Hatch et al., 1985; Plaunt and Hatch, 1988). In the latter, protein synthesis was shown to be sustained by addition of exogenous ATP for *C. psittaci* (Hatch et al., 1985) and *C. trachomatis* (Omsland et al., 2012). Their rigid outer membrane was suggested to be a permeability barrier (Bavoil et al., 1984). In fact, reducing their outer membrane using dithiothreitol (DTT) was shown to increase metabolic activity (Hackstadt et al., 1985). Moreover, ATPase activity could be detected in *C. trachomatis* EBs following treatment with reducing agents such as β-mercaptoethanol and glutathione (Peeling et al., 1989).

However, proteomics analyses showed that EBs were equipped with relatively more enzymes dedicated to energy metabolism than RBs (Saka et al., 2011). This was attributed to a higher energetic demand in the early phase of infection, at a stage when mechanisms for ATP scavenging from the host are not yet in place (Sixt et al., 2011; Skipp et al., 2005; Vandahl et al., 2001).

Omsland et al. (2012) developed a host cell-free growth conditions for *C. trachomatis* using axenic medium. They demonstrated that protein synthesis is active in EBs when they are supplied with G6P as an energy source, while, in contrast, RBs required ATP. This publication, together with the proteomic data revealing the enzymatic capacity of EBs changed the vision of the EBs from "inert" particles to metabolically capable entities (Omsland et al., 2012; Rother et al., 2018). The question of their energetic autonomy, i.e. their ability to sustain at least the first steps of infection, remains open.

e. Glucose metabolism of the host and the pathogen are tightly linked

i. The bacteria need glucose to develop

Glucose is the carbon source that fuels the major energy producing pathways. It was shown that lowering glucose concentration in the culture medium is detrimental for *C. trachomatis* development (Harper et al., 2000; Iliffe-Lee and McClarty, 2000; Maffei et al., 2020). Furthermore, bacterial growth was significantly reduced in cells supplied with other carbon sources than glucose. Those included glutamate, malate, α-ketoglutarate and oxaloacetate (Iliffe-Lee and McClarty, 2000) which are potential carbon sources for the gluconeogenesis pathway. In addition, the absence of fructose-1,6-bisphosphatase based on genomic data, which is an enzyme involved in gluconeogenesis, supports the hypothesis that the latter is not functional in *C. trachomatis*.

As described previously, bacteria rely on phosphorylated glucose from their host as they lack the HK enzyme (Omsland et al., 2012; Stephens, 1998; Vender and Moulder, 1967). The G6P transporter gene *UhpC* was found to be expressed throughout infection and could thus permit G6P import both in EBs and RBs (Gehre et al., 2016; Iliffe-Lee and McClarty, 1999; Schwoppe et al., 2002).

ii. *C. trachomatis* orchestrates glucose uptake by GLUT1/3

Glucose is an important actor for the metabolism of both host and bacteria, consequently, it is not surprising that one of the first impact of infection is the upregulation of glucose uptake, observed in several species of *Chlamydiaceae*. Indeed, Rupp et al. (2007) showed that infection with a *C. pneumoniae* strain results in an upregulation of glucose import during infection (Rupp et al., 2007). Moreover, infection with *C. caviae*, induced this time an upregulation of glucose transporter GLUT1 (Ojcius et al., 1998). As for *C. trachomatis*, infection was also shown to induce the same effect (Siegl et al., 2014). Wang and al. demonstrated that not only GLUT1 but also GLUT3 were upregulated at the transcriptional and protein level (Wang et al., 2017c). The increase in transcription of *GLUT1* and *GLUT3* was shown to be dependent on the transcription factor HIF-1 and on the activation of host transglutaminase 2 (Maffei et al., 2020). HIF-1 is a known regulator of key steps of the glycolysis pathway, as discussed extensively previously. HIF-1α, the HIF-1 subunit inducible by hypoxia, was shown to become stabilized in infections with both *C. trachomatis* (Sharma et al., 2011) and *C. pneumoniae* (Rupp et al.,

2007). Transglutaminase 2 is an enzyme responsible of post-translational modifications on its targets. It becomes activated upon infection, and the mechanism by which it regulates gene transcription remains unsolved (Maffei et al., 2020).

iii. *C. trachomatis* accumulates glycogen in the inclusion lumen

Glycogen accumulation in inclusions has been describe as early as 1965 by Gordon and Quan who observed that *C. trachomatis* infected cells stained positive for iodine (Gordon, 1965). Recently, Gehre et al. showed that glycogen and UDP-glucose are the glucose sources highjacked by *C. trachomatis* from its host cytoplasm to build luminal glycogen (Figure 21) (Gehre et al., 2016). UDP-glucose is translocated into the inclusion through at least one host transporter, the solute carrier family 35 member D2 (SLC35D2), itself being hijacked from the host by *C. trachomatis*. Once inside the inclusion, UDP-glucose is used as a starting point for *de novo* glycogen synthesis (Gehre et al., 2016). Indeed, two bacterial enzymes involved in glycogen synthesis, GlgA and GlgB, are secreted in the inclusion lumen, with GlgA being detected in the inclusion lumen as early as 12hpi (Lu et al., 2013). In parallel to this *de novo* glycogen synthesis in the inclusion membrane, a second pathway contributes to glycogen accumulation in the inclusion: bulk import of the polysaccharide directly from the host cytoplasm. However, the exact mechanism for this pathway remains to be elucidated (Gehre et al., 2016).

iv. The G1P/G6P conundrum

To perform glycolysis, *C. trachomatis* needs to import phosphorylated glucose molecules from the inclusion's lumen. Schöppe et al. (2002) had demonstrated that the *C. pneumoniae* UhpC transporter was only capable of importing G6P (Schwoppe et al., 2002), not glucose nor G1P, a finding that was confirmed using *C. trachomatis* EBs (Gehre et al., 2016).

The capture of glycogen in the lumen of the inclusion is presumably beneficial if it can be converted back to a form of glucose usable by the bacteria. However, glycogenolysis generates G1P, not G6P. This raises the question of the mechanism by which G1P is converted into G6P in the inclusion lumen.

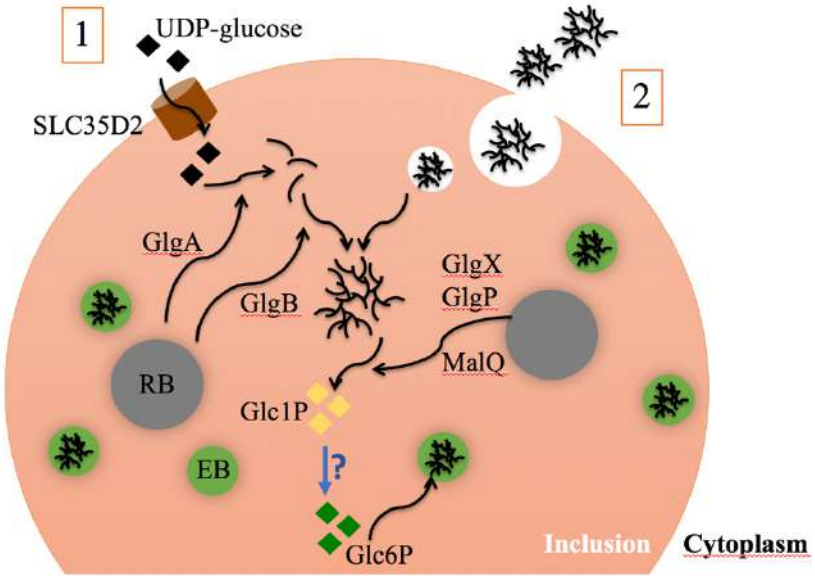

Figure 21. Glucose acquisition by *C. trachomatis*
C. trachomatis obtains glucose from the host under two different forms. It imports directly UDP-glucose (UDP-Glc) through the SLC35D2 transporter (1). Once inside the inclusion lumen, UPD-Glc can be converted into glycogen by the chlamydial glycogen synthase GlgA and GlgB. Host glycogen is also imported in bulk into the inclusion (2). Glycogen break-down generates G1P, which needs to be converted into G6P for uptake by the bacteria. Adapted from (Gehre et al., 2016)

v. Variation of the bacterial energetic demand over the infection cycle

Overall, the metabolic demand that *C. trachomatis* exert on the host cell evolves considerably during an infectious cycle. It is not known whether their glycogen reserve provide them with sufficient autonomy to establish the infectious niche and start replicating. Importantly, in the first hours of infection, the bacterial biomass is very small compared to that of their host, therefore their metabolism does not represent a significant burden. However, by 24 hpi, there is already an average of >300 bacteria per cell (Shaw et al., 2000). With about 10^6 bp for the bacterial genome against $3x10^9$ for the host, at that stage of infection, bacterial DNA represents about 10% of total DNA in an infected cell. Demand in ATP, amino acids, glucose has also become significant. Twenty-four hpi is about the time when RBs start converting into EBs in an asynchronous manner, with thus a gradual shift towards lower nutritional need per bacteria, but because the number of RBs continues to increase, the metabolic burden also does. Only by after ~30-32 hpi, when the number of RBs per inclusion starts decreasing (Lee et al., 2018), does the metabolic pressure follow. Although EBs rely on glucose-6-phosphate (G6P) for survival, even glucose demands probably also decreases by that time, because the bacteria obtain it from the degradation of the glycogen that they have accumulated in the inclusion lumen during the first half of their developmental cycle (Gehre et al., 2016).

3. Hosting an intracellular bacterium: metabolic consequences for the host

a. Cellular metabolic modulations

i. A metabolic switch seems to be promoted by chlamydial infection

Several features of chlamydial infection have suggested that infected cells go through a metabolic switch, favoring glycolysis over OxPhos. As mentioned earlier, chlamydial infection induces an upregulation of GLUT transporters. In HeLa cells, lactate production was enhanced by *C. caviae* infection (Ojcius et al., 1998). Moreover, the transcription factor HIF-1 which has been largely documented to favor glycolysis (Figure **17**) was shown to be upregulated in *C. trachomatis* infected cells (Sharma et al., 2011). In addition, the Protein kinase B/Akt (PKB) signaling pathway is activated throughout the infection (Rajalingam et al., 2008b). PKB is involved in multiple cellular processes such as cell survival and proliferation but also controls glucose uptake and utilization (Hajduch et al., 2001). Put together, these observations indicate that chlamydial infection might induced a metabolic switch similar to the Warburg effect. The parallel can be drawn further between infected cells and tumor cells: both undergo increased nutritional needs, to feed bacterial growth on one hand, and to feed increased cell division on the other hand.

ii. A metabolic snapshot of infected cells

Metabolic modifications upon infection has been increasingly investigated in the recent years. Rother et al. (2018) used GC-MS (gas chromatography-mass spectrometry) in order to generate a profile of various metabolites upon infection. They also performed a genome wide RNAi screen to identify host proteins important for bacterial development, among which metabolic enzymes. They found that many metabolites including G6P, lactate and pyruvate were upregulated upon infection. Furthermore, one enzyme involved in the metabolic switch of the Warburg Effect, Pyruvate dehydrogenase kinase 2 (PDK2), was also shown in to be essential for bacterial development (Rother et al., 2018). PDK2, as PDK1, block the pyruvate to acetyl-CoA conversion, forcing cells to perform aerobic glycolysis. All these observations support the hypothesis that *C. trachomatis* infected cells undergo a metabolic switch akin to the Warburg effect. However, this study was performed in HeLa cells, which are tumor derived cells, with an abnormal metabolism. Moreover, it could not distinguish host from bacterial metabolites, when more than one hundred bacteria are present in a single cell starting about 24

hpi, thus contribute significantly to the global picture (Lee et al., 2018). Thus, any change in concentration of a given metabolite needs to be interpreted with caution.

TCA cycle intermediates including succinate, fumarate, malate and citrate were also upregulated upon infection (Rother et al., 2018). However, upregulation of those metabolites could result from utilizing alternative carbon sources such as glutamate. Another possibility is that these metabolites could be produced by the bacterial TCA cycle, so it is not very informative on the potential changes in host metabolism. One important finding of that study was the demonstration that the *de novo* synthesis pathway for GMP, was essential for bacterial development. Exposure to a drug blocking inosine-5′-monophosphate dehydrogenase 2 (IMPDH), the first enzyme of this pathway, severely abrogated infection in cell cultures and *in vivo*. This validates the concept that drug targeting the host metabolism could give rise to a new generation of anti-chlamydial antibiotics (Rother et al., 2018).

b. p53 down regulation in infection and its consequences on host cell metabolism

The tumor suppressor protein p53 regulates many faces of cell homeostasis, one being the metabolic balance in the cell. Interestingly, p53 level is downregulated in *C. trachomatis* infected cells (González et al., 2014; Siegl et al., 2014) which necessarily has implications in the metabolic balance of the cell. Stabilizing p53 expression was detrimental to bacterial development, indicating that p53 downregulation benefits the bacteria. One known target of p53 is G6PD which regulates entry into the PPP (Jiang et al., 2011). Overexpression of G6PD, reversed the inhibitory effect of p53 stabilization on bacterial growth, indicating that the deleterious effect of p53 stabilization is due to its inhibitory effect on G6PD, and thus likely on the boost of PPP required in infection (Siegl et al., 2014).

On the mechanistic side, the downregulation of p53 during infection was shown to be mediated, on one hand, by activation of the phosphoinositide-3-kinase (PI3K)/Akt/HDM2 pathway leading to its proteasomal degradation (Siegl et al., 2014). On the other hand, p53 is also the target of a microRNA, miR-30, which is upregulated during infection (Chowdhury et al., 2017).

c. The impact of infection on the spatial distribution of key players in energy production in the cell

i. Mitochondrial network

Another consequence of p53 degradation during infection is the downregulation of Dynamin protein related 1 (Drp1) (Chowdhury et al., 2017). The role of the latter is to regulate mitochondrial fission, which had been shown to be modulated by miR-30 (Li et al., 2010; Wang et al., 2017a). Thus, infection induced elongation of mitochondria (Chowdhury et al., 2017). Kurihara et al (2019) also reported elongated mitochondria early in infection with *C. trachomatis* through a Drp1 inhibition mediated mechanism (Kurihara et al., 2019).

Mitochondria are dynamic organelles that are constantly fusing and breaking, and their architecture is tightly linked to their metabolic function and their quantity (Sarin et al., 2013; Touvier et al., 2015). Modulating their architecture is a strategy to adapt to various condition such as stress or apoptotic signals for instance (Suen et al., 2008; Wang et al., 2017b). In fact, ROS would promote fission, while starvation would instead induce more fusion (Frank et al., 2012; Gomes et al., 2011). In the context of infection, even though ROS production is induced (Abdul-Sater et al., 2010), mitochondria surprisingly end up elongated, at least early in infection. Indeed, Chowdhury et al. showed that mitochondria are not broken-down during infection, even upon treatment with excess peroxide which should normally fragment mitochondria (Chowdhury et al., 2017). However, Kurihara et al. (2019) only observed mitochondrial elongation at early stages of infection, while at late stages mitochondria did get fragmented (Kurihara et al., 2019).

As Drp1 mediated mitochondrial fission can be a pre-apoptotic signal (Frank et al., 2001; Röth et al., 2014), preventing fission could be one of *C. trachomatis'* strategies to prevent cell death. An additional role for maintaining mitochondrial integrity could be a means to maintain ATP production throughout infection, thus ensuring a constant energy source availability. Indeed, fragmented mitochondria were shown to be less efficient at energy production (Sarin et al., 2013).

ii. Glycolysis enzymes

A recent study revealed that three host glycolytic enzymes, PK, LDHA, and aldolase A (Aldo A), are recruited at the *C. trachomatis* inclusion membranes. The authors further showed that downregulating Aldo A decreased bacterial load in HeLa cells. Moreover, the expression of three bacterial glycolytic enzymes decreased over the course of infection, while the

percentage of inclusions positive for host glycolytic enzymes increased. The authors hypothesized that the localization of host glycolytic enzymes at the inclusion membrane could provide an easier access to host glycolysis substrates (Ende and Derré, 2020).

Another consequence of infection is the upregulation of the glycolysis regulator hexokinase II (HKII). This upregulation occurs at the transcriptional level and is dependent on the 3-phosphoinositide-dependent protein kinase-1 (PDPK1)-Myc signalling pathway. HKII becomes enriched at the mitochondrial surface, through association with the mitochondrial voltage dependent anion channel (VDAC), a feature that was needed for optimal bacterial growth (Al-Zeer et al., 2017). One known outcome of HKII association to VDAC on mitochondria is prevention of apoptosis. Indeed, HKII recruitment to mitochondria appears to play a role in the resistance of infected cells to apoptosis (Al-Zeer et al., 2017). Possible metabolic implications were not investigated.

V. Questions tackled during this research project: Investigating metabolic modifications and requirements during *C. trachomatis* infection

There has been an increasing effort to elucidate the metabolic modulations upon infection, though, multiple grey areas remain. Rother and al. (2018) provided an overview of the metabolic modifications upon *C. trachomatis* infection indicating that glycolysis is likely upregulated, nevertheless this study had some limits. Indeed, the metabolomics did not distinguish between host and bacterial metabolites. Moreover, as for multiple previous studies, the model used for the metabolomics experiment is HeLa cells which are highly glycolytic cells. In addition, as the focus of the study shifted to the purine synthesis pathway, the respective contribution to bacterial development of glycolysis and OxPhos, remains unanswered.

Beside Rother et al work, a previous study evaluated the metabolic changes induced by infection. Using NMR experiments Ojcius et al. (1998) showed that ATP production increases upon infection along with an increase in glucose consumption and lactate production, suggesting glycolysis is upregulated, and potentially OxPhos as well (Ojcius et al., 1998). Nonetheless, this study was performed in HeLa and using an animal strain *C.* caviae.

The goal of the present study was to address two main questions:

1) What is the effect of *C. trachomatis* infection on the main two glucose-derived, ATP synthesis pathways, glycolysis and OxPhos?
2) To what extent are these pathways necessary for *C. trachomatis* to undergo its developmental cycle?

The ambition of my project was to answer those questions in conditions as close as possible to physiological conditions. Ideally, we would have performed all our experiments using primary epithelial cells isolated from the ectocervix (Tang et al., 2021). However, the Covid19 pandemic made it difficult to obtain material from hospitals. To circumvent this limitation, we also performed experiments in the endo-cervix derived A2EN cell line, which was immortalized by E6/E7 transformation but conserved its epithelial phenotype, and which we cultivated in the same culture medium designed for epithelial cell selection as the primary cells (Herbst-Kralovetz et al., 2008). For all features we tested, primary cells and A2EN behaved identically, indicating that A2EN make an acceptable substitute for primary epithelial cells. In addition, we also performed experiments in HeLa cells because this is the reference cell line used in the field, and it was often interesting to compare the data obtained in the different cellular backgrounds. Beside this main project, I have been implicated in the project of a post-doctoral fellow, Sébastien Triboulet, aiming at solving the G1P/G6P conundrum. A first version of the results has been submitted for publication and is included in the Annex section.

Material and Methods

Cells and bacteria

Human cervix-derived epithelial HeLa cells (ATCC), human colon derived epithelial LS174T WT and GPI-KO cells (de Padua et al., 2017), monkey epithelial Vero cells (ATCC) were grown in Dulbecco's modified Eagle's medium with Glutamax (DMEM, Thermo Fisher Scientific), supplemented with 10 % (v/v) heat-inactivated fetal bovine serum (FBS) (complete medium). LS174T cells were a kind gift from Dr. J. Pouysségur (Institute for Research on Cancer and Aging, Nice). Primary epithelial cells were isolated from ectocervix biopsies of female patients and were cultivated in keratinocyte serum free medium (KSFM, Thermo Fisher Scientific) containing 50 mg/L of bovine pituitary extract (Thermo Fisher Scientific) and 5 µg/L of epidermal growth factor (EGF) human recombinant (Thermo Fisher Scientific) (Tang et al., 2021). A2EN cells (kind gift from Dr Alison Quayle, New Orleans, USA) were cultivated in the same conditions as the primary epithelial cells. *C. trachomatis* serovar D/UW-3/CX (CTD) and mCherry transformed serovar D/UW-3/CX (CTDm) were propagated in HeLa cells as described in (Scidmore, 2006). EBs were stored in sucrose-phosphate-glutamic acid buffer (SPG: 10 mM sodium phosphate [8 mM Na2HPO4- 2 mM NaH2PO4], 220 mM sucrose, 0.50 mM l-glutamic acid) at -80 °C.

Cell culture and treatment

Cells were cultured at 37 °C, in 5 % CO2 atmosphere and were routinely tested, with bacteria stocks, for mycoplasma using the standard PCR method. Confluent cultures of A2EN and primary cells were detached with 0.3% trypsin/EDTA for 3 min at 37 °C before a wash in RPMI 1640 (Thermo Fisher Scientific). Cells were centrifuged for 15 min at 2500 x*g* and the pellet was resuspended in KSFM to be seeded or passed. When confluent, HeLa cells and LS174T cells were detached with 0.5 mM EDTA in PBS before being seeded or passed in complete medium. For experiments of glucose deprivation from HeLa cells, cells were seeded in normal medium. On the following day, the medium was replaced with DMEM without glucose (Thermo Fisher Scientific, A14430) complemented with 5 mM sodium pyruvate (Sigma-Aldrich), 10% fetal bovine serum (FBS). Experiments were performed 48 h from the start of glucose deprivation. Experiments preceding lactate and ATP measurements in HeLa cells were performed in DMEM medium deprived of pyruvate (Thermo Fisher Scientific, 61965059). CTD and CTDm infections were always followed by a 30 min centrifugation step at 270x*g* at 37 °C, unless overwise stated.

Cells were treated with the following chemicals (stock solutions): Phenformin: 200 mM in H2O (Sigma-Aldrich, P7045); Oligomycin: 5 mM in DMSO (Cayman Chemical, 11341); GNE-140: 4 mM in DMSO (Sigma-Aldrich, SML2580). All chemicals were stored at -20 °C.

Bacterial transformation

The L2-based p2TK2-SW2 plasmid encoding the fluorescent protein mCherry under the control of the promoter of the early gene *incD* (Agaisse and Derré, 2013) was used to transform CTD. EBs (10^8 IFU) were incubated with 6 µg of plasmid in 0.05 M CaCl2 for 20 min. The resulting mixture was divided in 4 and plated in a 6 well plate containing Vero cells and warm complete medium, centrifuged at 1000x*g* 30 min and cells were allowed to grow for 48 h. At this point, cells were checked for inclusions before being detached and broken with glass beads to release EBs (48h). Broken cells were centrifuged at 190x*g* for 5 min and 0.5 mL of the EBs containing supernatant was used to infect two 6 well plates of Vero cells with complete medium supplemented with cycloheximine (1 µg/mL) and penicillin (1 U/mL), centrifuged at 1000x*g* 30 min. Subsequent passages were performed in a similar manner but using all lysate to infect fresh cells. At each passage, mCherry expression by the bacteria was verified. Once mCherry expression was detected, transformed *C. trachomatis* were amplified in Hela cells. Once infected HeLa cells were close to 100% infection, EBs were extracted by cells lysis in SPG buffer. Lysed cells were first centrifuged at 270x*g* 5 min to remove cell debris, after what the supernatant was centrifuged at 12,000x*g* at 4°C for 40 min. The pellet containing EBs was then re-suspended in SPG buffer and aliquots were frozen at -80 °C.

Adhesion assay

Adhesion assays were performed as previously described (Vromman et al., 2014). Hela cells were plated in a 24 well plate ($100*10^3$ cells/well) the day before the assay. Cells were pre-cooled 30 min at 4 °C after what they were incubated for 4 h at 4 °C (including a 30 min centrifugation step also at 4 °C) with either equal genome number of CTD or CTDm. Prior to infection, bacteria were sonicated in order to disrupt bacterial aggregates. Cells were then washed gently with cold PBS, lysed directly in the plate followed by genomic DNA (gDNA) extraction using the DNeasy Blood and Tissue Kit (Qiagen). Bacterial adhesion was determined through qPCR.

Progeny assay

Cells were seeded in a 24 well plate ($120*10^3$ cells/well for HeLa, $175*10^3$ cells/well for A2EN and primary cells, and $250*10^3$ cells/well for LS174T cells). For experiments using chemical inhibitors, GNE-140, oligomycin or phenformin were added to the culture medium at the indicated concentrations when infecting cells, unless otherwise stated. Cells with an infection lower than 30 % (checked by microscopy, and at least 50% for A2EN cells) were detached with 0.5 mM EDTA in PBS for HeLa cells or 0.3 %trypsin for LS174T cells, primary cells and A2EN cells, 48 hpi (or 30 hpi for the silencing experiment). They were lysed using glass beads and the supernatant was used to infect HeLa cells plated the day before ($120*10^3$ cells/well in a 24 well plate), in serial dilutions. In order to evaluate the first round of infection, cells from duplicate wells were fixed in 2 % paraformaldehyde (PFA, Merk-Millipore) 2% sucrose in PBS and analyzed by flow cytometry at 24 hpi to determine the bacterial titer (Vromman et al., 2014).

Flow cytometry

Cells were washed with PBS and gently detached using 0.5 mM EDTA in PBS. Samples were fixed in 2% PFA 2% sucrose in PBS and stored overnight at 4 °C. Cells infected using CTDm were analyzed directly on 1/10 of the sample diluted in PBS. Cells infected with CTD were stained with a mouse antibody against GroEL (Thermo Fisher Scientific) followed with Alexa488-coupled secondary antibody against mouse (Molecular Probes). Flow cytometry analysis was performed with a CytoFLEX S (Beckton Coulter). A minimum total of 10,000 gated events were collected for each sample. Data were then analyzed using FlowJo software (version 10.0.7) to determine the bacterial titer as described in (Vromman et al., 2014).

Immunofluorescence

All cells were grown on cover slips in a 24 well plate. After the indicated time of infection, the cells were fixed in 4% PFA (Merk-Millipore) 4% sucrose in PBS for 20 min and was followed with 10 min quenching with 50 mM NH4Cl, in PBS. Cells were then either stained for DNA then mounted or stained. Staining consisted of first permeabilizing cells in 0.05% Saponin (Sigma-Aldrich), 1 mg/mL bovine serum albumin (BSA Sigma-Aldrich) in PBS for 10 min. Primary antibodies used in this study were anti-*Chlamydia* antibody (a home-made mixture of rabbit polyclonal antibodies against several *Chlamydia* antigens) and rabbit anti-Cap1 antibody (Gehre et al., 2016). DNA was stained using 0.5 µg/mL of Hoechst 33342

(Thermo Fisher Scientific) which was added to the secondary antibody. Coverslips were then mounted in Mowiol (Sigma-Aldrich).

Images were acquired on an Axio observer Z1 microscope equipped with an ApoTome module (Zeiss, Germany) and a 63× Apochromat lens. Images were taken with an ORCAflash4.OLT camera (Hamamatsu, Japan) using the Zen software. Images were analyzed with ImageJ software. CTD and CTDm inclusions size was determined using the cell image analysis software CellProfiler.

qPCR

Total DNA was isolated with the DNeasy Blood and Tissue Kit (Qiagen). To determine plasmid number (pDNA) and bacterial genome number (gDNA), 100 uL of CTD and CTDm EBs were used for DNA extraction. DNA concentrations were determined with a spectrophotometer NanoDrop (Thermo Fisher Scientific) and normalized to equal contents. Quantitative PCR (qPCR) was performed using LightCycler 480 SYBR Green Master I (Roche) following the manufacturer's instructions. To normalize for equal genome number a standard curve was made using a plasmid containing the target gene g*lgA* used to measure genome number as described in the Applied Biosystem protocol "Creating Standard Curves with Genomic DNA or Plasmid DNA Templates for use in quantitative PCR" (2003). Primers against a conserved sequence within ORF2 were used to assess plasmid number, and then were analyzed using the ΔΔCt method (Schmittgen and Livak, 2008). To determine gDNA quantities relative to cell (adhesion assay, assessment of bacterial genomes in cells infected in the presence of oligomycin), primers for GlgA and for the *36B4* gene (encoding for an acidic ribosomal human phosphoprotein P0) were used to determine the relative number of bacteria per cell. Each qPCR experiment was performed in triplicate and repeated at least three times. The primer sequences are as follows:

- GlgA Forward: 5'-AATGATTGGAATGCGTTACGG-3',
- GlgA Reverse: 5'-CGGTAGGTTGTCACTGCTTCC-3';
- 36B4 Forward: 5'-TGCATCAGTACCCCATTCTATCAT-3';
- 36B4 Reverse: 5'-AAGGTGTAATCCGTCTCCACAGA-3';
- Ctrachplas Forward: 5'-CAGCTTGTAGTCCTGCTTGAGAGA-3';
- Ctrachplas Reverse: 5'-CAAGAGTACATCGGTCAACGAAGA-3'.

Measurement and quantification of intracellular ATP

Intracellular levels of ATP were analyzed using the CellTiter Glow luminescence assay (Promega) according to the manufacturer's instructions. Cells ($60*10^3$ for HeLa in a 48 well plate, $75*10^3$ for primary cells in a 48 well plate and $30*10^3$ for A2EN cells in a 96 well plate) were treated or infected for the indicated time in pyruvate free medium. The cell medium was then discarded or used for lactate measurement in the case of primary cells. Cells were then lysed directly in the plate with ATP Assay Buffer after what luminescence was measured with the Cytation 5 Cell Imaging Multi-Mode Reader (BioTek). ATP concentrations were calculated using an ATP (Sigma-Aldrich) standard curve (0 to 200 pmole). To normalize ATP levels to protein levels, duplicate wells of cells were lysed in 2 M urea buffer (Tris 30 mM, NaCl 150 mM, 2 M urea, 1 % SDS, pH=8.0) after what a BCA assay kit (Pierce) was used as indicated by the manufacturer to measure proteins levels.

Measurement of Lactate production

Cells ($60*10^3$ for HeLa in a 48 well plate, $75*10^3$ for primary cells in a 48 well plate and $30*10^3$ for A2EN cells in a 96 well plate) were treated or infected for the indicated time. Plates were then centrifuged for 5 min at 250x*g* then 56 uL of medium or lactate standard (Sigma-Aldrich) was used for the assay. Lactate produced was measured using a colorimetric lactate detection assay as described in (Powers et al., 2007) with the following reagents: nicotinamide adenine dinucleotide (14.3 mM NAD+, Sigma-Aldrich), 0.52 M Hydrazine (Sigma-Aldrich) both prepared in assay buffer (0.50 M Glycine (Sigma-Aldrich) and 2.5 mM, EDTA, pH 9.5); lactate dehydrogenase (19 U/mL, LDH, Sigma-Aldrich), 9.0 M urea buffer. Absorbance at 340 nm was measure with Cytation 5 Cell Imaging Multi-Mode Reader (BioTek). A lactate standard curve (0 - 4.6µmole) was used to calculate lactate concentrations. For normalization to protein levels, cells were lysed in 2 M urea buffer and proteins level was measured with Pierce BCA protein assay kit (Thermo Fisher Scientific), as indicated by the manufacturer.

RNA Interference

For siRNA experiments, $50*10^3$ HeLa cells were mixed with Lipofectamine RNAiMAX (Invitrogen), following the manufacturer's recommendation, with 10 nM siRNA, before being plated in a 24 well plate. The culture medium was changed the following day and progeny assay were performed two days post treatment with the siRNA. Downregulation efficiency was

verified by performing a lactate assay. Two sets of siRNA against glucose-6-phosphate isomerase (GPI) were used and their sequences are as follows:

- siGPI1-sense: 5'-CCAAGCUCACACCAUUCAU-3';
- siGPI1-antisense: 5'-AUGAAUGGUGUGAGCUUGG-3';
- siGPI2-sense: 5'-CAUGGAGUCCAAUGGGAAA-3';
- siGPI2-antisense: 5'-UUUCCCAU UGGACUCCAUG-3'

Metabolic flux analysis

Seahorse XF96 extracellular flux analyzer (Agilent Technologies) was used to measure oxygen consumption rates (OCR) and extracellular acidification rates (ECAR) of cells, in order to evaluated mitochondrial respiration and glycolysis, respectively. OCR and ECAR were measured following the Mito Stress test and Glyco stress test protocols, respectively. Cells were seeded (25,000 cells/well) on Seahorse 96 well-plate and were infected at various times, so that on the day of measurement, cells had been infected for 24, 30 or 48h, or left uninfected. One hour prior to the assay, cell media was replaced by Seahorse XF Base Medium (Agilent Technologies), 1 mM glutamine (Sigma-Aldrich) adjusted at pH 7.4 for the Glyco Stress test. For the Mito Stress test, the medium was replaced with Seahorse XF Base Medium (Agilent Technologies), 1 mM pyruvate (Sigma-Aldrich), 2 mM glutamine (Sigma-Aldrich), and 10 mM glucose (Sigma-Aldrich), pH 7.4) and the plates were incubated in a non-CO_2 incubator at 37 °C. For both tests, basal levels of OCR and ECAR were recorded for 30 min before consecutive addition of drugs that modulate OxPhos or glycolysis. In the Mito stress test, we added 2 µM oligomycin (Cayman Chemicals), 1 µM Carbonyl cyanide-4 (trifluoromethoxy) phenylhydrazone (FCCP (Cayman Chemicals), and a mix of 0.5 µM rotenone (Sigma-Aldrich) and 0.5 µM antimycin A (Sigma-Aldrich). In the Glyco Stress test, we added 10 mM glucose (Sigma-Aldrich), 2 µM oligomycin (Cayman Chemicals), 50 mM 2-Deoxy-D-glucose (2-DG) (Sigma-Aldrich). Unless otherwise stated, ECAR refers to glycolysis and OCR refers to ATP-linked respiration measurements.

In the Mito stress test, the roles of the above-mentioned drugs consist of:

- Oligomycin inhibits ATP synthase (complex V),
- FCCP uncouples oxygen consumption from ATP production transporting protons across the mitochondrial inner membrane, resulting in an increase of OCR
- Rotenone and antimycin A inhibit complexes I and III, respectively.

In the Glyco stress test, the roles of the above-mentioned drugs consist of:

- Glucose stimulates glycolysis
- Oligomycin inhibits OxPhos resulting in an increase of ECAR
- 2-DG inhibits glycolysis by competitively binding to hexokinase

Data were analyzed with the Wave software (Agilent Technologies).

Metabolic flux plates normalization

Following each experiment, plates were fixed in 2.5% PFA for 10 min then stained in 5 µg/mL DAPI (Invitrogen #D1306), 3% BSA in PBS. They were then washed three times with PBS then before analysis by a Cytation 5 Cell Imaging Multi-Mode Reader (BioTek) for cell count. Images were acquired on a 7x7 grid (394 µm x 291 µm for each square) and were analyzed with the cell image analysis software CellProfiler. In summary, the pipeline counted DAPI stained nuclei and subtracted mCherry stained inclusions from the nuclei to give the cell count per well. The obtained count was adjusted according to the actual number of pictures obtained per well and the size of the Seahorse 96 well plate well (0,106 cm^2). Normalization to cell number was performed in the Seahorse analysis Wave software and data were presented as mpH/min/cell for ECAR and as pmol/min/cell for OCR or as a ratio to the non-infected or non-treated cells.

Statistical analysis

The R environment v4.0.5 was used for all the analyses (R Core Team, 2020). Data were neither averaged nor normalized prior analyses. Data were fitted to a linear model that includes the variable of interest + the experiment date as covariate, but only when technical replicates are available (i.e., more than one value per variable of interest and per experiment date). Two by two effect comparisons (contrast comparisons) were performed with the emmeans() function of the emmeans package. Unequal variance t test (Welch test) was used in bivariate designs. Statistical significance was set to $P \leq 0.05$. In each figure, type I error was controlled by correcting the p values according to the Benjamini & Hochberg method ("BH" option in the p.adjust() function of R). Results are detailed in Table 1 in the annexe.

Results

I. Cell attachment and growth are enhanced in stably transformed *C. trachomatis* serovar D bacteria

The reference strain *C. trachomatis* D/UW-3/CX was stably transformed with the L2-based plasmid encoding the fluorescent protein mCherry under the control of the promoter of the early gene *incD* (Agaisse and Derré, 2013). mCherry expression allowed to quantitatively track infection by flow cytometry: at 18 hours post infection (hpi), mCherry expressing bacteria (CTDm) detached from the non-infected population, with a gradual increase in the fluorescent signal with time (Figure 22).

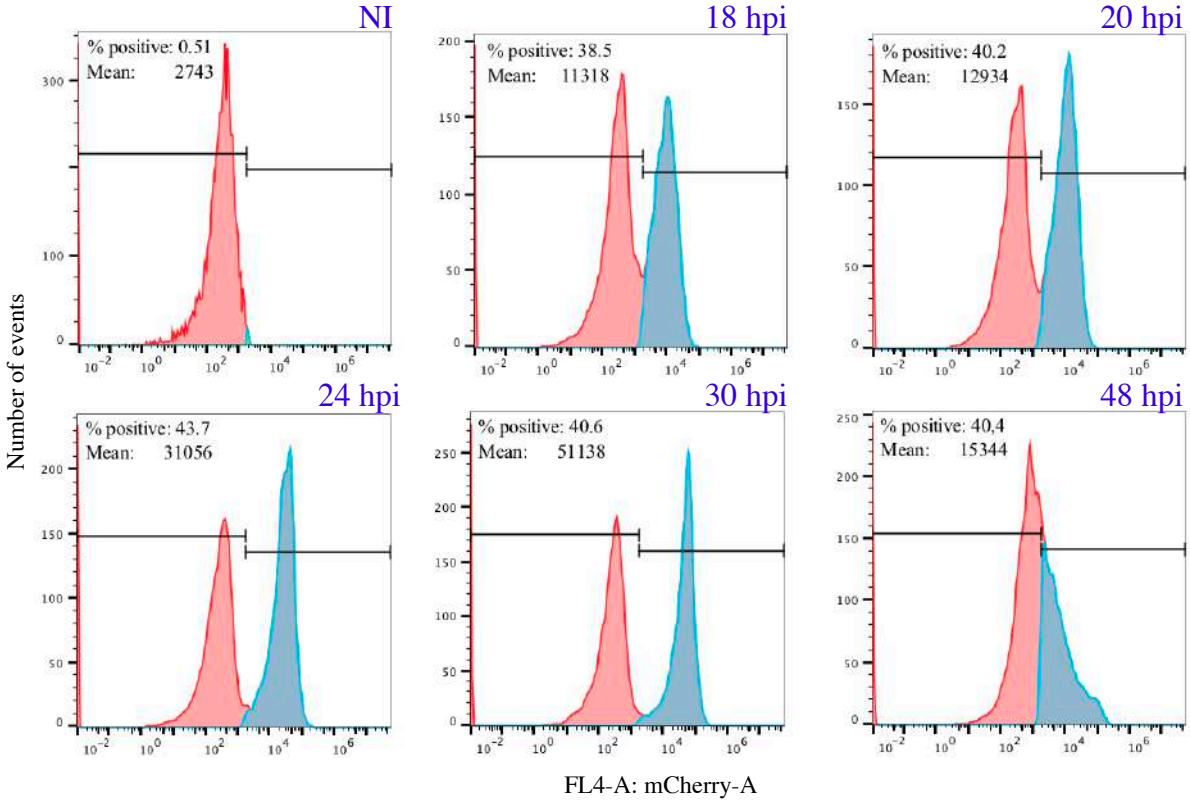

Figure 22. Quantification of mCherry expressing *C. trachomatis* D/UW-3/CX (CTDm) over time
Hela cells were infected with CTDm and fixed 18, 20, 24, 30 and 48 hpi. Samples were analyzed through flow cytometry in the red channel (FL4-A). mCherry negative cells are represented in red and the positive cells are in blue. The percentage of infection (out of total cells) and the mCherry mean fluorescence of the positive population (average signal per cell) are displayed on the graphs. This experiment is representative of two. Note that at 48 hpi reinfection events have occurred, precluding the distinction between the infected and non-infected population. Abbreviation: NI = non-infected.

We observed that even without the centrifugation step classically applied to facilitate infection with serovars of *C. trachomatis* others than LGV, we obtained good infection rates when using CTDm. When normalizing the stocks to equal genome number, we observed more and bigger inclusions in cells infected with CTDm than with CTD (Figure 23A, B). This suggested that bacteria gained in infectivity upon stable transformation. To verify this

hypothesis, we quantified the infectious forming units (IFU) obtained in cells infected with equal amounts of IFUs of the parental and of the stably transformed strain. CTDm gave rise to ~8-fold more IFU than the parental CTD strain (Figure 23C).

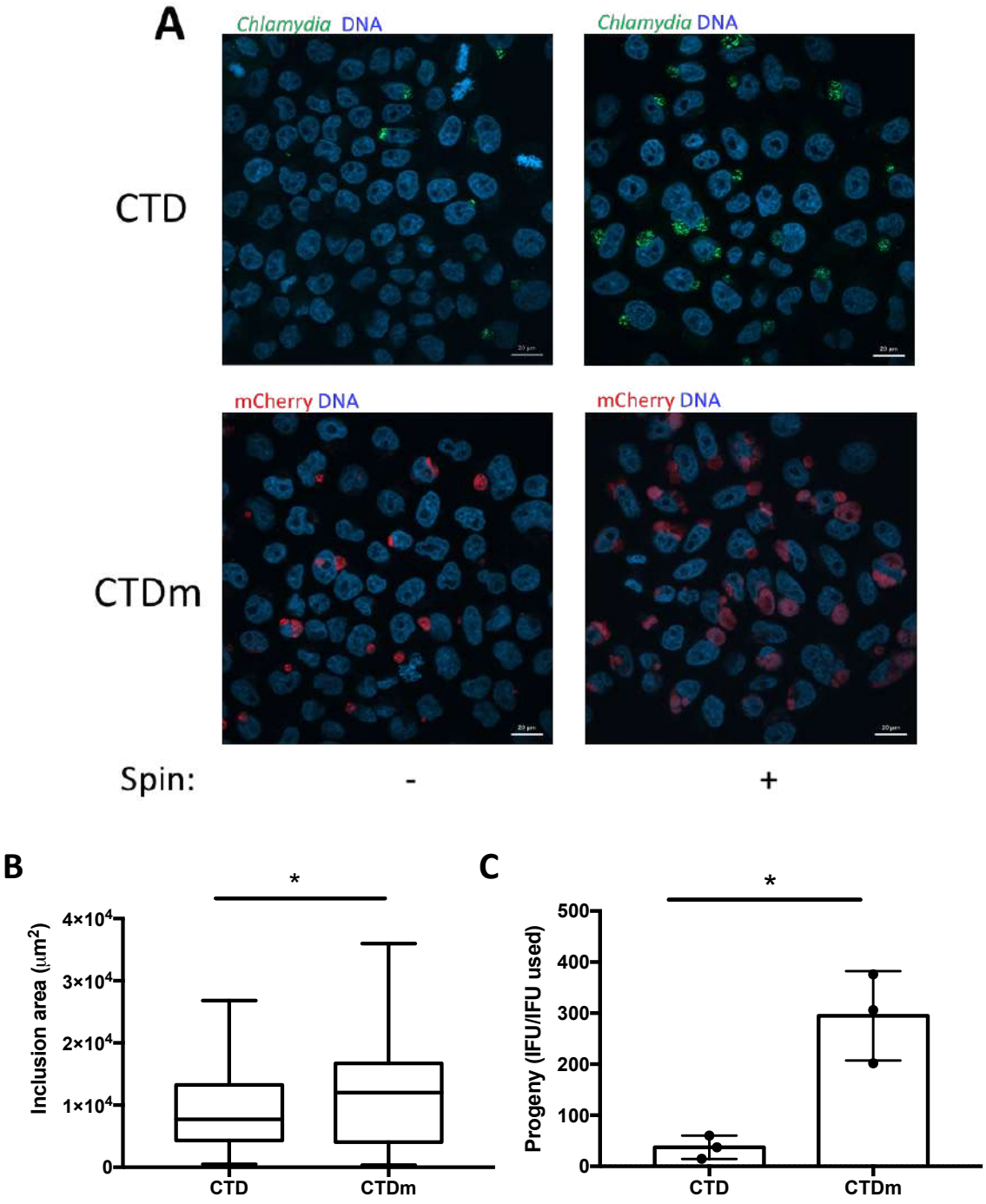

Figure 23. CTDm is more infectious than CTD
(**A**) Hela cells were infected with CTD or CTDm and fixed 24 hpi. CTD infected cells were permeabilized and immuno-stained with antibodies against *Chlamydia* followed with Alexa488-conjugated secondary antibodies (green). DNA is stained with Hoechst. Scale bar = 20 µm. (**B**) CTD and CTDm inclusion size was measured with the CellProfiler software. The graph displays the mean ± SD (n=38 inclusions/condition). (**C**) Hela cells were infected with equal IFUs of CTD and CTDm for 48 hpi. Cells were lysed and bacterial IFU were determined by re-infecting fresh HeLa cells as described in the methods. Significance is defined as: ns (not significant) = $P > 0.05$; (*)= $P \leq 0.05$

The plasmid used for the transformation is the natural plasmid of *C. trachomatis*, that was shown to provide a selection advantage over plasmid-free bacteria *in vitro* and *in vivo* (Russell et al., 2011). We hypothesized that selection of plasmid-transformed bacteria may have increased the quantity of plasmid per bacteria. This was indeed the case, since quantitative PCR (qPCR) measurement of the relative quantity of a plasmidic sequence over a chromosomal sequence revealed that CTDm bacteria displayed ~3 fold more plasmid copies per bacteria than the parental strain (Figure 24A). Thus, the gain in infectivity may be related to an increase in expression of plasmid-encoded genes. Among those, Pgp3 was shown to be required for full virulence of *C. muridarum in vitro* and *in vivo*, and might contribute to bacterial adhesion (Galaleldeen et al., 2013; Liu et al., 2014). We observed a ~3-fold increase in the adhesion capacity of the fluorescent strain (Figure 24B), consistent with the increase in the percentage of infected cells when using the CTDm compared to CTD (Figure 23A). Thus, stable transformation increases plasmid number and favors adhesion. At 24 hpi the sizes of the CTDm inclusions were about 30% larger (Figure 23B) than those of parental inclusions, indicating that the selection of stable transformants also provides an advantage on the growth rate.

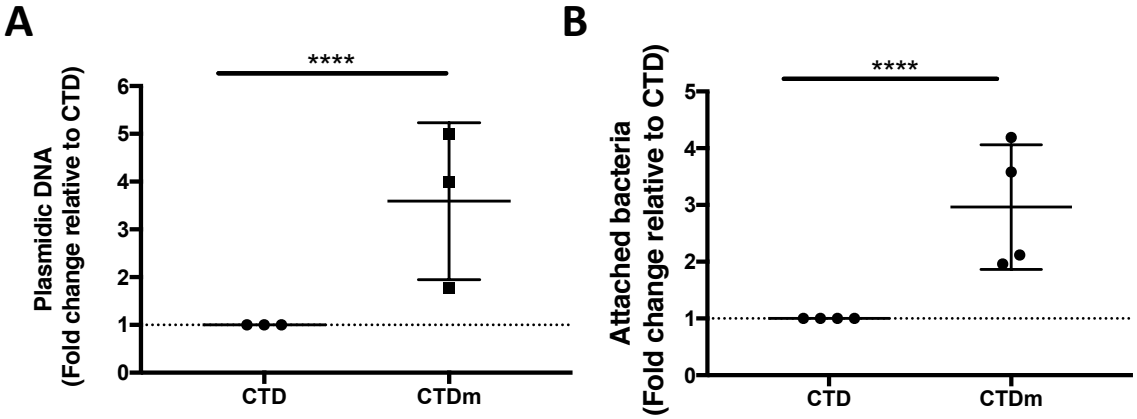

Figure 24. CTDm bacteria harbor more copies of the plasmid and display enhanced attachment capacity compared to the parental strain

(**A**) Total DNA was extracted from CTD and CTDm EBs. Bacterial plasmidic DNA (pDNA) was measured by qPCR and was normalized to bacterial genomic DNA (gDNA). The data are presented as the fold change pDNA over gDNA in CTDm relative to CTD. The mean ± SD are shown. Each experiment was performed in triplicate and repeated three times. (**B**) Pre-cooled HeLa cells were infected with equal genome number CTD and CTDm at 4°C, then incubated for 3h30 at 4 °C. Hela cells were then gently washed with cold PBS then lysed for total DNA extraction. Bacterial gDNA was measured by qPCR and was normalized to human gDNA. Each qPCR experiment was performed in triplicate and repeated at least three times. Significance is defined as: (****)= $P \leq 0.0001$

Altogether, CTDm bacteria represent a convenient model to follow *C. trachomatis* serovar D development, since it is easily tractable and develops better *in vitro*. Regarding the metabolic requirements during the course of infection, which is the focus of the present study, it is expected that the pressure exerted by the bacteria on the host metabolism occurs slightly earlier in time than with the parental strain, since the stably transformed bacteria multiply faster.

II. EBs energetic autonomy towards the early steps of the infectious cycle is incomplete.

The presence of glycogen and of glycolytic enzymes in EBs might cover the energetic needs of the bacteria in the first hours of the infectious cycle. To test this hypothesis and prevent the EBs from obtaining glucose from the host, we decided to use glucose-free medium. Since this formulation is not available for the culture medium used for primary cells, we performed this experiment in HeLa cells. Glucose deprivation for 48 h is expected to affect ATP production both through glycolysis and OxPhos. Indeed, we observed that ATP levels measured 48 h after deprivation were decreased by 50% (Figure 25A). As a read-out of the establishment of the early inclusion we used an antibody against Cap1. Cap1 is one of the bacterial proteins secreted early in the inclusion membrane (Fling et al., 2001). Six hours post infection the bacteria are expected to have clustered at the microtubule organizing center (MTOC), with a concomitant expansion of the inclusion membrane (Grieshaber, 2003). Indeed, in cells cultivated in the presence of glucose, many of the bacteria were already clustered near the nucleus, and Cap1 positive tubules were detected around them. In contrast, in glucose-deprived cells, bacteria were less clustered (Figure 25B). Cap1 staining was detected, but the tubules were shorter than in control cells. Thus, in the absence of glucose EBs are able to initiate the transcription and translation of early genes like *cap1*. However, some of the early steps of infection, e.g. clustering to the MTOC or inclusion tubule extension, necessitate glucose to be present in the culture medium. We concluded from these experiments that EBs have limited autonomy to initiate a successful infectious cycle.

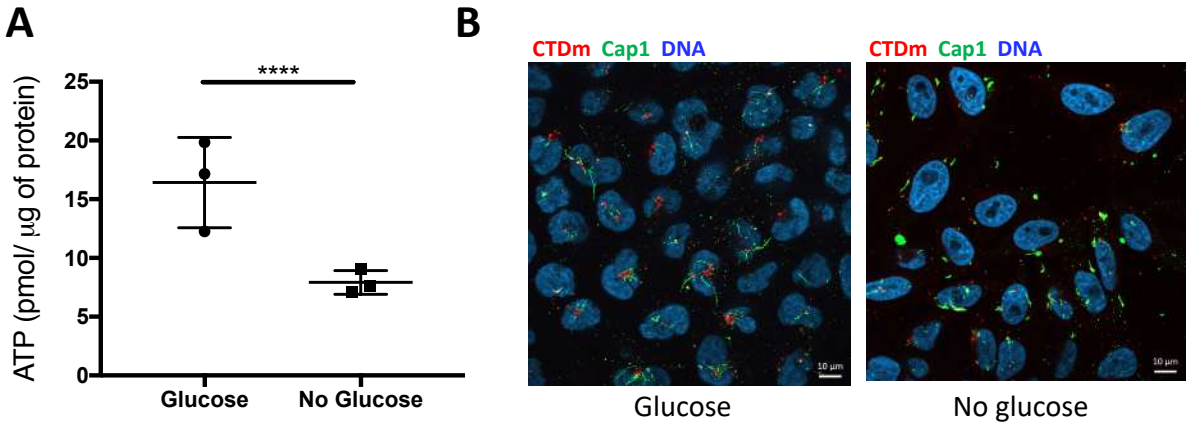

Figure 25. Chlamydial EBs energy source is not sufficient to sustain early bacterial development stages (**A**) HeLa cells were grown in medium containing glucose or not for 48 h. Intracellular ATP levels was then measured as described in the methods. (**B**) Hela cells were grown in medium containing glucose or not for 48 h before infection with CTDm. Cells were fixed 6 hpi then permeabilized before immunostaining with anti-Cap1 followed with Alexa488-conjugated secondary antibodies. DNA is stained with Hoechst. Scale bar = 10 µm. Significance is defined as: (****)= $P \leq 0.0001$

III. The ATP level remains stable in epithelial cells infected by *C. trachomatis* and is mostly generated by glycolysis.

To gain an overall picture of the energetic balance of infected cells we first measured the concentration of ATP over time in primary epithelial cells. We observed that ATP levels remained stable over the course of infection (Figure 26A). It was reported by Kurihara et al. (2019) that *C. trachomatis* infection induced an increase of ATP levels in HeLa cells early (8 hpi) in infection (Kurihara et al., 2019). However, we did not observe an increase in ATP at early time in this cell line, and we measured a small drop at 30 hpi (Figure 26B). ATP concentration is the result of production and consumption, by the host and by the bacteria. These data do not inform us on the rate of glycolysis nor OxPhos in the host but indicate that, in primary cells, supply meets demand even at the peak of bacterial proliferation.

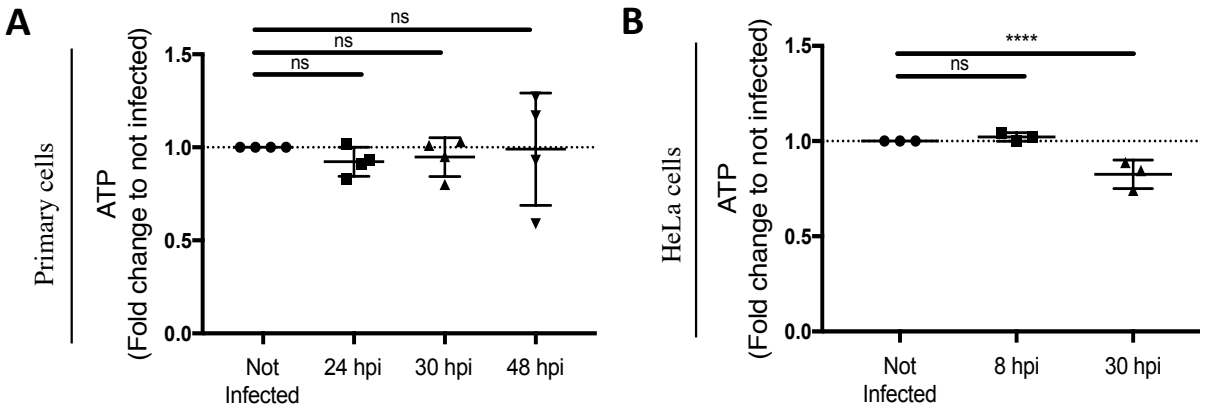

Figure 26. ATP levels remain stable over the course of infection by *C. trachomatis*
(**A**) Primary cells were infected with CTDm and intracellular ATP was measured 24, 30 and 48 hpi. Each experiment was repeated four times. (**B**) ATP levels were measured in CTDm infected HeLa cells at 8 and 30 hpi. Each experiment was repeated at least three times. Significance is defined as: ns (not significant) = $P > 0.05$; (*)= $P \leq 0.05$; (**)= $P \leq 0.01$; (***)= $P \leq 0.001$; (****)= $P \leq 0.0001$

Next, to understand which pathway makes the strongest contribution to the energetic balance in epithelial cells, we determined the consequences of chemical inhibition of glycolysis or OxPhos on ATP levels. Glycolysis is commonly determined through measurements of the extracellular acidification rate (ECAR) of the surrounding media. The latter is mostly governed by the excretion of lactic acid per unit time after its conversion from pyruvate, at the end of the glycolytic pathway. GNE-140 is a potent and specific lactate dehydrogenase (LDH) A/B inhibitor (Boudreau et al., 2016). Cells exposed to GNE-140 show an increase in levels of metabolites associated with glycolysis and the pentose phosphate pathway, which lie upstream of LDHA/B, but levels of metabolites associated with OxPhos remain fairly stable (Boudreau et al., 2016). In two different cancer cell line models GNE-140 was shown to block the glycolytic pathway and force cells towards oxidative phosphorylation (Ždralević et al., 2018). We first tested the efficiency of GNE-140 by measuring its effect on lactate production. Lactate production being below the sensitivity limit in the lactate assay for A2EN cells, GNE-140 effect was measured on ECAR in that cell line. Increasing doses of GNE reduced both lactate production in HeLa cells (Figure 27A) and ECAR in A2EN cells (Figure 27B). A representative experiment for the glycolytic stress test is represented in Figure 27C.

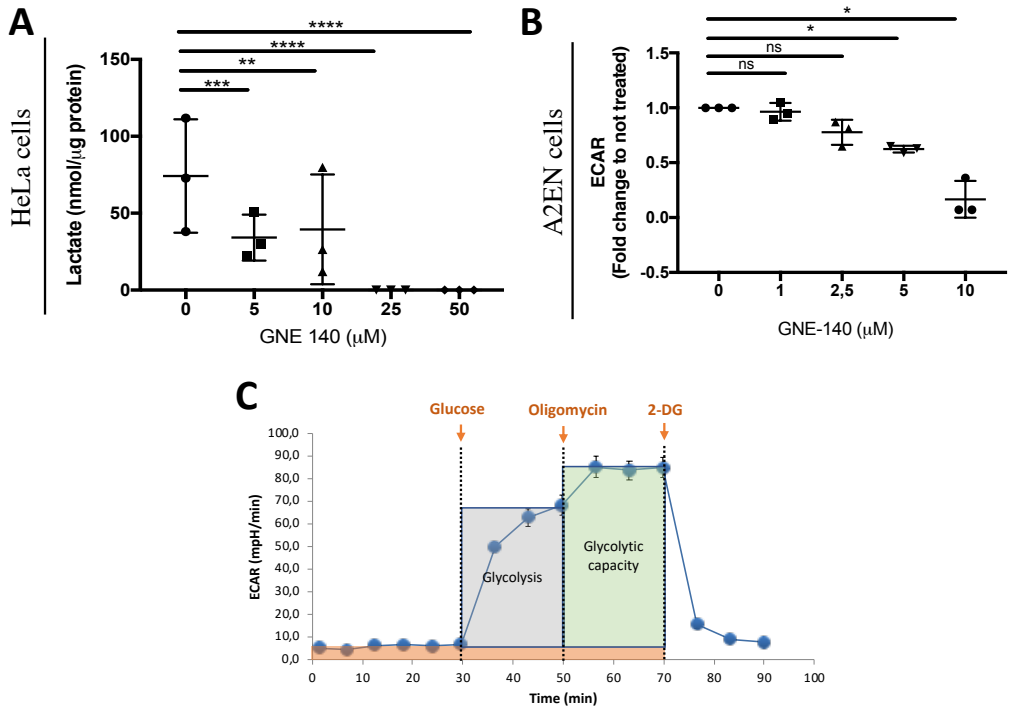

Figure 27. Dose dependent inhibition of lactate production by GNE-140
(**A**) Hela cells were treated with indicated GNE-140 concentrations and 24 h later lactate production was measured in the medium as described in the methods. Each experiment was repeated three times (**B**) A2EN cells were treated with indicated GNE-140 concentrations for 24 h then ECAR was measured as described in the methods. (**C**) Glycolysis Stress Test profile of one representative experiment using control A2EN cells. Sequential injections of the indicated compounds measure glycolysis (grey box), glycolytic capacity (green box), non-glycolytic acidification (orange box). ECAR values in (**B**) correspond to the "Glycolysis" measurements. Significance is defined as: ns (not significant) = $P > 0.05$; (*)= $P \leq 0.05$; (**)= $P \leq 0.01$; (***)= $P \leq 0.001$; (****)= $P \leq 0.0001$

We next measured the consequence of GNE-140 treatment on ATP levels in these cells. In A2EN cells, application of GNE-140 for 24 h induced a dose-dependent decrease in intracellular ATP (Figure 28A). The effect of the drug was actually very fast, since it was significant after only 2 h of treatment for 5 µM GNE-140 (Figure 28B). To exclude the possibility that GNE-140 affected ATP production both through glycolysis and OxPhos, thereby accounting for the strong drop in ATP, we measured the OCR upon 24 h of treatment with GNE-140. A representative experiment for the OCR measurements is represented in (Figure 28C). Our results indicate that OCR remains stable upon GNE-140 treatment, suggesting that OxPhos is not affected by the drug (Figure 28D). We concluded from these experiments that GNE-140 affects ATP levels in A2EN, likely through an inhibition of glycolysis, while OxPhos remains functional.

A different picture emerged from HeLa cells, with no significant effect of 2 h treatment with 10 µM GNE-140, and for long term treatment (24 h), a decrease in ATP levels was only

detected at the high concentration of 25 µM (Figure 28E, F). We were surprised with these results because the A2EN and the HeLa cells have a low and high glycolytic activity, respectively. We thus expected that glycolysis would contribute marginally to ATP production in A2EN, and significantly in HeLa cells, at odds with our observations.

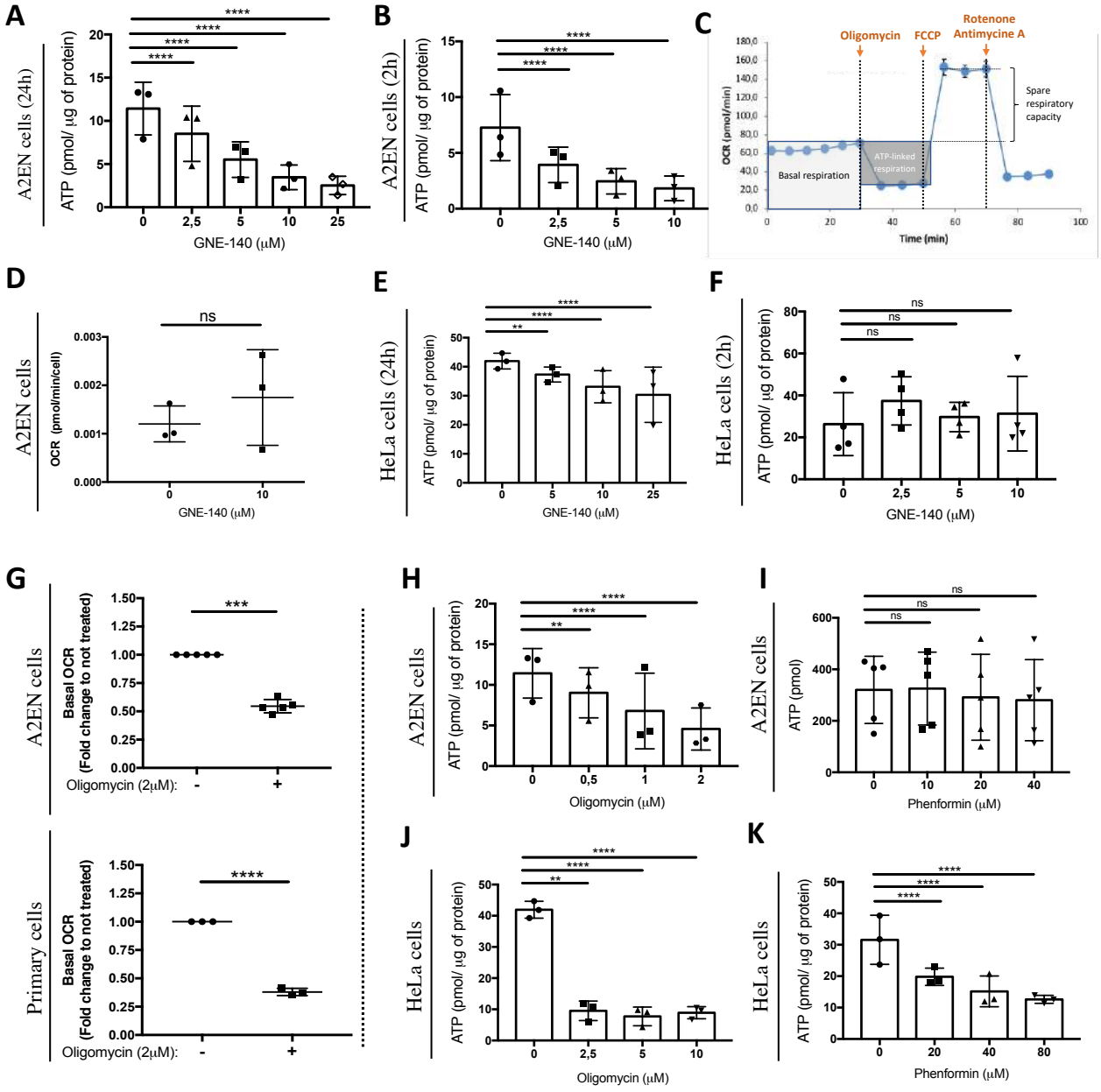

Figure 28. The effect of GNE-140 or OxPhos inhibitors on ATP levels is cell dependent
A2EN cells (**A**) (**B**) (**H**) (**I**) and HeLa cells (**E**) (**F**) (**J**) (**K**) were treated with the indicated concentrations of GNE-140, oligomycin or phenformin for 24 h except in (**B**) (**F**) where cells were treated for 2 h. ATP levels were measured as described in the methods. (**C**) Mito Stress Test profile of one representative experiment using control A2EN cells. OCR values in (**D**) correspond to the ATP-linked respiration measurements. (**D**) A2EN cells were treated or not for 24 h with 10 µM GNE-140 and Mito Stress Test was performed. (**G**) Basal level of OCR was measured on A2EN and primary cells upon addition of oligomycin (2 µM). Significance is defined as: ns (not significant) = $P > 0.05$; (*)= $P \leq 0.05$; (**)= $P \leq 0.01$; (***)= $P \leq 0.001$; (****)= $P \leq 0.0001$

To investigate the relative contribution of OxPhos and glycolysis to ATP levels in these cell lines further we next measured the effect of OxPhos inhibitors. Oligomycin is an inhibitor of the ATP synthase (complex V) of the respiratory chain commonly used to block OxPhos. Indeed, used at 2 μM in Mito stress test, it reduces efficiently mitochondrial oxygen consumption in A2EN and primary cells (Figure 28G). As an alternative drug, we used phenformin, an inhibitor of the complex I of the mitochondrial respiratory chain (García Rubiño et al., 2019). High concentrations of these drugs were toxic for A2EN, we thus used lower concentrations than in HeLa cells. Phenformin did not significantly affect ATP levels in A2EN cells, while oligomycin did, but to a lesser extent than what we had observed with GNE-140 (Figure 28H, I). Both OxPhos inhibitors had a stronger impact on ATP levels in HeLa cells than in A2EN (Figure 28, K). Altogether, we concluded from these experiments that the respective contribution of glycolysis and OxPhos to maintaining ATP levels are different in the two cellular backgrounds, with glycolysis being preponderant in A2EN cells, versus OxPhos in HeLa cells. We next moved on to understand the consequences of infection on these pathways.

IV. Glycolysis is not upregulated in cervical epithelial cells infected with *C. trachomatis* serovar D

In non-infected cells, ECAR, the rate of acidification of the culture medium, is mostly determined by the rate of excretion of lactic acid, itself a by-product of the glycolytic pathway. Since *C. trachomatis* lacks lactate dehydrogenase, it does not contribute to lactic acid production, and probably makes little contribution to the acidification of the extracellular medium. Thus, even in the context of the infection, it might be possible to use ECAR as a read-out of the glycolytic activity of the host cell. We thus compared the ECAR of A2EN infected or not with CTDm for 24, 30 or 48 h. ECAR increased by 30% starting at 24 hpi but remained stable up to 30 h of infection, when the energy demand of the bacteria is estimated to be at its peak (Figure 29A). A higher acidification was noticeable at 48 hpi, however at this time point there was a lot of cell death in the specific plates used for Seahorse assays. Thus, the increased stress endured by the cells at this time point might account for this high increase in ECAR, and the data should be considered with caution.

Seahorse experiments require a substantial number of cells. To validate these findings in primary epithelial cells we chose to measure directly lactate quantities in the supernatant of cell cultures, infected or not with CTDm, a technique that is less demanding in cell quantities. The second advantage of this readout is that lactate can only be produced by the host, and thus

constitute a more direct readout of glycolysis in the host than ECAR. No difference was seen between lactate concentration in the culture medium of infected and non-infected primary cells (Figure 29B). This was also the case in HeLa cells where we did not detect a significant increase in lactate production during *C. trachomatis* infection (Figure 29C).

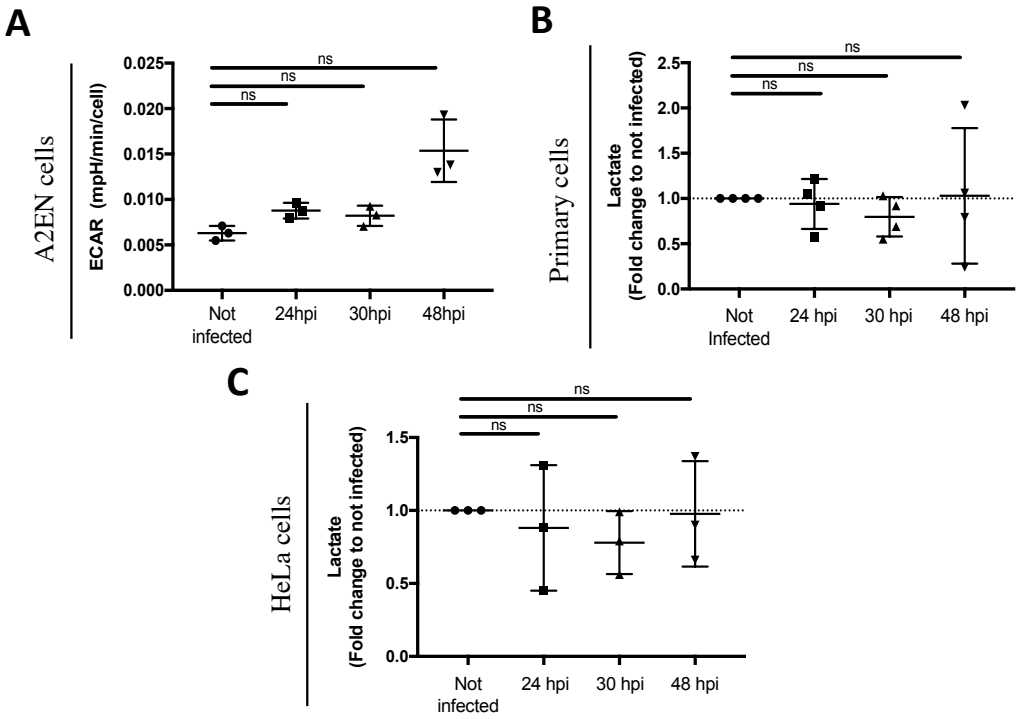

Figure 29 *C. trachomatis* infection does not significantly affect glycolysis
(**A**) A2EN cells were infected with CTDm for 24, 30 and 48 hpi followed by ECAR measurements as described in the methods. (**B**) Basal lactate levels were measured in HeLa and A2EN cells grown for 24 h. Primary cells (**C**) and HeLa cells (**D**) were infected with CTDm for 24, 30 and 48 hpi after what lactate measurements were performed. Significance is defined as: ns (not significant) = $P > 0.05$

In summary, our data indicate that the glycolytic pathway is not significantly up-regulated in epithelial cells infected by *C. trachomatis* serovar D, even at the peak of the metabolic demand.

V. OxPhos is not up-regulated in *C. trachomatis* infected cells

The level of OxPhos in eukaryotic cells is commonly measured by following oxygen consumption rate (OCR, see Figure 28C). *C. trachomatis* has an active respiratory metabolism, and it was estimated that up to 40% of the OCR in infected cells might represent bacterial oxygen consumption (Liang et al., 2018). Thus, basal OCR cannot be used as a read-out of the level of OxPhos in the host. However, the respiratory chain in *C. trachomatis* is very unusual, as it uses a sodium-linked respiratory chain to produce ATP (Liang et al., 2018). Addition of oligomycin, an inhibitor of the ATP synthase (complex V) of the respiratory chain of the host

allows to measure the mitochondrial respiration, as it has no effect on the bacteria that lack complex V. Similarly, addition of the cyanide-4 (trifluoromethoxy) phenylhydrazone (FCCP), an uncoupling agent that collapses the proton gradient, allows to assess the spare respiratory capacity of the host cell, whether infected or not. We thus decided to use these parameters to determine whether OxPhos was modified by infection in primary epithelial cells. We observed no significant difference in the mitochondrial dependent OCR (Figure 30A), nor in the spare respiratory capacity, in CTDm infected cells compared to control cells (Figure 30B). We observed similar results in A2EN cells (Figure 30C, D).

In summary, our data suggest that despite the significant bacterial load specially at late point of infection, cellular respiration remains stable.

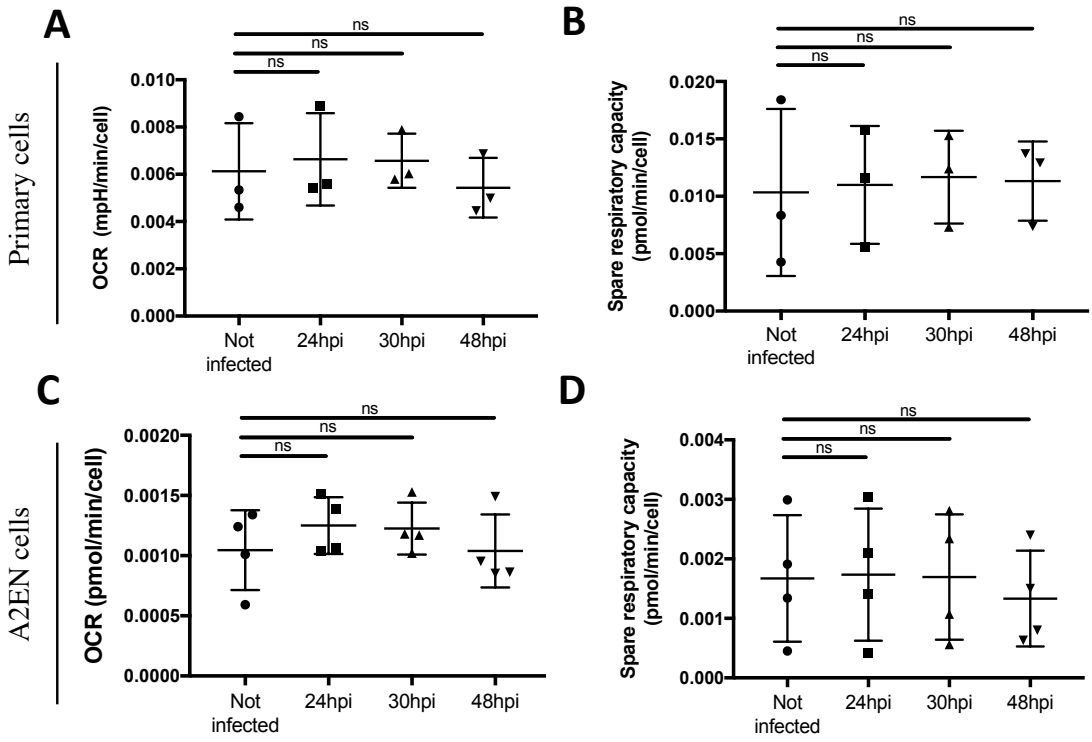

Figure 30. *C. trachomatis* infection does not affect OxPhos in epithelial cells
Primary cells (**A**) (**B**) and A2EN cells (**C**) (**D**) were infected with CTDm for 24, 30 and 48 hpi followed by OCR measurements as described in the methods. For each experiment the spare respiratory capacity was calculated and is reported in (**B**) (**D**). Significance is defined as: ns (not significant) = $P > 0.05$

VI. *C. trachomatis* development is impaired by a LDHA/B inhibitor in primary cells

The absence of up-regulation of glycolysis does not exclude the possibility that the bacteria rely on this pathway to sustain their metabolic need. Unfortunately, there is currently no specific drug that would specifically block glycolysis. Silencing techniques do not work in

the primary epithelial cells (*data not shown*) and their short life-span precludes gene disruption strategy. As shown above (Figure 28A, B), the LDHA/B inhibitor GNE-140 strongly reduces ATP production in A2EN cells, without affecting the mitochondrial oxygen consumption rate. It can be deduced from these observations that GNE-140 likely impairs glycolysis, but not OxPhos. Since the targets of GNE-140, LDHA/B, are absent in *C. trachomatis*, direct effect on the drug on the bacteria is unlikely. We thus decided to measure its effect on infectious progeny.

We first measured the effect of GNE-140 on the ability for the bacteria to undergo a complete developmental cycle. The progeny (IFU) collected after 48 hrs of infection in the absence or presence of the drug was measured by re-infecting fresh HeLa cells and counting the percentage of infected cells one day later. We observed a dose dependent reduction of the infectious progeny in A2EN cells treated with increasing doses of GNE-140, indicating that a functional glycolytic pathway in the host is required for bacterial development (Figure 31A). In mirror of the effect of GNE on IFU production, we observed that increasing concentration of the drug tends to reduce the percentage of infected cells and the mCherry signal in the primary infection (Figure 31B, C), a finding that we confirmed in primary cells (Figure 31D, E).

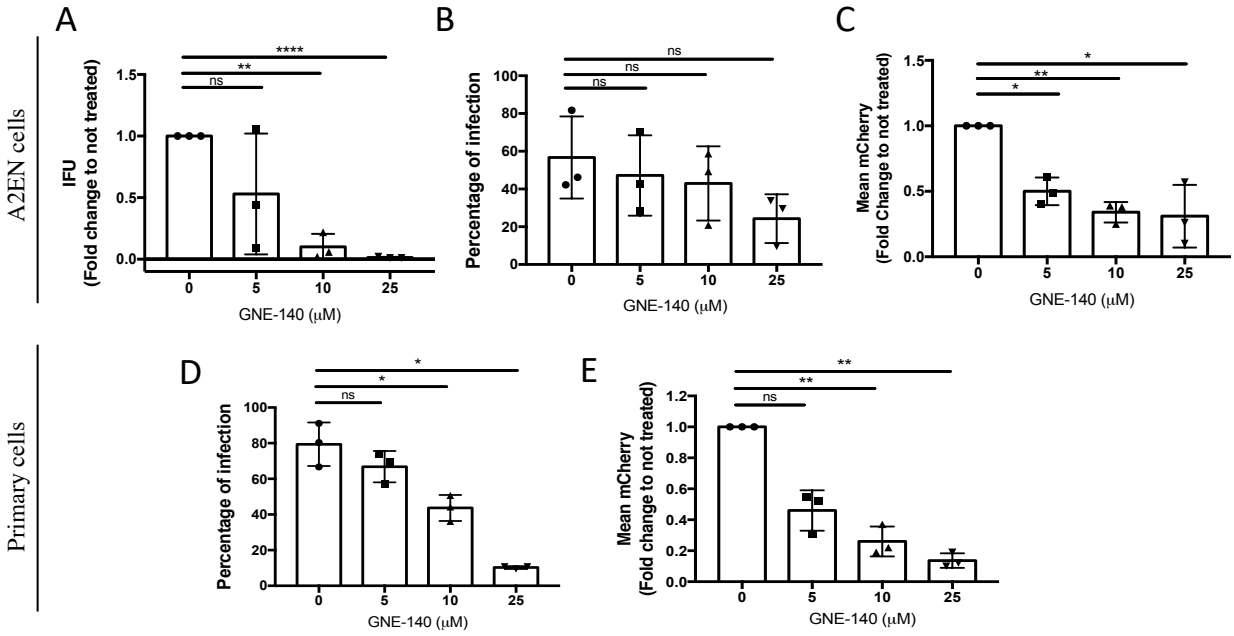

Figure 31. Glycolysis is required for *C. trachomatis* growth
(**A**) A2EN cells were infected with CTDm and treated with indicated concentrations of GNE-140 for 48 h. Cells were lysed and bacterial IFU were determined by re-infecting fresh HeLa cells as described in the methods. After 24 h, duplicate wells were fixed and analyzed by flow cytometry to determine the percentage of infected cells (**B**) and the mean fluorescence (mCherry) of the infected population (**C**). (**D**) (**E**) Primary cells were infected with CTDm and treated with indicated concentrations of GNE-140 for 30 h. Cells were fixed and the percentage of infection (**D**) and the mean mCherry signal (**E**) were determined by flow cytometry analysis. Significance is defined as: ns (not significant) = $P > 0.05$; (*)= $P \leq 0.05$; (**)= $P \leq 0.01$; (***)= $P \leq 0.001$; (****)= $P \leq 0.0001$

The decrease in the percentage of infection upon GNE-140 treatment suggests that establishment of the infection might be impaired. To address this question, we fixed cells 6 hpi in the absence of presence of the drug and stained them for the early inclusion marker Cap1 after a permeabilization step. GNE-140 treatment resulted in a decrease in bacteria clustering near the nucleus. Cap1-positive staining was observed in both non treated and GNE-140 treated cells, but appeared reduced in the drug-treated cells, possibly due to the clustering defect, which dispersed the signal throughout the cell volume. Note that the Cap1 staining is different in A2EN cells (Figure 32A) and HeLa cells (Figure 25), with much longer tubules in the latter. Thus, in GNE-140 treated A2EN cells migration to the MTOC, and inclusion formation were impaired, although some Cap1 synthesis and translocation still occurred.

To know if these early events were the only steps sensitive to the LDHA/B inhibitor, we postponed the addition of the GNE-140 to the culture medium to the mid-developmental stage, i.e. 12 hpi, and measured IFUs 48 hpi (Figure 32B). If anything, we observed a stronger effect of GNE-140 when applied 12 hpi versus at the onset of infection (compare Figure 31A and Figure 32B). The stronger effect is likely due to the drug losing activity with incubation time, and these data demonstrate that GNE-140 also impairs mid- and late steps of the *C. trachomatis* developmental cycle. Altogether, these observations indicate that host glycolysis is required to sustain multiple steps of *C. trachomatis* development.

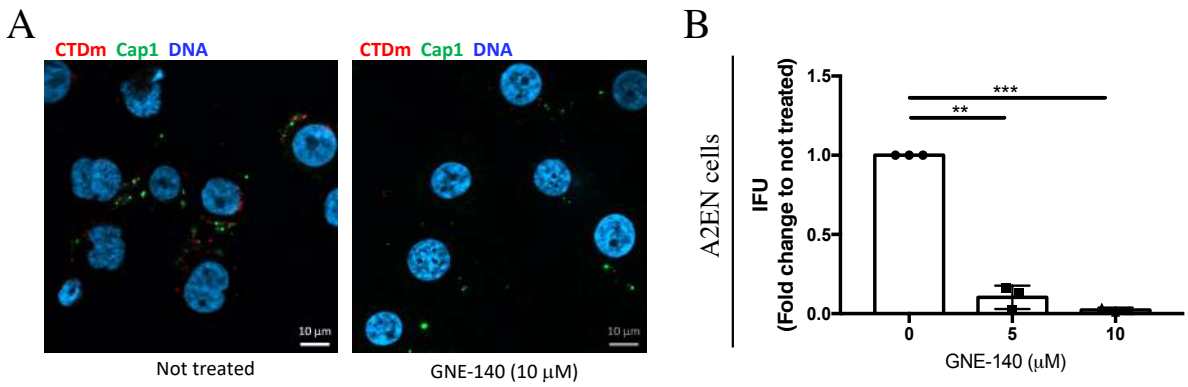

Figure 32. Glycolysis is required for early development steps of *C. trachomatis* in epithelial cells
(**A**) A2EN cells were infected CTDm and treated or not with 10 µM GNE-140. Cells were fixed 6 hpi then permeabilized before immunostaining with anti-Cap1 followed with Alexa488-conjugated secondary antibodies. DNA is stained with Hoechst. (**B**) A2EN cells were infected with CTDm and treated with indicated concentrations of GNE-140 12 hpi. Progeny assay was performed 48 hpi as described in the methods, and IFU was determined. Significance is defined as: ns (not significant) = $P > 0.05$; (*)= $P \leq 0.05$; (**)= $P \leq 0.01$; (***)= $P \leq 0.001$

Interestingly, GNE-140 had no significant effect on IFU production in HeLa cells (Figure 33A), even at concentration of 25 µM that completely blocked lactate production in this cell line (Figure 27A). 10 µM GNE-140, which strongly impaired early steps of infection in A2EN, had no effect on bacteria distribution and Cap1 secretion in HeLa (Figure 33B). Consistent with these findings, silencing glucose phosphate isomerase (GPI), one of the early enzymes that control the flux into the glycolytic pathway, had no effect on progeny in HeLa cells (Figure 33C). Efficiency of the siRNA was confirmed by running a lactate assay (Figure 33D). To test another cell line, we used epithelial cell line derived from the human colon, LS174T, in which *GPI* has been knock-out. These KO cells have been well-characterized and rely only on OxPhos for growth (de Padua et al., 2017). When IFU were titrated 48 hpi on two independent *GPI* KO clones, no difference was found compared to IFU obtained from infecting the parental wild-type LS174T cells (Figure 33E). Thus, the reliance of *C. trachomatis* on the glycolytic pathway was observed in A2EN and primary cells but not in two cell lines of tumoral origin. Another important implication of the absence of effect of GNE-140 on progeny in HeLa cells is that it rules out the possibility that its effect on progeny in A2EN cells was due to an off-target effect of the drug on the bacteria.

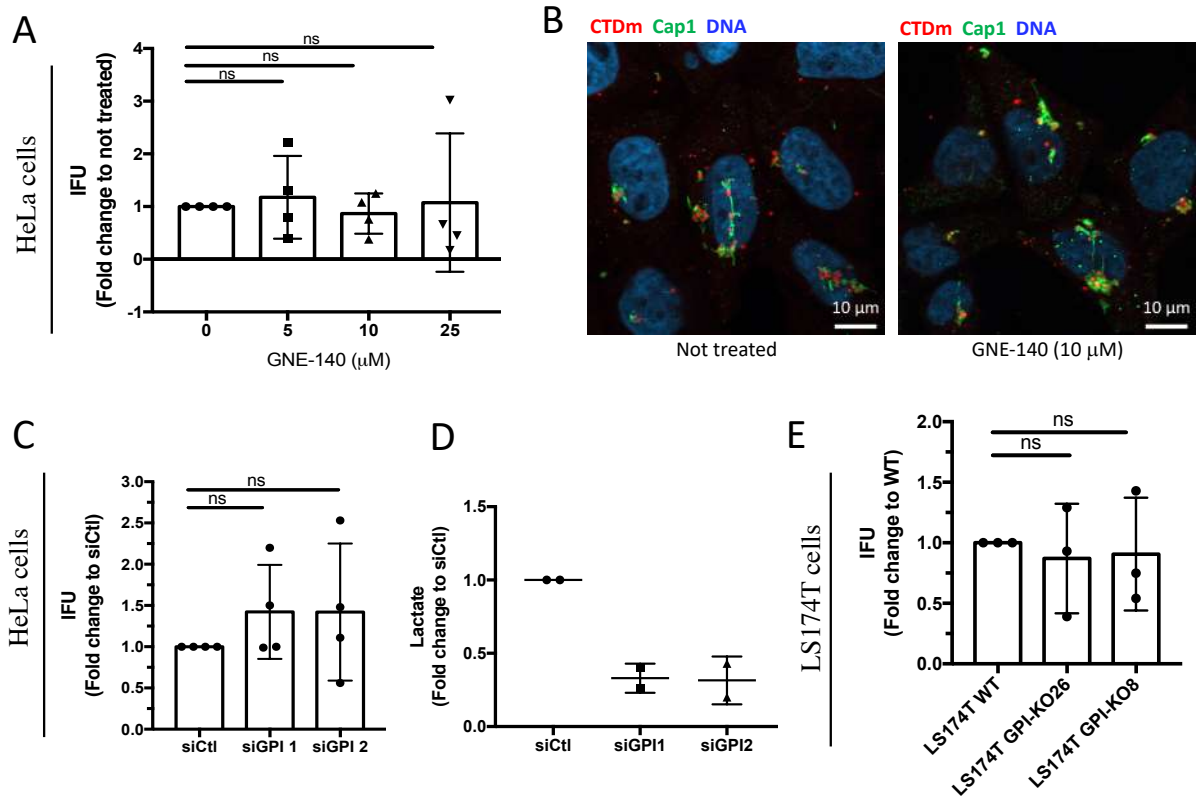

Figure 33. Glycolysis requirement for *C. trachomatis* growth is by-passed in two cancer cell lines
(**A**) HeLa cells were infected with CTDm and treated with indicated concentrations of GNE-140 for 48 h before a progeny assay was performed as described in the methods, and IFU was determined. (**B**) HeLa cells were infected CTDm and treated or not with 10 M GNE-140. Cells were fixed 6 hpi then permeabilized

before immunostaining with anti-Cap1 followed with Alexa488-conjugated secondary antibodies. DNA is stained with Hoechst. (**C**) GPI was silenced in HeLa cells with two siRNA for 48 h before cells were infected with CTDm. 30 hpi a progeny assay was performed, and IFU was determined. (**D**) Efficiency of siRNA treatment was evaluated through a lactate assay 48 h following siRNA treatment in HeLa cells. (**E**) LS174T WT or GPI-KO (clone #26 and #8) were infected with CTDm for 48 h before performing a progeny assay and determining IFU. Significance is defined as: ns (not significant) = $P > 0.05$; (*)= $P \leq 0.05$; (**)= $P \leq 0.01$; (***)= $P \leq 0.001$; (****)= $P \leq 0.0001$

VII. OxPhos inhibition impairs bacterial proliferation but not the early steps of development.

The absence of up-regulation of mitochondrial respiration does not exclude the possibility that the bacteria rely on this pathway to sustain their metabolic need. To address this question, we measured the effect of the OxPhos inhibitors oligomycin and phenformin on *C. trachomatis* developmental cycle. We observed a dose dependent reduction of the progeny for both drugs, with already 60-75 % reduction of the number of infectious particles collected from A2EN 48 hpi when the culture had been done in the presence of 0.5 μM oligomycin (Figure 34A) and 10 μM phenformin (Figure 34B). To directly measure the effect of these drugs on bacterial proliferation we used qPCR to estimate the relative number of bacterial genomes in the different culture conditions. We observed a similar decrease in the number of genomes as in the number of IFUs, indicating that the drop in IFU when OxPhos was impaired was reflecting a decrease in bacterial numbers at the previous infection round (Figure 34C).

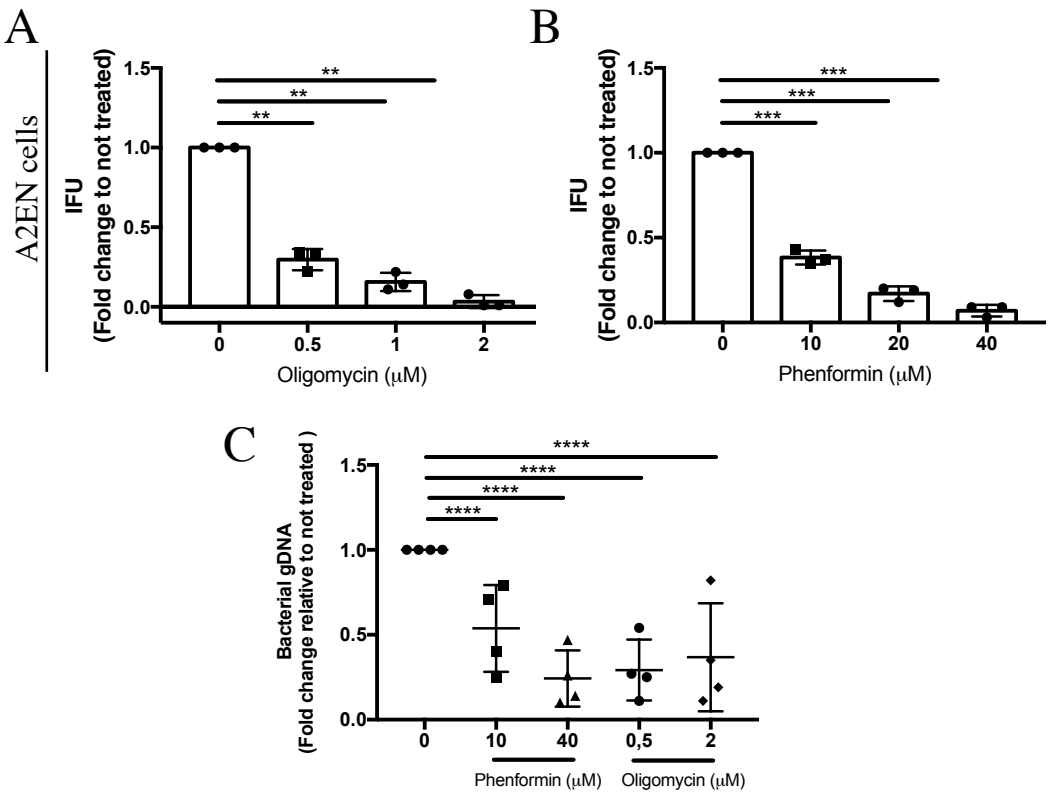

Figure 34. OxPhos is required for *C. trachomatis* growth
A2EN cells were infected with CTDm and treated with indicated concentrations of oligomycin (**A**) or phenformin (**B**). A progeny assay was performed for 48 hpi as described in the methods, and IFU was determined. (**C**) A2EN cells were infected with CTDm and treated with indicated concentrations of oligomycin or phenformin for 48 h. Cells were lysed for DNA extraction and samples were analyzed by qPCR. Bacterial load was determined by quantifying the bacterial *glgA* gene and normalizing it to cell number using the *36B4* gene. Significance is defined as: ns (not significant) = $P > 0.05$; (*)= $P \leq 0.05$; (**)= $P \leq 0.01$; (***)= $P \leq 0.001$; (****)= $P \leq 0.0001$

Interestingly, the presence of phenformin or oligomycin did not affect the percentage of infection in A2EN, although there was a trend to a decrease in the percentage of infected cells upon treatment with 2 μM oligomycin (Figure 35A). This observation indicated that the early steps of development proceeded normally even when OxPhos was not at full capacity. Indeed, inclusions fixed 6 hpi in the presence of 1 μM oligomycin (a concentration that resulted in 80% drop in IFUs, Figure 34A) displayed normal features of development, with the bacteria clustered at the MTOC, surrounded with Cap1-positive tubules (Figure 35B). At 2 μM oligomycin, failure of the bacteria to cluster started to appear. Finally, we postponed the addition of oligomycin to 12 hpi, and measured the impact on IFUs at 48 hpi (Figure 35C). As in the case of GNE-140, we observed an even stronger reduction in IFUs when the drug was applied during the proliferation phase instead of at the onset of infection (see Figure 34A for

comparison), likely because the efficacy of the drug wears off during the incubation time. These data confirm the importance of OxPhos to sustain bacterial replication in epithelial cells.

Altogether, these experiments show that OxPhos needs to work at full capacity to sustain bacterial proliferation in epithelial cells. However, the early steps of infection are more tolerant to suboptimal OxPhos.

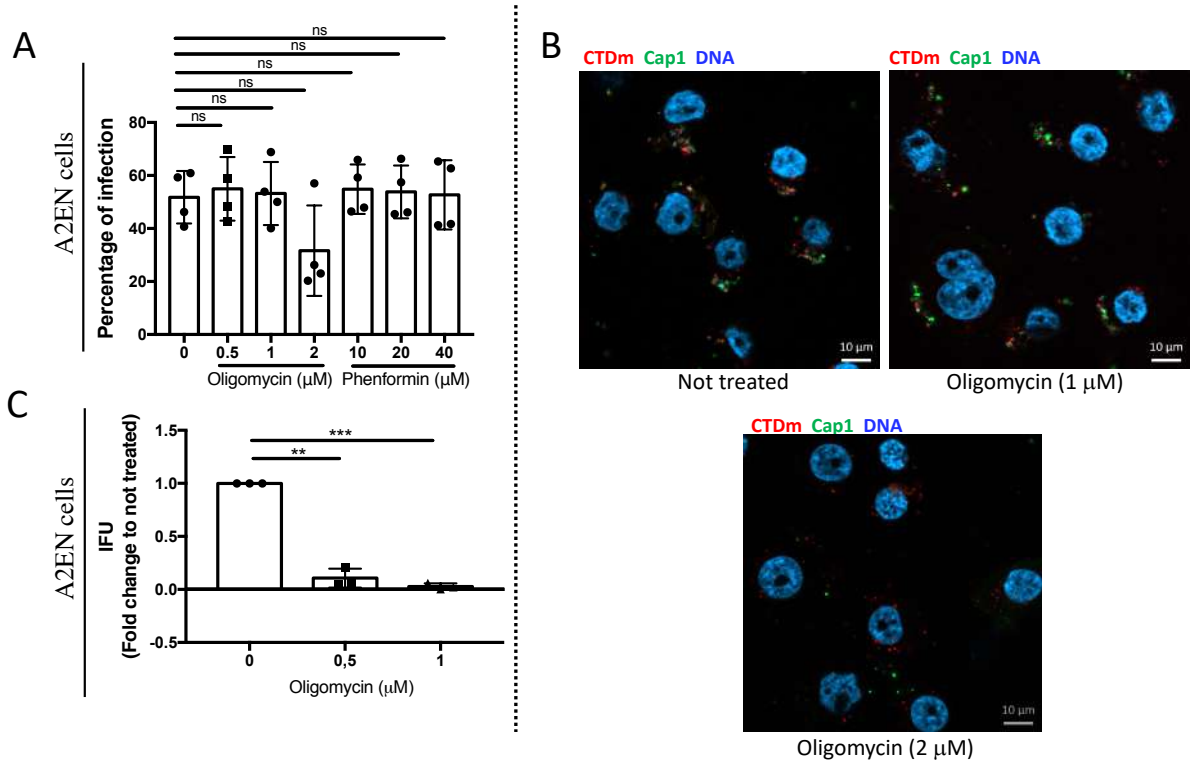

Figure 35. OxPhos is mostly required in the late phases of *C. trachomatis* developmental cycle
(**A**) Percentage of infected cells was measured 24 h following CTDm infection and oligomycin or phenformin treatment of A2EN (**B**) A2EN cells were infected CTDm and treated or not with 1 µM oligomycin. Cells were fixed 6 hpi then permeabilized before immunostaining with anti-Cap1 followed with Alexa488-conjugated secondary antibodies. DNA is stained with Hoechst. (**C**) A2EN cells were infected with CTDm and treated with indicated concentrations of oligomycin 12 hpi. Progeny assay was performed 48 hpi as described in the methods, and bacterial titer was determined. Significance is defined as: ns (not significant) = $P > 0.05$; (*)= $P \leq 0.05$; (**)= $P \leq 0.01$; (***)= $P \leq 0.001$; (****)= $P \leq 0.0001$

Discussion

At the start of this doctoral work, we made the hypothesis that *C. trachomatis* manipulated the metabolism of its host to produce the energy needed for the bacterial development. This hypothesis was mainly based on observations and speculations:

- The bacteria have been described to have a limited capacity for ATP production of their own, with their truncated TCA cycle (Stephens, 1998). They express an ATP transporter, indicating that they at least partly depend on ATP supply by the host (Tjaden 1999). In agreement with that, supply of ATP in the axenic medium is required for protein synthesis in RBs (Omsland et al., 2012).
- Some data in the literature reviewed in the introduction indicated that glycolysis might be up-regulated. However, these data needed to be taken with caution as they were mostly obtained in the cancerous cell line HeLa, and some were actually obtained with other species than *C. trachomatis*.
- Finally, it was tempting to make a parallel between infected cells and cancer cells: both face a need for increased consumption of some metabolites, to sustain bacterial growth in one case, and cellular proliferation in the other case. This parallel suggested that infected cell may undergo a metabolic shift towards high glycolysis, even in the presence of oxygen, as observed in tumoral cells.

Against our expectations, we observed that glycolysis and OxPhos remained very stable in infected epithelial cells, as we will discuss in detail below. The second question we asked was which of these ATP generating pathway, if any, was required for bacterial development, and at which step. Although glycolysis is rather low in primary cells, compared to tumor cells, it seems to be required throughout bacterial development, including early steps, while OxPhos was mostly important for the proliferative phase. Before discussing the data that led to these conclusions, and their implications, we will comment on the bacterial model that we used to obtain these results and we characterized in this work, i.e. *C. trachomatis* serovar D stably transformed with the *C. trachomatis* plasmid expressing the gene coding for mCherry.

I. Plasmid mCherry expressing bacteria display enhanced infectivity

This study was conducted with a serovar of *C. trachomatis* more representative of the circulating sexually transmitted infections that the more commonly used L2 serovar. For practical reasons, we generated a CTDm strain stably transformed with a *C. trachomatis* L2

derived plasmid engineered to constitutively express the fluorescent protein mCherry. As previously shown for GFP expressing *C. trachomatis* L2, it enabled us to easily quantify infected cells by flow cytometry. However, unlike GFP (Vromman et al., 2014), the mCherry signal was slightly too weak for reliable detection by immunofluorescence on single EBs. Interestingly, we observed that the fluorescent bacteria were more infectious than the parental ones, due to enhanced attachment and intracellular growth. This is in contrast to stably transformed serovar L2 strains, that did not differ from the parental strain for these two parameters (Vromman et al., 2014). To the best of our knowledge this is the first detailed investigation of the difference *in vitro* between a plasmid-bearing parental strain and the transformed strain for a non LGV strain. In the LGV serovars of *C. trachomatis*, in which transformation protocols were initially implemented, comparison of parental and transformed strains led to the conclusion that there was no significant difference in infectivity (Agaisse and Derré, 2013; Wang et al., 2011). Importantly, LGV strains are more infectious than the ocular or other genital serovars *in vitro*. It might be that the advantage provided by the transformation is not significant in the LGV background, that is proliferate already extremely efficiently in tissue culture.

We measured that the CTDm contained on average 3-fold more copies of the plasmid than the parental bacteria. The chlamydial plasmid was shown to provide a selection advantage over plasmid-free bacteria *in vitro* and *in vivo* (Russell et al., 2011). In particular Pgp3, one of the eight proteins coded by this plasmid, is required for full virulence *in vitro* and *in vivo* (Liu et al., 2014) and might be exposed on the EB surface (Hou et al., 2015). Thus, increase in Pgp3 expression might account for the enhanced infectivity observed with the fluorescent strain. It is unknown whether the increase in plasmid copy number accounts for the increase in inclusion size we observed, and if so, by which mechanism. Plasmid-free bacteria lose their ability to store glycogen in the inclusion lumen, and display different inclusion morphology (Miyashita et al., 2000). This original study does not report on difference in inclusion growth in the absence of plasmid, but one study measuring the number of genome copy in a plasmid-less strain of the ocular serovar A also observed a decrease in the replication rate in the first half of infection compared to the parental strain (Porcella et al., 2015). In any case, we concluded from these preliminary experiments that, if anything, the fluorescent bacteria might exert a metabolic pressure slightly earlier than the parental strain, and make a suitable and convenient tool to study the intracellular development of *C. trachomatis* serovar D.

II. *C. trachomatis* infection does not significantly modify glycolysis nor OxPhos

As explained above, we expected the need for ATP of the bacteria to translate into a manipulation of at least one of the two main ATP generating pathways in host cells, glycolysis and OxPhos. Surprisingly, we observed stability for both pathways. This was measured in particular at 30 hpi, which is estimated to correspond to the peak of the metabolic demand. The measure of ECAR indicate that there might be a small increase in glycolysis, however this was not confirmed when directly measuring lactate production, which constitute a more direct readout of the shift of pyruvate consumption by fermentation rather than OxPhos.

Contrasting with our observation, increase in ATP level was reported in HeLa cells infected for 8 h with *C. trachomatis* (Kurihara et al., 2019), an observation we did not reproduce. Moreover, at odds with our observations, mitochondrial activity was reported to increase in CTD infected HeLa cells at 24 hpi (Shima et al., 2021). The main difference between these studies and ours is the cellular background. Our results provide several illustrations of the difference in basal metabolism between HeLa cells and primary epithelial cells, and it is likely that infection has different effects on the metabolism of these two cell types. These difference in cell type might also explain the increase in lactate observed late in infection in HeLa cells (Rother et al., 2018) but not in primary cells.

Interestingly, while our data indicate that glycolysis remains fairly stable in cells infected by *C. trachomatis*, at least one glucose-derived pathways is up-regulated by infection. Indeed, we demonstrated that the hexosamine biosynthesis pathway (HBP) is boosted upon infection both in HeLa cells and in primary epithelial cells (Maffei et al., 2020). This occurs through the activation of a host enzyme called transglutaminase 2 (TG2), which modifies GFPT, the enzyme controlling entry into HBP, and increases its activity. Moreover, several studies have demonstrated that preservation of the pentose phosphate pathway is a key to a successful infection. Siegl et al. (2014) proved that PPP downregulation interfered with bacterial development (Siegl et al., 2014). And Rother et al. (2018) demonstrated that inhibition of the purine synthesis pathway, which is downstream the PPP, is detrimental for bacterial development (Rother et al., 2018). Whether this pathway is upregulated has not been investigated. The phosphoribosyl pyrophosphate amidotransferase (PPAT) enzyme, which converts the activated form of ribose 5 phosphate (R5P), phosphoribosyl pyrophosphate (PRPP), into 5'-phosphoribosylamine (PRA) could be the target of *C. trachomatis* infection as we identified it as another putative substrate of TG2. During my PhD, I started investigating

this question. However, my data remain very preliminary at this stage, and the question will need further work.

III. Individual EB display limited autonomy in the initiation of infection

Glycogen synthesis genes are present in all known families of *Chlamydiae*, including *Estrella lausannensis* and *Waddlia chondrophila*, which use a very original pathway for its synthesis (Colpaert et al., 2021). This observation is surprising since glycogen metabolism loss appears to be universal to most if not all obligate intracellular bacterial pathogens or symbionts that went through genome reduction throughout evolution (Henrissat et al., 2002). This strongly suggests that glycogen plays an essential role in the developmental cycle of *Chlamydia*e. In *C. trachomatis*, proteomics studies have shown a very strong enrichment for enzymes involved in glycogen synthesis and degradation in EBs compared to RBs (Saka et al., 2011). Indeed, glycogen was shown to only be present in EBs (Gehre et al., 2016). These observations support the hypothesis that EBs, more than RBs, uses glycogen to sustain their metabolic need.

We demonstrated that the phosphoglucomutase activity in *C. trachomatis* is exerted by the protein CT295, and not by the related protein CT815. CT295 is one of the metabolic enzymes enriched in EBs (Saka et al., 2011). Catabolism of intra-bacterial glycogen into G1P, and conversion to G6P with CT295, should allow to feed the glycolysis pathway and generate ATP during the extracellular stage, and in the very early stages of intracellular development, when import of host ATP has not been put in place yet. We thus hypothesized that EBs might have some degree of autonomy, and that early steps of infection might occur normally even if glycolysis or oxidative phosphorylation were not functioning at full capacity.

We first investigated this question in HeLa cells, as we could use glucose-free medium to bridle the access of EBs to glucose (a glucose-free formulation for the KSF medium used to grow A2EN or primary epithelial cells does not exist). As expected from previous work, 6 hpi most bacteria were clustered at the MTOC in HeLa cells, and numerous, long Cap1-positive tubules emanating from the inclusion were observed. In glucose-deprived cultures, the bacteria were more dispersed, and the tubules were fewer and shorter. The detection of Cap1, even in the absence of glucose, confirms that the EBs have some metabolic autonomy that allow them to transcribe and express at least some of the early genes of their developmental cycle. However, we observed that several steps of the early development of the bacteria, such as clustering to the MTOC or inclusion formation were affected by glucose deprivation.

Motor-driven transport along microtubules and fusion with host compartments for building the inclusion membrane are host-driven processes that require energy. Thus, we hypothesized that the sensibility of the early steps of development to glucose deprivation is related to the drop of ATP we observed in glucose-deprived cells. Experiments in A2EN corroborated this hypothesis. Indeed, in that cellular background, GNE-140 treatment also decreased bacterial clustering and Cap1 secretion, while OxPhos inhibition did so only at high drug concentration. These phenotypes correlated with the effect of these drugs on ATP levels in the host, with GNE-140 inducing a sharp decrease in ATP, even as early as 2 h after treatment, while OxPhos inhibitors had a milder effect. Also, in HeLa cells, 10 μM GNE-140 does not affect ATP levels and does not affect the initiation of infection. This experiment is an important control since it allows us a rule out a direct effect of the drug on the bacteria.

A rapid effect of GNE-140 on ATP levels was also observed in a pancreatic cell line within 6 h of treatment with 10 μM of GNE-140 (Boudreau et al., 2016). We did not expect this strong effect in the primary cells nor in A2EN cells, since they have low glycolysis activity, but our data suggest that this activity contributes to the majority of ATP production in these cells. Consistent with this conclusion, OxPhos inhibitors had a lower impact on ATP levels in A2EN cells than GNE-140.

We concluded from these observations that EBs exhibit some degree of metabolic autonomy, but heavily rely on energy-driven processes of the host to establish the nascent inclusion. It should be noted that Omsland and al. showed that G6P needs to be added to the axenic medium to detect a significant protein synthesis activity over a 6 h incubation period, suggesting that autonomous metabolic capacity of EBs might be limited, at least in these experimental conditions (Omsland et al., 2012).

IV. Reliance on glycolysis and OxPhos for intracellular replication

The next question we investigated was the requirement for glycolysis and OxPhos for a successful infection in epithelial cells.

In A2EN cells, we had no other mean of intervention on glycolysis than the use of the chemical inhibitor GNE-140, as other "glycolysis inhibitors" have pleiotropic effects, and gene silencing or disruption did not work in this cell line. We showed that 10 μM GNE-140 induced a rapid and significant drop in ATP levels in A2EN without affecting OxPhos, implicating that it blocks glycolysis-driven ATP production. We need to keep in mind that GNE-140 affects a

step downstream of glycolysis, meaning that glycolytic intermediates may still be present and even increased in GNE-140 treated cells, as was shown in a pancreatic cell line (Boudreau et al., 2016). Our data indicate that glycolysis is required not only to enable the formation of nascent inclusions, as discussed above, but also to sustain the proliferative stage of the development. Indeed, inhibition LDH A/B, either from the beginning or during mid-stages of infection, severely reduced bacterial progeny measured 48 hpi. Importantly, treatments with 10 μM GNE-140 had no effect on bacterial progeny in HeLa cells, ruling out the possibility that the drug is acting directly on the bacteria. Considering the strong effect of GNE-140 on ATP levels in primary cells, it is likely that GNE-140 delays bacterial replication by limiting bacterial access to host ATP.

Nevertheless, we cannot exclude the possibility that the effect of GNE-140 treatment is linked to other metabolic changes. Indeed, on one hand, GNE-140 treatment induces an accumulation of some PPP intermediates which could be utilized for bacterial nucleotides synthesis and higher ROS levels which has been described as beneficial for the bacteria, through HIF-1α activation (Prusty et al., 2012). On the other hand, GNE-140 treatment also decreases NAD^+/NADH ratio, with both a decrease in NAD^+ and an increase of NADH, which could be detrimental to bacterial development, as discussed below. Furthermore, a recent study demonstrated that three glycolytic enzymes, aldolase A, pyruvate kinase (PK) and lactate dehydrogenase (PDH), were enriched at the inclusion membrane, and the former was proven to be important for inclusion formation and bacterial development. The authors suggested that recruitment of host glycolytic enzymes at the inclusion membrane could be a way by which the bacteria have an easier access to ATP or small metabolites produced through the glycolytic pathways or to nucleotides produced vis the PPP (Ende and Derré, 2020). GNE-140 treatment might affect the localization of these enzymes, so that even if the intermediates of glycolysis are still being made in the presence of the drug, they might have lost in accessibility for the bacteria.

Our data show that OxPhos is also required for bacterial growth in primary epithelial cells, as two distinct OxPhos inhibitors decreased IFU production in a drug dependent manner. Early studies by Gill and Stewart (1970) and Becker and Asher (1972) had demonstrated that inhibiting mitochondrial function reduces bacterial load in L-cells (Becker and Asher, 1972). However, the debate was still open since Tipples and McClarty (1993) showed that *C. trachomatis* grew normally in a cell line deficient of mitochondrial function, concluding that mitochondrial ATP was dispensable (Tipples and McClarty, 1993). A more recent work in

HeLa cells showed that infection preserves the mitochondrial network by upregulating the microRNA, miR-30c leading to a p53-mediated downregulation of the mitochondrial fission regulator Drp1, and that mitochondrial ATP is required for bacterial development (Chowdhury et al., 2017). Reduction of inclusion size upon oligomycin treatment in HeLa cells was also reported by Liang et al. (2018).

Together with our own observations made in primary and A2EN cells we can conclude that OxPhos needs to function at full capacity in the host for optimal *C. trachomatis* growth. The requirement for both OxPhos and glycolysis for the replication phase of the *C. trachomatis* supports the hypothesis that they are indeed partly metabolically dependent on their host, especially for this step of their development. Of course, the bacterial need for host ATP might again be the reason for the effect of the drugs on bacterial proliferation. However, the comparison of the effect of GNE-140 and oligomycin on progeny and on ATP level call for additional explanations. Indeed, when applied 12 hpi, 0.5 μM oligomycin reduced IFUs by 95% while 5 μM GNE did so by 90%. However, 0.5 μM oligomycin reduced ATP levels in 24 h by only 20%, when 5 μM GNE did so by 50%. One metabolic imbalance caused by blocking OxPhos that is likely to affect bacterial growth is the decrease in NAD^+ regeneration. Indeed, NAD is essential in bacterial development, and a wide variety of pathogens have developed ways to steal it or it precursors from their host (Mesquita et al., 2016). *C. trachomatis* uses its ATP/ADP transporter, Ntp1, for NAD transport (Fisher et al., 2013) and increasing presence of NADH and NAD(P)H in the inclusion has been demonstrated by fluorescence lifetime imaging (Szászák et al., 2011). Reduction in NAD import from the host is expected to limit oxidative phosphorylation in the bacteria, thereby affecting their growth. Imbalance of other metabolites in the host as a consequence of OxPhos inhibition might also contribute to the strong decrease in IFUs observed.

A crucial observation we made during this project was the importance of using either primary cells, or cells with a background close to those, in our case A2EN cells, in order to perform metabolic investigations. In fact, inhibition of the glycolytic pathway in two cell lines, HeLa cells and LS174T cells, using either gene silencing or gene disruption, had no impact on CTDm progenies. Inhibition of LDH A/B had also no effect in HeLa cells, while it had a strong effect on progenies in A2EN cells. There are advantages to using cell lines compared to primary cells, especially an easier access to them, which is one major difficulty we faced during this project. However primary cells reflect better physiological conditions as they retain cell physiology and important *in vivo* function and markers (Alge et al., 2006; Pan et al., 2009).

HeLa cells are cancer cells with upregulated glycolysis. Still, OxPhos inhibitors had a strong effect on ATP levels. Thus, OxPhos is the major contributor to their ATP levels a conclusion already documented for multiple cancer cell lines, including HeLa cells (Guppy et al., 2002; Zu and Guppy, 2004; Rodriguez-Enriquez et al., 2006; Moreno-Sánchez et al., 2007).

V. What about other intracellular bacteria?

While we concluded here that *C. trachomatis* has little effect on glycolysis and OxPhos in primary epithelial cells, what was observed in the case of other intracellular bacteria, and are these pathways important for bacterial growth? These questions were essentially addressed in macrophages, which are the targets of many intracellular pathogens. A common theme that emerges is that infection commonly upregulates glycolysis, a phenomenon which is required to mount the host inflammatory response to infection (Pearce and Pearce, 2013). Many pathogens have evolved strategies to dampen this shift to glycolysis in the host, thereby limiting the inflammatory response. One recent report shows that *Mycobacterium tuberculosis* infection of macrophages limits metabolic reprogramming over time through sustained induction of anti-inflammatory microRNA-21 (miR-21). This microRNA represses the expression of the phosphofructokinase muscle (PFK-M) isoform, thereby slowing down glycolysis and the production of pro-inflammatory mediators (Hackett et al., 2020). The enhancement of the inflammatory response to infection through the metabolic reprogramming of macrophages is also observed in the case of infection by *Salmonella enterica* serovar Typhimurium. To adapt to that shift to aerobic glycolysis, *Salmonella typhimurium* developed a strategy to promotes its survival by sensing shift in levels of the TCA cycle intermediate succinate, which activates its virulence (Rosenberg et al., 2021). Another recent report described that decreased glucose levels in the macrophages, upon increase in glycolysis, lead to upregulated bacterial uptake of 2- and 3-phosphoglycerate and phosphoenolpyruvate (carbon sources), while increased pyruvate and lactate levels induce upregulation of a pathogenicity island known to encode virulence factors (Jiang et al., 2021). The facultative intracellular bacteria *Francisella tularensis* mainly rely on host amino acid as major gluconeogenic substrates (Ziveri et al., 2017). Inhibition of glycolysis in the macrophage is also important for the bacteria to counteract host defense, a process that requires the capsule. Interestingly, inhibition of glycolysis is also required for early replication of virulent *Francisella* (Wyatt et al., 2016).

Thus, in these cases, the shift to glycolysis is part of the host response to limit infection but can in some cases be exploited by the bacteria to increase its virulence. A favorable consequence of the increase in glycolysis has also been described for the facultative intracellular pathogen *Legionella (L.) pneumophila*. Its effector protein MitF was shown to induce mitochondrial fission in human monocyte-derived macrophages. This leads to a reduction in OxPhos, while glycolysis is upregulated (Escoll et al., 2017). The authors concluded to a Warburg effect in the host cells, that would be necessary to sustain bacterial growth. Up-regulation of glycolysis was also reported in bone marrow-derived macrophages infected with *L. pneumophila,* as well as a sensitivity of the bacteria to the glucose derivative 2-DeoxyGlucose (2-DG) which cannot enter glycolysis (Price et al., 2018). However, it was shown that bacterial sensitivity to 2-DG is only due to its hexose-phosphate transporter UhpC sensitivity to the drug. Indeed, pathogens deficient for UhpC grew normally in bone marrow-derived macrophages in the presence of 2-DG Further investigation showed that inhibition of macrophage glycolysis had only a marginal effect on intracellular *L. pneumophila* replication, bringing the authors to the conclusion that *L. pneumophila* can employ diverse metabolic strategies to exploit its host cells.

The difficulty to obtain primary epithelial cells might explain why only few studies have tried to address the metabolic changes occurring upon infection in this cell type. One precursor study was conducted by the Bumann lab, and although it mostly used HeLa cells, several of the conclusions were validated in human umbilical vein endothelial cells (Kentner et al., 2014). Using metabolomics, proteomics, and genetic experiments to examine the metabolism of the facultative intracellular bacterium *Shigella flexneri* and that of epithelial host cells, the authors came to the conclusions that "infected host cells maintain largely normal fluxes through glycolytic pathways, but the entire output of these pathways is captured by *Shigella*, most likely in the form of pyruvate. This striking strategy provides *Shigella* with an abundant favorable energy source, while preserving host cell ATP generation, energy charge maintenance, and survival, despite ongoing vigorous exploitation". These conclusions are very similar to our own regarding *C. trachomatis* infection in epithelial cells. More studies on infection in epithelial cells are necessary to generalize this picture. However, coming back to the case of *C. trachomatis*, that engage in long-term relationship with their epithelial host cells, and capture a lot of glucose as glycogen in the inclusion lumen as a carbon source, there might simply not be sufficient glucose to also shift the host metabolism towards glycolysis.

Finally, it is intriguing to note that the fine metabolic equilibrium reached by *C. trachomatis* and epithelial cells of the genital tract might be achieved by different means with

other *Chlamydia* species, even among the same family of *Chlamydiaceae*. Indeed, we have demonstrated that CT295 plays the role of chlamydial phosphoglucomutase, and that its secretion in the lumen of the inclusion accounts for conversion of G1P to G6P, that can be taken up by the bacteria through UhpC. Surprisingly, we found that this ability to convert G1P to G6P in the lumen of the inclusion is limited to a few *Chlamydiaceae* (*C. trachomatis, C. muridarum, C. suis*), which are also the only known chlamydiae to accumulate glycogen in the inclusion lumen. This probably reflects different metabolic strategies between these species. Interestingly, among *Chlamydiaceae*, some species like *C. psittaci* display inclusions surrounded by mitochondria, while others like *C. pneumoniae* or *C. trachomatis* do not (Matsumoto et al., 1991). Another indication that *Chlamydiaceae* species have adopted different metabolic strategies is that *C. pneumoniae* growth is promoted in hypoxic conditions, i.e. when mitochondrial functions are impaired, while hypoxia had no effect on *C. trachomatis* progeny in primary cells derived from Fallopian tubes (Käding et al., 2017; Roth et al., 2010). Furthermore, silencing the ATP synthase promoted *C. pneumoniae* growth in both normoxia and hypoxia (Käding et al., 2017), while we observed here that OxPhos is essential for optimal growth of *C. trachomatis*. Thus, we anticipate that the fine metabolic equilibrium reached by *C. trachomatis* and epithelial cells of the genital tract might not hold true for other *Chlamydia* species, and might play a role in the tissue tropism of this species.

References

1. Abby, S.S., and Rocha, E.P.C. (2012). The Non-Flagellar Type III Secretion System Evolved from the Bacterial Flagellum and Diversified into Host-Cell Adapted Systems. PLoS Genetics 8, e1002983.

2. AbdelRahman, Y.M., and Belland, R.J. (2005). The chlamydial developmental cycle: Figure 1. FEMS Microbiology Reviews 29, 949–959.

3. Abdelrahman, Y., Ouellette, S.P., Belland, R.J., and Cox, J.V. (2016). Polarized Cell Division of Chlamydia trachomatis. PLOS Pathogens 12, e1005822.

4. Abdul-Sater, A.A., Saïd-Sadier, N., Lam, V.M., Singh, B., Pettengill, M.A., Soares, F., Tattoli, I., Lipinski, S., Girardin, S.E., Rosenstiel, P., et al. (2010). Enhancement of Reactive Oxygen Species Production and Chlamydial Infection by the Mitochondrial Nod-like Family Member NLRX1. Journal of Biological Chemistry 285, 41637–41645.

5. Abraham, S., Bang, P., Cheeseman, H.M., Dohn, R.B., Cole, T., Kristiansen, M.P., Korsholm, K.S., Lewis, D., Olsen, A.W., McFarlane, L.R., et al. (2019). Safety and immunogenicity of the chlamydia vaccine candidate CTH522 adjuvanted with CAF01 liposomes or aluminium hydroxide: a first-in-human, randomised, double-blind, placebo-controlled, phase 1 trial. The Lancet Infectious Diseases 19, 1091–1100.

6. Abromaitis, S., and Stephens, R.S. (2009). Attachment and Entry of Chlamydia Have Distinct Requirements for Host Protein Disulfide Isomerase. PLoS Pathogens 5, e1000357.

7. Aeberhard, L., Banhart, S., Fischer, M., Jehmlich, N., Rose, L., Koch, S., Laue, M., Renard, B.Y., Schmidt, F., and Heuer, D. (2015). The Proteome of the Isolated Chlamydia trachomatis Containing Vacuole Reveals a Complex Trafficking Platform Enriched for Retromer Components. PLOS Pathogens 11, e1004883.

8. Agaisse, H., and Derré, I. (2013). A C. trachomatis Cloning Vector and the Generation of C. trachomatis Strains Expressing Fluorescent Proteins under the Control of a C. trachomatis Promoter. PLoS ONE 8, e57090.

9. Agaisse, H., and Derré, I. (2014). Expression of the Effector Protein IncD in Chlamydia trachomatis Mediates Recruitment of the Lipid Transfer Protein CERT and the Endoplasmic Reticulum-Resident Protein VAPB to the Inclusion Membrane. Infection and Immunity 82, 2037–2047.

10. Ajonuma, C.L., Lam Fok, K., Sze Ho, L., Kay Sheung Chan, P., Chow, P.H., Ling Tsang, L., Hau Yan Wong, C., Chen, J., Li, S., Kenneth Rowlands, D., et al. (2010). CFTR is required for cellular entry and internalization of Chlamydia trachomatis. Cell Biology International 34, 593–600.

11. Alge, C.S., Hauck, S.M., Priglinger, S.G., Kampik, A., and Ueffing, M. (2006). Differential Protein Profiling of Primary versus Immortalized Human RPE Cells Identifies Expression Patterns Associated with Cytoskeletal Remodeling and Cell Survival. J. Proteome Res. 5, 862–878.

12. Allan, I., and Pearce, J.H. (1983). Amino acid requirements of strains of Chlamydia trachomatis and C. psittaci growing in McCoy cells: relationship with clinical syndrome and host origin. J Gen Microbiol 129, 2001–2007.

13. Allen, E.G., and Bovarnick, M.R. (1957). ASSOCIATION OF REDUCED DIPHOSPHOPYRIDINE NUCLEOTIDE CYTOCHROME C REDUCTASE ACTIVITY WITH MENINGOPNEUMONITIS VIRUS. Journal of Experimental Medicine 105, 539–547.

14. Al-Younes, H.M., Brinkmann, V., and Meyer, T.F. (2004). Interaction of Chlamydia trachomatis Serovar L2 with the Host Autophagic Pathway. Infection and Immunity 72, 4751–4762.

15. Al-Zeer, M.A., Al-Younes, H.M., Kerr, M., Abu-Lubad, M., Gonzalez, E., Brinkmann, V., and Meyer, T.F. (2014). Chlamydia trachomatis remodels stable microtubules to coordinate Golgi stack recruitment to the chlamydial inclusion surface. Molecular Microbiology 94, 1285–1297.

16. Al-Zeer, M.A., Xavier, A., Abu Lubad, M., Sigulla, J., Kessler, M., Hurwitz, R., and Meyer, T.F. (2017). Chlamydia trachomatis Prevents Apoptosis Via Activation of PDPK1-MYC and Enhanced Mitochondrial Binding of Hexokinase II. EBioMedicine 23, 100–110.

17. An, Y., Wang, J., Li, C., Leier, A., Marquez-Lago, T., Wilksch, J., Zhang, Y., Webb, G.I., Song, J., and Lithgow, T. (2016). Comprehensive assessment and performance improvement of effector protein predictors for bacterial secretion systems III, IV and VI. Briefings in Bioinformatics bbw100.

18. Anastasiou, D., Poulogiannis, G., Asara, J.M., Boxer, M.B., Jiang, J. -k., Shen, M., Bellinger, G., Sasaki, A.T., Locasale, J.W., Auld, D.S., et al. (2011). Inhibition of Pyruvate Kinase M2 by Reactive Oxygen Species Contributes to Cellular Antioxidant Responses. Science 334, 1278–1283.

19. Assrir, N., Richez, C., Durand, P., Guittet, E., Badet, B., Lescop, E., and Badet-Denisot, M.-A. (2014). Mapping the UDP-N-acetylglucosamine regulatory site of human glucosamine-6P synthase by saturation-transfer difference NMR and site-directed mutagenesis. Biochimie 97, 39–48.

20. Bader, J.P., and Morgan, H.R. (1958). LATENT VIRAL INFECTION OF CELLS IN TISSUE CULTURE : VI. ROLE OF AMINO ACIDS, GLUTAMINE, AND GLUCOSE IN PSITTACOSIS VIRUS PROPAGATION IN L CELLS. Journal of Experimental Medicine 108, 617–630.

21. Balana, M.E. (2005). ARF6 GTPase controls bacterial invasion by actin remodelling. Journal of Cell Science 118, 2201–2210.

22. Bannantine, Griffiths, Viratyosin, Brown, and Rockey (2000). A secondary structure motif predictive of protein localization to the chlamydial inclusion membrane. Cellular Microbiology 2, 35–47.

23. Barbour, A.G., Amano, K., Hackstadt, T., Perry, L., and Caldwell, H.D. (1982). Chlamydia trachomatis has penicillin-binding proteins but not detectable muramic acid. Journal of Bacteriology 151, 420–428.

24. Barry, C.E., Brickman, T.J., and Hackstadt, T. (1993). Hc1-mediated effects on DNA structure: a potential regulator of chlamydial development. Molecular Microbiology 9, 273–283.

25. Bastidas, R.J., Elwell, C.A., Engel, J.N., and Valdivia, R.H. (2013). Chlamydial Intracellular Survival Strategies. Cold Spring Harbor Perspectives in Medicine 3, a010256–a010256.

26. Bavoil, P., Ohlin, A., and Schachter, J. (1984). Role of disulfide bonding in outer membrane structure and permeability in Chlamydia trachomatis. Infection and Immunity 44, 479–485.

27. Beatty, W.L. (2006). Trafficking from CD63-positive late endocytic multivesicular bodies is essential for intracellular development of Chlamydia trachomatis. Journal of Cell Science 119, 350–359.

28. Becker, E., and Hegemann, J.H. (2014). All subtypes of the Pmp adhesin family are implicated in chlamydial virulence and show species-specific function. MicrobiologyOpen 3, 544–556.

29. Becker, Y., and Asher, Y. (1972). Obligate Parasitism of Trachoma Agent: Lack of Trachoma Development in Ethidium Bromide-Treated Cells. Antimicrob Agents Chemother 1, 171–173.

30. Bedson, S.P., and Bland, J.O.W. (1932). A MORPHOLOGICAL STU'DY OF PSITTACOSIS VIRUS, WITH THE DESCRTPTION OF A DEVELOPMENTAL CYCLE. Br J Exp Pathol 13, 8.

31. Belland, R.J., Zhong, G., Crane, D.D., Hogan, D., Sturdevant, D., Sharma, J., Beatty, W.L., and Caldwell, H.D. (2003). Genomic transcriptional profiling of the developmental cycle of Chlamydia trachomatis. Proceedings of the National Academy of Sciences 100, 8478–8483.

32. Betts-Hampikian, H.J., and Fields, K.A. (2011). Disulfide Bonding within Components of the Chlamydia Type III Secretion Apparatus Correlates with Development. Journal of Bacteriology 193, 6950–6959.

33. Black, C.M. (2013). Chlamydial Infection_Introduction. In Issues in Infectious Diseases, C.M. Black, ed. (Basel: S. KARGER AG), pp. 1–8.

34. Boncompain, G., Lazarow, P.B., and Subtil, A. (2014). The Intracellular Bacteria Chlamydia Hijack Peroxisomes and Utilize Their Enzymatic Capacity to Produce Bacteria-Specific Phospholipids. PLOS ONE 9, 9.

35. Boudreau, A., Purkey, H.E., Hitz, A., Robarge, K., Peterson, D., Labadie, S., Kwong, M., Hong, R., Gao, M., Del Nagro, C., et al. (2016). Metabolic plasticity underpins innate and acquired resistance to LDHA inhibition. Nat Chem Biol 12, 779–786.

36. Braun, P.R., Al-Younes, H., Gussmann, J., Klein, J., Schneider, E., and Meyer, T.F. (2008). Competitive Inhibition of Amino Acid Uptake Suppresses Chlamydial Growth: Involvement of the Chlamydial Amino Acid Transporter BrnQ. Journal of Bacteriology 190, 1822–1830.

37. Brickman, T.J., Barry, C.E., and Hackstadt, T. (1993). Molecular cloning and expression of hctB encoding a strain-variant chlamydial histone-like protein with DNA-binding activity. Journal of Bacteriology 175, 4274–4281.

38. Bugalhão, J.N., and Mota, L.J. (2019). The multiple functions of the numerous Chlamydia trachomatis secreted proteins: the tip of the iceberg. Microb Cell 6, 414–449.

39. Burnet, F.M., and Rountree, P.M. (1935). Psittacosis in the developing egg. The Journal of Pathology and Bacteriology 40, 471–481.

40. Burton, M.J., and Mabey, D.C.W. (2009). The Global Burden of Trachoma: A Review. PLoS Neglected Tropical Diseases 3, e460.

41. Carabeo, R.A., Grieshaber, S.S., Fischer, E., and Hackstadt, T. (2002). Chlamydia trachomatis Induces Remodeling of the Actin Cytoskeleton during Attachment and Entry into HeLa Cells. Infection and Immunity 70, 3793–3803.

42. Carabeo, R.A., Grieshaber, S.S., Hasenkrug, A., Dooley, C., and Hackstadt, T. (2004). Requirement for the Rac GTPase in Chlamydia trachomatis Invasion of Non-phagocytic Cells: Chlamydial Requirement for Rac. Traffic 5, 418–425.

43. Carabeo, R.A., Dooley, C.A., Grieshaber, S.S., and Hackstadt, T. (2007). Rac interacts with Abi-1 and WAVE2 to promote an Arp2/3-dependent actin recruitment during chlamydial invasion. Cellular Microbiology 9, 2278–2288.

44. Carpenter, V., Chen, Y.-S., Dolat, L., and Valdivia, R.H. (2017). The Effector TepP Mediates Recruitment and Activation of Phosphoinositide 3- Kinase on Early Chlamydia trachomatis Vacuoles. MSphere 2, 15.

45. Chen, D., Lei, L., Lu, C., Flores, R., DeLisa, M.P., Roberts, T.C., Romesberg, F.E., and Zhong, G. (2010). Secretion of the chlamydial virulence factor CPAF requires the Sec-dependent pathway. Microbiology 156, 3031–3040.

46. Chen, H., Wen, Y., and Li, Z. (2019). Clear Victory for Chlamydia: The Subversion of Host Innate Immunity. Frontiers in Microbiology 10.

47. Chen, Y.-S., Bastidas, R.J., Saka, H.A., Carpenter, V.K., Richards, K.L., Plano, G.V., and Valdivia, R.H. (2014). The Chlamydia trachomatis Type III Secretion Chaperone Slc1 Engages Multiple Early Effectors, Including TepP, a Tyrosine-phosphorylated Protein Required for the Recruitment of CrkI-II to Nascent Inclusions and Innate Immune Signaling. PLOS Pathogens 10, 17.

48. Chiarelli, T.J., Grieshaber, N.A., Omsland, A., Remien, C.H., and Grieshaber, S.S. (2020). Single-Inclusion Kinetics of Chlamydia trachomatis Development. MSystems 5.

49. Chowdhury, S.R., Reimer, A., Sharan, M., Kozjak-Pavlovic, V., Eulalio, A., Prusty, B.K., Fraunholz, M., Karunakaran, K., and Rudel, T. (2017). Chlamydia preserves the mitochondrial network necessary for replication via microRNA-dependent inhibition of fission. Journal of Cell Biology 216, 19.

50. Christiansen, G. (1993). Interaction between the Chlamydia trachomatis Histone Hl-Like Protein (Hcl) and DNA. J. BACTERIOL. 11.

51. Clifton, D.R., Dooley, C.A., Grieshaber, S.S., Carabeo, R.A., Fields, K.A., and Hackstadt, T. (2005). Tyrosine Phosphorylation of the Chlamydial Effector Protein Tarp Is Species Specific and Not Required for Recruitment of Actin. INFECT. IMMUN. 73, 9.

52. Cocchiaro, J.L., Kumar, Y., Fischer, E.R., Hackstadt, T., and Valdivia, R.H. (2008). Cytoplasmic lipid droplets are translocated into the lumen of the Chlamydia trachomatis parasitophorous vacuole. Proceedings of the National Academy of Sciences 105, 9379–9384.

53. Collingro, A., Köstlbacher, S., Mussmann, M., Stepanauskas, R., Hallam, S.J., and Horn, M. (2017). Unexpected genomic features in widespread intracellular bacteria: evidence for motility of marine chlamydiae. The ISME Journal 11, 2334–2344.

54. Colpaert, M., Kadouche, D., Ducatez, M., Pillonel, T., Kebbi-Beghdadi, C., Cenci, U., Huang, B., Chabi, M., Maes, E., Coddeville, B., et al. (2021). Conservation of the glycogen metabolism pathway underlines a pivotal function of storage polysaccharides in Chlamydiae. Commun Biol 4, 296.

55. Conant, C.G., and Stephens, R.S. (2007). Chlamydia attachment to mammalian cells requires protein disulfide isomerase. Cellular Microbiology 9, 222–232.

56. Cossé, M.M., Barta, M.L., Fisher, D.J., Oesterlin, L.K., Niragire, B., Perrinet, S., Millot, G.A., Hefty, P.S., and Subtil, A. (2018). The Loss of Expression of a Single Type 3 Effector (CT622) Strongly Reduces Chlamydia trachomatis Infectivity and Growth. Front Cell Infect Microbiol 8, 145.

57. Cox, J.V., Naher, N., Abdelrahman, Y.M., and Belland, R.J. (2012). Host HDL biogenesis machinery is recruited to the inclusion of Chlamydia trachomatis -infected cells and regulates chlamydial growth: Phospholipid acquisition by Chlamydia. Cellular Microbiology 14, 1497–1512.

58. Crenshaw, R.W., Fahr, M.J., Wichlan, D.G., and Hatch, T.P. (1990). Developmental cycle-specific host-free RNA synthesis in Chlamydia spp. Infect Immun 58, 3194–3201.

59. da Cunha, M., Milho, C., Almeida, F., Pais, S.V., Borges, V., Maurício, R., Borrego, M.J., Gomes, J.P., and Mota, L.J. (2014). Identification of type III secretion substrates of Chlamydia trachomatis using Yersinia enterocolitica as a heterologous system. BMC Microbiology 14, 40.

60. Dai, W., and Li, Z. (2014). Conserved type III secretion system exerts important roles in Chlamydia trachomatis. Int J Clin Exp Pathol 11.

61. Damiani, M.T., Gambarte Tudela, J., and Capmany, A. (2014). Targeting eukaryotic Rab proteins: a smart strategy for chlamydial survival and replication: Chlamydia co-opt Rab-controlled vesicular transport. Cellular Microbiology 16, 1329–1338.

62. Dehoux, P., Flores, R., Dauga, C., Zhong, G., and Subtil, A. (2011). Multi-genome identification and characterization of chlamydiae-specific type III secretion substrates: the Inc proteins. BMC Genomics 12.

63. Delevoye, C., Nilges, M., Dehoux, P., Paumet, F., Perrinet, S., Dautry-Varsat, A., and Subtil, A. (2008). SNARE protein mimicry by an intracellular bacterium.pdf. PLOS Pathogens 4.

64. Denzel, M.S., Storm, N.J., Gutschmidt, A., Baddi, R., Hinze, Y., Jarosch, E., Sommer, T., Hoppe, T., and Antebi, A. (2014). Hexosamine Pathway Metabolites Enhance Protein Quality Control and Prolong Life. Cell 156, 1167–1178.

65. Derré, I., Swiss, R., and Agaisse, H. (2011). The Lipid Transfer Protein CERT Interacts with the Chlamydia Inclusion Protein IncD and Participates to ER-Chlamydia Inclusion Membrane Contact Sites. PLoS Pathogens 7, e1002092.

66. Dharamshi, J.E., Tamarit, D., Eme, L., Stairs, C.W., Martijn, J., Homa, F., Jørgensen, S.L., Spang, A., and Ettema, T.J.G. (2020). Marine Sediments Illuminate Chlamydiae Diversity and Evolution. Current Biology 30, 1032-1048.e7.

67. Dibrov, P., Dibrov, E., Pierce, G.N., and Galperin, M.Y. (2004). Salt in the Wound: A Possible Role of Na+ Gradient in Chlamydial Infection. J Mol Microbiol Biotechnol 8, 1–6.

68. Doherty, J.R., and Cleveland, J.L. (2013). Targeting lactate metabolism for cancer therapeutics. Journal of Clinical Investigation 123, 3685–3692.

69. Dumoux, M., Menny, A., Delacour, D., and Hayward, R.D. (2015). A Chlamydia effector recruits CEP170 to reprogram host microtubule organization. Journal of Cell Science 128, 3420–3434.

70. Ebert, B.L., Firth, J.D., and Ratcliffe, P.J. (1995). Hypoxia and Mitochondrial Inhibitors Regulate Expression of Glucose Transporter-1 via Distinct Cis-acting Sequences (*). Journal of Biological Chemistry 270, 29083–29089.

71. Ebert, B.L., Gleadle, J.M., O'Rourke, J.F., Bartlett, S.M., Poulton, J., and Ratcliffe, P.J. (1996). Isoenzyme-specific regulation of genes involved in energy metabolism by hypoxia: similarities with the regulation of erythropoietin. Biochemical Journal 313, 809–814.

72. Elwell, C.A., and Engel, J.N. (2012). Lipid acquisition by intracellular Chlamydiae: Lipid acquisition by Chlamydiae. Cellular Microbiology 14, 1010–1018.

73. Elwell, C., Mirrashidi, K., and Engel, J. (2016). Chlamydia cell biology and pathogenesis. Nature Reviews Microbiology 14, 385–400.

74. Elwell, C.A., Ceesay, A., Kim, J.H., Kalman, D., and Engel, J.N. (2008). RNA Interference Screen Identifies Abl Kinase and PDGFR Signaling in Chlamydia trachomatis Entry. PLoS Pathogens 4, e1000021.

75. Elwell, C.A., Jiang, S., Kim, J.H., Lee, A., Wittmann, T., Hanada, K., Melancon, P., and Engel, J.N. (2011). Chlamydia trachomatis Co-opts GBF1 and CERT to Acquire Host Sphingomyelin for Distinct Roles during Intracellular Development. PLoS Pathogens 7, e1002198.

76. Ende, R.J., and Derré, I. (2020). Host and Bacterial Glycolysis during Chlamydia trachomatis Infection. Infect Immun 88, e00545-20, /iai/88/12/IAI.00545-20.atom.

77. Escoll, P., Song, O.-R., Viana, F., Steiner, B., Lagache, T., Olivo-Marin, J.-C., Impens, F., Brodin, P., Hilbi, H., and Buchrieser, C. (2017). Legionella pneumophila Modulates Mitochondrial Dynamics to Trigger Metabolic Repurposing of Infected Macrophages. Cell Host & Microbe 22, 302-316.e7.

78. Fadel, S., and Eley, A. (2007). Chlamydia trachomatis OmcB protein is a surface-exposed glycosaminoglycan-dependent adhesin. Journal of Medical Microbiology 56, 15–22.

79. Fadel, S., and Eley, A. (2008). Differential glycosaminoglycan binding of Chlamydia trachomatis OmcB protein from serovars E and LGV. Journal of Medical Microbiology 57, 1058–1061.

80. Faris, R., Merling, M., Andersen, S.E., Dooley, C.A., Hackstadt, T., and Weber, M.M. (2019). Chlamydia trachomatis CT229 Subverts Rab GTPase-Dependent CCV Trafficking Pathways to Promote Chlamydial Infection. Cell Reports 26, 3380-3390.e5.

81. Fehr, A., Walther, E., Schmidt-Posthaus, H., Nufer, L., Wilson, A., Svercel, M., Richter, D., Segner, H., Pospischil, A., and Vaughan, L. (2013). Candidatus Syngnamydia Venezia, a Novel Member of the Phylum Chlamydiae from the Broad Nosed Pipefish, Syngnathus typhle. PLoS ONE 8, e70853.

82. Fields, K.A. (2012). Protein Secretion and Chlamydia Pathogenesis. In Intracellular Pathogens I: Chlamydiales, Tan and Bavoil, eds. (American Society of Microbiology), pp. 192–216.

83. Fisher, A.B., and Zhang, Q. (2006). NADPH AND NADPH OXIDASE. In Encyclopedia of Respiratory Medicine, (Elsevier), pp. 77–84.

84. Fisher, D.J., Fernández, R.E., Adams, N.E., and Maurelli, A.T. (2012). Uptake of Biotin by Chlamydia Spp. through the Use of a Bacterial Transporter (BioY) and a Host-Cell Transporter (SMVT). PLoS ONE 7, e46052.

85. Fisher, D.J., Fernandez, R.E., and Maurelli, A.T. (2013). Chlamydia trachomatis Transports NAD via the Npt1 ATP/ADP Translocase. Journal of Bacteriology 195, 3381–3386.

86. Fling, S.P., Sutherland, R.A., Steele, L.N., Hess, B., D'Orazio, S.E.F., Maisonneuve, J.-F., Lampe, M.F., Probst, P., and Starnbach, M.N. (2001). CD8+ T cells recognize an inclusion membrane-associated protein from the vacuolar pathogen Chlamydia trachomatis. Proceedings of the National Academy of Sciences 98, 1160–1165.

87. Fox, A., Rogers, J.C., Gilbart, J., Morgan, S., Davis, C.H., Knight, S., and Wyrick, P.B. (1990). Muramic acid is not detectable in Chlamydia psittaci or Chlamydia trachomatis by gas chromatography-mass spectrometry. Infection and Immunity 58, 835–837.

88. Frank, M., Duvezin-Caubet, S., Koob, S., Occhipinti, A., Jagasia, R., Petcherski, A., Ruonala, M.O., Priault, M., Salin, B., and Reichert, A.S. (2012). Mitophagy is triggered by mild oxidative stress in a mitochondrial fission dependent manner. Biochimica et Biophysica Acta (BBA) - Molecular Cell Research 1823, 2297–2310.

89. Frank, S., Gaume, B., Bergmann-Leitner, E.S., Leitner, W.W., Robert, E.G., Catez, F., Smith, C.L., and Youle, R.J. (2001). The Role of Dynamin-Related Protein 1, a Mediator of Mitochondrial Fission, in Apoptosis. Developmental Cell 1, 515–525.

90. Galaleldeen, A., Taylor, A.B., Chen, D., Schuermann, J.P., Holloway, S.P., Hou, S., Gong, S., Zhong, G., and Hart, P.J. (2013). Structure of the Chlamydia trachomatis Immunodominant Antigen Pgp3. J Biol Chem 288, 22068–22079.

91. Galán, J.E., Lara-Tejero, M., Marlovits, T.C., and Wagner, S. (2014). Bacterial type III secretion systems: specialized nanomachines for protein delivery into target cells. Annual Review of Microbiology 26.

92. Gambarte Tudela, J., Capmany, A., Romao, M., Quintero, C., Miserey-Lenkei, S., Raposo, G., Goud, B., and Damiani, M.T. (2015). The late endocytic Rab39a GTPase regulates the interaction between multivesicular bodies and chlamydial inclusions. Journal of Cell Science 128, 3068–3081.

93. García Rubiño, M.E., Carrillo, E., Ruiz Alcalá, G., Domínguez-Martín, A., A. Marchal, J., and Boulaiz, H. (2019). Phenformin as an Anticancer Agent: Challenges and Prospects. International Journal of Molecular Sciences 20, 3316.

94. Ge, T., Yang, J., Zhou, S., Wang, Y., Li, Y., and Tong, X. (2020). The Role of the Pentose Phosphate Pathway in Diabetes and Cancer. Front Endocrinol (Lausanne) 11, 365.

95. Gehre, L., Gorgette, O., Perrinet, S., Prevost, M.-C., Ducatez, M., Giebel, A.M., Nelson, D.E., Ball, S.G., and Subtil, A. (2016). Sequestration of host metabolism by an intracellular pathogen. ELife 5.

96. Gitsels, A., Sanders, N., and Vanrompay, D. (2019). Chlamydial Infection From Outside to Inside. Frontiers in Microbiology 10.

97. Gomes, L.C., Benedetto, G.D., and Scorrano, L. (2011). During autophagy mitochondria elongate, are spared from degradation and sustain cell viability. Nature Cell Biology 13, 589–598.

98. González, E., Rother, M., Kerr, M.C., Al-Zeer, M.A., Abu-Lubad, M., Kessler, M., Brinkmann, V., Loewer, A., and Meyer, T.F. (2014). Chlamydia infection depends on a functional MDM2-p53 axis. Nature Communications 5.

99. Gordon, F.B. (1965). OCCURRENCE OF GLYCOGEN IN INCLCSIONS OF THE PSITTACOSIS-LYMPHOGRANULOMA VENEREUM-TRACHOMA AGENTS. 11.

100. Grieshaber, S.S. (2003). Chlamydia trachomatis uses host cell dynein to traffic to the microtubule-organizing center in a p50 dynamitin-independent process. Journal of Cell Science 116, 3793–3802.

101. Grieshaber, S., Swanson, J.A., and Hackstadt, T. (2002). Determination of the physical environment within the Chlamydia trachomatis inclusion using ion-selective ratiometric probes. Cellular Microbiology 11.

102. Guppy, M., Leedman, P., Zu, X., and Russell, V. (2002). Contribution by different fuels and metabolic pathways to the total ATP turnover of proliferating MCF-7 breast cancer cells. Biochem J 364, 309–315.

103. Gurumurthy, R.K., Chumduri, C., Karlas, A., Kimmig, S., Gonzalez, E., Machuy, N., Rudel, T., and Meyer, T.F. (2014). Dynamin-mediated lipid acquisition is essential for C hlamydia trachomatis development: Dynamin-mediated lipid acquisition in C. trachomatis infection. Molecular Microbiology 94, 186–201.

104. Hackett, E.E., Charles-Messance, H., O'Leary, S.M., Gleeson, L.E., Muñoz-Wolf, N., Case, S., Wedderburn, A., Johnston, D.G.W., Williams, M.A., Smyth, A., et al. (2020). Mycobacterium tuberculosis Limits Host Glycolysis and IL-1β by Restriction of PFK-M via MicroRNA-21. Cell Reports 30, 124-136.e4.

105. Hackstadt, T., Todd, W.J., and Caldwell, H.D. (1985). Disulfide-mediated interactions of the chlamydial major outer membrane protein: role in the differentiation of chlamydiae? Journal of Bacteriology 161, 25–31.

106. Haider, S., Wagner, M., Schmid, M.C., Sixt, B.S., Christian, J.G., Häcker, G., Pichler, P., Mechtler, K., Müller, A., Baranyi, C., et al. (2010). Raman microspectroscopy reveals long-term extracellular activity of chlamydiae: Intra- and extracellular activity of chlamydiae. Molecular Microbiology 77, 687–700.

107. Hajduch, E., Litherland, G.J., and Hundal, H.S. (2001). Protein kinase B (PKB/Akt) - a key regulator of glucose transport? FEBS Letters 492, 199–203.

108. Harper, A., Pogson, C.I., Jones, M.L., and Pearce, J.H. (2000). Chlamydial Development Is Adversely Affected by Minor Changes in Amino Acid Supply, Blood Plasma Amino Acid Levels, and Glucose Deprivation. Infection and Immunity 68, 1457–1464.

109. Harris, S.R., Clarke, I.N., Seth-Smith, H.M.B., Solomon, A.W., Cutcliffe, L.T., Marsh, P., Skilton, R.J., Holland, M.J., Mabey, D., Peeling, R.W., et al. (2012). Whole-genome analysis of diverse Chlamydia trachomatis strains identifies phylogenetic relationships masked by current clinical typing. Nature Genetics 44, 413–419.

110. Hatch, T.P. (1975a). Utilization of L-cell nucleoside triphosphates by Chlamydia psittaci for ribonucleic acid synthesis. Journal of Bacteriology 122, 393–400.

111. Hatch, T.P. (1975b). Competition between Chlamydia psittaci and L cells for host isoleucine pools: a limiting factor in chlamydial multiplication. Infection and Immunity 12, 211–220.

112. Hatch, T.P., Al-Hossainy, E., and Silverman, J.A. (1982). Adenine nucleotide and lysine transport in Chlamydia psittaci. Journal of Bacteriology 150, 662–670.

113. Hatch, T.P., Miceli, M., and Silverman, J.A. (1985). Synthesis of protein in host-free reticulate bodies of Chlamydia psittaci and Chlamydia trachomatis. Journal of Bacteriology 162, 938–942.

114. Hatch, T.P., Miceli, M., and Sublett, J.E. (1986). Synthesis of disulfide-bonded outer membrane proteins during the developmental cycle of Chlamydia psittaci and Chlamydia trachomatis. Journal of Bacteriology 165, 379–385.

115. Heinzen, R.A., and Hackstadt, T. (1997). The Chlamydia trachomatis Parasitophorous Vacuolar Membrane Is Not Passively Permeable to Low-Molecular-Weight Compounds. INFECT. IMMUN. 65, 7.

116. Henderson, I.R., and Lam, A.C. (2001). Polymorphic proteins of Chlamydia spp. – autotransporters beyond the Proteobacteria. Trends in Microbiology 9, 573–578.

117. Henrissat, B., Deleury, E., and Coutinho, P.M. (2002). Glycogen metabolism loss: a common marker of parasitic behaviour in bacteria? Trends in Genetics 18, 437–440.

118. Herbst-Kralovetz, M.M., Quayle, A.J., Ficarra, M., Greene, S., Rose, W.A., Chesson, R., Spagnuolo, R.A., and Pyles, R.B. (2008). ORIGINAL ARTICLE: Quantification and Comparison of Toll-Like Receptor Expression and Responsiveness in Primary and Immortalized Human Female Lower Genital Tract Epithelia. American Journal of Reproductive Immunology 59, 212–224.

119. Herweg, J.-A., Hansmeier, N., Otto, A., Geffken, A.C., Subbarayal, P., Prusty, B.K., Becher, D., Hensel, M., Schaible, U.E., Rudel, T., et al. (2015). Purification and proteomics of pathogen-modified vacuoles and membranes. Frontiers in Cellular and Infection Microbiology 5.

120. Heuer, D., Lipinski, A.R., Machuy, N., Karlas, A., Wehrens, A., Siedler, F., Brinkmann, V., and Meyer, T.F. (2009). Chlamydia causes fragmentation of the Golgi compartment to ensure reproduction. Nature 457, 731–735.

121. Horn, M. (2008). Chlamydiae as Symbionts in Eukaryotes. Annual Review of Microbiology 62, 113–131.

122. Hou, S., Dong, X., Yang, Z., Li, Z., Liu, Q., and Zhong, G. (2015). Chlamydial Plasmid-Encoded Virulence Factor Pgp3 Neutralizes the Antichlamydial Activity of Human Cathelicidin LL-37. Infection and Immunity 83, 4701–4709.

123. Hybiske, K., and Stephens, R.S. (2007). Mechanisms of host cell exit by the intracellular bacterium Chlamydia. Proceedings of the National Academy of Sciences 104, 11430–11435.

124. Iliffe-Lee, E.R., and McClarty, G. (1999). Glucose metabolism in Chlamydia trachomatis: the “energy parasite” hypothesis revisited. Molecular Microbiology 33, 177–187.

125. Iliffe-Lee, E.R., and McClarty, G. (2000). Regulation of carbon metabolism in Chlamydia trachomatis. Molecular Microbiology 38, 20–30.

126. Jewett, T.J., Fischer, E.R., Mead, D.J., and Hackstadt, T. (2006). Chlamydial TARP is a bacterial nucleator of actin. Proceedings of the National Academy of Sciences 103, 15599–15604.

127. Jiang, L., Wang, P., Song, X., Zhang, H., Ma, S., Wang, J., Li, W., Lv, R., Liu, X., Ma, S., et al. (2021). Salmonella Typhimurium reprograms macrophage metabolism via T3SS effector SopE2 to promote intracellular replication and virulence. Nat Commun 12, 879.

128. Jiang, P., Du, W., Wang, X., Mancuso, A., Gao, X., Wu, M., and Yang, X. (2011). p53 regulates biosynthesis through direct inactivation of glucose-6-phosphate dehydrogenase. Nature Cell Biology 13, 310–316.

129. Jm, B., Jl, T., and Biochemistry, S.L. (2002). Section 16.4 Gluconeogenesis and Glycolysis Are Reciprocally Regulated. Section 16.4 5.

130. Käding, N., Kaufhold, I., Müller, C., Szaszák, M., Shima, K., Weinmaier, T., Lomas, R., Conesa, A., Schmitt-Kopplin, P., Rattei, T., et al. (2017). Growth of Chlamydia

pneumoniae Is Enhanced in Cells with Impaired Mitochondrial Function. Frontiers in Cellular and Infection Microbiology 7.

131. Keb, G., Ferrell, J., Scanlon, K.R., Jewett, T.J., and Fields, K.A. (2021). Chlamydia trachomatis TmeA Directly Activates N-WASP To Promote Actin Polymerization and Functions Synergistically with TarP during Invasion. MBio 12.

132. Kentner, D., Martano, G., Callon, M., Chiquet, P., Brodmann, M., Burton, O., Wahlander, A., Nanni, P., Delmotte, N., Grossmann, J., et al. (2014). Shigella reroutes host cell central metabolism to obtain high-flux nutrient supply for vigorous intracellular growth. PNAS 111, 9929–9934.

133. Kim, J., Tchernyshyov, I., Semenza, G.L., and Dang, C.V. (2006). HIF-1-mediated expression of pyruvate dehydrogenase kinase: A metabolic switch required for cellular adaptation to hypoxia. Cell Metabolism 3, 177–185.

134. Kim, J., Gao, P., Liu, Y.-C., Semenza, G.L., and Dang, C.V. (2007). Hypoxia-Inducible Factor 1 and Dysregulated c-Myc Cooperatively Induce Vascular Endothelial Growth Factor and Metabolic Switches Hexokinase 2 and Pyruvate Dehydrogenase Kinase 1. Mol Cell Biol 27, 7381–7393.

135. Kim, J.H., Jiang, S., Elwell, C.A., and Engel, J.N. (2011). Chlamydia trachomatis Co-opts the FGF2 Signaling Pathway to Enhance Infection. PLoS Pathogens 7, e1002285.

136. Kokes, M., and Valdivia, R.H. (2012). Cell Biology of the Chlamydial Inclusion. In Intracellular Pathogens I: Chlamydiales, Tan and Bavoil, eds. (American Society of Microbiology), pp. 170–191.

137. Kokes, M., Dunn, J.D., Granek, J.A., Nguyen, B.D., Barker, J.R., Valdivia, R.H., and Bastidas, R.J. (2015). Integrating Chemical Mutagenesis and Whole-Genome Sequencing as a Platform for Forward and Reverse Genetic Analysis of Chlamydia. Cell Host & Microbe 17, 716–725.

138. Kumar, Y., and Valdivia, R.H. (2008a). Reorganization of the host cytoskeleton by the intracellular pathogen Chlamydia trachomatis. Communicative & Integrative Biology 1, 175–177.

139. Kumar, Y., and Valdivia, R.H. (2008b). Actin and Intermediate Filaments Stabilize the Chlamydia trachomatis Vacuole by Forming Dynamic Structural Scaffolds. Cell Host & Microbe 4, 159–169.

140. Kurihara, Y., Itoh, R., Shimizu, A., Walenna, N.F., Chou, B., Ishii, K., Soejima, T., Fujikane, A., and Hiromatsu, K. (2019). Chlamydia trachomatis targets mitochondrial dynamics to promote intracellular survival and proliferation. Cellular Microbiology 21, e12962.

141. Lagkouvardos, I., Weinmaier, T., Lauro, F.M., Cavicchioli, R., Rattei, T., and Horn, M. (2014). Integrating metagenomic and amplicon databases to resolve the phylogenetic and ecological diversity of the Chlamydiae. The ISME Journal 8, 115–125.

142. Lee, J.K., Enciso, G.A., Boassa, D., Chander, C.N., Lou, T.H., Pairawan, S.S., Guo, M.C., Wan, F.Y.M., Ellisman, M.H., Sütterlin, C., et al. (2018). Replication-dependent size reduction precedes differentiation in Chlamydia trachomatis. Nature Communications 9.

143. Li, J., Donath, S., Li, Y., Qin, D., Prabhakar, B.S., and Li, P. (2010). miR-30 Regulates Mitochondrial Fission through Targeting p53 and the Dynamin-Related Protein-1 Pathway. PLoS Genetics 6, e1000795.

144. Li, Z., Chen, C., Chen, D., Wu, Y., Zhong, Y., and Zhong, G. (2008). Characterization of Fifty Putative Inclusion Membrane Proteins Encoded in the Chlamydia trachomatis Genome. Infection and Immunity 76, 2746–2757.

145. Liang, P., Rosas-Lemus, M., Patel, D., Fang, X., Tuz, K., and Juárez, O. (2018). Dynamic energy dependency of Chlamydia trachomatis on host cell metabolism during intracellular growth: Role of sodium-based energetics in chlamydial ATP generation. Journal of Biological Chemistry 293, 510–522.

146. Liechti, G., Kuru, E., Packiam, M., Hsu, Y.-P., Tekkam, S., Hall, E., Rittichier, J.T., VanNieuwenhze, M., Brun, Y.V., and Maurelli, A.T. (2016). Pathogenic Chlamydia Lack a Classical Sacculus but Synthesize a Narrow, Mid-cell Peptidoglycan Ring, Regulated by MreB, for Cell Division. PLOS Pathogens 12, e1005590.

147. Liechti, G.W., Kuru, E., Hall, E., Kalinda, A., Brun, Y.V., VanNieuwenhze, M., and Maurelli, A.T. (2014). A new metabolic cell-wall labelling method reveals peptidoglycan in Chlamydia trachomatis. Nature 506, 507–510.

148. Liu, Y., Huang, Y., Yang, Z., Sun, Y., Gong, S., Hou, S., Chen, C., Li, Z., Liu, Q., Wu, Y., et al. (2014). Plasmid-Encoded Pgp3 Is a Major Virulence Factor for Chlamydia muridarum To Induce Hydrosalpinx in Mice. Infection and Immunity 82, 5327–5335.

149. Love, D.C., and Hanover, J.A. (2005). The Hexosamine Signaling Pathway: Deciphering the “O-GlcNAc Code.” Science Signaling 2005, re13–re13.

150. Lu, C., Lei, L., Peng, B., Tang, L., Ding, H., Gong, S., Li, Z., Wu, Y., and Zhong, G. (2013). Chlamydia trachomatis GlgA Is Secreted into Host Cell Cytoplasm. PLoS ONE 8, e68764.

151. Luo, W., Hu, H., Chang, R., Zhong, J., Knabel, M., O’Meally, R., Cole, R.N., Pandey, A., and Semenza, G.L. (2011). Pyruvate Kinase M2 Is a PHD3-Stimulated Coactivator for Hypoxia-Inducible Factor 1. Cell 145, 732–744.

152. Lutter, E.I., Martens, C., and Hackstadt, T. (2012). Evolution and Conservation of Predicted Inclusion Membrane Proteins in Chlamydiae. Comparative and Functional Genomics 13.

153. Lutter, E.I., Barger, A.C., Nair, V., and Hackstadt, T. (2013). Chlamydia trachomatis Inclusion Membrane Protein CT228 Recruits Elements of the Myosin Phosphatase Pathway to Regulate Release Mechanisms. Cell Reports 3, 1921–1931.

154. Maffei, B. (2018). Investigation of the role of tissue transglutaminase (TG2) in the infection by Chlamydia trachomatis : a key player in the metabolic rewiring of the host cell. phdthesis. Sorbonne Université.

155. Maffei, B., Laverrière, M., Wu, Y., Triboulet, S., Perrinet, S., Duchateau, M., Matondo, M., Hollis, R.L., Gourley, C., Rupp, J., et al. (2020). Infection-driven activation of transglutaminase 2 boosts glucose uptake and hexosamine biosynthesis in epithelial cells. EMBO J 39.

156. Mamelak, D., Mylvaganam, M., Whetstone, H., Hartmann, E., Lennarz, W., Wyrick, P.B., Raulston, J., Han, H., Hoffman, P., and Lingwood, C.A. (2001). Hsp70s Contain a Specific Sulfogalactolipid Binding Site. Differential Aglycone Influence on Sulfogalactosyl Ceramide Binding by Recombinant Prokaryotic and Eukaryotic Hsp70 Family Members †. Biochemistry 40, 3572–3582.

157. Marsin, A.-S., Bouzin, C., Bertrand, L., and Hue, L. (2002). The Stimulation of Glycolysis by Hypoxia in Activated Monocytes Is Mediated by AMP-activated Protein Kinase and Inducible 6-Phosphofructo-2-kinase. Journal of Biological Chemistry 277, 30778–30783.

158. Martin, S., and Parton, R.G. (2006). Lipid droplets- a unified view of a dynamic organelle. Nature Reviews Molecular Cell Biology 7, 373–378.

159. Matsumoto, A., Bessho, H., Uehira, K., and Suda, T. (1991). Morphological studies of the association of mitochondria with chlamydial inclusions and the fusion of chlamydial inclusions. J Electron Microsc (Tokyo) 40, 356–363.

160. de la Maza, L.M., Darville, T.L., and Pal, S. (2021). Chlamydia trachomatis vaccines for genital infections: where are we and how far is there to go? Expert Review of Vaccines 20, 421–435.

161. Mazurek, S. (2011). Pyruvate kinase type M2: A key regulator of the metabolic budget system in tumor cells. The International Journal of Biochemistry & Cell Biology 43, 969–980.

162. Mehlitz, A., Eylert, E., Huber, C., Lindner, B., Vollmuth, N., Karunakaran, K., Goebel, W., Eisenreich, W., and Rudel, T. (2017). Metabolic adaptation of Chlamydia trachomatis to mammalian host cells: Metabolism of intracellular chlamydia trachomatis. Molecular Microbiology 103, 1004–1019.

163. Mesquita, I., Varela, P., Belinha, A., Gaifem, J., Laforge, M., Vergnes, B., Estaquier, J., and Silvestre, R. (2016). Exploring NAD+ metabolism in host–pathogen interactions. Cell. Mol. Life Sci. 73, 1225–1236.

164. Minchenko, A., Leshchinsky, I., Opentanova, I., Sang, N., Srinivas, V., Armstead, V., and Caro, J. (2002). Hypoxia-inducible Factor-1-mediated Expression of the 6-Phosphofructo-2-kinase/fructose-2,6-bisphosphatase-3 (PFKFB3) Gene. Journal of Biological Chemistry 277, 6183–6187.

165. Mital, J., and Hackstadt, T. (2011). Diverse Requirements for Src-Family Tyrosine Kinases Distinguish Chlamydial Species. MBio 2.

166. Mital, J., Miller, N.J., Fischer, E.R., and Hackstadt, T. (2010). Specific chlamydial inclusion membrane proteins associate with active Src family kinases in microdomains that interact with the host microtubule network: Chlamydial inclusion microdomains. Cellular Microbiology 12, 1235–1249.

167. Mital, J., Lutter, E.I., Barger, A.C., Dooley, C.A., and Hackstadt, T. (2015). Chlamydia trachomatis inclusion membrane protein CT850 interacts with the dynein light chain DYNLT1 (Tctex1). Biochemical and Biophysical Research Communications 462, 165–170.

168. Miyashita, N., Matsumoto, A., and Matsushima, T. (2000). In Vitro Susceptibility of 7.5-kb Common Plasmid-Free Chlamydia trachomatis Strains. Microbiology and Immunology 44, 267–269.

169. Moore, E.R., and Ouellette, S.P. (2014). Reconceptualizing the chlamydial inclusion as a pathogen-specified parasitic organelle: an expanded role for Inc proteins. Frontiers in Cellular and Infection Microbiology 4.

170. Moorhead, A.M., Jung, J.-Y., Smirnov, A., Kaufer, S., and Scidmore, M.A. (2010). Multiple Host Proteins That Function in Phosphatidylinositol-4-Phosphate Metabolism Are Recruited to the Chlamydial Inclusion. Infection and Immunity 78, 1990–2007.

171. Moreno-Sánchez, R., Rodríguez-Enríquez, S., Marín-Hernández, A., and Saavedra, E. (2007). Energy metabolism in tumor cells. The FEBS Journal 274, 1393–1418.

172. Moulder, J.W. (1966). The Relation of the Psittacosis Group (Chlamydiae) to Bacteria and Viruses. Annu. Rev. Microbiol. 20, 107–130.

173. Moulder, J.W., Grisso, D.L., and Brubaker, R.R. (1965). Enzymes of Glucose Catabolism in a Member of the Psittacosis Group. Journal of Bacteriology 89, 810–812.

174. Mpiga, P., and Ravaoarinoro, M. (2006). Chlamydia trachomatis persistence: An update. Microbiological Research 161, 9–19.

175. Nans, A., Saibil, H.R., and Hayward, R.D. (2014). Pathogen-host reorganization during Chlamydia invasion revealed by cryo-electron tomography. Cellular Microbiology 16.

176. Nguyen, P.H., Lutter, E.I., and Hackstadt, T. (2018). Chlamydia trachomatis inclusion membrane protein MrcA interacts with the inositol 1,4,5-trisphosphate receptor type 3 (ITPR3) to regulate extrusion formation. PLOS Pathogens 14, e1006911.

177. Nunes, A., and Gomes, J.P. (2014). Evolution, phylogeny, and molecular epidemiology of Chlamydia. Infection, Genetics and Evolution 23, 49–64.

178. O'Connell, C.M., and Ferone, M.E. (2016). Chlamydia trachomatis Genital Infections. Microbial Cell 3, 390–403.

179. Ojcius, D.M., Degani, H., Mispelter, J., and Dautry-Varsat, A. (1998). Enhancement of ATP Levels and Glucose Metabolism during an Infection by Chlamydia: NMR STUDIES OF LIVING CELLS. Journal of Biological Chemistry 273, 7052–7058.

180. Omsland, A., Sager, J., Nair, V., Sturdevant, D.E., and Hackstadt, T. (2012). Developmental stage-specific metabolic and transcriptional activity of Chlamydia trachomatis in an axenic medium. Proceedings of the National Academy of Sciences 109, 19781–19785.

181. Omsland, A., Sixt, B.S., Horn, M., and Hackstadt, T. (2014). Chlamydial metabolism revisited: interspecies metabolic variability and developmental stage-specific physiologic activities. FEMS Microbiology Reviews 38, 779–801.

182. Ormsbee, R.A., and Weiss, E. (1963). Trachoma Agemt: Glucose Utilization by Purified Suspensions. Science 142, 1077–1078.

183. Ouellette, S.P., and Carabeo, R.A. (2010). A Functional Slow Recycling Pathway of Transferrin is Required for Growth of Chlamydia. Frontiers in Microbiology 1.

184. Ouellette, S.P., Dorsey, F.C., Moshiach, S., Cleveland, J.L., and Carabeo, R.A. (2011). Chlamydia Species-Dependent Differences in the Growth Requirement for Lysosomes. PLoS ONE 6, 16.

185. Packiam, M., Weinrick, B., Jacobs, W.R., and Maurelli, A.T. (2015). Structural characterization of muropeptides from Chlamydia trachomatis peptidoglycan by mass spectrometry resolves "chlamydial anomaly." Proceedings of the National Academy of Sciences 112, 11660–11665.

186. de Padua, M.C., Delodi, G., Vučetić, M., Durivault, J., Vial, V., Bayer, P., Noleto, G.R., Mazure, N.M., Ždralević, M., and Pouysségur, J. (2017). Disrupting glucose-6-phosphate isomerase fully suppresses the "Warburg effect" and activates OXPHOS with minimal impact on tumor growth except in hypoxia. Oncotarget 8, 87623–87637.

187. Pais, S.V., Milho, C., Almeida, F., and Mota, L.J. (2013). Identification of Novel Type III Secretion Chaperone-Substrate Complexes of Chlamydia trachomatis. PLoS ONE 8, e56292.

188. Pan, C., Kumar, C., Bohl, S., Klingmueller, U., and Mann, M. (2009). Comparative Proteomic Phenotyping of Cell Lines and Primary Cells to Assess Preservation of Cell Type-specific Functions. Molecular & Cellular Proteomics 8, 443–450.

189. Parsot, C. (2003). The various and varying roles of specific chaperones in type III secretion systems. Current Opinion in Microbiology 6, 7–14.

190. Patel, A.L., Chen, X., Wood, S.T., Stuart, E.S., Arcaro, K.F., Molina, D.P., Petrovic, S., Furdui, C.M., and Tsang, A.W. (2014). Activation of epidermal growth factor receptor is required for Chlamydia trachomatis development. BMC Microbiology 14.

191. Patton, M.J., McCorrister, S., Grant, C., Westmacott, G., Fariss, R., Hu, P., Zhao, K., Blake, M., Whitmire, B., Yang, C., et al. (2016). Chlamydial Protease-Like Activity Factor and Type III Secreted Effectors Cooperate in Inhibition of p65 Nuclear Translocation. MBio 7, 9.

192. Paul, B., Kim, H.S., Kerr, M.C., Huston, W.M., Teasdale, R.D., and Collins, B.M. (2017). Structural basis for the hijacking of endosomal sorting nexin proteins by. ELife 23.

193. Pearce, E.L., and Pearce, E.J. (2013). Metabolic Pathways In Immune Cell Activation And Quiescence. Immunity 38, 633–643.

194. Peeling, R.W., Peeling, J., and Brunham, R.C. (1989). High-resolution 31P nuclear magnetic resonance study of Chlamydia trachomatis: induction of ATPase activity in elementary bodies. Infect Immun 57, 3338–3344.

195. Perrin, J. (1952). Observations on the Relationship between Viruses of the Psittacosis-Lymphogranuloma Group and the Rickettsiae. Journal of General Microbiology 6, 143–148.

196. Pillonel, T., Bertelli, C., and Greub, G. (2018). Environmental Metagenomic Assemblies Reveal Seven New Highly Divergent Chlamydial Lineages and Hallmarks of a Conserved Intracellular Lifestyle. Frontiers in Microbiology 9.

197. Plaunt, M.R., and Hatch, T.P. (1988). Protein synthesis early in the developmental cycle of Chlamydia psittaci. Infection and Immunity 56, 3021–3025.

198. Porcella, S.F., Carlson, J.H., Sturdevant, D.E., Sturdevant, G.L., Kanakabandi, K., Virtaneva, K., Wilder, H., Whitmire, W.M., Song, L., and Caldwell, H.D. (2015). Transcriptional Profiling of Human Epithelial Cells Infected with Plasmid-Bearing and Plasmid-Deficient Chlamydia trachomatis. Infection and Immunity 83, 534–543.

199. Porporato, P.E., Dhup, S., Dadhich, R.K., Copetti, T., and Sonveaux, P. (2011). Anticancer Targets in the Glycolytic Metabolism of Tumors: A Comprehensive Review. Frontiers in Pharmacology 2.

200. Pouysségur, J., Dayan, F., and Mazure, N.M. (2006). Hypoxia signalling in cancer and approaches to enforce tumour regression. Nature 441, 437–443.

201. Powers, J.L., Kiesman, N.E., Tran, C.M., Brown, J.H., and Bevilacqua, V.L.H. (2007). Lactate dehydrogenase kinetics and inhibition using a microplate reader. Biochem. Mol. Biol. Educ. 35, 287–292.

202. Price, J.V., Jiang, K., Galantowicz, A., Freifeld, A., and Vance, R.E. (2018). Legionella pneumophila Is Directly Sensitive to 2-Deoxyglucose-Phosphate via Its UhpC Transporter but Is Indifferent to Shifts in Host Cell Glycolytic Metabolism. J Bacteriol 200.

203. Prusty, B.K., Böhme, L., Bergmann, B., Siegl, C., Krause, E., Mehlitz, A., and Rudel, T. (2012). Imbalanced Oxidative Stress Causes Chlamydial Persistence during Non-Productive Human Herpes Virus Co-Infection. PLoS ONE 7, e47427.

204. R Core Team, *R: A language and environment for statistical computing*. 2020, R Foundation for Statistical Computing, Vienna, Austria.

205. Rajalingam, K., Sharma, M., Lohmann, C., Oswald, M., Thieck, O., Froelich, C.J., and Rudel, T. (2008a). Mcl-1 Is a Key Regulator of Apoptosis Resistance in Chlamydia trachomatis-Infected Cells. PLoS ONE 3, 11.

206. Rajalingam, K., Sharma, M., Lohmann, C., Oswald, M., Thieck, O., Froelich, C.J., and Rudel, T. (2008b). Mcl-1 Is a Key Regulator of Apoptosis Resistance in Chlamydia trachomatis-Infected Cells. PLoS ONE 3, e3102.

207. Rajeeve, K. (2018). Chlamydia trachomatis paralyses neutrophils to evade the host innate immune response. Nature Microbiology 3, 16.

208. Rajeeve, K., Vollmuth, N., Janaki-Raman, S., Wulff, T.F., Baluapuri, A., Dejure, F.R., Huber, C., Fink, J., Schmalhofer, M., Schmitz, W., et al. (2020). Reprogramming of host glutamine metabolism during Chlamydia trachomatis infection and its key role in peptidoglycan synthesis. Nat Microbiol 5, 1390–1402.

209. Read, T.D. (2000). Genome sequences of Chlamydia trachomatis MoPn and Chlamydia pneumoniae AR39. Nucleic Acids Research 28, 1397–1406.

210. Rodriguez-Enriquez, S., Vitalgonzalez, P., Floresrodriguez, F., Marinhernandez, A., Ruizazuara, L., and Morenosanchez, R. (2006). Control of cellular proliferation by modulation of oxidative phosphorylation in human and rodent fast-growing tumor cells. Toxicology and Applied Pharmacology 215, 208–217.

211. Ronzone, E., and Paumet, F. (2013). Two Coiled-Coil Domains of Chlamydia trachomatis IncA Affect Membrane Fusion Events during Infection. PLoS ONE 8, e69769.

212. Rosenberg, G., Yehezkel, D., Hoffman, D., Mattioli, C.C., Fremder, M., Ben-Arosh, H., Vainman, L., Nissani, N., Hen-Avivi, S., Brenner, S., et al. (2021). Host succinate is an activation signal for Salmonella virulence during intracellular infection. Science 371, 400–405.

213. Roth, A., Konig, P., van Zandbergen, G., Klinger, M., Hellwig-Burgel, T., Daubener, W., Bohlmann, M.K., and Rupp, J. (2010). Hypoxia abrogates antichlamydial properties of IFN- in human fallopian tube cells in vitro and ex vivo. Proceedings of the National Academy of Sciences 107, 19502–19507.

214. Röth, D., Krammer, P.H., and Gülow, K. (2014). Dynamin related protein 1-dependent mitochondrial fission regulates oxidative signalling in T cells. FEBS Letters 588, 1749–1754.

215. Rother, M., Gonzalez, E., Teixeira da Costa, A.R., Wask, L., Gravenstein, I., Pardo, M., Pietzke, M., Gurumurthy, R.K., Angermann, J., Laudeley, R., et al. (2018). Combined Human Genome-wide RNAi and Metabolite Analyses Identify IMPDH as a Host-Directed Target against Chlamydia Infection. Cell Host & Microbe 23, 661-671.e8.

216. Rowley, J., Vander Hoorn, S., Korenromp, E., Low, N., Unemo, M., Abu-Raddad, L.J., Chico, R.M., Smolak, A., Newman, L., Gottlieb, S., et al. (2019). Chlamydia, gonorrhoea, trichomoniasis and syphilis: global prevalence and incidence estimates, 2016. Bulletin of the World Health Organization 97, 548-562P.

217. Rupp, J., Gieffers, J., Klinger, M., Zandbergen, G.V., Wrase, R., Maass, M., Solbach, W., Deiwick, J., and Hellwig-Burgel, T. (2007). Chlamydia pneumoniae directly interferes with HIF-1α stabilization in human host cells. Cellular Microbiology 9, 2181–2191.

218. Russell, M., Darville, T., Chandra-Kuntal, K., Smith, B., Andrews, C.W., and O'Connell, C.M. (2011). Infectivity Acts as In Vivo Selection for Maintenance of the Chlamydial Cryptic Plasmid. Infect Immun 79, 98–107.

219. Rzomp, K.A., Scholtes, L.D., Briggs, B.J., Whittaker, G.R., and Scidmore, M.A. (2003). Rab GTPases Are Recruited to Chlamydial Inclusions in Both a Species-Dependent and Species-Independent Manner. Infection and Immunity 71, 5855–5870.

220. Saka, H.A., Thompson, J.W., Chen, Y.-S., Kumar, Y., Dubois, L.G., Moseley, M.A., and Valdivia, R.H. (2011). Quantitative proteomics reveals metabolic and pathogenic properties of Chlamydia trachomatis developmental forms: Quantitative proteomics analysis of C. trachomatis developmental forms. Molecular Microbiology 82, 1185–1203.

221. Saka, H.A., Thompson, J.W., Chen, Y.-S., Dubois, L.G., Haas, J.T., Moseley, A., and Valdivia, R.H. (2015). Chlamydia trachomatis Infection Leads to Defined Alterations to the Lipid Droplet Proteome in Epithelial Cells. PLOS ONE 10, e0124630.

222. Samanta, D., Mulye, M., Clemente, T.M., Justis, A.V., and Gilk, S.D. (2017). Manipulation of Host Cholesterol by Obligate Intracellular Bacteria. Frontiers in Cellular and Infection Microbiology 7.

223. Sarin, M., Wang, Y., Zhang, F., Rothermund, K., Zhang, Y., Lu, J., Sims-Lucas, S., Beer-Stolz, D., Van Houten, B.E., Vockley, J., et al. (2013). Alterations in c-Myc phenotypes resulting from dynamin-related protein 1 (Drp1)-mediated mitochondrial fission. Cell Death & Disease 4, e670–e670.

224. Sarkar, A. (2015). Mechanisms of apoptosis inhibition in Chlamydia pneumoniae-infected neutrophils. International Journal of Medical Microbiology 8.

225. Schmittgen, T.D., and Livak, K.J. (2008). Analyzing real-time PCR data by the comparative CT method. Nat Protoc 3, 1101–1108.

226. Schwoppe, C., Winkler, H.H., and Neuhaus, H.E. (2002). Properties of the Glucose-6-Phosphate Transporter from Chlamydia pneumoniae (HPTcp) and the Glucose-6-Phosphate Sensor from Escherichia coli (UhpC). Journal of Bacteriology 184, 2108–2115.

227. Scidmore, M.A. (2006). Cultivation and Laboratory Maintenance of Chlamydia trachomatis. Current Protocols in Microbiology 00, 11A.1.1-11A.1.25.

228. Sharma, M., Machuy, N., Böhme, L., Karunakaran, K., Mäurer, A.P., Meyer, T.F., and Rudel, T. (2011). HIF-1α is involved in mediating apoptosis resistance to Chlamydia trachomatis-infected cells: Inhibition of apoptosis by C. trachomatis infection. Cellular Microbiology 13, 1573–1585.

229. Shaw, E.I., Dooley, C.A., Fischer, E.R., Scidmore, M.A., Fields, K.A., and Hackstadt, T. (2000). Three temporal classes of gene expression during the Chlamydia trachomatis developmental cycle. Molecular Microbiology 37, 913–925.

230. Sherrid, A.M., and Hybiske, K. (2017). Chlamydia trachomatis Cellular Exit Alters Interactions with Host Dendritic Cells. Infection and Immunity 85.

231. Shima, K., Kaufhold, I., Eder, T., Käding, N., Schmidt, N., Ogunsulire, I.M., Deenen, R., Köhrer, K., Friedrich, D., Isay, S.E., et al. (2021). Regulation of the Mitochondrion-Fatty Acid Axis for the Metabolic Reprogramming of Chlamydia trachomatis during Treatment with β-Lactam Antimicrobials. MBio 12.

232. Siegl, C., Prusty, B.K., Karunakaran, K., Wischhusen, J., and Rudel, T. (2014). Tumor Suppressor p53 Alters Host Cell Metabolism to Limit Chlamydia trachomatis Infection. Cell Reports 9, 918–929.

233. Sixt, B.S., Heinz, C., Pichler, P., Heinz, E., Montanaro, J., Camp, H.J.M.O. den, Ammerer, G., Mechtler, K., Wagner, M., and Horn, M. (2011). Proteomic analysis reveals a virtually complete set of proteins for translation and energy generation in elementary bodies of the amoeba symbiont Protochlamydia amoebophila. PROTEOMICS 11, 1868–1892.

234. Sixt, B.S., Bastidas, R.J., Finethy, R., Baxter, R.M., Carpenter, V.K., Kroemer, G., Coers, J., and Valdivia, R.H. (2017). The Chlamydia trachomatis Inclusion Membrane Protein CpoS Counteracts STING-Mediated Cellular Surveillance and Suicide Programs. Cell Host & Microbe 21, 113–121.

235. Skipp, P., Robinson, J., O'Connor, C.D., and Clarke, I.N. (2005). Shotgun proteomic analysis of Chlamydia trachomatis. PROTEOMICS 5, 1558–1573.

236. Soupene, E., Rothschild, J., Kuypers, F.A., and Dean, D. (2012). Eukaryotic Protein Recruitment into the Chlamydia Inclusion: Implications for Survival and Growth. PLoS ONE 7, e36843.

237. Soupene, E., Wang, D., and Kuypers, F.A. (2015). Remodeling of host phosphatidylcholine by Chlamydia acyltransferase is regulated by acyl-CoA binding protein ACBD6 associated with lipid droplets. MicrobiologyOpen 4, 235–251.

238. Spaeth, K.E., Chen, Y.-S., and Valdivia, R.H. (2009). The Chlamydia Type III Secretion System C-ring Engages a Chaperone-Effector Protein Complex. PLoS Pathogens 5, 11.

239. Stallmann, S., and Hegemann, J.H. (2016). The Chlamydia trachomatis Ctad1 invasin exploits the human integrin β1 receptor for host cell entry: Chlamydia trachomatis Ctad1 binds to integrin β1. Cellular Microbiology 18, 761–775.

240. Stanhope, R., Flora, E., Bayne, C., and Derré, I. (2017). IncV, a FFAT motif-containing Chlamydia protein, tethers the endoplasmic reticulum to the pathogen-containing vacuole. Pnas 6.

241. Stephens, R.S. (1998). Genome Sequence of an Obligate Intracellular Pathogen of Humans: Chlamydia trachomatis. Science 282, 754–759.

242. Stephens, R.S., Koshiyama, K., Lewis, E., and Kubo, A. (2001). Heparin-binding outer membrane protein of chlamydiae: Chlamydial heparin-binding protein. Molecular Microbiology 40, 691–699.

243. Su, H., Raymond, L., Rockey, D.D., Fischer, E., Hackstadt, T., and Caldwell, H.D. (1996). A recombinant Chlamydia trachomatis major outer membrane protein binds to heparan sulfate receptors on epithelial cells. Proceedings of the National Academy of Sciences 93, 11143–11148.

244. Su, H., McClarty, G., Dong, F., Hatch, G.M., Pan, Z.K., and Zhong, G. (2004). Activation of Raf/MEK/ERK/cPLA2 Signaling Pathway Is Essential for Chlamydial Acquisition of Host Glycerophospholipids. Journal of Biological Chemistry 279, 9409–9416.

245. Subbarayal, P., Karunakaran, K., Winkler, A.-C., Rother, M., Gonzalez, E., Meyer, T.F., and Rudel, T. (2015). EphrinA2 Receptor (EphA2) Is an Invasion and Intracellular Signaling Receptor for Chlamydia trachomatis. PLOS Pathogens 11, e1004846.

246. Subtil, A., Delevoye, C., Balañá, M.-E., Tastevin, L., Perrinet, S., and Dautry-Varsat, A. (2005). A directed screen for chlamydial proteins secreted by a type III mechanism identifies a translocated protein and numerous other new candidates: Identification of secreted chlamydial proteins. Molecular Microbiology 56, 1636–1647.

247. Suen, D.-F., Norris, K.L., and Youle, R.J. (2008). Mitochondrial dynamics and apoptosis. Genes & Development 22, 1577–1590.

248. Swietach, P., Vaughan-Jones, R.D., and Harris, A.L. (2007). Regulation of tumor pH and the role of carbonic anhydrase 9. Cancer Metastasis Rev 26, 299–310.

249. Szászák, M., Steven, P., Shima, K., Orzekowsky-Schröder, R., Hüttmann, G., König, I.R., Solbach, W., and Rupp, J. (2011). Fluorescence Lifetime Imaging Unravels C. trachomatis Metabolism and Its Crosstalk with the Host Cell. PLoS Pathog 7, e1002108.

250. Tang, C., Liu, C., Maffei, B., Niragire, B., Cohen, H., Kane, A., Donnadieu, A.-C., Levy-Zauberman, Y., Vernay, T., Hugueny, J., et al. (2021). Primary ectocervical epithelial cells display lower permissivity to Chlamydia trachomatis than HeLa cells and a globally higher pro-inflammatory profile. Sci Rep 11, 5848.

251. Tarbet, H.J., Dolat, L., Smith, T.J., Condon, B.M., O'Brien, E.T., Valdivia, R.H., and Boyce, M. (2018). Site-specific glycosylation regulates the form and function of the intermediate filament cytoskeleton. ELife 7.

252. Taylor-Brown, A., Vaughan, L., Greub, G., Timms, P., and Polkinghorne, A. (2015). Twenty years of research into Chlamydia-like organisms: a revolution in our understanding of the biology and pathogenicity of members of the phylum Chlamydiae. Pathogens and Disease 73, 1–15.

253. Taylor-Brown, A., Bachmann, N.L., Borel, N., and Polkinghorne, A. (2016). Culture-independent genomic characterisation of Candidatus Chlamydia sanzinia, a novel uncultivated bacterium infecting snakes. BMC Genomics 17.

254. Taylor-Brown, A., Pillonel, T., Bridle, A., Qi, W., Bachmann, N.L., Miller, T.L., Greub, G., Nowak, B., Seth-Smith, H.M.B., Vaughan, L., et al. (2017). Culture-independent genomics of a novel chlamydial pathogen of fish provides new insight into host-specific adaptations utilized by these intracellular bacteria: Novel chlamydial epitheliocystis agent in grouper. Environmental Microbiology 19, 1899–1913.

255. Thalmann, J., Janik, K., May, M., Sommer, K., Ebeling, J., Hofmann, F., Genth, H., and Klos, A. (2010). Actin Re-Organization Induced by Chlamydia trachomatis Serovar D - Evidence for a Critical Role of the Effector Protein CT166 Targeting Rac. PLoS ONE 5, e9887.

256. Thomson, N.R., Holden, M.T.G., Carder, C., Lennard, N., Lockey, S.J., Marsh, P., Skipp, P., O'Connor, C.D., Goodhead, I., Norbertzcak, H., et al. (2007). Chlamydia trachomatis: Genome sequence analysis of lymphogranuloma venereum isolates. Genome Research 18, 161–171.

257. Tipples, G., and McClarty, G. (1993). The obligate intracellular bacterium Chlamydia trachomatis is auxotrophic for three of the four ribonucleoside triphosphates. Molecular Microbiology 8, 1105–1114.

258. Tjaden, J., Winkler, H.H., Ppe, C.S., Hlmann, T.M., and Neuhaus, H.E. (1999). Two Nucleotide Transport Proteins in Chlamydia trachomatis, One for Net Nucleoside Triphosphate Uptake and the Other for Transport of Energy. J. BACTERIOL. 181, 7.

259. Touvier, T., De Palma, C., Rigamonti, E., Scagliola, A., Incerti, E., Mazelin, L., Thomas, J.-L., D'Antonio, M., Politi, L., Schaeffer, L., et al. (2015). Muscle-specific Drp1 overexpression impairs skeletal muscle growth via translational attenuation. Cell Death & Disease 6, e1663–e1663.

260. Triboulet, S., and Subtil, A. (2019). Make It a Sweet Home: Responses of Chlamydia trachomatis to the Challenges of an Intravacuolar Lifestyle. Microbiology Spectrum 7, 7.2.06.

261. Vandahl, B.B., Birkelund, S., Demol, H., Hoorelbeke, B., Christiansen, G., Vandekerckhove, J., and Gevaert, K. (2001). Proteome analysis of the Chlamydia pneumoniaeelementary body. ELECTROPHORESIS 22, 1204–1223.

262. Vandahl, B.B.S., Birkelund, S., and Christiansen, G. (2004). Genome and proteome analysis of Chlamydia. PROTEOMICS 4, 2831–2842.

263. Vander Heiden, M.G., Cantley, L.C., and Thompson, C.B. (2009). Understanding the Warburg Effect: The Metabolic Requirements of Cell Proliferation. Science 324, 1029–1033.

264. Vanrompay, D., Charlier, G., Ducatelle, R., and Haesebrouck, F. (1996). Ultrastructural changes in avian Chlamydia psittaci serovar A-, B-, and D-infected Buffalo Green Monkey cells. Infection and Immunity 64, 1265–1271.

265. Vender, J., and Moulder, J.W. (1967). Initial Step in Catabolism of Glucose by the Meningopneumonitis Agent. Journal of Bacteriology 94, 867–869.

266. Vizán, P., Alcarraz-Vizán, G., Díaz-Moralli, S., Solovjeva, O.N., Frederiks, W.M., and Cascante, M. (2009). Modulation of pentose phosphate pathway during cell cycle progression in human colon adenocarcinoma cell line HT29. International Journal of Cancer 124, 2789–2796.

267. Volceanov, L., Herbst, K., Biniossek, M., Schilling, O., Haller, D., Nölke, T., Subbarayal, P., Rudel, T., Zieger, B., and Häcker, G. (2014). Septins Arrange F-Actin-Containing Fibers on the Chlamydia trachomatis Inclusion and Are Required for Normal Release of the Inclusion by Extrusion. MBio 5.

268. Vromman, F., Laverrière, M., Perrinet, S., Dufour, A., and Subtil, A. (2014). Quantitative Monitoring of the Chlamydia trachomatis Developmental Cycle Using GFP-Expressing Bacteria, Microscopy and Flow Cytometry. PLoS ONE 9, e99197.

269. Wang, J., Jiao, Y., Cui, L., and Jiang, L. (2017a). miR-30 functions as an oncomiR in gastric cancer cells through regulation of P53-mediated mitochondrial apoptotic pathway. Bioscience, Biotechnology, and Biochemistry 81, 119–126.

270. Wang, S., Mao, Y., Xi, S., Wang, X., and Sun, L. (2017b). Nutrient Starvation Sensitizes Human Ovarian Cancer SKOV3 Cells to BH3 Mimetic via Modulation of Mitochondrial Dynamics: SENSITIZATION OF SKOV3 CELLS TO BH3 MIMETIC. Anat. Rec. 300, 326–339.

271. Wang, X., Hybiske, K., and Stephens, R.S. (2017c). Orchestration of the mammalian host cell glucose transporter proteins-1 and 3 by Chlamydia contributes to intracellular growth and infectivity. Pathogens and Disease 75.

272. Wang, Y., Kahane, S., Cutcliffe, L.T., Skilton, R.J., Lambden, P.R., and Clarke, I.N. (2011). Development of a Transformation System for Chlamydia trachomatis: Restoration of Glycogen Biosynthesis by Acquisition of a Plasmid Shuttle Vector. PLoS Pathogens 7, e1002258.

273. Weber, M.M., Lam, J.L., Dooley, C.A., Noriea, N.F., Hansen, B.T., Hoyt, F.H., Carmody, A.B., Sturdevant, G.L., and Hackstadt, T. (2017). Absence of Specific Chlamydia trachomatis Inclusion Membrane Proteins Triggers Premature Inclusion Membrane Lysis and Host Cell Death. Cell Reports 19, 1406–1417.

274. Weiss, E. (1965). Adenosine Triphosphate and Other Requirements for the Utilization of Glucose by Agents of the Psittacosis-Trachoma Group1. Journal of Bacteriology 90, 243–253.

275. Weiss, E. (1967). Transaminase Activity and Other Enzymatic Reactions Involving Pyruvate and Glutamate in Chlamydia (Psittacosis-Trachoma Group)1. Journal of Bacteriology 93, 177–184.

276. Weiss, E., Myers, W.F., Dressler, H.R., and Chun-Hoon, H. (1964). Glucose metabolism by agents of the psittacosis-trachoma group. Virology 22, 551–562.

277. Wesolowski, J., and Paumet, F. (2017). Taking control: reorganization of the host cytoskeleton by Chlamydia. F1000Research 6, 2058.

278. Wesolowski, J., Weber, M.M., Nawrotek, A., Dooley, C.A., Calderon, M., and Paumet, F. (2017). Chlamydia Hijacks ARF GTPases To Coordinate Microtubule Posttranslational Modifications and Golgi Complex Positioning. MBio 8, 14.

279. Wilson, D.P., Timms, P., Mcelwain, D.L.S., and Bavoil, P.M. (2006). Type III Secretion, Contact-dependent Model for the Intracellular Development of Chlamydia. Bltn. Mathcal. Biology 68, 161–178.

280. Wilson, D.P., Whittum-Hudson, J.A., Timms, P., and Bavoil, P.M. (2009). Kinematics of Intracellular Chlamydiae Provide Evidence for Contact-Dependent Development. Journal of Bacteriology 191, 5734–5742.

281. Wyatt, E.V., Diaz, K., Griffin, A.J., Rassmussen, J.A., Crane, D.D., Jones, B.D., and Bosio, C.M. (2016). Metabolic reprogramming of host cells by virulent Francisella tularensis for optimal replication and modulation of inflammation. J Immunol 196, 4227–4236.

282. Wylie, J.L., Hatch, G.M., and McClarty, G. (1997). Host cell phospholipids are trafficked to and then modified by Chlamydia trachomatis. J Bacteriol 179, 7233–7242.

283. Yao, J., Abdelrahman, Y.M., Robertson, R.M., Cox, J.V., Belland, R.J., White, S.W., and Rock, C.O. (2014). Type II Fatty Acid Synthesis Is Essential for the Replication of Chlamydia trachomatis. Journal of Biological Chemistry 289, 22365–22376.

284. Yao, J., Cherian, P.T., Frank, M.W., and Rock, C.O. (2015a). Chlamydia trachomatis Relies on Autonomous Phospholipid Synthesis for Membrane Biogenesis. Journal of Biological Chemistry 290, 18874–18888.

285. Yao, J., Dodson, V.J., Frank, M.W., and Rock, C.O. (2015b). Chlamydia trachomatis Scavenges Host Fatty Acids for Phospholipid Synthesis via an Acyl-Acyl Carrier Protein Synthetase. Journal of Biological Chemistry 290, 22163–22173.

286. Ždralević, M., Vučetić, M., Daher, B., Marchiq, I., Parks, S.K., and Pouysségur, J. (2018). Disrupting the 'Warburg effect' re-routes cancer cells to OXPHOS offering a vulnerability point via 'ferroptosis'-induced cell death. Advances in Biological Regulation 68, 55–63.

287. Zhang, J.P., and Stephens, R.S. (1992). Mechanism of C. trachomatis Attachment to Eukaryotic Host Cells. 9.

288. Ziveri, J., Barel, M., and Charbit, A. (2017). Importance of Metabolic Adaptations in Francisella Pathogenesis. Front. Cell. Infect. Microbiol. 7.

289. Zu, X.L., and Guppy, M. (2004). Cancer metabolism: facts, fantasy, and fiction. Biochemical and Biophysical Research Communications 313, 459–465.

290. Zuck, M., Ellis, T., Venida, A., and Hybiske, K. (2017). Extrusions are phagocytosed and promote Chlamydia survival within macrophages: Extrusions are phagocytosed and promote Chlamydia survival within macrophages. Cellular Microbiology 19, e12683.

291. CDC | National overview of STDs (2019)

292. WHO | Homepage on Trachoma. WHO (2021)

293. WHO | Report on Global Adult Estimates for 4 STIs. WHO (2016)

294. WHO | Fact sheets on Sexually transmitted infections. WHO (2019)

Annexe

Table 1: Statistical analyses

Figure #	Comparison	Alternative hypothesis	Sample size	Test	p-value	Adjusted p-value
23. B	CTD and CTDm	mean difference	n = 76, n = 76	Welch test	0,02	*nr*
23. C	CTD and CTDm	mean difference	n = 3, n = 3	Welch test	0,03	*nr*
24. A	CTD and CTDm	effect difference	n = 9, n =9 | df = 13	Contrast test in linear model	2e-5	*nr*
24. B	CTD and CTDm	effect difference	n = 9, n =9 | df = 14	Contrast test in linear model	1e-6	*nr*
25. A	No Glucose and Glucose	effect difference	n = 11, n =11 | df = 18	Contrast test in linear model	2e-11	*nr*
26. A	Infected 24 h and Not infected	effect difference	n = 14, n =14 | df = 78	Contrast test in linear model	0.29	0.57
	Infected 30 h and Not infected	effect difference	n = 14, n =14 | df = 78	Contrast test in linear model	0.65	0.65
	Infected 48 h and Not infected	effect difference	n = 14, n =14 | df = 78	Contrast test in linear model	0.39	0.58
26. B	Infected 8 h and Not infected	effect difference	n = 12, n =12 | df = 42	Contrast test in linear model	0.51	0,51
	Infected 30 h and Not infected	effect difference	n = 12, n =12 | df = 42	Contrast test in linear model	1e-5	2e-5
27. A	0 and 5	effect difference	n = 12, n =12 | df = 53	Contrast test in linear model	4e-4	5e-4
	0 and 10	effect difference	n = 12, n =12 | df = 53	Contrast test in linear model	3e-3	3e-3
	0 and 25	effect difference	n = 12, n =12 | df = 53	Contrast test in linear model	4e-9	9e-9
	0 and 50	effect difference	n = 12, n =12 | df = 53	Contrast test in linear model	4e-9	9e-9
27. B	0 and 1	mean difference	n = 6, n = 3	Welch test	0.51	0.51
	0 and 2.5	mean difference	n = 6, n = 3	Welch test	0.09	0.12
	0 and 5	mean difference	n = 6, n = 3	Welch test	0.02	0.03
	0 and 10	mean difference	n = 6, n = 3	Welch test	0.01	0.04

28. A	0 and 2.5	effect difference	n = 12, n =12 | df = 49	Contrast test in linear model	1e-13	3e-13
	0 and 5	effect difference	n = 12, n =11 | df = 49	Contrast test in linear model	6e-12	8e-12
	0 and 10	effect difference	n = 12, n =11 | df = 49	Contrast test in linear model	4e-8	4e-8
	0 and 25	effect difference	n = 12, n =10 | df = 49	Contrast test in linear model	1e-14	5e-14
28.B	0 and 5	effect difference	n = 12, n =11 | df = 41	Contrast test in linear model	1e-9	1e-9
	0 and 10	effect difference	n = 12, n =12 | df = 41	Contrast test in linear model	2e-14	3e-14
	0 and 25	effect difference	n = 12, n =12 | df = 41	Contrast test in linear model	4e-16	1e-15
28. D	0 and 10	mean difference	n = 3, n = 3	Welch test	0.45	*nr*
28. E	0 and 5	effect difference	n = 11, n =10 | df = 36	Contrast test in linear model	8e-3	8e-3
	0 and 10	effect difference	n = 11, n =10 | df = 36	Contrast test in linear model	9e-6	1e-5
	0 and 25	effect difference	n = 11, n =11 | df = 36	Contrast test in linear model	6e-8	2e-7
28. F	0 and 2.5	effect difference	n = 11, n =10 | df = 36	Contrast test in linear model	0.02	0.06
	0 and 5	effect difference	n = 11, n =10 | df = 36	Contrast test in linear model	0.48	0.48
	0 and 10	effect difference	n = 11, n =11 | df = 36	Contrast test in linear model	0.31	0.46
28. G A2EN cells	Not treated and Oligomycin	mean difference	n = 5, n = 5	Welch test	7e-4	*nr*
28. G Primary cells	Not treated and Oligomycin	mean difference	n = 3, n = 3	Welch test	9e-5	*nr*
28. H	0 and 0.5	effect difference	n = 12, n =9 | df = 35	Contrast test in linear model	2e-3	2e-3
	0 and 1	effect difference	n = 12, n =10 | df = 35	Contrast test in linear model	1e-7	2e-7
	0 and 2	effect difference	n = 12, n =10 | df = 35	Contrast test in linear model	4e-11	1e-10

28. I	0 and 5	effect difference	n = 5, n =5 | df = 16	Contrast test in linear model	0.55	0.73
	0 and 10	effect difference	n = 5, n =5 | df = 16	Contrast test in linear model	0.83	0.83
	0 and 20	effect difference	n = 5, n =5 | df = 16	Contrast test in linear model	0.24	0.48
	0 and 40	effect difference	n = 5, n =5 | df = 16	Contrast test in linear model	0.11	0.14
28. J	0 and 2.5	effect difference	n = 11, n =12 | df = 40	Contrast test in linear model	2e-3	2e-3
	0 and 5	effect difference	n = 11, n =11 | df = 40	Contrast test in linear model	1e-7	2e-7
	0 and 10	effect difference	n = 11, n =12 | df = 40	Contrast test in linear model	4e-11	1e-10
28. K	0 and 20	effect difference	n = 10, n =10 | df = 32	Contrast test in linear model	3e-7	3e-7
	0 and 40	effect difference	n = 10, n =9 | df = 32	Contrast test in linear model	1e-9	2e-9
	0 and 80	effect difference	n = 10, n =9 | df = 32	Contrast test in linear model	4e-11	1e-10
29. A	Not treated and 24h	mean difference	n = 3, n = 3	Welch test	0.02	0.06
	Not treated and 30h	mean difference	n = 3, n = 3	Welch test	0.08	0.08
	Not treated and 48h	mean difference	n = 3, n = 3	Welch test	0.04	0.06
29. B	Infected 24 h and Not infected	effect difference	n = 11, n =13 | df = 74	Contrast test in linear model	0.60	0.79
	Infected 30 h and Not infected	effect difference	n = 16, n =13 | df = 74	Contrast test in linear model	0.12	0.35
	Infected 48 h and Not infected	effect difference	n = 13, n =13 | df = 74	Contrast test in linear model	0.79	0.79
29. C	Infected 24 h and Not infected	effect difference	n = 10, n =10 | df = 53	Contrast test in linear model	0.30	0.45
	Infected 30 h and Not infected	effect difference	n = 11, n =10 | df = 53	Contrast test in linear model	0.06	0.18
	Infected 48 h and Not infected	effect difference	n = 11, n =10 | df = 53	Contrast test in linear model	0.62	0.62

30. A	Infected 24 h and Not infected	mean difference	n = 3, n = 3	Welch test	0.77	0.77
	Infected 30 h and Not infected	mean difference	n = 3, n = 3	Welch test	0.76	0.77
	Infected 48 h and Not infected	mean difference	n = 3, n = 3	Welch test	0.65	0.77
30. B	Not treated and 24h	mean difference	n = 3, n = 3	Welch test	0.90	0.91
	Not treated and 30h	mean difference	n = 3, n = 3	Welch test	0.80	0.91
	Not treated and 48h	mean difference	n = 3, n = 3	Welch test	0.85	0.91
30. C	Not treated and 24h	mean difference	n = 4, n = 4	Welch test	0.35	0.60
	Not treated and 30h	mean difference	n = 4, n = 4	Welch test	0.40	0.60
	Not treated and 48h	mean difference	n = 4, n = 4	Welch test	0.98	0.98
30. D	Not treated and 24h	mean difference	n = 4, n = 4	Welch test	0.94	0.98
	Not treated and 30h	mean difference	n = 4, n = 4	Welch test	0.98	0.98
	Not treated and 48h	mean difference	n = 4, n = 4	Welch test	0.93	0.98
31. A	0 and 5	mean difference	n = 3, n = 3	Welch test	0.24	0.26
	0 and 10	mean difference	n = 3, n = 3	Welch test	4e-3	0.01
	0 and 25	mean difference	n = 3, n = 3	Welch test	2e-7	1e-6
31. B	0 and 5	mean difference	n = 3, n = 3	Welch test	0.62	0.62
	0 and 10	mean difference	n = 3, n = 3	Welch test	0.46	0.62
	0 and 25	mean difference	n = 3, n = 3	Welch test	0.10	0.32
31. C	0 and 5	mean difference	n = 3, n = 3	Welch test	0.01	0.02
	0 and 10	mean difference	n = 3, n = 3	Welch test	5e-3	0.01
	0 and 25	mean difference	n = 3, n = 3	Welch test	0.04	0.04
31. D	0 and 5	mean difference	n = 3, n = 3	Welch test	0.23	0.23
	0 and 10	mean difference	n = 3, n = 3	Welch test	0.02	0.03
	0 and 25	mean difference	n = 3, n = 3	Welch test	0.01	0.03
31. E	0 and 5	mean difference	n = 3, n = 3	Welch test	0.02	0.02
	0 and 10	mean difference	n = 3, n = 3	Welch test	5e-3	8e-3
	0 and 25	mean difference	n = 3, n = 3	Welch test	1e-3	3e-3
32. B	0 and 5	mean difference	n = 3, n = 3	Welch test	2e-3	2e-3
	0 and 10	mean difference	n = 3, n = 3	Welch test	8e-5	2e-4
33. A	0 and 5	mean difference	n = 4, n = 4	Welch test	0.69	0.92
	0 and 10	mean difference	n = 4, n = 4	Welch test	0.54	0.92
	0 and 25	mean difference	n = 4, n = 4	Welch test	0.92	0.92

33. C	Not.treated - siGPI1	mean difference	n = 4, n = 4	Welch test	0.49	0.77
	Not.treated - siGPI2	mean difference	n = 4, n = 4	Welch test	0.52	0.77
	siGPI1 - siGPI2	mean difference	n = 4, n = 4	Welch test	0.93	0.93
33. E	GPI.KO26 - GPI.KO8	mean difference	n = 3, n = 3	Welch test	0.93	0.93
	GPI.KO26 - WT	mean difference	n = 3, n = 3	Welch test	0.67	0.93
	GPI.KO8 - WT	mean difference	n = 3, n = 3	Welch test	0.76	0.93
34. A	0 and 0.5	mean difference	n = 3, n = 3	Welch test	3e-3	3e-3
	0 and 1	mean difference	n = 3, n = 3	Welch test	1e-3	2e-3
	0 and 2	mean difference	n = 3, n = 3	Welch test	5e-4	2e-3
34. B	0 and 10	mean difference	n = 3, n = 3	Welch test	1e-3	1e-3
	0 and 20	mean difference	n = 3, n = 3	Welch test	9e-4	1e-3
	0 and 40	mean difference	n = 3, n = 3	Welch test	4e-3	1e-3
34. C	0 and 0.5	effect difference	n = 12, n =12 | df = 52	Contrast test in linear model	1e-13	3e-13
	0 and 2	effect difference	n = 12, n =12 | df = 52	Contrast test in linear model	6e-12	8e-12
	0 and 10	effect difference	n = 12, n =12 | df = 52	Contrast test in linear model	4e-8	4e-8
	0 and 40	effect difference	n = 12, n =12 | df = 52	Contrast test in linear model	1e-14	5e-14
35. A	Not treated and 0.5	mean difference	n = 4, n = 4	Welch test	0.70	0.91
	Not treated and 1	mean difference	n = 4, n = 4	Welch test	0.86	0.91
	Not treated and 2	mean difference	n = 4, n = 4	Welch test	0.10	0.59
	Not treated and 10	mean difference	n = 4, n = 4	Welch test	0.67	0.91
	Not treated and 20	mean difference	n = 4, n = 4	Welch test	0.78	0.91
	Not treated and 40	mean difference	n = 4, n = 4	Welch test	0.91	0.91
35. B	0 and 0.5	mean difference	n = 3, n = 3	Welch test	3e-3	3e-3
	0 and 1	mean difference	n = 3, n = 3	Welch test	3e-4	6e-4
[a] n, sample size for each class tested, respectively; df, degree of freedom; nr, not relevant; adjusted p values from the same panel, according to Benjamini & Hochberg						

Acquisition of a type 3 secretion signal in an housekeeping enzyme shaped glycogen metabolism in *Chlamydia*

Sébastien Triboulet[1,2], Maimouna D. N'Gadjaga[1,2,3], Béatrice Niragire[1,2], Stephan Köstlbacher[4], Matthias Horn[4] and Agathe Subtil[1,2*]

[1] Institut Pasteur, Unité de Biologie cellulaire de l'infection microbienne, 25 rue du Dr Roux, 75015 Paris, France

[2] CNRS UMR3691, Paris, France

[3] Sorbonne Université, Collège Doctoral, F-75005 Paris, France

[4] Centre for Microbiology and Ecosystem Science, University of Vienna, Vienna, Austria;

Short Title: PGM activity in *C. trachomatis*

[*] Corresponding author: Unité de Biologie cellulaire de l'infection microbienne
25 rue du Dr Roux, 75015 Paris, France
Tel: +33 1 40 61 30 49
Fax: + 33 1 40 61 32 38
E-mail: asubtil@pasteur.fr

ABSTRACT

The obligate intracellular bacteria *Chlamydia trachomatis* store glycogen in the lumen of the vacuoles in which they grow. Glycogen catabolism generates glucose-1-phosphate (Glc1P), while the bacteria are capable of taking up only glucose-6-phosphate (Glc6P). We tested whether the conversion of Glc1P into Glc6P could be catalyzed by a phosphoglucomutase (PGM) of host or bacterial origin. We found no evidence for the presence of the host enzyme in the vacuole. In *C. trachomatis*, two proteins are potential PGMs. By reconstituting the reaction, and by complementing PGM deficient fibroblasts, we demonstrated that only CT295 displayed robust PGM activity. Furthermore, we showed that glycogen accumulation by a subset of *Chlamydia* species correlated with the presence of a type three secretion (T3S) signal in their PGM. In conclusion, we established that the conversion of Glc1P into Glc6P was accomplished by a bacterial PGM, through the acquisition of a T3S signal in a "housekeeping" gene.

INTRODUCTION

Many bacteria and parasites develop inside vacuolar compartments within eukaryotic cells. Such enclosed replication niches provide a shelter against extracellular and cytosolic host defense. They can also be further exploited to sequester cytoplasmic components and make them accessible only to the intruder. One striking example of this behavior is the vacuole in which the human adapted pathogen *Chlamydia trachomatis* grows, also called the inclusion (1). Glucose is the main carbon source for these obligate intracellular bacteria (2-5). Over the course of their developmental cycle they hijack a considerable amount of glucose from their host, and accumulate it as a polysaccharide, i.e. glycogen, in the lumen of the inclusion (6, 7). The *C. trachomatis* genome encodes for all the enzymes necessary for a functional glycogenesis and glycogenolysis, a surprising observation given that this pathway is absent in most intracellular bacteria (8). Glycogen starts accumulating in the lumen of the inclusion about 20 hours post infection (hpi), a time of intensive bacterial replication (9). Shortly later, while luminal glycogen continues to accumulate, a fraction of the dividing bacteria, called reticulate bodies (RB), initiate conversion into the non-dividing, infectious, form of the bacterium, the elementary body (EB). Electron microscopy studies showed that, in contrast to RBs, EBs contain glycogen, but in modest quantities compared to the luminal glycogen. While part of the luminal glycogen is imported in bulk from the host cytoplasm, the majority is synthesized *de novo* through the action of bacterial enzymes (9). Bacterial glycogen synthase GlgA, and branching enzyme GlgB, have acquired type 3 secretion (T3S) signals that allow their secretion in the lumen of the inclusion, where they ensure glycogen synthesis out of UDP-glucose imported from the host cytosol (9). T3S of these enzymes is likely shut down once the bacteria have converted into EBs. This simple mechanism might account for the appearance of glycogen in EBs, once GlgA and GlgB can accumulate within the bacteria.

Bacterial enzymes responsible for glycogen catabolism into Glc1P, i.e. the glycogen phosphorylase GlgP, the debranching enzyme GlgX, and the amylomaltase MalQ, have also acquired T3S signals (9). In *C. trachomatis* infection, they are expressed as early as 3-8 hpi, indicating that even if glycogen is only detected 20 hpi, there is a continuous flux of Glc1P generation in the inclusion lumen earlier on (9, 10). However, Glc1P cannot sustain bacterial growth directly because the glucose transporter UhpC can only import Glc6P, not free glucose nor Glc1P (9, 11). Thus, while the rate of expression and distribution of *C. trachomatis* glycogen enzymes and the strategy of glycogen storage in the inclusion lumen by RBs point to a sophisticated pathway for hijacking host glucose, this metabolite would not be able to fuel bacterial metabolism due to a lack of an import mechanism.

To solve this conundrum, we had hypothesized that an enzyme with PGM activity was present in the inclusion lumen (9). In the present work we tested this hypothesis in depth by investigating two non-mutually exclusive possibilities as to its origin: the translocation of a host enzyme into the inclusion, and the secretion of a bacterial enzyme. We provide evidence for the second hypothesis and identify CT295 as *C. trachomatis* PGM. In addition, we show that this feature is characteristic of the glycogen-accumulating *Chlamydiaceae* as opposed to the glycogen-free species.

RESULTS

Absence of evidence for the import of host phosphoglucomutase in the inclusion lumen.

PGM activity in human cells is carried out by the enzyme PGM1. PGM1 deficiency leads to defects in glycogen storage, and to several disorders resulting from insufficient protein glycosylation (12, 13). To test for the presence of this enzyme in *C. trachomatis* inclusions we expressed PGM1 with either an amino-terminal (Flag-PGM1) or a carboxy-terminal (PGM1-Flag) Flag tag in HeLa cells, which were further infected with *C. trachomatis* L2. The cells were fixed 24 h later and stained with a mouse antibody against the Flag tag and a rabbit antibody against the inclusion protein Cap1. An irrelevant Flag-tagged protein (Flag-CymR) was included as a negative control, and Flag-tagged chlamydial glycogen synthase (Flag-GlgA), as a positive control (9). Flag-PGM1 and PGM1-Flag had a cytosolic distribution, as expected (Fig. 1A). In infected cells, it was often abundant in the vicinity of the inclusion membrane, especially with the carboxy-terminal tag. However, no signal was detected in the inclusion lumen, indicating that PGM1 is not translocated in this compartment. We next tested whether silencing PGM1 expression had any effect on bacterial development. Cells were infected 24 h after siRNA transfection with two different siRNA (si*pgm1*_1 and si*pgm1*_2), and the resulting progeny was measured 48 hours post infection (hpi). The efficacy of each of the siRNA against PGM1 was validated by western blot (Fig. 1B). Transfection of si*pgm1*_2 had no effect on progeny, while transfection of si*pgm1*_1 reduced it by about two-fold (Fig. 1C). However, transfection with si*pgm1*_1 reduced cell viability, which likely accounts for the decrease in progeny. Altogether, silencing PGM1 expression did not significantly affect bacterial development.

We concluded from this series of experiments that host PGM1 does not reach the inclusion lumen, at least not in detectable amount, and is not essential for the generation of infectious bacteria. Therefore, it is unlikely that the conversion of Glc1P into Glc6P in the inclusion lumen relies on the host PGM activity by PGM1.

CT295 is the main PGM in *C. trachomatis*, while CT815 displays low activity towards Glc1P

CT295 and CT815 are two *C. trachomatis* proteins that belong to the eggNOG cluster of orthologous groups COG1109 (Fig. S1A, (14)). Members of this large group of bacterial, archaeal and eukaryotic proteins display PGM activity and related functions such as phosphomannomutase or phosphoglucosamine mutase activities. CT295 and CT815 homologs are found among all known chlamydiae. These proteins represent separate monophyletic clades in COG1109 and are related to proteins from diverse bacterial taxa (Fig. S1A). CT295 and CT815 are only distantly related with each other and thus do not originate from a recent gene duplication event (Fig. S1B).

To test if CT295 and/or CT815 displayed PGM activity we expressed them in *Escherichia coli* with an amino-terminal histidine tag. HIS-CT295 was not produced by *E. coli*, and after testing the orthologous protein in different *Chlamydiaceae* we chose the *C. caviae* ortholog, CCA00034, which displayed 59 % amino acid identity with CT295. HIS-CCA00034 and HIS-CT815 were purified from *E. coli* extracts (Fig. S2A). As a positive control we also produced the *E. coli* phosphomannomutase CpsG, because our initial attempts to produce the *E. coli* PGM failed, and CpsG turned out to display good PGM activity *in vitro*. To test the ability of these recombinant proteins to convert Glc1P into Glc6P we first incubated them with Glc1P in the presence of glucose 1,6-diPhosphate (Glc1,6diP), a cofactor for the PGM reaction in *E. coli* (15). The samples were incubated for 20 min at 37 °C, before stopping the reaction by boiling for 5 min. Sugars present in the samples were analyzed by high performance anion exchange chromatography with pulsed amperometric detection (HPAEC-PAD) (Fig. S2B). Incubation of Glc1P in the presence of HIS-CCA00034 led to its full conversion into Glc6P, while only low levels of Glc6P were detected in the presence of HIS-CT815 (Fig. 2A). Interestingly we noted that while we confirmed that HIS-CpsG required the presence of Glc1,6diP to convert Glc1P into Glc6P, HIS-CCA00034 did not, indicating that the chlamydial enzyme evolved to bypass co-factor requirement (Fig. S2C). Also, HIS-CCA00034 favored the conversion of α-Glc6P into β-Glc6P, a property that we did not observed in CT815 nor CpsG (Fig. 2 and Fig. S2).

When we monitored the reverse reaction, supplying Glc6P and following the appearance of Glc1P, very low amounts of Glc1P were detected after incubation with HIS-CCA00034 or HIS-CpsG, and none with HIS-CT815 (Fig. 2B and Fig. S2). This indicates that, *in vitro*, the conversion of Glc1P into Glc6P is more favorable than the reverse reaction. To confirm that CT295 was nonetheless capable of catalyzing the reverse reaction, we made use of human fibroblasts deficient for PGM1. One of the phenotypes associated with PGM1 deficiency is a defect in protein glycosylation, due to the inability to convert Glc6P into Glc1P to feed UDP-Glc synthesis and thereby protein glycosylation (13). As a consequence, several glycosylated proteins like the cell-surface glycoprotein intercellular adhesion molecule 1 (ICAM-1) are hardly expressed at the cell surface in PGM1 deficient cells (13). ICAM-1 expression can thus be used as a read-out for PGM activity. As expected, ICAM-1 was hardly detected at the surface of PGM1 deficient fibroblasts. Transfection of an irrelevant protein, Flag-CymR, had a marginal effect on ICAM-1 expression. In contrast, as expected, transfection of the wild-type human PGM1 restored ICAM1 expression in the PGM1 deficient fibroblasts. Transfection of CT295 also restored ICAM-1 expression, confirming its ability to catalyze the conversion of Glc6P into Glc1P. Transfection of CT815 also resulted in increased ICAM-1 expression, but to a lesser extent, supporting the hypothesis that while CT815 displays some phosphoglucomutase activity, it is likely that it uses a different sugar than glucose as a favorite substrate (Fig. 2C).

Altogether, these data demonstrate that CT295, and its ortholog in *C. caviae*, are bona fide phosphoglucomutases.

CT295 is a T3S substrate

If CT295 is the PGM that converts Glc1P into Glc6P in the inclusion lumen it needs to be secreted out of the bacteria. We have shown that *C. trachomatis* glycogen metabolism enzymes were secreted by a T3S mechanism (9). To explore if this was also true for CT295, we tested for the presence of a functional T3S signal within its amino-terminus using a heterologous secretion assay in *Shigella flexneri* as described previously (16). Briefly, we fused these amino-terminal sequences to the reporter protein calmodulin-dependent adenylate cyclase (Cya). The chimeric proteins were then expressed in *S. flexneri ipaB* (constitutive T3S) or *mxiD* (deficient in T3S) null strains. When we analyzed the culture supernatant versus the bacterial pellet, we found the Cya reporter in the supernatant of *ipaB* cultures (Fig. 3A). The same expression pattern was observed for an endogenous *Shigella* T3S substrate, IpaD. Conversely, we found the cAMP receptor protein (CRP), a non-secreted protein, exclusively in the bacterial pellet. This control shows that Cya detection in the supernatant was not due to bacterial lysis. Finally, the Cya reporter was not recovered in the supernatants of the *mxiD* strain, demonstrating that its secretion was dependent on the T3S system.

Evidence for the direct secretion of CT295 in the inclusion lumen

C. trachomatis GlgA is detected both in the inclusion lumen and in the cytoplasm (17). When expressed ectopically by the host in the cytoplasm, this bacterial enzyme was able to translocate into the inclusion lumen (9). These observations suggested that some T3S substrates might be first translocated in the cytoplasm, before being transferred into the inclusion lumen. To test whether this was also the case for CT295, we first transformed *C. trachomatis* with an expression plasmid constitutively expressing the green fluorescent protein (GFP), as well as CT295 with a carboxy-terminal Flag tag under the control of an inducible promoter, as an initial attempt using the endogenous promoter showed no protein expression. Bacteria expressing GlgA-Flag under the control of its endogenous promoter were used for comparison. The cells were fixed 48 hpi, permeabilized, and stained with a mouse antibody against the Flag tag and a rabbit antibody against the inclusion membrane protein Cap1. As expected, a cytoplasmic staining was observed for GlgA-Flag, although only in ~ 10% of the infected cells (n=150 infected cells from 2 independent experiments). A faint Flag staining was detected in the inclusions upon induction of cells infected with bacteria expressing CT295-Flag (Fig. 3B). No signal was detected in the host cell cytoplasm, indicating that the protein is not translocated there. However, the expression level of CT295-Flag was much lower than that of GlgA-Flag, whose cytoplasmic location is only visible in ~ 10% of the cells. Thus, this assay might not be sensitive enough to detect CT295 in the cytoplasm.

As an alternative approach to test for CT295 presence in the host cytoplasm we tested whether infection could restore PGM activity in the cytoplasm of PGM1 deficient fibroblasts. Indeed, if CT295 reached the cytoplasm, it might lead to at least a partial recovery of ICAM-1 glycosylation. Cells transfected with Flag-PGM1 served as a positive control. We observed that ICAM-1 expression, which was undetectable at the surface of PGM1 deficient fibroblast, remained absent from the surface of cells infected for 40 h with *C. trachomatis* (Fig. 3C). One

pitfall of this experiment is that *C. trachomatis* L2 takes up UDP-glucose from the host cytoplasm to accumulate glycogen in the inclusion lumen (9). Therefore, the presence of a bacterial PGM in the cytoplasm might not be sufficient to restore ICAM-1 glycosylation. We thus also used the plasmid-less L2(25667R), which is less likely to deplete the host UDP-glucose stores, as it does not accumulate glycogen in the inclusion (18). Infection with L2(25667R) did not restore ICAM-1expression at the cell surface either. These experiments indicate that CT295 is translocated directly into the inclusion lumen, without an intermediate cytoplasmic step (Fig. 3C).

Presence of a T3S in CT295 orthologs among *Chlamydiaceae* correlates with their capacity to accumulate glycogen in the inclusion lumen

We next asked whether the secretion of a PGM was a conserved feature among *Chlamydiaceae*. Previous studies have reported glycogen accumulation in *C. suis* and *C. muridarum* inclusions, but the polysaccharide was not observed in the inclusions of more phylogenetically distant *Chlamydia* species such as *C. caviae* or *C. pneumoniae*. We verified this feature by performing periodic acid-Schiff staining (PAS) on cells infected with these different species. Inclusion staining was observed only on cells infected with *C. trachomatis*, *C. suis* and *C. muridarum* (Fig. 4A). Two amino-terminal amino-acids (W23L24) are conserved in the orthologs of CT295 in all chlamydiae, and the preceding amino acids show low levels of conservation (Fig. 4B). To test whether these different peptides also function as T3S signals in other species than *C. trachomatis* we constructed chimeras between the amino-terminal 22 amino-acids of the different CT295 orthologs and the Cya reporter gene, and tested their secretion when expressed in the *S. flexneri ipaB* strain. The chimera made out of the amino-terminal segment of *C. suis* and *C. muriarum* PGMs were recovered in the supernatant, but not those originating from *C. caviae* or *C. pneumoniae*. Secretion was dependent on the T3S system since the chimera were not recovered in the supernatant when expressed by the *S. flexneri mxiD* strain (Fig. 4C). Thus, the accumulation of glycogen in the inclusion of *Chlamydiaceae* correlates with their ability to secrete a phosphoglucomutase.

DISCUSSION

To be of metabolic use for the bacteria the glycogen stored in the inclusion lumen needs to be converted into glucose moieties. Glycogen degradation in the inclusion generates Glc1P, and the single glucose transporter of *C. trachomatis*, UhpC, displays transport activity exclusively towards Glc6P. We show here that this conundrum is solved by the secretion of a bacterial PGM, CT295, by the T3S system. Host PGM1 was not translocated into the inclusion lumen, at least not at levels detectable by immunofluorescence. Silencing *pgm1* did not affect the generation of infectious bacteria. Thus, while we cannot exclude that imported host PGM1 also contributes to Glc1P to Glc6P conversion in the inclusion lumen, our data suggest that such activity would only be marginal compared to that of secreted CT295.

In vitro and *in cellulo* assays demonstrated that CT295 and its ortholog in *C. caviae* displayed *bona fide* PGM activity. Interestingly, unlike what had been observed in *E. coli* (15), the chlamydial activity did not require the co-factor glucose 1,6-diPhosphate (Glc1,6diP). This may represent an adaptation to the inclusion environment, where this metabolite might be absent. The second *C. trachomatis* enzyme with predicted PGM activity, CT815, diverged from CT295 early in the evolution of the phylum, possibly even before its emergence. It displayed a poor ability to interconvert Glc1P and Glc6P *in vitro* and *in vivo*, indicating that its preferred substrate is different, possibly phosphoglucosamine, as shown for at least one member or the same clade (19).

Transcriptomic studies detected transcription of *ct295* 8 hpi, a timing that coincides with the start of expression of the Glc6P transporter *uhpC* (10). Interestingly, the protein CT295 was hardly detected by proteomics in the replicative form of the bacteria, the reticulate bodies (RBs), while it was rather abundant in the infectious form, the elementary bodies (EBs) that accumulate at the end of the developmental cycle (20). This difference in abundance in the two bacterial forms is consistent with the observation that glycogen is detectable in EBs, not in RBs (9). It might be explained by the fact that most CT295 synthesized by RBs is secreted to convert Glc1P to Glc6P in the inclusion lumen, and thus absent from purified RBs. Like other T3S substrates, secretion of CT295 probably stops during conversion to the EB stage, and the enzymatic activity is then mostly exerted inside the bacteria. Here, it is likely used for the conversion of Glc6P into Glc1P, which serves as a substrate for the ADP-Glc pyrophosphorylase GlgC to initiate glycogen synthesis in the bacteria.

We and others have shown that several T3S substrates are detected in the inclusion lumen (9, 21, 22). This observation was at first surprising considering that most T3S machineries have been described to deliver proteins across a eukaryotic membrane, through the translocon pore. Here, we considered the possibility that CT295 was first translocated into the cytoplasm before being transported back inside the inclusion lumen. However, we found no evidence of an increase in PGM activity in the host cytoplasm upon infection. It is therefore likely that CT295 is secreted directly into the lumen of the inclusion. Of note, several T3S substrates have been detected on the surface of different Gram-negative bacteria before being translocated into a mammalian cell (23, 24). These observations support the hypothesis of direct secretion of T3S substrates into the inclusion lumen rather than via the T3S translocon pore into the host cell. Future work will be needed to understand how these substrates are sorted from those that are translocated into the cytoplasm.

Finally, we made the intriguing observation that chlamydial PGMs possess functional T3S signals only in species that accumulate glycogen in the inclusion lumen. These species are phylogenetically apart from other *Chlamydiaceae*, and differ by several other features (25). We lack sufficient information on the translocation, in the inclusion lumen or in the host cytoplasm, of glycogen metabolism enzymes of *Chlamydiaceae* other than *C. trachomatis* to draw solid hypotheses on the evolutionary path that led to this situation, we can however try to elaborate on this observation. We have shown that T3S signals were present in glycogen metabolism enzymes of several environmental chlamydiae, indicating that the ability to take

control of glycogen storage capacity of the host was acquired early upon evolution of the phylum (26, 27). One possibility is that the acquisition of T3S signal in the PGM of the *Chlamydia* lineage (as opposed to species of the formerly called *Chlamydophila* lineage, e.g. *C. pneumoniae* and *C. Caviae*) opened the way to a positive selection of the capacity to store glycogen in the inclusion. Indeed, once Glc1P became convertible to Glc6P, it might have become advantageous to store a lot of glycogen, possibly to compete out the rest of the microbiota, or to weaken host cell defense, as previously discussed (9). Of note, expression of the glycogen synthase GlgA is the limiting factor for glycogen accumulation in the inclusion. In *C. trachomatis*, this gene is under transcriptional control by the *C. trachomatis* plasmid (18). Acquisition of this transcriptional control was likely also an important step along the path towards the glycogen storage strategy.

One question left open is whether a more direct mechanism for Glc6P supply in the inclusion lumen of *C. trachomatis* also takes place? An alternative mechanism must exist at least in the *Chlamydiaceae* of the former *Chlamydophila* lineage, considering the absence of glycogen and phosphoglucomutase in their inclusions, and the fact that UhpC transports only Glc6P also in *C. pneumoniae* (11). The situation is different in environmental chlamydiae because, unlike *Chlamydiaceae*, environmental chlamydiae express a hexokinase activity (28-30), and are likely able to import glucose, as demonstrated in the case of *Protochlamydia amoebophila* (31).

In conclusion, we have shown that several "housekeeping" chlamydial proteins are secreted outside the bacteria. This possibility has seldom been investigated in other bacteria, but was also observed for glyceraldehyde-3-phosphate dehydrogenase in enteropathogenic *E. coli* (32). In that case, the broad range type 3 secretion chaperone CesT was involved, and whether such a chaperone is required for the secretion of chlamydial enzymes remains to be investigated. In any case, the secretion of bacterial enzymes opens the door to a direct modification of the metabolism of the host cell to the benefit of the bacteria, and might therefore occur more frequently than currently known.

MATERIAL AND METHODS

Cells and bacteria

HeLa cells (ATCC) were cultured in Dulbecco's modified Eagle's medium (DMEM) with Glutamax (Gibco™ #31966), supplemented with 10 % (v/v) fetal bovine serum (FBS). Fibroblast CDG_0072 deficient in PGM1, a kind gift from Pr. Hudson Freeze (La Jolla, CA), were grown in DMEM (Gibco™ # A1443001) supplemented with 1 g/L glucose, 584 mg/mL L-glutamine, 110 mg/mL sodium pyruvate, and 10% FBS. Cells were routinely checked for absence of mycoplasma contamination by PCR. *C. trachomatis* LGV serovar L2 strain 434/Bu (ATCC), the plasmid-less strain LGV L2 25667R (33) and GFP-expressing L2 ($L2^{IncD}GFP$) (34) were purified on density gradients as previously described (35). Other *Chlamydia* strains used were *C. suis* SWA107, a kind gift from Nicole Borel (Zürich, Switzerand), *C. pneumoniae* CWL029, *C. muridarum* MoPn and *C. caviae* GPIC. The *Shigella flexneri ipaB* and *mxiD* strains

are derivates of M90T, the virulent wild-type strain, in which the respective genes (*ipaB* and *mxiD*) have been inactivated (36). The *Escherichia coli* strain *DH5α* was used for cloning purposes and plasmid amplification. Both *S. flexneri* and *E. coli* strains were grown in Luria-Bertani (LB) medium.

Phylogenetic analysis of CT295 and CT815

Protein sequences of CT295 and CT815 were analyzed with eggNOG v4.5.1 (14). They are both members of COG1109 at the last universal common ancestor (LUCA) taxonomic level (including all domains of life). At the bacteria-specific eggNOG clustering, CT295 and CT815 belong to two distinct EggNOGs, ENOG4107QSU and ENOG4107QJF. To identify closely related sequences we used eggNOG-mapper v1.0.1 (37) with the bacteria optimized database using the "--database bact" option and default settings on a broad selection of published chlamydial genomes. We downloaded all COG1109 sequences (n=4,829; http://eggnogapi45.embl.de/nog_data/text/fasta/COG1109), added all chlamydial ENOG4107QSU (n=104) and ENOG4107QJF (n=69) sequences and aligned them using the COG1109 hidden markov model (http://eggnogapi45.embl.de/nog_data/file/hmm/COG1109). To reduce redundancy we clustered the alignment with the cd-hit program (38) at 80% sequence identity over at least 90% of the shorter sequence ("-aS 0.9 -c 0.8"). We performed de novo multiple sequence alignment of the clustered sequences (n=2,869) with MAFFT 7.222 (39) using the "--localpair" and "--maxiterate 1000" parameter and trimmed the alignment with trimAl "-gappyout" (40). Only sequences with a gap-rate < 50% were retained (n=2,829). We performed model testing under the empirical LG model (41), and with the empirical mixture models C10 to C60 (best model: C60+LG+G+F) and maximum likelihood tree reconstruction with IQ-TREE 1.6.2 (42). We inferred support values from 1,000 ultrafast bootstrap replicates (43) with the "-bnni" option for bootstrap tree optimization and from 1,000 replicates of the SH-like approximate likelihood ratio test (44).We next extracted the sister clade of CT295 (n=93) and used it as an outgroup for a more detailed analysis of CT295 related proteins. Sequence alignment, trimming, and initial phylogenetic reconstruction (best model: C60+LG+G+F) was performed as described above. We then used the resulting best tree as a guide tree for the posterior mean site frequency (PMSF) model (45) for improved site heterogeneity modeling under C60+LG+G+F and inferred 100 non-parametric bootstraps. Phylogenetic trees were visualized and edited using the Interactive Tree Of Life v4 (46).

Cloning

Primer sequences and cloning methods are described in Table S1. The gene *ct815* was cloned as follows: the gene was amplified with primers 1 and 4, and with primers 2 and 3. PCR products were mixed, heated to 65 °C for 10 minutes, and annealed at 37 °C for 30 minutes. The mix was then cloned into the pET28a previously digested by NcoI and XhoI restriction enzymes. Chimeras to test for the presence of T3S signal were constructed like in (16), using the first 22 codons of the gene of interest. Flag-GlgA is described in (9) and the negative

control, CymR, that corresponds to a bacterial repressor for gene expression from *Pseudomonas putida* (47) was constructed through Gateway cloning like Flag-PGM1 and PGM1-Flag. The *ctl0547* gene (CT295 in the *C. trachomatis* L2/434/Bu strain) followed by a nucleotide sequence coding for a flag tag immediately upstream of the stop codon was cloned using NotI and SalI restriction sites into the pBOMB4-Tet-mCherry plasmid after removing the mCherry insert (48). For GlgA, cloning was performed in pBOMB4 using the endogenous promoter of the *ctl0167* gene. The strain LGV L2 25667R was stably transformed with these plasmid as described (49).

Production and purification of recombinant proteins.

E. coli BL21 (DE3) was used for the production of recombinant CCA00034, CT815, and CpsG harboring a polyhistidine tag at the C-terminal part of the protein. Bacteria were grown at 37 °C to an optical density at 600 nm of 0.9 in 2 liters of LB with 30 µg/mL of kanamycin under shaking. 0.5 mM of isopropyl-β-D-thiogalactopyranoside (IPTG) was added and incubation was continued for 18 h at 16 °C. Bacteria were harvested by centrifugation, and proteins were purified from clarified lysate by affinity chromatography on Ni^{2+}-nitrilotriaceta-agarose (Qiagen) in 20 mM Tris-HCl 500 mM NaCl pH 8.0 buffer and by size exclusion chromatography on Superdex 200 HL 16/600 column (GE Healthcare) in 20 mM Tris-HCl 500 mM NaCl pH 7.0 buffer. All purified proteins were stored at 4 °C.

Phosphoglucomutase activity assay.

HIS-tagged CCA00034, CT815 or CpsG (0,1 mg/mL) were incubated for 20 minutes at 37 °C with 0.2 mg/mL of glucose-1,6-diphosphate and either 0.66 mg/ml glucose-1-phosphate or 0.33 mg/ml glucose-6-phosphate in 10 mM Tris-HCl buffer (pH 8.0) and then boiled for 5 minutes to stop the reaction. Reaction products were analyzed by High Performance Anion Exchange Chromatography with Pulse Amperometric Detection (Dionex, model ICS3000). The samples were loaded on a CarboPAC-PA100 column (Dionex) pre-equilibrated for 20 minutes with 98% of 50 mM NaOH (eluant A) and 2% of 50 mM NaOH 500 mM NaOAc (eluant B). After injection a gradient run (flow rate of 0.350 $mL.min^{-1}$) was performed as follows: 0-2 min 98% A + 2% B – 88.8% A + 11.2% B, 2-20 min 88.8% A + 11.2% B – 65% A + 35% B, 20-35 min 65% A + 35% B – 40% A + 60% B, 35-37 min 40% A + 60% B – 100% B.

Transfections, immunofluorescence and PAS staining.

Cells were transfected with the indicated plasmids using the JetPrime kit (Polyplus Transfection) according the manufacturer recommendations. Twenty-four hours post transfection, cells were fixed with 2% (w/v) paraformaldehyde (PFA) 2% (w/v) sucrose in PBS for 30 minutes at room temperature, then washed with PBS twice. For the panel shown in Fig.1, a 4% PFA 4 % sucrose solution was used for fixation. Cells were blocked with 10 mg/mL bovine serum albumin (BSA) for 30 minutes before being stained with antibodies anti-ICAM-1 coupled to APC (Invitrogen 17.0549.42) at dilution 1/1000. Cells were then washed twice with PBS, permeabilized with 0.5% saponin in PBS and DNA was stained with Hoechst 33342

(Molecular Probes). For the panel shown in Fig. 3D the cells were permeabilized after ICAM-1-APC staining to probe for Flag (rabbit, Sigma F7425) or Hsp60 (rabbit, homemade) followed with A488-conjugated secondary antibodies. For the panel shown in Fig.1 and 3C, the cells were permeabilized in 0.5% saponin in PBS and stained with mouse anti-Flag M2 antibody (Sigma) and homemade rabbit anti-Cap1 antibody, followed with species-specific secondary antibodies. Images were acquired on an Axio observer Z1 microscope equipped with an ApoTome module (Zeiss, Germany) and a 63× Apochromat lens. Images were taken with an ORCA-flash4.OLT camera (Hamamatsu, Japan) using the software Zen.

For periodic-acid-Schiff (PAS) stain cells were fixed in 4 % PFA 4% sucrose in PBS for 30 min at room temperature and staining was performed as described (50). Briefly, cells were incubated in 1 % periodic acid (Sigma) for 5 min. Thereafter coverslips were put in tap water for 1 min, quickly rinsed in mQ-H_20 and then applied to Schiff reagent (Sigma) for 15 min at room temperature. Afterwards the coverslips were rinsed again in mQ-H_20, incubated in tap water for 10 min followed by an incubation step in PBS for 5 min. Periodic acid oxidizes the vicinal diols in sugars such as glycogen to aldehydes, which now in turn react with the Schiff reagent to give a purple colour. Coverslips infected with *C. caviae* and *C. pneumoniae* were further stained with home-made rabbit antibody against *C. muridarum* GroEL, that cross-reacts with the orthologous proteins in these species, followed with Alexa488-conjugated secondary antibodies. Images were acquired using transmission light or green fluorescence excitation on an Axio Vert.A1 microscope (Zeiss, Germany) and an LD A-Plan 40x lense. Images were taken with an AxioCam ICc 1 camera using the software Zen.

Progeny assays

For siRNA transfection 50 000 cells were plated in a 24-well plate and immediately mixed with Lipofectamine RNAiMAX (Invitrogen) following the manufacturer's recommendation, using 10 nM of siRNA (see Table S1 for sequences). Cells treated with siRNA for 24 h (J1) were infected with $L2^{IncD}$GFP bacteria at a MOI = 0.2. Transfection of siRNAs was repeated on J2. On J3 (48 hpi), cells were detached, lysed using glass beads and the supernatant was used to infect new untreated cells plated the day before (100 000 cells/well in a 24-well plate), in serial dilution. The next day, 3 wells per condition with an infection lower than 30 % (checked by microscopy) were detached, fixed and analyzed by flow cytometry to determine the bacterial titer as described (34).

***Shigella* heterologous secretion assays and immunoblots**

Analysis of secreted proteins was performed as described previously (16), except that the *ipaB* or *mxiD Shigella flexneri* were co-transformed with the pMM100 plasmid that codes for the *lacI* repressor (selection with tetracyclin) (51) and with the indicated Cya chimera (selection with ampicillin). This was done to avoid the very strong expression of some of the chimeras in the absence of *lacI* repressor. Briefly, 1 ml of a 30 °C overnight culture of *S. flexneri ipaB* or *mxiD* transformed with different Cya chimeras was inoculated in 15 ml of LB broth and incubated at 37 °C for 1 h. Expression of the Cya chimeras was induced by adding 10 µM IPTG

for all chimera except PGMtracho/Cya which was induced at 100 µM IPTG. Bacteria were harvested by centrifugation 3 h later and the supernatant was filtered through a Millipore filter (0.2 µm). To precipitate the proteins 1/10 (v/v) of trichloroacetic acid was added to the supernatants. The pellet fraction and the supernatant fraction (concentrated 40-fold compared to the pellet fraction) were resuspended in sample buffer for SDS-PAGE, transferred to Immobilon-P (PVDF) membranes and immunoblotted with the proper primary antibodies diluted in 1X PBS containing 5% milk and 0.01% Tween-20. Primary antibodies used were mouse anti-cya, rabbit anti-CRP and rabbit anti-IpaD antibodies generously given by Drs N. Guiso, A. Ullmann and C. Parsot, respectively (Institut Pasteur, Paris). Goat anti-mouse and anti-rabbit IgG-HRP (GE Healthcare) were used at 1:10000 dilution. Blots were developed using the Western Lightning Chemiluminescence Reagent (GE Healthcare).

ACKNOWLEDGEMENTS

We thank Dr. Hudson Freeze (Sanford-Burnham Medical Research Institute, La Jolla, USA) for the generous gift of PGM1-deficient fibroblasts, Dr. Hanna Marti (University of Zürich) for the *C. suis* strain and Dr. Lena Gehre for the GlgA-Flag expressing bacteria. This work was supported by the Agence Nationale pour la Recherche (ANR-14-CE11-0024-02 “Expendo”), the Institut Pasteur and the Centre National de la Recherche Scientifique. D.N’G. received financial support from the Fondation pour la recherche médicale (FDT202012010504). MH received financial support from the Austrian Science Fund FWF (DOC 69-B).

REFERENCES

1. Elwell C, Mirrashidi K, & Engel J (2016) *Chlamydia* cell biology and pathogenesis. *Nat Rev Microbiol* 14(6):385-400.
2. Harper A, Pogson CI, Jones ML, & Pearce JH (2000) Chlamydial development is adversely affected by minor changes in amino acid supply, blood plasma amino acid levels, and glucose deprivation. *Infect. Immun.* 68(3):1457-1464.
3. Iliffe-Lee ER & McClarty G (2000) Regulation of carbon metabolism in Chlamydia trachomatis. *Mol. Microbiol.* 38(1):20-30.
4. Nicholson TL, Chiu K, & Stephens RS (2004) Chlamydia trachomatis lacks an adaptive response to changes in carbon source availability. *Infect. Immun.* 72(7):4286-4289.
5. Mehlitz A*, et al.* (2017) Metabolic adaptation of Chlamydia trachomatisto mammalian host cells. *Mol. Microbiol.* 103(6):1004-1019.
6. Gordon FB & Quan AL (1965) Occurence of glycogen in inclusions of the pisttacosis-lymphogranuloma venereum-trachoma agents. *J. Infect. Dis.* 115:186-196.
7. Chiappino ML, Dawson C, Schachter J, & Nichols BA (1995) Cytochemical localization of glycogen in Chlamydia trachomatis inclusions. *J. Bacteriol.* 177(18):5358-5363.
8. Henrissat B, Deleury E, & Coutinho PM (2002) Glycogen metabolism loss: a common marker of parasitic behaviour in bacteria? *Trends Genet.* 18(9):437-440.
9. Gehre L*, et al.* (2016) Sequestration of host metabolism by an intracellular pathogen. *Elife* 5:e12552.
10. Belland R*, et al.* (2003) Genomic transcriptional profiling of the developmental cycle of Chlamydia trachomatis. *Proc. Natl. Acad. Sci. U. S. A.* 100(14):8478-8483.
11. Schwoppe C, Winkler HH, & Neuhaus HE (2002) Properties of the glucose-6-phosphate transporter from Chlamydia pneumoniae (HPTcp) and the glucose-6-phosphate sensor from Escherichia coli (UhpC). *J. Bacteriol.* 184(8):2108-2115.
12. Stojkovic T*, et al.* (2009) Muscle glycogenosis due to phosphoglucomutase 1 deficiency. *N. Engl. J. Med.* 361(4):425-427.
13. Tegtmeyer LC*, et al.* (2014) Multiple Phenotypes in Phosphoglucomutase 1 Deficiency. *N. Engl. J. Med.* 370(6):533-542.
14. Huerta-Cepas J*, et al.* (2016) eggNOG 4.5: a hierarchical orthology framework with improved functional annotations for eukaryotic, prokaryotic and viral sequences. *Nucleic Acids Res.* 44(D1):D286-D293.
15. Ray WJ, Jr. & Roscelli GA (1964) A KINETIC STUDY OF THE PHOSPHOGLUCOMUTASE PATHWAY. *J. Biol. Chem.* 239:1228-1236.
16. Subtil A, Parsot C, & Dautry-Varsat A (2001) Secretion of predicted Inc proteins of *Chlamydia pneumoniae* by a heterologous type III machinery. *Mol. Microbiol.* 39(3):792-800.
17. Lu C*, et al.* (2013) Chlamydia trachomatis GlgA is secreted into host cell cytoplasm. *PLoS One* 8(7):e68764.
18. Carlson JH*, et al.* (2008) The Chlamydia trachomatis plasmid is a transcriptional regulator of chromosomal genes and a virulence factor. *Infect. Immun.* 76(6):2273-2283.
19. Jolly L*, et al.* (1999) Reaction mechanism of phosphoglucosamine mutase from Escherichia coli. *Eur. J. Biochem.* 262(1):202-210.
20. Saka HA*, et al.* (2011) Quantitative proteomics reveals metabolic and pathogenic properties of *Chlamydia trachomatis* developmental forms. *Mol. Microbiol.* 82(5):1185-1203.
21. Muschiol S*, et al.* (2011) Identification of a family of type III secreted effectors conserved in pathogenic *Chlamydiae*. *Infect. Immun.* 79:571-580.

22. da Cunha M, Pais SV, Bugalhão JN, & Mota LJ (2017) The Chlamydia trachomatis type III secretion substrates CT142, CT143, and CT144 are secreted into the lumen of the inclusion. *PLoS ONE* 12(6):e0178856.
23. Akopyan K*, et al.* (2011) Translocation of surface-localized effectors in type III secretion. *Proc. Natl. Acad. Sci. U. S. A.* 108(4):1639-1644.
24. Tejeda-Dominguez F, Huerta-Cantillo J, Chavez-Dueñas L, & Navarro-Garcia F (2017) A Novel Mechanism for Protein Delivery by the Type 3 Secretion System for Extracellularly Secreted Proteins. *mBio* 8(2).
25. Bush RM & Everett KDE (2001) Molecular evolution of the Chlamydiaceae. *International Journal of Systematic and Evolutionary Microbiology* 51:203-220.
26. Ball SG*, et al.* (2013) Metabolic effectors secreted by bacterial pathogens: essential facilitators of plastid endosymbiosis? *Plant Cell* 25(1):7-21.
27. Collingro A, Köstlbacher S, & Horn M (2020) Chlamydiae in the Environment. *Trends Microbiol.*
28. Horn M*, et al.* (2004) Illuminating the evolutionary history of chlamydiae. *Science* 304(5671):728-730.
29. Omsland A, Sixt BS, Horn M, & Hackstadt T (2014) Chlamydial metabolism revisited: interspecies metabolic variability and developmental stage-specific physiologic activities. *FEMS Microbiol. Rev.* 38(4):779-801.
30. Dharamshi JE*, et al.* (2020) Marine Sediments Illuminate Chlamydiae Diversity and Evolution. *Curr. Biol.* 30(6):1032-1048.e1037.
31. Sixt BS*, et al.* (2013) Metabolic features of Protochlamydia amoebophila elementary bodies--a link between activity and infectivity in Chlamydiae. *PLoS Pathog* 9(8):e1003553.
32. Aguilera L*, et al.* (2012) Secretion of the housekeeping protein glyceraldehyde-3-phosphate dehydrogenase by the LEE-encoded type III secretion system in enteropathogenic Escherichia coli. *The International Journal of Biochemistry & Cell Biology* 44(6):955-962.
33. Peterson EM, Markoff BA, Schachter J, & de la Maza LM (1990) The 7.5-kb plasmid present in Chlamydia trachomatis is not essential for the growth of this microorganism. *Plasmid* 23(2):144-148.
34. Vromman F, Laverriere M, Perrinet S, Dufour A, & Subtil A (2014) Quantitative Monitoring of the *Chlamydia trachomatis* Developmental Cycle Using GFP-Expressing Bacteria, Microscopy and Flow Cytometry. *PLoS One* 9(6):e99197.
35. Scidmore MA (2005) Cultivation and laboratory maintenance of *Chlamydia trachomatis*. *Curr Protocols Microbiol*:11A11.11-11A11.25.
36. Allaoui A, Sansonetti P, & Parsot C (1993) MxiD, an outer membrane protein necessary for the secretion of the Shigella flexneri lpa invasins. *Mol. Microbiol.* 7(1):59-68.
37. Huerta-Cepas J*, et al.* (2017) Fast Genome-Wide Functional Annotation through Orthology Assignment by eggNOG-Mapper. *Mol. Biol. Evol.* 34(8):2115-2122.
38. Fu L, Niu B, Zhu Z, Wu S, & Li W (2012) CD-HIT: accelerated for clustering the next-generation sequencing data. *Bioinformatics* 28(23):3150-3152.
39. Katoh K, Misawa K, Kuma K, & Miyata T (2002) MAFFT: a novel method for rapid multiple sequence alignment based on fast Fourier transform. *Nucleic Acids Res* 30(14):3059-3066.
40. Capella-Gutiérrez S, Silla-Martínez JM, & Gabaldón T (2009) trimAl: a tool for automated alignment trimming in large-scale phylogenetic analyses. *Bioinformatics* 25(15):1972-1973.

41. Le SQ & Gascuel O (2008) An improved general amino acid replacement matrix. *Mol. Biol. Evol.* 25(7):1307-1320.
42. Minh BQ, Nguyen MA, & von Haeseler A (2013) Ultrafast approximation for phylogenetic bootstrap. *Mol. Biol. Evol.* 30(5):1188-1195.
43. Hoang DT, Chernomor O, von Haeseler A, Minh BQ, & Vinh LS (2018) UFBoot2: Improving the Ultrafast Bootstrap Approximation. *Mol. Biol. Evol.* 35(2):518-522.
44. Guindon S*, et al.* (2010) New algorithms and methods to estimate maximum-likelihood phylogenies: assessing the performance of PhyML 3.0. *Systematic biology* 59(3):307-321.
45. Wang HC, Minh BQ, Susko E, & Roger AJ (2018) Modeling Site Heterogeneity with Posterior Mean Site Frequency Profiles Accelerates Accurate Phylogenomic Estimation. *Systematic biology* 67(2):216-235.
46. Letunic I & Bork P (2019) Interactive Tree Of Life (iTOL) v4: recent updates and new developments. *Nucleic Acids Res* 47(W1):W256-w259.
47. Mullick A*, et al.* (2006) The cumate gene-switch: a system for regulated expression in mammalian cells. *BMC Biotechnology* 6(1):43.
48. Bauler LD & Hackstadt T (2014) Expression and Targeting of Secreted Proteins from Chlamydia trachomatis. *J. Bacteriol.* 196(7):1325-1334.
49. Wang Y*, et al.* (2011) Development of a transformation system for *Chlamydia trachomatis*: restoration of glycogen biosynthesis by acquisition of a plasmid shuttle vector. *PLoS Pathog* 7(9):e1002258.
50. Schaart G*, et al.* (2004) A modified PAS stain combined with immunofluorescence for quantitative analyses of glycogen in muscle sections. *Histochem. Cell Biol.* 122(2):161-169.
51. Jaumouillé V, Francetic O, Sansonetti PJ, & Tran Van Nhieu G (2008) Cytoplasmic targeting of IpaC to the bacterial pole directs polar type III secretion in Shigella. *The EMBO Journal* 27(2):447-457.

Figure 1

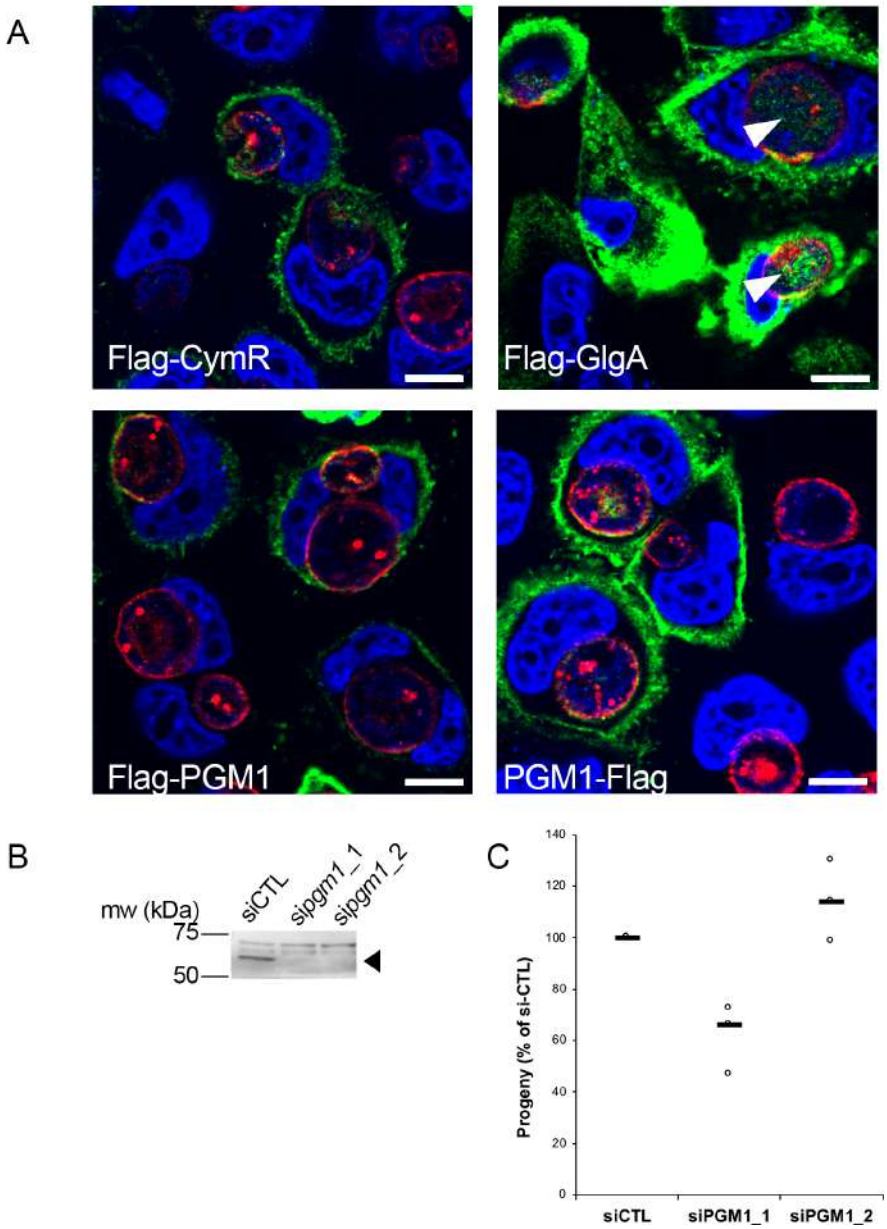

Fig. 1. Host PGM1 does not accumulate in the inclusion lumen and is dispensable for *C. trachomatis* development. A – HeLa cells were transfected with the indicated Flag-tagged constructs, infected with *C. trachomatis* L2 and fixed 24 h later. Cells were permeabilized and stained for the inclusion membrane protein Cap1 (red) and Flag (green). DNA was stained with Hoechst (blue). The merge image is shown. Only Flag-GlgA was detected in the inclusion lumen (arrowheads). Bar is 10 μm. B – Two different siRNA were used to silence *pgm1* expression and the effect on PGM1 level was measured by western blot. The arrowhead points to PGM1 (mw=61.5 kDa), higher bands are non specific. C – The effect of *pgm1* silencing on bacterial progeny was measured 48 hpi. Dot plot distribution of the progeny relative to cells treated with control siRNA, for three independent experiments, is shown. Gray bar, median.

Figure 2

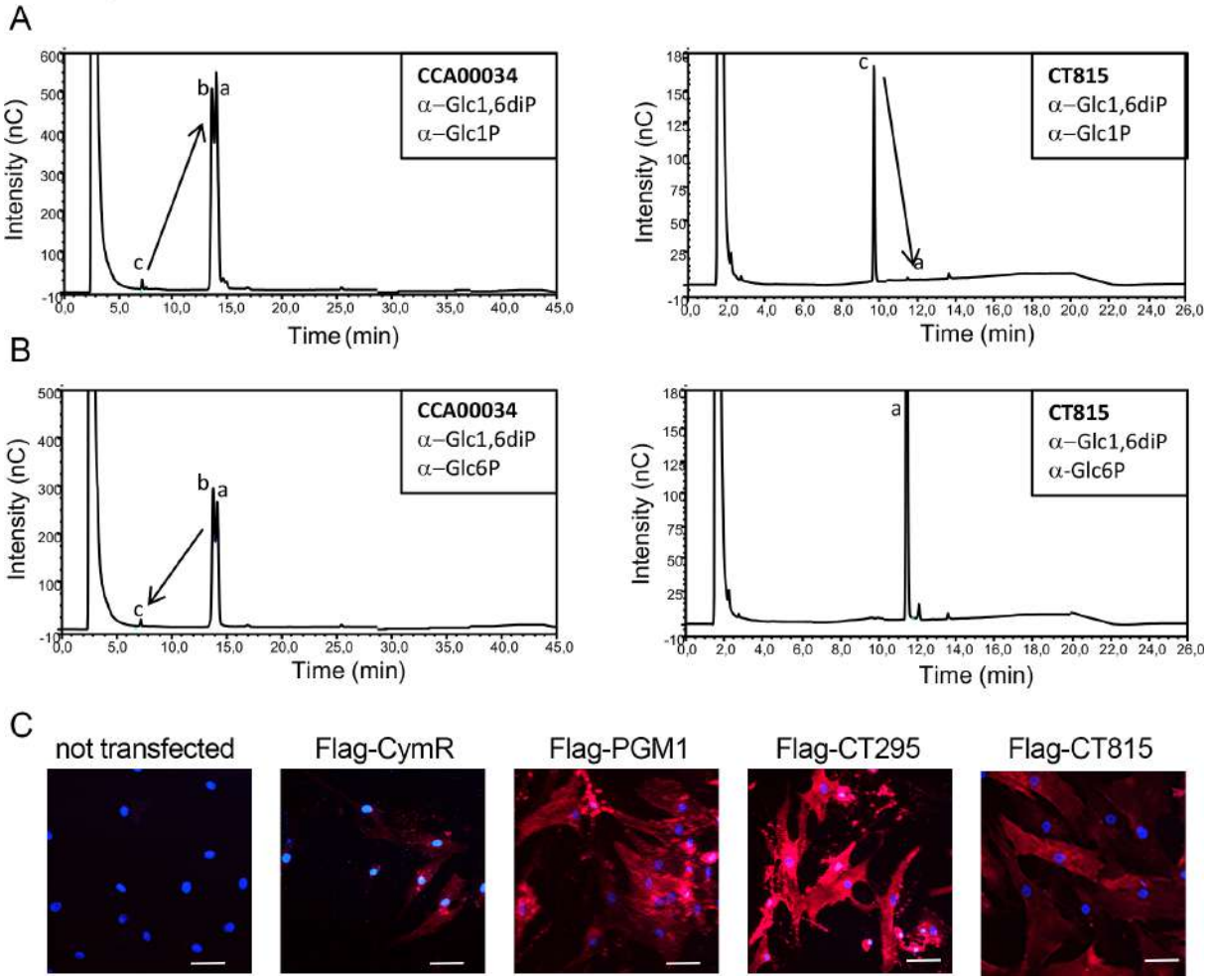

Fig. 2. CT295 is a phosphoglucomutase. A – The indicated purified proteins (bold letters) were incubated with Glc1P in the presence of the co-factor Glc1,6diP. The substrates and reaction products were identified by HPAEC. Incubation of Glc1P (peak c) with CCA00034 resulted in full conversion into Glc6P (peaks a and b), while Glc6P was hardly detectable when CT815 was tested. Note that the samples were run on two different columns, resulting in different elution profiles. B – The reverse reaction was tested. A very low conversion of Glc6P into Glc1P was observed for CCA00034 and was totally absent for CT815. Of note, CCA00034 favors the conversion of α-Glc6P (peak a) into β-Glc6P (peak b) while CT815 does not. C – PGM1 deficient fibroblasts were transfected or not with the indicated constructs. One day later, ICAM1 expression at the cell surface was probed with Cy5-coupled anti-ICAM1 antibody (red). Nuclei were stained with Hoechst (blue). Bar is 50 μm.

Figure 3

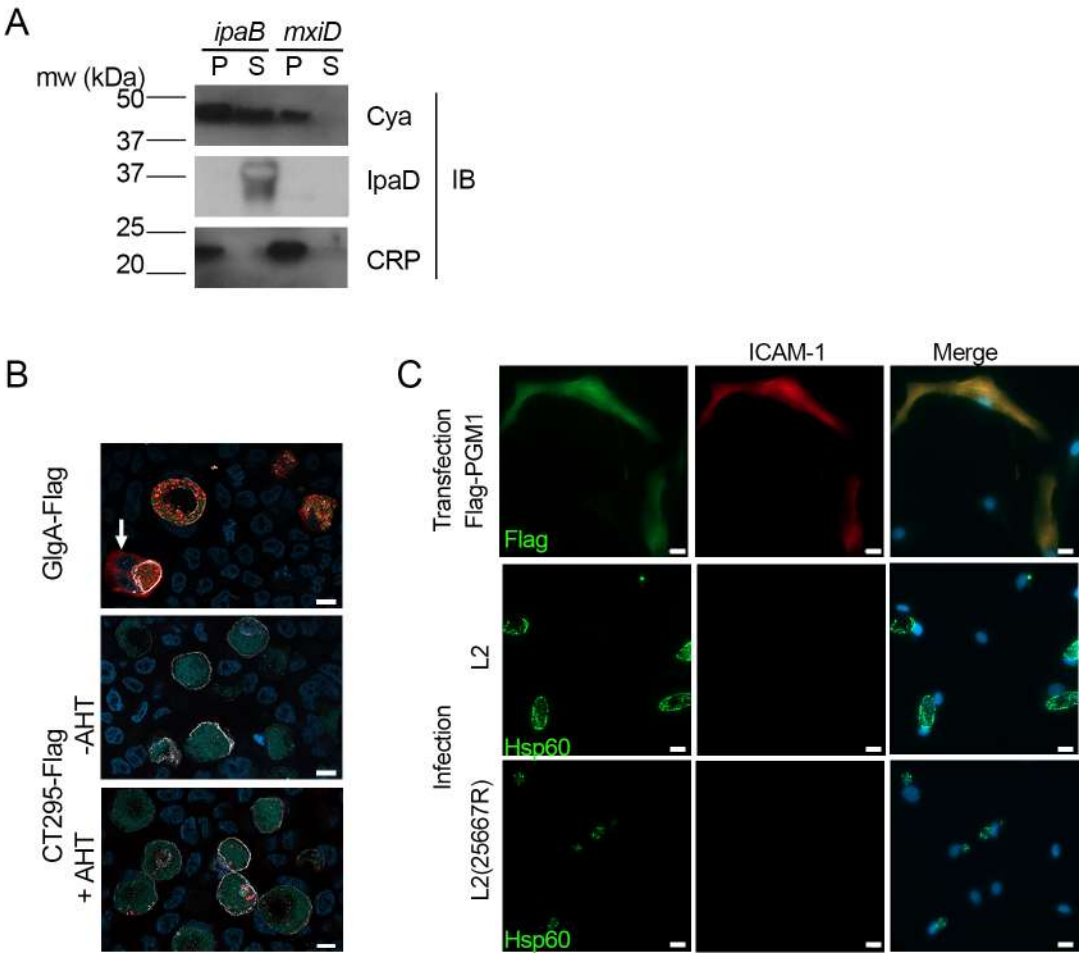

Fig. 3. CT295 is secreted in the inclusion lumen. A – The first 22 amino acids of CT295 were fused to the Cya reporter protein and expressed in a S. *flexneri ipaB* (constitutive T3S) or *mxiD* (defective T3S) strain. Exponential phase cultures expressing the reporter fusion protein were fractionated into supernatants (S) and pellets (P). Samples were resolved by SDS-PAGE, transferred to a PVDF membrane, and probed with anti-Cya (to detect the fusion protein), anti-IpaD (*Shigella* secreted protein), or anti-CRP (*Shigella* non-secreted protein) antibodies. B – Cells were infected with *C. trachomatis* L2 strain stably expressing GFP together with either GlgA-Flag (endogenous promoter), or CT295-Flag (Tet-inducible promoter), and incubated in the absence of presence of 5 nM anhydrotetracycline (AHT) for 48 h before fixation, permeabilization and staining. Bacteria are visible in the green channel, the inclusion membrane is labeled with antibodies against Cap1 followed with Cy3-coupled anti-rabbit antibodies (white), secondaries antibodies for the Flag-tagged were Alexa647-coupled anti-mouse antibodies (red), the DNA was stained with Hoechst (blue). The white arrow points to GlgA-Flag detected in the cytoplasm of one infected cell. Bar is 10 μm. C – PGM1 deficient fibroblasts were transfected with Flag-PGM1 or infected with the indicated *C. trachomatis* L2 strain. Forty-eight hours later the cells were fixed, permeabilized and stained with the indicated antibodies. Nuclei were stained with Hoechst (blue). Bar is 20 μm.

Figure 4

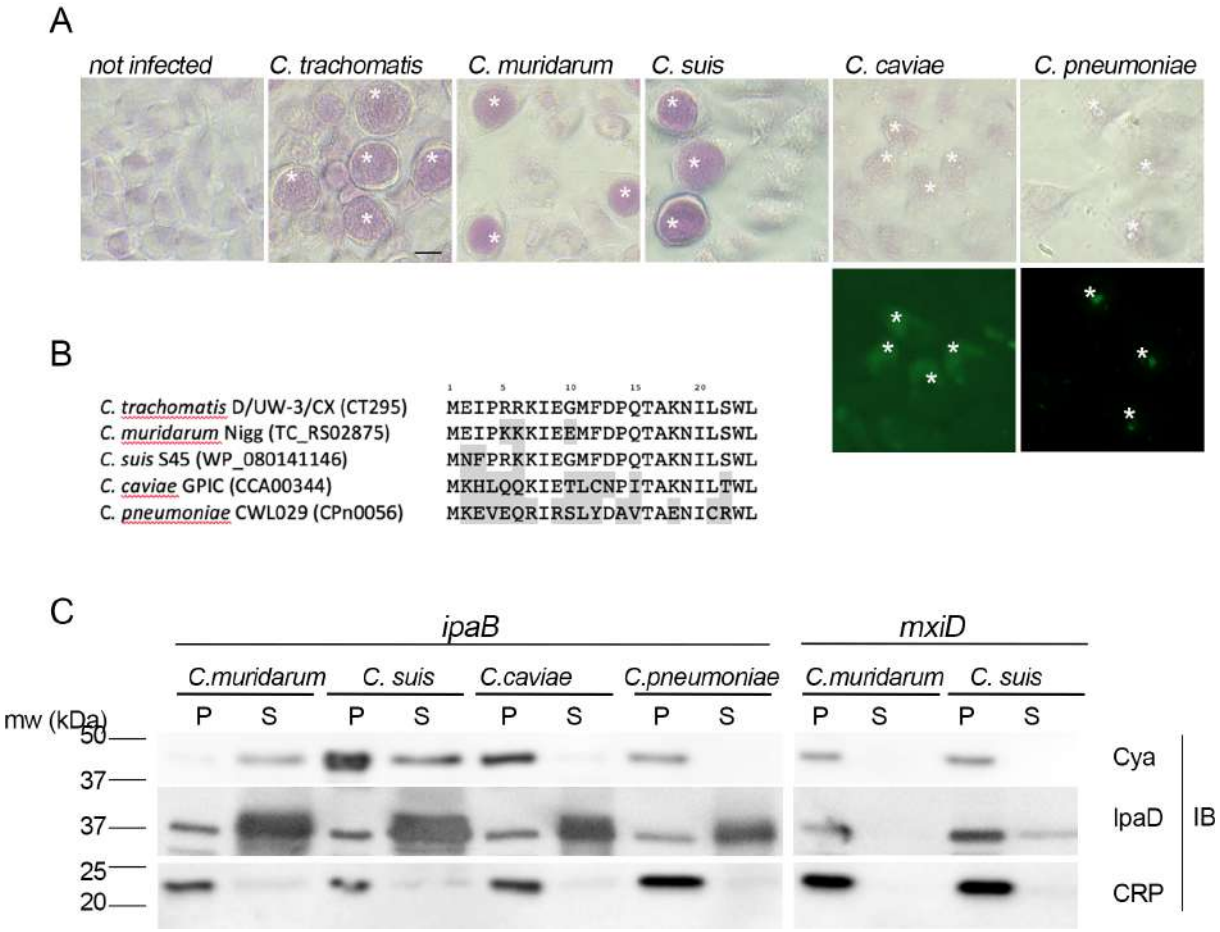

Fig. 4. Secretion of a PGM activity correlates with glycogen accumulation among *Chlamydiaceae*. A – Top panels: PAS staining of cells infected with the indicated strains. Bottom panels: *C. caviae* and *C. pneumoniae* infected cells were further stained with anti-mGroEL antibody followed with Alexa488-conjugated secondary antibodies to detect the inclusions (asterisks). Bar is 20 μm. B – Alignement of the first 24 amino acids of CT295 and its orthologs in the indicated *Chlamydiaceae* species. Amino acids that differ from the *C. trachomatis* sequence are shadowed. C – The first 22 amino acids of the indicated CT295 orthologs were fused to the Cya reporter protein and expressed in a S*. flexneri ipaB* (left) or *mxiD* (right) strains. Secretion was analyzed like in Fig. 3A.

Figure S1

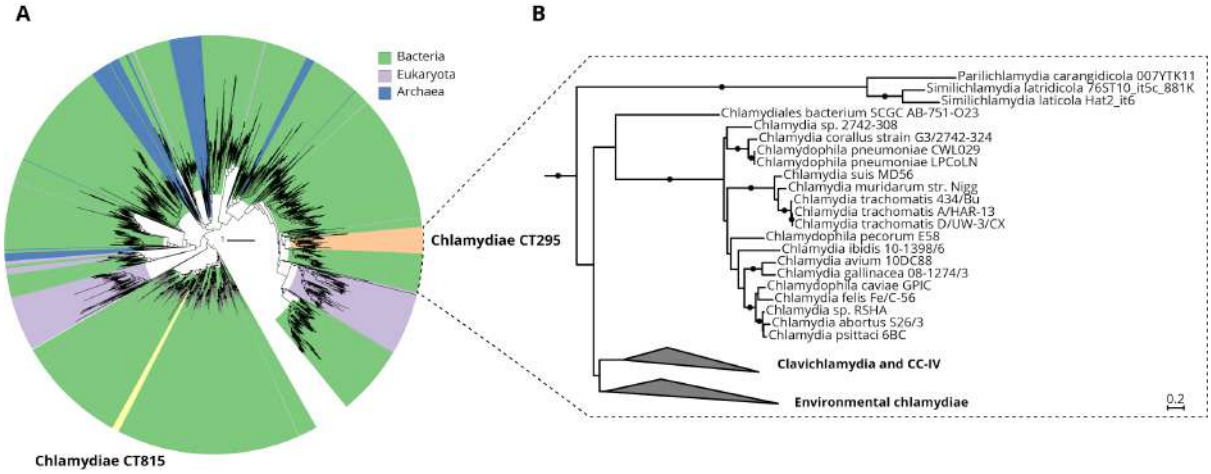

Supplementary figure 1: The chlamydial candidate PGMs CT295 and CT815 are related with other bacterial PGMs, stem from an ancient gene duplication event and are both monophyletic. (**A**) Phylogenetic analysis of chlamydial CT295 and CT815 homologs in eggNOG COG1109 (annotated as "phosphomannomutase"; 456 aligned positions; http://eggnogapi45.embl.de/nog_data/text/fasta/COG1109) clustered at 80% amino acid identity over 90% query coverage (n=2,829). Clades are colored by their affiliation to bacteria, eukaryota, and archaea in green, violet, and blue, respectively. Orange indicates the chlamydial CT295 clade (bacterial eggNOG ENOG4107QSU), and yellow indicates the chlamydial CT815 clade (bacterial eggNOG ENOG4107QJF). Maximum likelihood phylogenetic trees with best fit model LG+C60+G+F with 1,000 ultrafast bootstraps are shown. Bootstrap support for monophyly of chlamydial clades in the tree is ≥ 95%, and the SH-like approximate likelihood ratio is ≥ 80%. (**B**) Phylogenetic analysis of chlamydial CT295 homologs (bacterial eggNOG ENOG4107QSU; n=104) with its sister clade from COG1109 (575 aligned positions) used as outgroup (n=93). Maximum likelihood phylogenetic tree based on LG+C60+G+F best tree using the posterior mean site frequency model and 100 non-parametric bootstraps. Bootstraps ≥ 70% are indicated by filled circles at splits in the tree. Scale bar indicates 0.2 substitution per position.

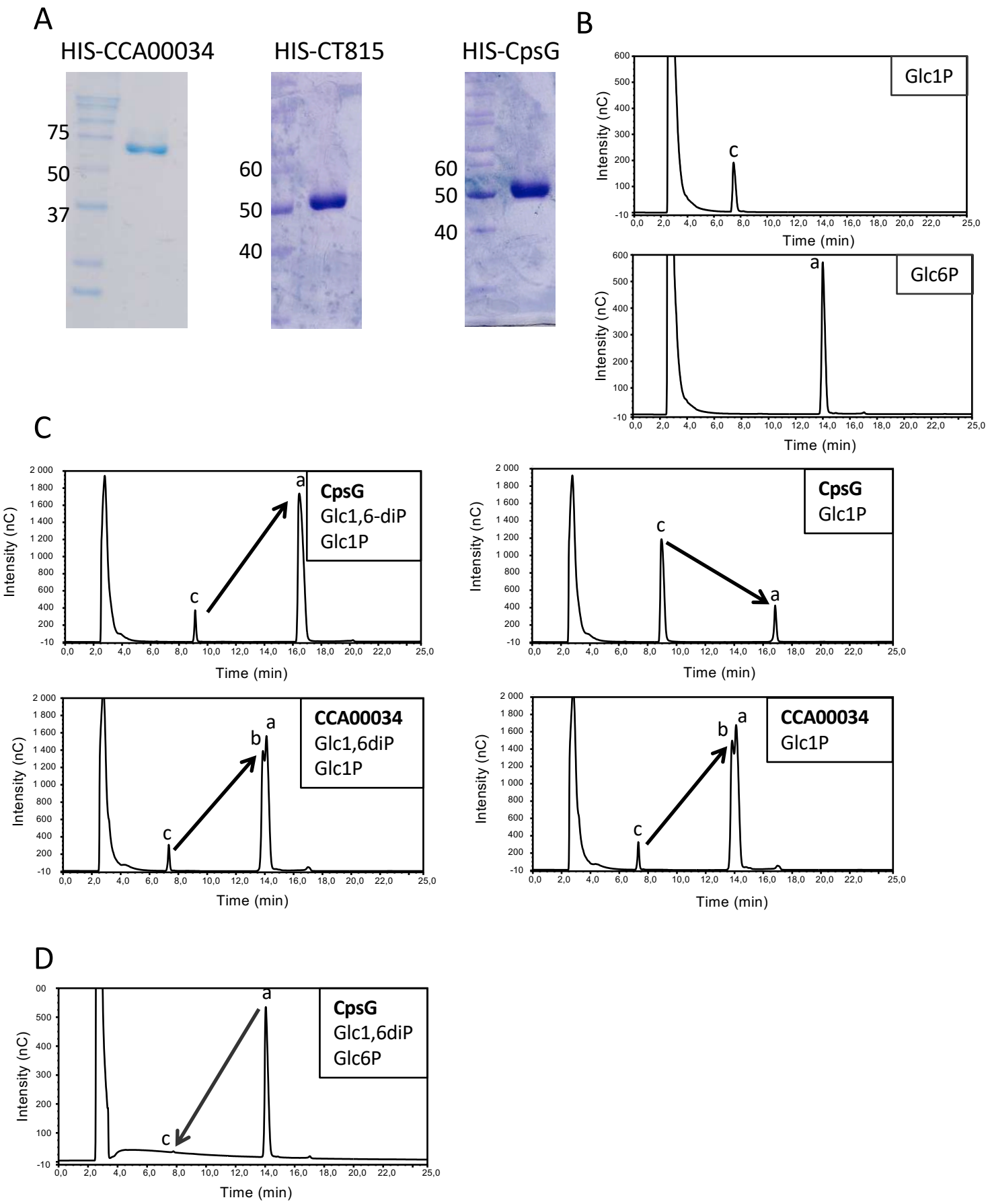

Figure S2 A – Migration profile of purified proteins. Purified His-tagged proteins were run on SDS-PAGE and stained with Coomassie blue. Molecular weights are indicated. B – Elution profiles of α-Glc1P (peak c) and α–Glc6P (peak a). C – HIS-CpsG (top) or HIS-CCA00034 (bottom) were incubated with Glc1P in the presence (left) or absence (right) of the co-factor Glc1,6diP. The substrates and reaction products were identified by HPAEC-PAD. CpsG required the presence of Glc1,6diP for optimal conversion of Glc1P into Glc6P, while CCA00034 did not. Also, CCA00034 favored the conversion of α-Glc6P (peak a) into β-Glc6P (peak b), while CpsG did not. D- HIS-CpsG was incubated with Glc6P in the presence of Glc1,6diP. Conversion of Glc6P into Glc1P was hardly detectable.

Table S1: Oligonucleotides and plasmids used

Construct name	Gene	DNA Template	Vector	Tag	Primers	Restriction sites	Cloning method	Resistance
HIS-CpsG	*cpsG*	*E. coli* BW25113	pET28a	6xHis	5'-AAAACCATGGGGAAAAAATTAACCTGCTTTAA-3' 5'-TTTTTCTCGAGCTCGTTCAGCAACGTCAGCA-3'	NcoI-XhoI	Restriction enzyme	Kanamycin
HIS-CCA00034	*cca00034*	*C. caviae* GPIC	pET28a	6xHis	5'-TCTAGAAATAATTTTGTTTAACTTTAAGAAGGAGATATACCATGAAGCATCTTCAACAGAA-3' 5'-TTTGTTAGCAGCCGGATCTCAGTGGTGGTGGTGGTGGTGCTCGAGTTCAGGCTTTAAAGAAGAGA-3'	NcoI-XhoI	Gibson assembly	Kanamycin
HIS-CT815	*ctl0187*	*C. trachomatis L2/434/Bu*	pET28a	6xHis	5'-CATGGGGACACGTGATGTGAGCCAGCT-3' (1) 5'-CGGGACACGTGATGTGAGCCAGCT-3' (2) 5'-TCGAGTTCGGAAATCCCGGCTCCAA-3' (3) 5'-GTTCGGAAATCCCGGCTCCAA-3' (4)	NcoI-XhoI	See main text	Kanamycin
Flag-CT295	*ctl0547*	*C. trachomatis L2/434/Bu*	pDEST-pCINeoFlag	Flag (Nter)	5'-GGGGACAAGTTTGTACAAAAAAGCAGGCTTGATGGAAATTCCTAGAAGGA-3' 5'-GGGGACCACTTTGTACAAGAAAGCTGGGTCTTACTACTAAGAGTAAAAAAGGTGAC-3'	NA	Gateway cloning	Ampicillin
Flag-CT815	*ctl0187*	*C. trachomatis L2/434/Bu*	pDEST-pCINeoFlag	Flag (Nter)	5'-GGGGACAAGTTTGTACAAAAAAGCAGGCTTGATGACACGTGATGTGAGCCA-3' 5'-GGGGACCACTTTGTACAAGAAAGCTGGGTCTTACTATTATTCGGAAATCCCGGCTC-3'	NA	Gateway cloning	Ampicillin
Flag-CymR	*CymR*	Entry vector was a gift from Y. Jacob, Institut Pasteur	pDEST-pCINeoFlag	Flag (Nter)		NA	Gateway cloning	Ampicillin
Flag-PGM1	*pgm1*	HeLa cells	pDEST-pCINeoFlag	Flag (Nter)	5'-GGGGACAAGTTTGTACAAAAAAGCAGGCTTGATGGTGAAGATCGTGACAGT-3' 5'-GGGGACCACTTTGTACAAGAAAGCTGGGTCTTACTATTAGGTGATGACAGTGGGTG-3'	NA	Gateway cloning	Ampicillin
PGM1-Flag	*pgm1*	HeLa cells	2Flag-pDEST-C Addgene #118372	Flag (Cter)	5'-GGGGACAAGTTTGTACAAAAAAGCAGGCTgccaccATGGTGAAGATCGTGACAGTTA-3' 5'-GGGGACCACTTTGTACAAGAAAGCTGGGTcGGTGATGACAGTGGGTGC-3'	NA	Gateway cloning	Ampicillin
PGM_Ctrachomatis	*ctl0547* (22 codons)	*C. trachomatis L2/434/Bu*	pUC19Cya	Cya	5'-agtcaagcttgTAAagtaccaggagaaattaactATGGAAATTCCTAGAAGGAAAATAGAG-3' 5'-agtctctagaAGACAAAATGTTTTTGGCTGTTT-3'	HindIII-XbaI	Restriction enzyme	Ampicillin
PGM_muridarum-c	*TC_RS02875* (22 codons)	*C. muridarum MoPn*	pUC19Cya	Cya	5'-AGTCaagcttgTAAagtaccAGGAGAaattaactATGGAAATTCCAAAAAAGAAAATTGAGG-3' 5'-AGTCtctagaAGATAAAATATTTTTGGCAGTTTGAGG-3'	HindIII-XbaI	Restriction enzyme	Ampicillin
PGM_suis-cya	*WP_080141146* (22 codons)	*C. suis* 4.29b	pUC19Cya	Cya	5'-AGTCaagcttgTAAagtaccAGGAGAaattaactATGAATTTTCCAAGAAAAAAAATAGAAGGG-3' 5'-AGTCtctagaAGAGAGAATATTCCTAGCTGTTTGA-3'	HindIII-XbaI	Restriction enzyme	Ampicillin
PGM_caviae-cya	*cca0034* (22 codons)	*C. caviae GPIC*	pUC19Cya	Cya	5'-AGTCaagcttgTAAagtaccAGGAGAaattaactATGAAGCATCTTCAACAGAAAATAGAA-3' 5'-AGTCtctagaGGTTAAGATATTCTTCGCTGTTATAGGG-3'	HindIII-XbaI	Restriction enzyme	Ampicillin
PGM_pneumoniae-	*cpn0056* (22 codons)	*C. pneumoniae CWL029*	pUC19Cya	Cya	5'-AGTCaagcttgTAAagtaccAGGAGAaattaactATGAAAGAAGTAGAACAACGTATCCGG-3' 5'-AGTCtctagaTCTACAAATATTTTCAGCTGTTACTG-3'	HindIII-XbaI	Restriction enzyme	Ampicillin
CT295-Flag	*ctl0547*	*C. trachomatis* L2/434/Bu	pBOMB4-Tet	Flag (Cter)	5'-ttttGCGGCCGCATGGAAATTCCTAGAAGGAAAATAGAGGGA -3' 5'-cgatgtcgacCTATTACTTGTCGTCATCGTCTTTGTAGTCagagtaaaaaaggtcactcttggtttctt-3'	NotI-SalI	Restriction enzyme	Ampicillin
GlgA-Flag	*ctl0167 (glgA)*	*C. trachomatis L2/434/Bu*	pBOMB4	Flag (Cter)	5'-ttatccgcggccgcCCTTCTATGAGCAGAAACTATCCAT-3' 5'-cgatgtcgacCTATTACTTGTCGTCATCGTCTTTGTAGTCttgtttataaatttctaaatatttattggcgg-3'	NotI-SalI	Restriction enzyme	Ampicillin

siRNA sequences: si*pgm1*_ 1 CCACAUCCGUGAGAAAGAU dTdT
si*pgm1* _2 GCAAGACAAUUGAAGAAUA dTdT

Résumé

Les microorganismes à développement intracellulaire exercent une pression importante sur le métabolisme de leur hôte, car ils obtiennent tous leurs nutriments de son cytoplasme. Les bactéries intracellulaires obligatoires *Chlamydia trachomatis* en sont une illustration extrême : elles dépendent de leur hôte non seulement pour l'apport en glucose, leur source principale de carbone, mais probablement aussi, au moins partiellement, pour l'obtention de la monnaie énergétique issue du catabolisme du glucose, l'adénosine triphosphate (ATP). Ces bactéries effectuent un cycle de développement biphasique: les bactéries infectieuses, ou corps élémentaires (EBs), adhèrent à la membrane d'une cellule hôte, typiquement une cellules épithéliale du tractus génital, et provoquent leur internalisation. Une fois à l'intérieur d'un compartiment délimité par une membrane, appelé inclusion, les bactéries expriment un nouveau jeu de gènes et se transforment en corps réticulés (RBs). Le métabolisme des RBs, qui constitue la seule forme réplicative des bactéries, est plus élevé que celui des EBs. Les bactéries se multiplient plusieurs fois dans l'inclusion jusqu'à ce que les RBs se convertissent en EBs, qui, une fois relargués de la cellule-hôte, peuvent initier un nouveau cycle infectieux. La pression métabolique exercée par les bactéries sur leur hôte évolue donc tout au cours du temps. Savoir si l'infection module le métabolisme de son hôte, et dans quelle mesure les différentes étapes du cycle de développement dépendent de ce métabolisme, demeurent des questions ouvertes. Dans ce travail, en utilisant des cellules épithéliales primaires et une lignée cellulaire d'origine non tumorale, nous avons montré que les deux voies métaboliques principales pour la production d'ATP chez l'hôte, la glycolyse et la phosphorylation oxydative, restaient largement stables durant l'infection. Ces résultats indiquent que contrairement à nos attentes, il n'y a pas de basculement significatif du métabolisme de l'hôte vers la glycolyse durant l'infection. L'inhibition de l'une ou l'autre de ces deux voies diminue fortement la capacité des bactéries à effectuer leur cycle de développement. Bien que les EBs démontrent un certain degré d'autonomie énergétique pour la synthèse des protéines exprimées dans la phase initiale de l'infection, une glycolyse fonctionnelle est requise pour accompagner la formation des inclusions, tandis que la phosphorylation oxydative est moins nécessaire à ce stade précoce du développement. L'importance relative des deux voies pour soutenir les étapes initiales de l'infection corrèle avec leur contribution respective à maintenir le niveau d'ATP dans les cellules épithéliales, la glycolyse étant le contributeur principal. En conclusion, ce travail confirme la dépendance des bactéries vis à vis de la capacité de production d'ATP de l'hôte. Cependant, la consommation d'ATP par les bactéries semble en équilibre avec la production normale des cellules épithéliales et la production autonome par les bactéries, en sorte que le métabolisme de l'hôte ne nécessite pas de remodelage profond pour répondre aux besoins des bactéries.